



FACULTY OF SCIENCE AND TECHNOLOGY

MASTER'S THESIS

Study Program/Specialization: Offshore Technology / Marine and Subsea Technology	Spring Semester, 2011 Open / Confidential
Author: Iswan Herlianto	(signature author)
Instructor : Prof. Daniel Karunakaran Ph.D (University of Stavanger, Subsea 7 Norway) Supervisor(s) : Dr. Qiang Chen (Subsea 7 Norway) Dr. Dasharatha Achani (Subsea 7 Norway)	
Title of Master's Thesis: Lateral Buckling Induced by Trawl Gears Pull-over Loads on High Temperature / High Pressure Subsea Pipeline	
ECTS: 30	
Subject Headings: Lateral buckling, HP/HT subsea pipeline, Trawl gears, Pull-over loads, ANSYS	Pages: xiii + 68 + attachments/other : 75 Stavanger, 14 th June 2011

Abstract

This thesis work is performed to study and understand the pipeline global response as a result of trawl gears pull-over loads triggering lateral buckling on high temperature/high pressure subsea pipeline. The external interference from trawl gears pull-over loads may create substantial imperfection or out-of-straightness on the pipeline to trigger lateral buckling. The pull-over loads also may induce excessive bending moments and strains in the buckle region.

To be able to understand the global response of the pipeline under pull-over loading condition, a finite element analysis is carried out based on DNV OS F101 [1], DNV RP F110 [2] and DNV RP F111 [1]. The analysis is carried out using general finite element analysis software ANSYS v13. Nonlinear-transient analysis is used to incorporate the non-linear effects, such as the nonlinearities of pipeline material, and the response of a structure under the action of pull-over time-dependent loads.

The finite element analysis covers two period of duration i.e. during pull-over loads duration and after pull-over loads duration. The analysis during pull-over loads duration deals with the pipeline global response as a result of trawl gears pull-over loads. The pipeline is subjected to substantial horizontal and vertical pull-over forces from the trawl gears. The pull-over forces are applied based on force-time history as recommended in DNV RP F111 [3].

This thesis work also study the pipeline post buckling condition. After pull-over loads duration, the pipeline global response may be different. The analysis is carried out for additional 5 seconds from the end of pull-over loads duration. In this period, the pull-over loads are no longer applied. The pipeline may expand further more caused by temperature and pressure loads on pipeline.

There are four (4) types of trawl gear considered in the analysis i.e. polyvalent and rectangular trawl gear, industrial v-board, beam trawl and clump weight. All the trawl gears data are taken from DNV RP F111 [3]. The thesis work calculates the pull-over loads and durations from all type of trawl gears. In the finite element analysis, only the pull-over loads from polyvalent and rectangular trawl gear are used as this is considered to adequately represent the cases.

The finite element analysis of trawl gear pull-over shows the trawl gears pull-over loads induces lateral buckling on pipeline. The pipeline deform laterally at the pull-over loads location. High bending moments and strain occur at the apex of the buckle. The DNV displacement condition code check shows that the integrity of the pipeline is not satisfy the safety level hence the pipeline cannot withstand the trawl gears pull-over loads.

The analysis with variation of operating temperature and pressure should be carried out as further works. The further works shall also take into account a full comparison of lateral and axial soil friction combination. This way, a more accurate result can be obtained and better conclusion can be verified.

Keywords: Lateral buckling, HP/HT subsea pipeline, Trawl gears, Pull-over loads, finite element analysis, ANSYS.

Acknowledgement

This thesis is carried out to fulfill the requirement for Master of Science degree in the Offshore Technology Master's Degree program at the Department of Mechanical and Structural Engineering and Materials Science, Faculty of Science and Technology, University of Stavanger, Norway. This thesis work is carried out at Subsea 7 Norway, started from January 2011 and completed in June in the same year.

First of all, I would like to take this opportunity to thank my supervisor Prof. Daniel Karunakaran Ph.D for giving me the opportunity to work this thesis under his supervision. I would like to thank also for his advice, time for discussion and his great support. It is an honor for me to work with him.

I would also like to thank to Subsea 7 Norway for providing me an office space, computer system, full support and access to ANSYS finite element software and other softwares. I would especially like to thank my day to day supervisor, Dr. Qiang Chen for his guidance, time for sharing knowledge and discussion. My great thanks also to Dr. Dasharatha Achani for his great help and tutorial for finite element works in ANSYS

My sincere thanks go to my beloved wife Airindy Ayu Felisita, for her love, patience and her calls when she was away onboard every day. Thank you for your encouragement, great support and time for discussion. Your great support made this thesis work can be finished on time.

Last but not least, I would like to thank my family in Indonesia, my mother and father, my brother and sisters. Your love, your prayers and your support are big encouragement to finish this thesis and my master degree program.

Stavanger, 14th June 2011

Iswan Herlianto

Nomenclature

Abbreviations

BE	Best Estimate
DNV	Det Norske Veritas
FEA	Finite Element Analysis
LB	Lower Bound
OOS	Out-of-Straightness
OD	Outside Diameter
OS	Offshore Standard
RP	Recommended Practice
SMYS	Specified Minimum Yield Strength
UB	Upper Bound

Symbols

C_F	Coefficient of pull-over force	t	Pipe wall thickness
C_T	Coefficient of pull-over duration	T_{amb}	Ambient Temperature
D	Diameter	T_{op}	Operating Temperature
E	Young's modulus of the steel pipe	T_P	Pull-over duration
F_P	Maximum pull-over load on pipe in horizontal direction	Z_s	Section modulus of the steel pipe
f_T	Annual trawling frequency per relevant pipeline section	α_h	Maximum allowed yield to tensile ratio
F_T	Characteristic pull-over load	α_{gw}	Girth weld factor
F_Z	Maximum pull-over load on pipe in vertical direction	α_t	Coefficient thermal expansion
H	Residual lay tension	α_U	Material strength factor
I	Second moment of area	δ_p	Displacement of the pipe at the point of interaction
k_b	Trawl gear bending board stiffness	ΔT	Temperature difference
k_i	Trawl gear in plane stiffness	ϵ_{endcap}	Strain due to end cap effect
M_b	Bending moment	$\epsilon_{poisson}$	Strain due to <i>Poisson's</i> effect
N_a	Axial force	ϵ_t	Thermal strain
P_e	External pressure	γ_ϵ	Strain resistance factor
P_i	Internal pressure	γ_m	Material resistance factor
S	Effective axial force	γ_{sc}	Safety class resistance factor

μ_a	Coefficient of axial soil friction	σ_{lc}	Longitudinal stress due to end cap effect
μ_l	Coefficient of lateral soil friction	σ_{lh}	Longitudinal stress due to <i>Poisson's</i> Effect
σ_h	Hoop stress	σ_{lt}	Longitudinal stress due to temperature difference
σ_l	Longitudinal stress	ν	Poisson's ratio
σ_{la}	Longitudinal stress due to axial stress		
σ_{lb}	Longitudinal stress due to bending moment		

Table of Content

Abstract	i
Acknowledgement	ii
Nomenclature	iii
Table of Content	v
Table of Tables	viii
Table of Figures	ix
Chapter 1 Introduction	1
1.1. General.....	1
1.2. State of The Art	2
1.2.1. Lateral Buckling	2
1.2.2. Trawling Gears	4
1.3. Study Objectives	6
Chapter 2 Theoretical Background	8
2.1. General.....	8
2.2. Stresses in Pipeline.....	8
2.2.1. Hoop Stress (σ_h)	8
2.2.2. Longitudinal Stress (σ_l).....	8
2.2.3. Combined Stress (σ_c).....	10
2.3. Hydrodynamic loads.....	11
2.4. Pipeline Expansion.....	11
2.4.1. Thermal Strain ($\epsilon_{\text{thermal}}$)	11
2.4.2. Pressure Strain ($\epsilon_{\text{pressure}}$).....	11
2.4.3. Combined Strain (ϵ_{total}).....	12
2.4.4. Restraining/Anchor Force	12
2.4.5. Soil Frictional Resistance Force	13
2.4.6. Pipeline End Expansion.....	13
2.5. Lateral Buckling.....	14
2.5.1. Buckle Modes	14
2.5.2. Feed-in Zone	15

2.5.3.	Lateral Imperfection	15
2.5.4.	Hobbs' Analytical Method	16
2.6.	Pull-Over Analysis	17
2.6.1.	Trawl Boards and Beam Trawls Pull-Over Loads	18
2.6.2.	Clump Weight Pull-Over Loads	19
2.6.3.	Pull-Over Durations	20
2.7.	DNV Combined Loading Criteria	21
Chapter 3	Methodology	23
3.1.	General.....	23
3.2.	Preparation Works.....	23
3.2.1.	Pipeline End Expansion.....	23
3.2.2.	Hobbs' Critical Buckling Force.....	23
3.2.3.	Pull-Over Forces and Duration	24
3.3.	Finite Element Model.....	24
3.3.1.	Pipeline Model	24
3.3.2.	Seabed Model.....	26
3.3.3.	Initial Imperfection.....	27
3.3.4.	Soil Friction	27
3.3.5.	Pull-over loads	27
3.4.	Load Cases	28
3.5.	Finite Element Analysis	29
3.5.1.	Initial Condition Step.....	29
3.5.2.	Pull-over Analysis	30
Chapter 4	Case Study	31
4.1.	General.....	31
4.2.	Pipeline Parameter	31
4.3.	Pipe Material Yield Stress	32
4.4.	Operating Data	33
4.5.	Environmental Data	33
4.6.	Soil Data	33
4.7.	Trawl Gear Parameter	33
4.8.	Pull-over Loads and Durations	34
4.9.	Displacement Controlled Condition	36
4.9.1.	Safety Factors.....	36
4.9.2.	Load Combinations and Load Effect Factors	37

Chapter 5	Results & Discussion	38
5.1.	Model Validation	38
5.2.	Effective Axial Force	38
5.3.	Hobbs's Critical Buckling Limiting Load	39
5.4.	Trawl Boards Pull-Over Analysis Results	40
5.4.1.	Lateral Displacement	40
5.4.2.	Axial Displacement	45
5.4.3.	Bending Moments	49
5.4.4.	Effective Axial Force	53
5.4.5.	Equivalent Strain	56
5.5.	Discussion	59
5.5.1.	During Pull-over Loads Duration (t: 2.0s – 2.9s)	59
5.5.2.	After Pull-over Loads Duration (t: 3.0s-8.0s)	60
5.5.3.	Buckle Amplitude	61
5.5.4.	Lateral Soil Friction	62
5.5.5.	Bending Moments	63
5.5.6.	Equivalent Strain	64
5.5.7.	DNV Displacement Controlled Checked	65
Chapter 6	Conclusion and Further Works	66
6.1.	Summary	66
6.2.	Conclusion	67
6.3.	Further Works	67
References		xii
Appendix A	Preparation Works	
Appendix A-1	Pipeline End Expansion	
Appendix A-2	Hobbs' Critical Buckling	
Appendix A-3	Pull-over Forces and Durations	
Appendix B	Finite Element Analysis- ANSYS Script	
Appendix C	FE Analysis Result Graphs	
Appendix D	DNV Displacement Controlled Condition Code Check	

Table of Tables

Table 2 - 1 Hobbs' Lateral Buckling Coefficient	16
Table 2 - 2 Trawl Pull-over loads Characteristic [2]	17
Table 3 - 1 Scenarios of lateral soil resistance and trawl pull-over loads	28
Table 3 - 2 Initial Condition Time Steps	29
Table 3 - 3 Trawl Gear Pull-over Analysis Time Steps	30
Table 4 - 1 Pipe Design Data and Material Properties	31
Table 4 - 2 Coating Parameter	31
Table 4 - 3 Stress-Strain Data	32
Table 4 - 4 Operating Parameters	33
Table 4 - 5 Environmental Data	33
Table 4 - 6 Friction Factors	33
Table 4 - 7 Trawl Gears Data [3]	34
Table 4 - 8 Pull-over Horizontal and Vertical Loads and Durations	34
Table 4 - 9 Safety factors	36
Table 4 - 10 Load combinations and load effect factors	37
Table 5 - 1 Pipeline End Expansion	38
Table 5 - 2 Friction Force and Axial Restrained Force	38
Table 5 - 3 Hobbs's Critical Buckling Force	39
Table 5 - 4 Pipeline lateral (Z-direction) displacement during pull-over loads	42
Table 5 - 5 Pipeline lateral (Z-direction) displacement after pull-over loads duration	44
Table 5 - 6 Pipeline axial (X-direction) displacement During Pull-Over Load	47
Table 5 - 7 Pipeline axial (X-direction) displacement after pull-over loads duration	49
Table 5 - 8 Pipeline bending moments during pull-over loads duration	51
Table 5 - 9 Pipeline bending moments after pull-over loads duration	53
Table 5 - 10 Equivalent strain during pull-over loads duration	57
Table 5 - 11 Pipeline equivalent strain after pull-over loads duration	59
Table 5 - 12 Summary of maximum lateral displacement	60
Table 5 - 13 Summary of maximum bending moments, equivalent strain and DNV code check	64

Table of Figures

Figure 1 - 1 Typical Deepwater Field Layout – Shell St. Malo fields, Gulf of Mexico [19]	1
Figure 1 - 2 Thyborøn Trawl Door Pairs Cross on Pipeline [16]	2
Figure 1 - 3 Lateral Buckle from seabed side scan survey [13]	2
Figure 1 - 4 Snake Lay Configuration[10]	3
Figure 1 - 5 Typical Mid-line Expansion Spool [10]	3
Figure 1 - 6 Vertical Trigger/Sleeper [10]	4
Figure 1 - 7 Illustration of Fishing Activity using Trawl Gears [18].	4
Figure 1 - 8 Typical Beam Trawl Shoe [3].	5
Figure 1 - 9 Beam Trawl and Components [22].	5
Figure 1 - 10 Polyvalent and Rectangular Trawl Boards [22].	5
Figure 1 - 11 Steel V-board [22]	6
Figure 1 - 12 Typical Clump Weight [22].	6
Figure 2 - 1 Stresses due to internal pressure in thin-wall pipes [5].	9
Figure 2 - 2 Longitudinal stress components [5].	10
Figure 2 - 3 Typical Effective Axial Force Diagrams [7]	13
Figure 2 - 4 Lateral Buckling Modes [9]	14
Figure 2 - 5 Buckle Region [10]	15
Figure 2 - 6 Feed –in to a Single Buckle in an Infinite Pipeline [11]	15
Figure 2 - 7 Pipeline – Trawl Gears Interaction Laboratorial Model [15]	17
Figure 2 - 8 Typical clump weight (roller type) [3].	19
Figure 2 - 9 Clump weight (roller type) interaction with pipeline [3]	20
Figure 2 - 10 Force-time history for trawl boards pull-over forces [3].	20
Figure 2 - 11 Force-time history for beam trawls pull-over forces [3].	21
Figure 2 - 12 Force-time history for roller type clump weight pull-over forces [3]	21
Figure 3 - 1 PIPE288 Geometry [14]	24
Figure 3 - 2 Pipe element using PIPE288 in ANSYS.	25
Figure 3 - 3 Pipeline Model in ANSYS	25
Figure 3 - 4 TARGE170 Geometry [14]	26
Figure 3 - 5 TARGE170 Segment Types [14]	26
Figure 3 - 6 Pull-over Forces on Pipeline	27
Figure 3 - 7 Combined lateral soil resistance and trawl load matrix [2].	28

Figure 4 - 1 Pipe Material Yield Stress De-Rating [1]	32
Figure 4 - 2 Steel Pipe Stress-Strain Curve	32
Figure 4 - 3 C_h coefficient for effect of span height on impact velocity [3]	34
Figure 4 - 4 Polyvalent & rectangular pull-over force-time history	35
Figure 4 - 5 Industrial v-board pull-over force-time history	35
Figure 4 - 6 Beam trawl pull-over force-time history	36
Figure 5 - 1 Hobbs's Buckle Length Vs Axial force for each buckle modes for lateral soil friction of 0.7	39
Figure 5 - 2 Lateral displacement during pull-over loads duration (t:2.0-2.9s)	40
Figure 5 - 3 Lateral displacement during pull-over loads duration (t:2.0-2.9s) for load case 5.	41
Figure 5 - 4 Lateral displacement after pull-over loads duration (t:3.0-8.0s)	43
Figure 5 - 5 Lateral displacement after pull-over loads duration (t:3.0-8.0s) for load case 5.	44
Figure 5 - 6 Axial displacement during pull-over loads duration (t:2.0-2.9s)	45
Figure 5 - 7 Axial displacement during pull-over loads duration (t:2.0-2.9s) for load case 5.	46
Figure 5 - 8 Axial displacement after pull-over loads duration (t:3.0-8.0s)	48
Figure 5 - 9 Axial displacement after pull-over load duration (t:3.0-8.0s) for load case 5.	49
Figure 5 - 10 Bending moments during pull-over loads duration (t:2.0-2.9s)	50
Figure 5 - 11 Bending moments after pull-over loads duration (t:3.0-8.0s)	52
Figure 5 - 12 Effective axial force during pull-over loads durations (t:2.0-2.9s)	54
Figure 5 - 13 Effective axial force after pull-over loads duration (t:3.0-8.0s)	55
Figure 5 - 14 Equivalent strain during pull-over loads duration (t:2.0-2.9s)	56
Figure 5 - 15 Equivalent strain after pull-over loads duration (t:3.0-8.0s)	58
Figure 5 - 16 FEA result: pipeline lateral buckling profile for load case 1	59
Figure 5 - 17 Pipeline maximum lateral displacement from time 2.0s to 8.0s	61
Figure 5 - 18 Pipeline lateral displacement at buckle region from time 2.5 to 4.5s for load case 1.	61
Figure C - 1 Axial displacement during pull-over loads duration (t:2.0-2.9s) for load case 2	C-3
Figure C - 2 Axial displacement during pull-over loads duration (t:2.0-2.9s) for load case 3	C-3
Figure C - 3 Axial displacement during pull-over loads duration (t:2.0-2.9s) for load case 6	C-4
Figure C - 4 Axial displacement after pull-over loads duration (t:3.0-8.0s) for load case 2	C-4
Figure C - 5 Axial displacement after pull-over loads duration (t:3.0-8.0s) for load case 3	C-5
Figure C - 6 Axial displacement after pull-over loads duration (t:3.0-8.0s) for load case 6	C-5
Figure C - 7 Lateral displacement during pull-over loads duration (t:2.0-2.9s) for load case 2	C-7
Figure C - 8 Lateral displacement during pull-over loads duration (t:2.0-2.9s) for load case 3	C-7
Figure C - 9 Lateral displacement during pull-over loads duration (t:2.0-2.9s) for load case 6	C-8
Figure C - 10 Lateral displacement after pull-over loads duration (t:3.0-8.0s) for load case 2	C-8

Figure C - 11 Lateral displacement after pull-over loads duration (t:3.0-8.0s) for load case 3	C-9
Figure C - 12 Lateral displacement after pull-over loads duration (t:3.0-8.0s) for load case 6	C-9
Figure C - 13 Bending moments during pull-over loads duration (t:2.0-2.9s) for load case 2	C-11
Figure C - 14 Bending moments during pull-over loads duration (t:2.0-2.9s) for load case 3	C-11
Figure C - 15 Bending moments during pull-over loads duration (t:2.0-2.9s) for load case 6	C-12
Figure C - 16 Bending moments after pull-over loads duration (t:3.0-8.0s) for load case 2	C-12
Figure C - 17 Bending moments after pull-over loads duration (t:3.0-8.0s) for load case 3	C-13
Figure C - 18 Bending moments after pull-over loads duration (t:3.0-8.0s) for load case 6	C-13
Figure C - 19 Effective axial force during pull-over loads durations (t:2.0-2.9s) for load case 2	C-15
Figure C - 20 Effective axial force during pull-over loads durations (t:2.0-2.9s) for load case 3	C-15
Figure C - 21 Effective axial force during pull-over loads durations (t:2.0-2.9s) for load case 6	C-16
Figure C - 22 Effective axial force after pull-over loads duration (t:3.0-8.0s) for load case 2	C-16
Figure C - 23 Effective axial force after pull-over loads duration (t:3.0-8.0s) for load case 3	C-17
Figure C - 24 Effective axial force after pull-over loads duration (t:3.0-8.0s) for load case 6	C-17
Figure C - 25 Equivalent strain during pull-over loads duration (t:2.0-2.9s) for load case 2	C-19
Figure C - 26 Equivalent strain during pull-over loads duration (t:2.0-2.9s) for load case 3	C-19
Figure C - 27 Equivalent strain during pull-over loads duration (t:2.0-2.9s) for load case 6	C-20
Figure C - 28 Equivalent strain after pull-over loads duration (t:3.0-8.0s) for load case 2	C-20
Figure C - 29 Equivalent strain after pull-over loads duration (t:3.0-8.0s) for load case 3	C-21
Figure C - 30 Equivalent strain after pull-over loads duration (t:3.0-8.0s) for load case 6	C-21

Chapter 1 Introduction

1.1. General

In many part of the world, oil and gas industry has increased significantly and has expanded into deeper water. As one of the key point facilities, pipeline must also improve in order to cope the technology with the trend.

Deepwater pipeline has to face very challenging parameters from both environment and operational condition, e.g. higher operating pressure, higher operating temperature, and also higher hydrostatic pressure. Thus, pipeline operation in deeper waters puts high requirement. The high pressure and elevated temperature of the reservoirs, the high ambient external pressure and extremely cold external temperature, the large force involved in the installation phase, and the hostility of the surrounding environment can result in a large number of limit states that must be addressed.

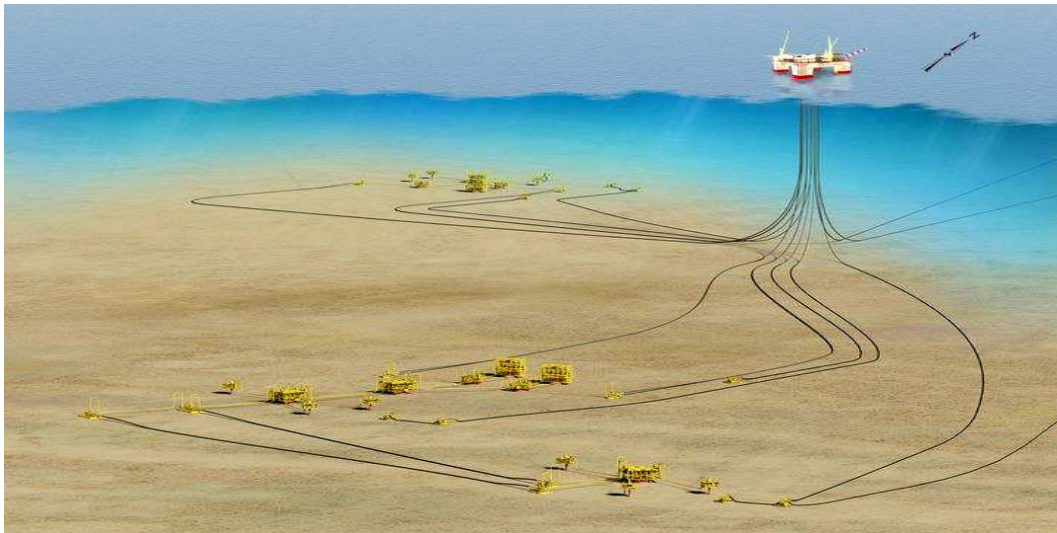


Figure 1 - 1 Typical Deepwater Field Layout – Shell St. Malo fields, Gulf of Mexico [19]

Pipeline with higher operational temperature compared to the surrounding environment tend to expand due to thermal and pressure loading. If the pipeline is constrained, either partially or fully, a compressive axial force will develop in the pipeline. The magnitude of this compressive force depends on the extent of constraint applied to oppose the expansion. Combining these factors, deepwater pipeline are very critical against lateral and vertical buckling cases.

Those situations are quite dangerous especially in area supporting major commercial fishing industry activities e.g. North Sea in Norway and Atlantic Margin in UK. Fishing activities such as bottom trawling, poses a number of engineering problems [12]. Equipment used for bottom trawling can expose a pipeline to substantial loads that may damage the pipeline. Such load is associated with the instantaneous impact and the subsequent pull-over load as the trawl gear hits and drags over the pipeline [3].

On average an area equivalent to 48% of the North Sea is disturbed annually by beam trawling, one type of fishing gears. It is concentrated in the South, reaching 54% off the English coast, 112% in the central southern North Sea (some areas are hit more than once), 153% off the Danish coast, and a staggering 321% off the Dutch coast [21].

Figure 1 - 1 shows the typical subsea field layout on the development of deepwater area. Several subsea wells or manifolds are tied few kilometers back to the platform or floating facilities. These subsea structures and pipelines are likely to attract the fish. The establishment of fish colonies or populations might also attract fisherman. As the fish colonies grow, the fishing activities also increase. As a consequence, the use of trawl gears more frequent on this area. The fishing trawls are the common method used in the fishing industry recently.

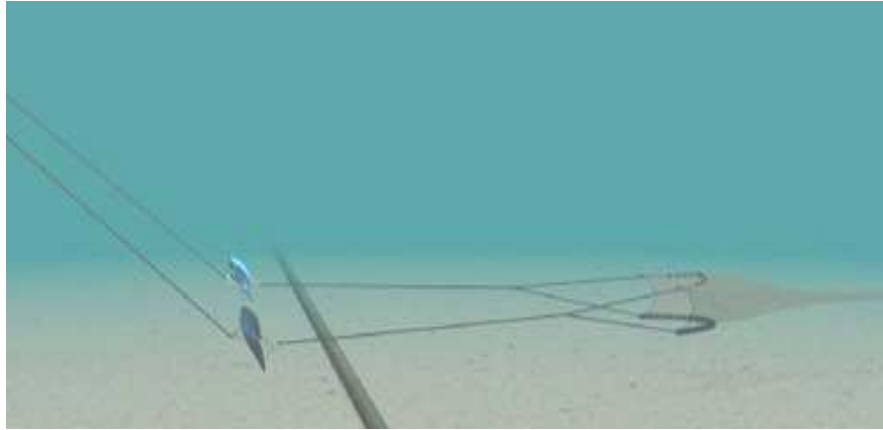


Figure 1 - 2 Thyborøn Trawl Door Pairs Cross on Pipeline [16]

The risk of the pipeline getting hit and dragged over by the trawl gears is increase as the fishing activity near the subsea facilities more frequent. Figure 1 - 2 shows the fishing trawl cross over the pipeline. The trawl gear may hit and dragged over the pipeline as the trawl gear is forced to cross over the pipeline. The pipeline will be subjected to substantial horizontal (lateral) and vertical forces from the trawl gears. These forces will make the pipeline deform locally and globally and may damage it.

1.2. State of The Art

1.2.1. Lateral Buckling

The problem of pipeline buckling had been considered analytically by Hobbs [9] in 1984. Experimental work performed as part of his study has found that pipeline can buckle into different lateral mode shapes. The common types of buckle shapes are presented in section 2.5.1.

Lateral buckling commonly happen on unburied pipeline and takes the form of “snaking” on the seabed. This laterally deformed shape of the pipeline occurs in order to reduce the compression force in the pipeline created by restrained thermal expansion. The magnitude of the compressive force depends on the extent of constrained applied to oppose the expansion [10].

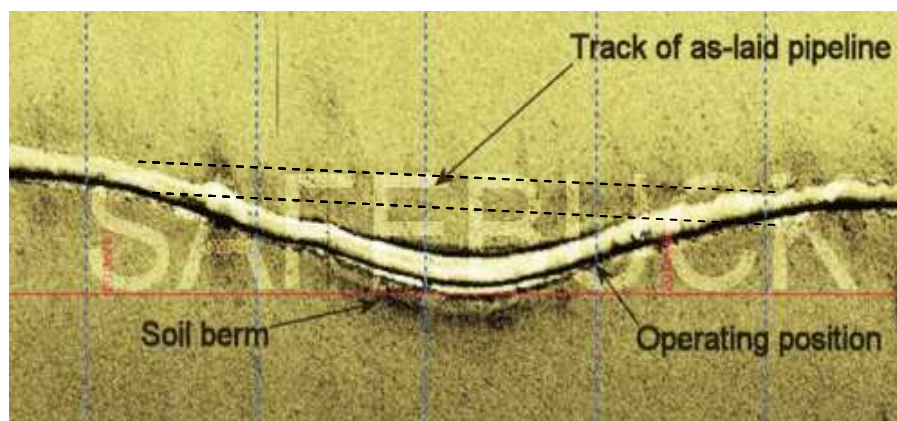


Figure 1 - 3 Lateral Buckle from seabed side scan survey [13]

Generally, submarine pipeline will be trenched and buried to restrain it and prevent buckling. However, in deeper water, trenching and burying is less practical and with the higher operating pressures and temperatures that we often experience in deepwater developments, this solution simply does not work. The pipeline is left on the seabed and allowed to buckle laterally.

Even though lateral buckling can be a safe way to accommodate expansion created by temperature and pressure loads, but detailed analysis should be taken to control the buckles. Uncontrolled lateral buckling can lead to excessive plastic deformation of the pipe or fatigue failure in operation due to continuous heat-up and cool-down cycles [10].

There are several ways to mitigate or accommodate the lateral buckling. Some of them that are commonly used in the industry are [10]:

a) Snake-Lay Configuration

Snake lay configuration is used to introduce horizontal imperfection to the pipeline. The pipeline is laid in the form of curves of given radius of curvature at predetermined location. The crown of the snake then behaves as a large curvature expansion spool while the pitch dictates the amount of pipe feed-in at the crown.

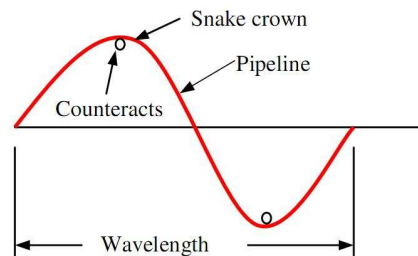


Figure 1 - 4 Snake Lay Configuration [10]

b) Mid-line expansion spools

The spool is modeled in 'U' shape with thermal expansion imposed to both ends of the spool. The expansion spool acts as compression relief points.

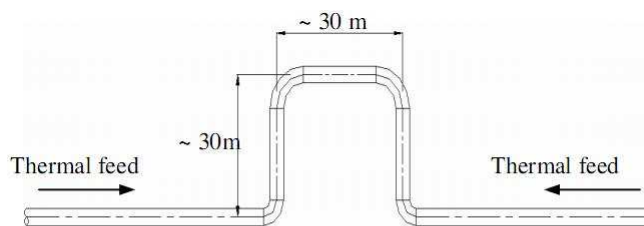


Figure 1 - 5 Typical Mid-line Expansion Spool [10]

c) Vertical triggers/sleepers

To initiate a lateral buckle, the initial vertical out-of-straightness (OSS) is used. A sleeper, pre-laid across the route of the pipeline. The sleeper would rise and support the pipeline off the seabed to create vertical OSS. The elevated pipeline above the sleeper also has benefit of reduction in lateral frictional resistance.

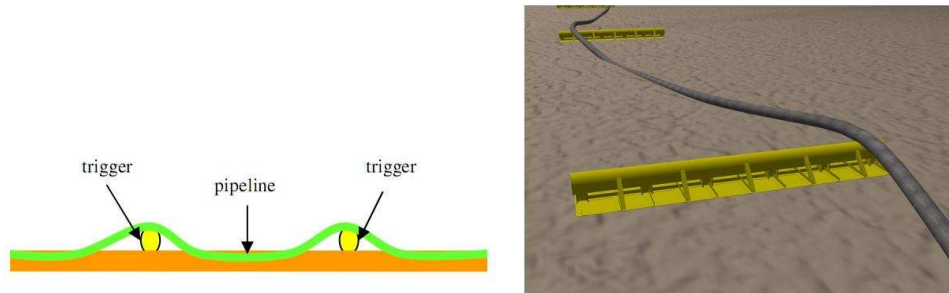


Figure 1 - 6 Vertical Trigger/Sleeper [10]

1.2.2. Trawling Gears

Nowdays, trawling is commonly used in the commercial fishing industry especially in the North Sea and the Norwegian Sea. Figure 1 - 7 shows the illustration of trawling activity. The trawling method is an active fishing technique by pulls a trawl gears through the water behind one or more fishing boats. The trawl nets are dragged along the seabed or in midwater at a specified depth. Two or more trawl nets can be operated simultaneously (double-rig and multi-rig) [20].

The heaviest twin trawls equipment used in the Barents Sea and outside Greenland has typical mass up to 9-10 tonnes based on 2005 data [3]. This equipment may also use in the North Sea and the Norwegian Sea. While, the largest trawl board in the North Sea and the Norwegian Sea has mass about 4000kg in the same year.

There are many variants of trawling gears. The local traditions, bottom sea conditions and the capacity and size of trawling boats are governing the variation of trawling gears [20]. The main trawl gears commonly use in the North Sea and the Norwegian Sea are conventional otter trawl gear and beam trawl gear [3]. The otter trawls use trawl boards to keep open the trawl net. While, the beam trawl use transverse beams.

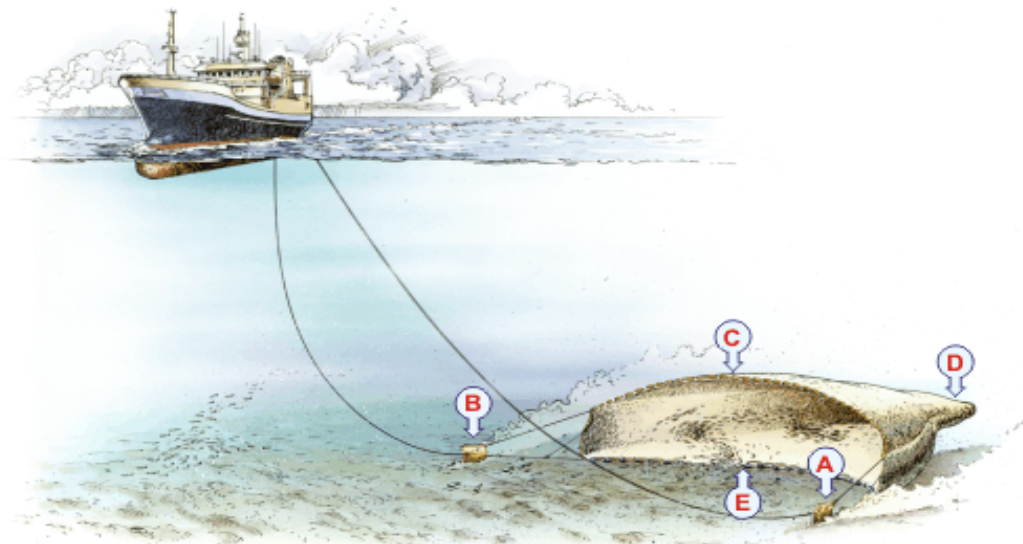


Figure 1 - 7 Illustration of Fishing Activity using Trawl Gears [18].

Beam trawl is the simplest of trawls. The transverse beam which is made by steel or wood, keeps a funnel shaped trawl net open. The transverse beam is mounted on steel blades called shoes or on heavy rubber wheels [17]. The outriggers or booms are used to tow the trawl. These outriggers are fastened to, or at the foot of the mast and extend out over the sides of the vessel during fishing operations. The beam

trawling method uses a very strong outrigger boom in each side. Each outrigger boom tows a beam trawl [20]. Beam trawls mainly used on sandy flat seabed in the Southern North Sea.

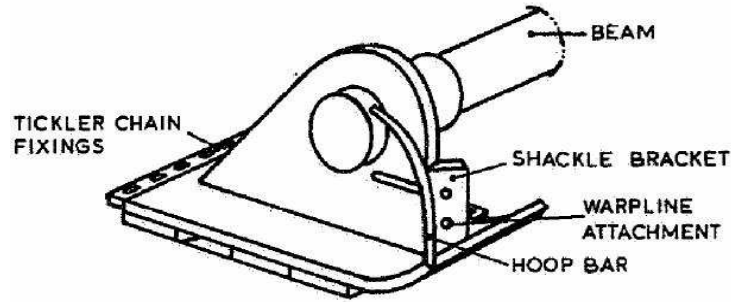


Figure 1 - 8 Typical Beam Trawl Shoe [3].

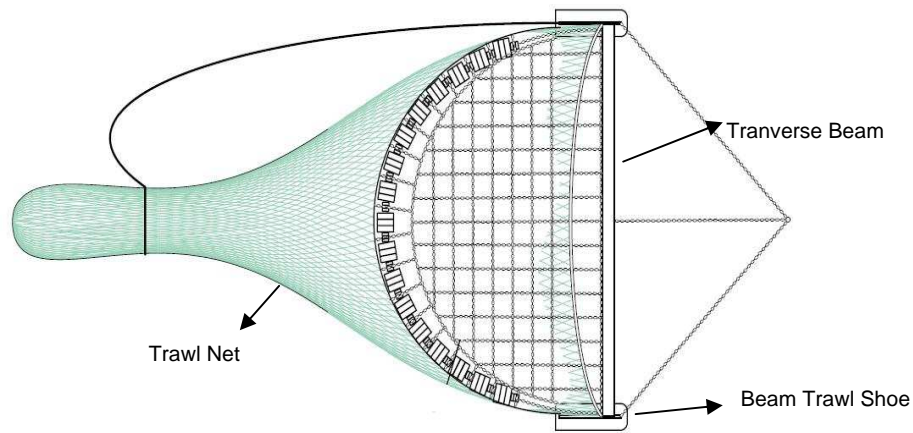


Figure 1 - 9 Beam Trawl and Components [22].

The otter trawl has several types of trawls boards. The trawl boards are shown as point A and B in Figure 1 - 7. The size of the trawl board depends on the type of the trawl net being used. The common types of trawl boards based on DNV RP F111 [3] are:

a) Polyvalent and Rectangular trawl board

The polyvalent and rectangular trawl boards have a curved surface with an oval shape. This construction of the trawl boards improves the ability to slide over the obstacles. The complex geometry of these trawl gear type cause high costs to fabricate. These types of trawl board have been found to give the highest loads on pipeline [3]. Figure 1 - 10 shows those two typical trawl boards.

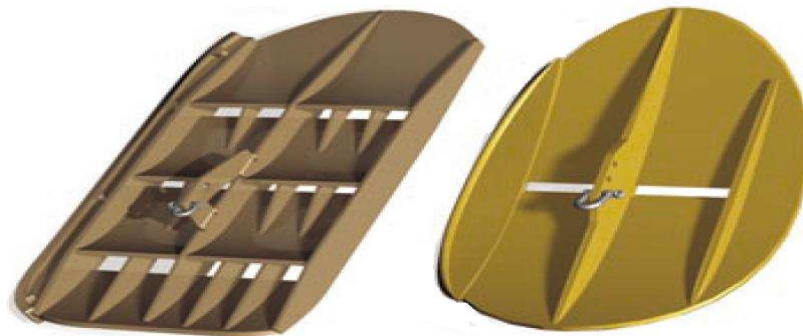


Figure 1 - 10 Polyvalent and Rectangular Trawl Boards [22].

b) V-shaped board

V-shape board has a knuckle line in the longitudinal direction. This knuckle line gives different attack lines of the hydrodynamic lift forces on the upper and lower part. This type of trawl gear is easy to use and maintain. The V-board also has good ability on spreading the trawl net [22].



Figure 1 - 11 Steel V-board [22]

The other type of trawling is twin rig trawling. The twin rig trawling used two set of nets side by side and a clump weight. The clump weight is a heavy weight that designed to roll rather than be dragged along the sea bottom [22]. The clump weight can consist of short lengths of chain cables shackled together or custom made device. There are two common types of clump weight i.e. bobbin type and roller type.



Figure 1 - 12 Typical Clump Weight [22].

1.3. Study Objectives

Most of the deepwater subsea pipelines are laid directly on the seabed without a concrete weight coating depending on the pipeline on-bottom stability. In combination also with the lower resistance provided by the soil on the seabed, the restrained high temperature/high pressure subsea pipeline is susceptible to movement in lateral direction as a result of temperature and pressure driven loads.

In some area, such as in North Sea, unburied pipelines, even temporarily, can be subjected to frequent crossing of bottom trawl/fishing gears. Hence, these unburied pipelines are susceptible to the combined effect of lateral buckling and trawling/fishing gear interaction under operating conditions. The trawl gears normally hit and drag over the pipeline on the seabed and giving it a short impact. In some cases, the trawl gears may actually get hooked under the pipeline and move it along with the trawl equipment, leading to a very severe loading situation.

The objectives of this thesis work is to study and understand the relevant pipeline global response as a result of trawl gear pull-over loads on high temperature/high pressure subsea pipelines. The interaction between pipeline and trawl gears highly susceptible to lateral buckling. The trawl gears pull-over loads induce substantial horizontal (lateral) and vertical force on pipeline. The pipeline may deform globally and trigger lateral buckling during pull-over loads duration. The pipeline also may continue to expand and buckle further after pull-over loads duration.

To be able study and understand the global response of the pipeline under the trawl gears pull-over loading condition, a finite element analysis is carried out. The analysis is carried out using general finite element analysis software ANSYS v13 based on DNV OS F101 [1], DNV RP F110 [2], DNV RP F111 [3] and Subsea 7 Lateral Buckling Analysis Design Guideline [7].

Chapter 2 Theoretical Background

2.1. General

The following chapter covers the theoretical backgrounds for the areas that need to be considered when carrying out the analysis. Most important subjects related to the analysis are the temperature and pressure loading on the pipeline. This section also gives brief explanation on lateral buckling phenomenon, i.e. buckle modes and forces.

The trawl gears pull-over loads are also important in this analysis. The formulae used to calculate the pull-over loads are described in this chapter.

2.2. Stresses in Pipeline

2.2.1. Hoop Stress (σ_h)

The pipe is assumed as thin-wall pipe since the ratio of D/t is greater than 20 from [5]. If the internal pressure, P , exist, the action of radial force distributed around the circumference will produce a circumferential or hoop stress, σ_h , given by:

$$\sigma_h = \frac{PD}{2t}$$

where: σ_h = hoop stress
 D = internal diameter
 T = wall thickness
 P = net internal pressure

For deeper water pipeline, the effect of external pressure should be also considered. Hence, the equation for hoop stress is [5]:

$$\sigma_h = (P_i - P_e) \frac{D}{2t}$$

where: D = nominal outside diameter of the pipe
 P_e = external pressure

2.2.2. Longitudinal Stress (σ_l)

The longitudinal stress (σ_l), is defined as the axial stress experienced by the pipe wall. The longitudinal stress, consists of stresses due to end cap effect (σ_{lc}), hoop stress (Poisson's effect) (σ_{lh}), bending stress (σ_{lb}), axial stress (σ_{la}) and thermal stress (σ_{lt}) [7].

a) End Cap Effect (σ_{lc})

From [5], the longitudinal stress due to end cap effect (σ_{lc}) is calculated as follow:

$$\sigma_{lc} = \frac{PD}{4t}$$

where: σ_l = longitudinal stress
 D = internal diameter
 t = wall thickness
 P = net internal pressure

b) Hoop Stress (Poisson's Effect) (σ_{lh})

The longitudinal stress due to hoop stress (*Poisson's effect*) (σ_{lh}), is calculated as follow based on [5]:

$$\sigma_{lh} = \nu \cdot \sigma_h$$

where: σ_h = hoop stress
 ν = Poisson's ratio, 0.3 for steel pipe

If the pipe is under restrained condition, the end cap force is countered by the restraining force. Therefore no longitudinal stress from end cap effect will occur. In the other hand, the longitudinal stress due to Poisson's effect will present [6]. The stresses due to internal pressure in thin-wall pipes are illustrated below.

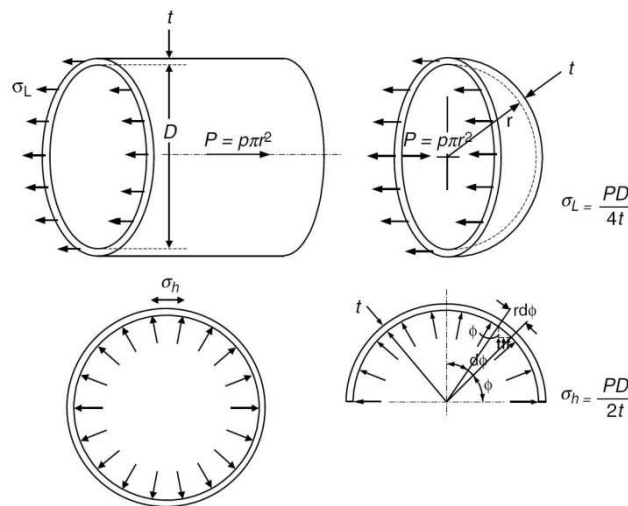


Figure 2 - 1 Stresses due to internal pressure in thin-wall pipes [5].

c) Bending Stress (σ_{lb})

From [6], the longitudinal stress due to bending stress (σ_{lb}) is calculated as follow:

$$\sigma_{lb} = \frac{M_b}{Z_s}$$

where: M_b = bending moment
 Z_s = section modulus of the steel pipe

$$= \frac{\pi(D^4 - D_i^4)}{64(D/2)}$$

d) Axial Stress (σ_{la})

From [6], the longitudinal stress due to axial stress (σ_{la}), is calculated as follow:

$$\sigma_{la} = \frac{N_a}{A_s}$$

where: N_a = axial force

A_s = cross sectional area of the steel pipe, $\frac{\pi}{4}(D^2 - D_i^2)$

e) Thermal Stress (σ_{lt})

In the restrained condition, the prevention of expansion gives rise to the compressive stresses, but the longitudinal strain is zero. The compressive stress, σ_{lt} , generated by the restrained expansion is given by [5]:

$$\sigma_{lt} = -\alpha_t \cdot E \cdot \Delta T$$

where: E = Young's modulus of the steel pipe

The stresses are acting axially. The negative sign on the thermal stress reflects that the pipe is under compressive for a positive temperature increase under restrained conditions.

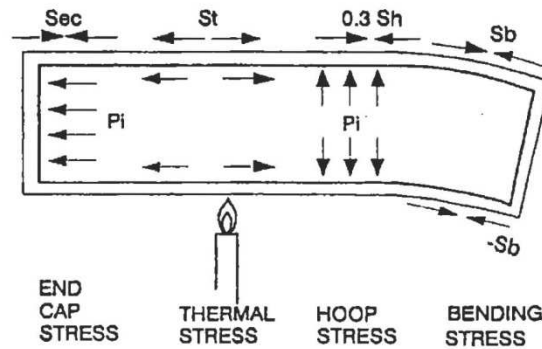


Figure 2 - 2 Longitudinal stress components [5].

f) Total Longitudinal stress

From [5], the total longitudinal stress can be determined using the following equation. It should be ensured that sign conventions are utilized when employing this equation, i.e. tensile stress is positive.

$$\sigma_l = \sigma_{lc} + \sigma_{lh} + \sigma_{lb} + \sigma_{la} + \sigma_{lt}$$

2.2.3. Combined Stress (σ_l)

The combined stress is determined differently depending on the code/standards utilized. The combined stress shall meet the following requirement [3]:

$$\sqrt{\sigma_h^2 + \sigma_l^2} - \sigma_h \sigma_l \leq F_3 \cdot SMYS$$

where: F_3 = Combined stress design factor

2.3. Hydrodynamic loads

The pipeline resting on seabed is subjected to the hydrodynamic forces. The hydrodynamic forces on the seabed are functions of the wave and current climate. The waves can be either locally generated wind waves or swell and the currents can be tidal currents, as e.g. in the southern North Sea, or circulation currents prevalent in some deepwater.

The recommended practice DNV RP F110 [2] recommends that the hydrodynamic forces not to be included in the pull-over analysis. The hydrodynamic forces may reduce the lateral pipe-soil resistance due to lift effects.

2.4. Pipeline Expansion

Pipelines operating at temperature above the ambient temperature will tend to expand, both radially and longitudinally, due to thermal and pressure loading. The pipeline expansion will occur at pipeline ends under unrestrained condition. There are three main reasons contributing to end forces and expansions leading to lateral buckling are temperature (thermal), pressure - end cap effect and pressure - Poisson contraction [6].

2.4.1. Thermal Strain ($\epsilon_{\text{thermal}}$)

In the unrestrained condition, the thermal strain will present due to temperature difference between the maximum operating temperature and the minimum installation temperature. The longitudinal strain is proportional to the magnitude of the temperature difference [5]. The temperature rise causes an expansion due to the thermal strain but the longitudinal thermal stress is zero. The thermal strain, ϵ_t , is given by:

$$\epsilon_t = \alpha_t \cdot \Delta T$$

where: α_t = coefficient thermal expansion (1.17×10^{-5} /deg Celsius)
 ΔT = temperature difference relative to as laid ($^{\circ}\text{C}$)

2.4.2. Pressure Strain ($\epsilon_{\text{pressure}}$)

There are two potential effects on strain due to pressure loads:

a) End Cap Effect

The differential pressure loading across the pipe wall induces axial loadings which contribute to the expansion of the pipeline, i.e. compression. The strain at pipeline due to end cap effect if neglect the external pressure, is [6]:

$$\epsilon_{\text{end cap}} = \frac{P \cdot D}{4t \cdot E}$$

where: P = differential internal pressure across the pipe wall
 D = internal diameter
 t = pipe wall thickness

b) Poisson Effect

The internal pressure induces hoop stress and corresponding circumferential strain. The circumferential expansion/strain gives axial contraction on pipeline. The hoop expansion causes a longitudinal contraction of the pipe, i.e. the pipe expands in the hoop direction and the Poisson effect

results in an axial contraction (opposite to end cap pressure effect). Under unrestrained condition, the expansion/strain due to Poisson effect is [6]:

$$\varepsilon_{poisson} = -\nu \cdot \frac{\sigma_h}{E}$$

where: σ_h = hoop stress
 ν = Poisson's ratio of steel pipe

2.4.3. Combined Strain (ε_{total})

Hence, the combined thermal and pressure strains for unrestrained case is given by [6]:

$$\varepsilon_{total} = \alpha \cdot \Delta T + \frac{\sigma_h}{2} \cdot \frac{(1 - 2\nu)}{E}$$

2.4.4. Restraining/Anchor Force

A pipeline may experience fully restrained. The force required to fully restrain the pipeline is a result of the thermal, end cap and Poisson effect. This force is known also known as the anchor force or restrained axial force, and given by [6]:

$$F_{ax} = A_{steel} \cdot E \cdot \alpha \cdot \Delta T + \frac{P \cdot \pi \cdot D^2}{4} (1 - 2\nu)$$

where: P = Internal pressure difference relative to as laid
 D = internal diameter
 A_{steel} = cross sectional area of the steel pipe
 $= \pi D t$

If the residual lay tension, H from laying operation is taken into account, hence the total restrained axial force, S for a totally restrained pipeline is given by [1]:

$$S = H - F_{ax}$$

$$S = H - \left(A_{steel} \cdot E \cdot \alpha \cdot \Delta T + \frac{P \cdot \pi \cdot D^2}{4} (1 - 2\nu) \right)$$

where: S = effective axial force (negative sign indicates compression, positive sign indicates tensile)
 H = residual lay tension

The effective axial force close to the pipeline end is reduced from maximum of the total restrained axial force due to expansion. The reduction is governed by the axial friction between the pipe and the seabed. If the total axial friction is sufficient to constrain the pipeline fully, it is called a "short" pipeline.

For a sufficiently "long" pipeline, the build-up frictional resistance will exceed the axial force required to fully constrain the pipeline and some part of the pipeline will be fully constrained. The typical effective forces along the pipeline for short and long pipeline are shown below. The equilibrium point where the friction force changes direction and equal to restraining force is known as a virtual anchor point, hence no axial expansion occurs.

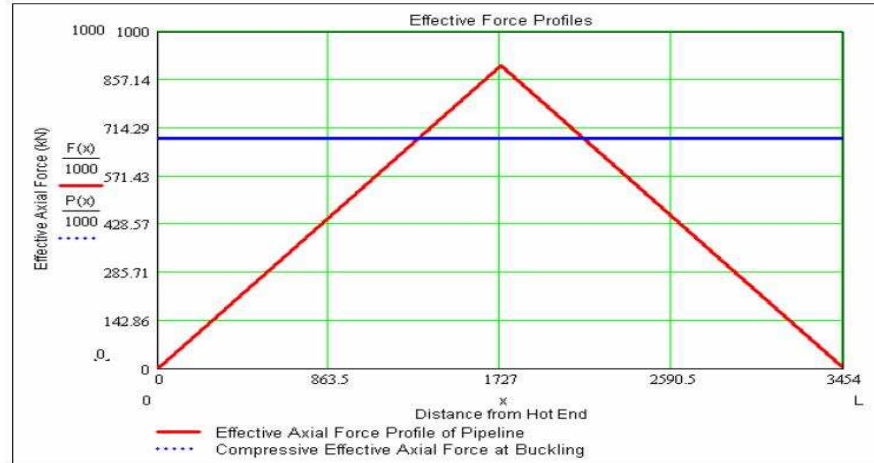


Figure 2 - 3 Typical Effective Axial Force Diagrams [7]

2.4.5. Soil Frictional Resistance Force

Expansion along the pipeline length is restrained by axial friction between the pipe and seabed causing axial compressive forces to develop in the pipeline system. Frictional strain only acts in response to expansion movement. This builds up a compressive strain opposing the net tensile strain effects resulting from temperature and pressure effects. Hence, a high resistance will give higher forces close to the end and potential triggering buckles. The frictional resistance provided by the seabed soil can be calculated based on the operational submerged weight along the pipeline length. This is given by [6]:

$$F_{Fric} = \mu \cdot Ws$$

where: F_{fric} = frictional resistance force
 μ = coefficient of friction between the pipe and seabed
 Ws = pipe submerged weight include the content

This thesis only considers for the pipeline laid on the seabed, hence buried and trenched pipeline are not discussed.

2.4.6. Pipeline End Expansion

The expansion can be calculated by integrating the pipe strain between the free end and the fixed anchor point [8]. Strain in the pipe is due to the difference between the applied axial force and the frictional resistance. Taking an anchor point at the hot end and the cool end of the pipe the following expressions can be derived based on the relationship, $\epsilon = \sigma / E$ [8].

$$\delta_{hot} = \int_{L_{ancpt}(X1)}^{KP_0} \frac{F_{ax}(x) - F_{Fric}(x)}{E \cdot A_{st}} dx$$

$$\delta_{cold} = \int_{KP_{n-1}}^{L_{ancpt}(X2)} \frac{F_{ax}(x) - F_{Fric}(x)}{E \cdot A_{st}} dx$$

where:

$F_{ax}(x)$	= resultant effective axial force
$F_{Fric}(x)$	= friction restraint along full beam
$L_{ancpt}(x1)$	= hot end anchor point (KP)
$L_{ancpt}(x2)$	= cold end anchor point (KP)
KP_0	= pipeline start KP
KP_{n-1}	= end of pipeline KP
δ_{hot}	= hot end expansion
δ_{cold}	= cold end expansion

2.5. Lateral Buckling

The frictional resistance from the interaction between pipe and soil and the flexibility of the pipe end will restrain the expansion along the pipeline. Under restrained condition, a compressive axial force will arise on pipeline. The magnitude of the compressive axial force depends on the extent of constraint applied to oppose the expansion [10]. To release the compressive axial force, the pipe will deform into a new shape and obtain a new equilibrium state by seeking a large deflection. This structural response of the pipeline is called buckling and the amount of load to initiate buckling is the critical buckling load. A buckle of originally straight pipeline is similar to the bending deformation occurring in the elastic (Euler) buckling of a column that loaded axially [9].

The pipeline response under compression depends on the level of the compression developed under the thermal loading. A high effective axial compressive force can cause the pipeline to buckle laterally or vertically. The lateral buckle mode occurs at a lower axial load than vertical mode [9]. Hence, the lateral buckling is dominant unless sufficient lateral resistant is provided by trenching for example.

For pipeline that is exposed on the seabed, lateral buckling will occur naturally at interval along the pipeline if the effective axial compressive force is sufficient for the pipe to buckle. There are several factors govern the lateral buckle to occur, such as pressure and temperature, pipe weight, pipe-soil interaction (frictional resistance), initial imperfection from the lay process due to vessel motion, wave or current loading, imperfection caused by seabed variations and external interference e.g. trawl impact and pull-over.

2.5.1. Buckle Modes

The buckle is considered as a sequence of half-wave. The pipeline can buckle into either symmetric or asymmetric modes, where the symmetric is referred to an axis drawn through the centre of the buckle and perpendicular to the original centerline of the pipeline [11]. Experimental work performed by Hobbs [9] has found that pipeline can buckle into different lateral mode shapes. The most common lateral buckle modes from modes 1 to modes 4 are shown in Figure 2 - 4.

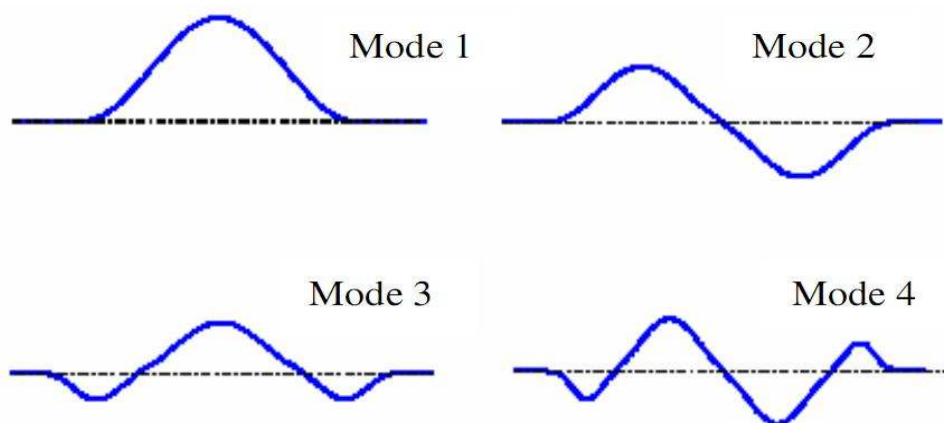


Figure 2 - 4 Lateral Buckling Modes [9]

Figure 2 - 5 shows the regions of a buckle. A buckle region consists of the buckle and two slipping region flank on both sides. The slip region will continue to expand and feed into the buckle as temperature increase further after the buckle has developed. The available frictional resistance to oppose the feed in will determine the slip region length.

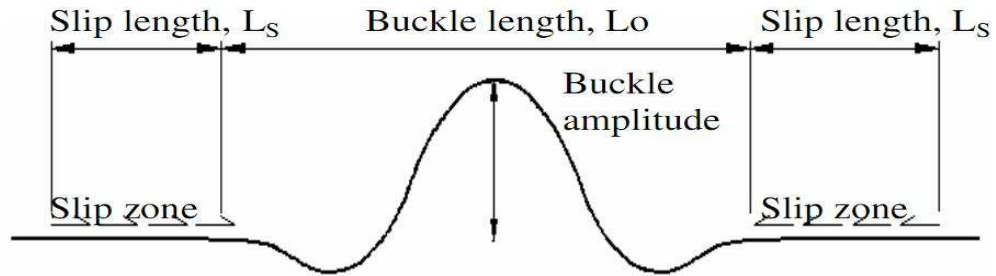


Figure 2 - 5 Buckle Region [10]

2.5.2. Feed-in Zone

The formation of a buckle involves the movement of the pipe. The total length of pipe over the half-waves of the buckle is greater than length of the initial straight pipe over the same section [11]. The formation of the buckle also leads to new distribution of axial force of the pipeline. The illustration of axial feed-in movement is illustrated in Figure 2 - 6.

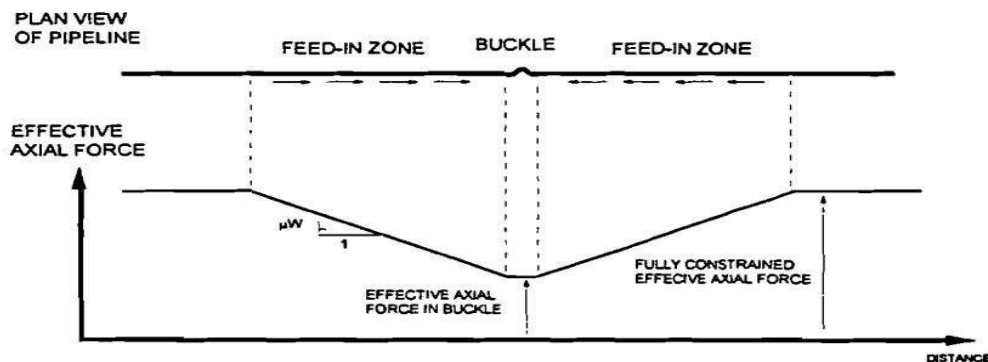


Figure 2 - 6 Feed -in to a Single Buckle in an Infinite Pipeline [11]

Figure 2 - 6 shows, the effective axial forces at the feed-in zone are higher than at the buckle region. These effective axial forces are compressive forces induce by pipeline expansion due to the temperature and pressure load. These compressive axial forces will feed into the buckle and push the pipeline to expand and buckle further more.

2.5.3. Lateral Imperfection

Lateral imperfection or also know as out-of-straightness (OOS) has a significant effect on the critical force at which the buckling first occur as shown by Andrew Palmer and associates shown in his paper [8]. The lateral imperfection and the corresponding wavelength are key factors in the prediction of the onset of lateral buckling of the pipeline [7]. The lateral imperfections are introduced in the pipeline due to the pipe-lay vessel sway motion during the installation process and due to seabed irregularities. Depending on the pipe-lay tension and lateral soil friction coefficient, the pipeline will tend to move laterally on the seabed as the installation proceeds.

The lateral imperfection or OOS also may induced by external interference such as by trawl gears. Trawl gears may hit and skid over the pipeline and create an out-of-straightness on the pipeline as the trawl gear is pulled or forced to cross over the pipeline. This will usually give a global response of the pipeline.

2.5.4. Hobbs' Analytical Method

The pipeline may buckle into a number of different alternative post-buckled shapes as discussed in section 2.5.1. Each mode requires a different minimum axial force for the onset of lateral buckling. The analytical method of Hobbs [7] [9] is used to predict the critical buckling force for a given buckle modes.

The theory is based on force equilibrium and displacement compatibility after a lateral buckle has formed in a theoretically straight pipe. The pipeline is assumed as a beam-column under axial load with uniform lateral support. The linear differential equation of the buckled portion is solved for the deflected shape [7]. The pipe material is assumed to remain elastic and no initial imperfections is considered. The method is also restricted to small rotations.

The analytical method of Hobbs [9] traces the equilibrium path in terms of buckle length and fully restrained axial force. The relationship between effective axial force and buckle length is given by [7][9]:

$$P_0 = P + k_3 \mu_a WL \left[\sqrt{\left(1 + k_2 \frac{E \cdot A \cdot \mu_l^2 \cdot WL^5}{\mu_a (EI)^2} \right)} - 1 \right]$$

- Where: P_0 = post-buckle axial force
 μ_a = coefficient of axial friction
 μ_l = coefficient of lateral friction
 W = submerged weight of the pipeline
 A = steel area
 I = second moment of area
 L = buckle length corresponding to P_0

The effective compressive axial force within the buckle, P , is given by [7]: $P = k_1 \frac{EI}{L^2}$

And, the maximum corresponding buckle amplitude, y , is given by [7]: $y = k_4 \frac{\mu_l W}{EI} L^4$

The maximum bending moment, M , is calculated from [7]: $M = k_5 \mu_l WL^2$

Table 2 – 1 lists the coefficient k_1 - k_5 for the fundamental modes [9].

Table 2 - 1 Hobbs' Lateral Buckling Coefficient

Mode	k_1	k_2	k_3	k_4	k_5
1	80.76	6.391×10^{-5}	0.500	2.407×10^{-3}	0.06938
2	$4\pi^2$	1.743×10^{-4}	1.000	5.532×10^{-3}	0.1088
3	34.06	1.668×10^{-4}	1.294	1.032×10^{-2}	0.1434
4	28.20	2.144×10^{-4}	1.608	1.047×10^{-2}	0.1483
$5(\infty)$	$4\pi^2$	4.705×10^{-5}	4.705×10^{-5}	4.4495×10^{-3}	0.05066

2.6. Pull-Over Analysis

The trawl gear for some reason is completely stop and pulled or forced to cross the pipe. shows the experimental of pull-over load in the laboratories. The pipeline will be subjected to substantial horizontal (lateral) and vertical forces. The global response of the pipeline will be analyzed. The analysis will be based on the DNV OS F101 [1], DNV RP F110 [2] and DNV RP F111 [3]. The most critical position for trawl pull-over depends on [3]:

- Length, height and shoulder support of free spans,
- Effective axial force,
- Lateral curvature of the pipeline, and
- Lateral or axial support or restraint.



Figure 2 - 7 Pipeline – Trawl Gears Interaction Laboratorial Model [15]

The pull-over analysis is carried out using finite element analysis software, ANSYS v13. The finite element analysis use non-linear transient analysis type to analyze the pull-over load on pipeline. All relevant non-linear effects shall also be taken into account in the finite element analysis of trawl gear pull-over. The non-linear effects may include non-linear material behavior, soil resistance, large displacement including geometrical stiffness, and buckling effects caused by effective axial force [3].

The trawl pull-over load (F_T) depends on the trawl frequency (f_T) and trawl boards type among other parameters. In this thesis work, the trawling frequency is assumed between 10^{-4} to 1 annually. Table 2 - 2 is applied to define the trawl pull-over loads characteristic [2] and used to evaluate the triggering of a pipe to buckle.

Table 2 - 2 Trawl Pull-over loads Characteristic [2]

Pull-over load	Trawling Frequency
	$10^{-4} < f_T < 1$
F_T^{UB}	$1.0 F_p$
F_T^{BE}	$0.8 F_p$
F_T^{LB}	$0.3 F_p$

Different types of trawl gears have a different distribution of pull-over forces horizontally and vertically. The duration of pull-over loads are also different from type to type of trawl gears. The following section will present the horizontal and vertical pull-over forces applied on the pipeline and also the duration with respect to the trawl gear types.

2.6.1. Trawl Boards and Beam Trawls Pull-Over Loads

The pull-over loads from trawl boards shall be applied as a single point load or concentrated load horizontally and vertically as long as its pull-over duration [3]. The beam trawl pull-over loads may be applied as two concentrated forces at a distance equal to the width of the trawl beam. Each concentrated force apply half of the pull-over loads. The maximum forces for these types of trawl gears can be calculated as follow as recommended in [3]:

a) Maximum Horizontal Loads

The maximum horizontal force applied to the pipe, F_p , is given as follow:

- For trawl board: $F_p = C_F \cdot V(m_t \cdot k_w)^{1/2}$
- For beam trawls: $F_p = C_F \cdot V[(m_t + m_a)k_w]^{1/2}$

Where k_w = warp line stiffness

V = trawling velocity

m_t = board or beam with shoes steel mass

m_a = hydrodynamic added mass and mass of entrained water.

The empirical coefficient, C_F , for trawl board is a function of trawl gear type and some geometrical parameters characterizing the trawl-pipeline interaction.

- For polyvalent and rectangular boards:

$$C_F = 8.0 \cdot (1 - e^{-0.8 \cdot \bar{H}})$$

- For V-shaped boards:

$$C_F = 5.8 \cdot (1 - e^{-1.1 \cdot \bar{H}})$$

Here, \bar{H} is a dimensionless height:

$$\bar{H} = \frac{H_{sp} + \frac{OD}{2} + 0.2}{B}$$

Where H_{sp} = span height

B = half of the trawl board height

Meanwhile, the beam trawls is assumed without hoop bars as recommend by DNV RP F111 [3] if the detail information is not available. Hence, the empirical coefficient, C_F , for beam trawls is defined as:

$$C_F = \begin{cases} 5.0 & OD/H_a < 2 \\ 8.0 - 1.5OD/H_a & \text{for } 2 < OD/H_a < 3 \\ 3.5 & OD/H_a > 3 \end{cases}$$

Where H_a = attachment point of the warp line, set to 0.2m

The warp stiffness, k_w , is calculated based on DNV RP F111 [3] recommendation for one single wire (typically 32-38mm dia.):

Where L_w = length of the warp line (set to 3 x water depth)

For beam trawls, it is assumed that 3 pieces of 32mm diameter warp lines are used.

b) Maximum Vertical Loads

The maximum vertical loads for trawls boards are acting in the downward direction and calculated as below:

- Polyvalent and rectangular boards:
- V-shaped boards:

The equations above are valid for one trawl boards. While, these equations are for total pull-over force from both beam shoes for beam trawls.

2.6.2. Clump Weight Pull-Over Loads

The typical clump weight used in this thesis work is roller type. Figure 2 - 8 shows the illustration of typical clump weight (roller type) and pull-over mechanism on pipeline laid on seabed.

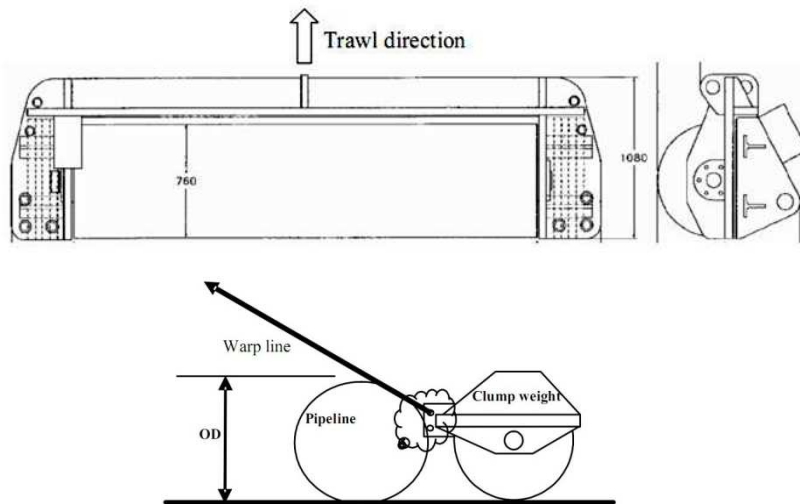


Figure 2 - 8 Typical clump weight (roller type) [3].

The maximum horizontal pull-over force for clump weight is taken from DNV RP F111 [3] as follow:

Where L_{clump} = distance from reaction point to the CoG of clump weight (0.7m for roller type with drum dia. of 0.76m)
 m_t = steel mass
 g = gravitational acceleration
 h' = $(H_{sp} + OD) / L_{clump}$

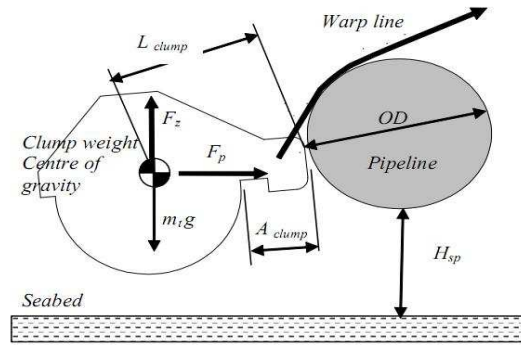


Figure 2 - 9 Clump weight (roller type) interaction with pipeline [3]

The maximum vertical pull-over force for clump weight is calculated in upward and downward direction. In each case it should be considered which one give the most critical load combination.

- Maximum upward pull-over force: $F_z = 0.3F_p - 0.4m_t \cdot g$
- Maximum downward pull-over force: $F_z = 0.1F_p - 1.1m_t \cdot g$

2.6.3. Pull-Over Durations

a) Trawl Boards and Beam Trawls

The total pull-over time, T_p , for trawl boards and beam trawls are given by:

$$T_p = C_T \cdot C_F \left(\frac{m_t}{k_w} \right)^{0.5} + \frac{\delta_p}{V}$$

Where C_T = pull-over duration coefficient (2.0 for trawl boards and 1.5 for beam trawls)

δ_p = displacement of the pipe at the point of interaction

The value of δ_p/V is unknown prior to analysis. Therefore, it is assumed that $\frac{\delta_p}{V} = \frac{C_T \cdot C_F \left(\frac{m_t}{k_w} \right)^{0.5}}{10}$ in the analysis as recommended by DNV RP F111 [3] in section 4.5. Hence, the total pull-over time, T_p , equation becomes:

$$T_p = C_T \cdot C_F \left(\frac{m_t}{k_w} \right)^{0.5} (1 + 0.1)$$

Figure 2 - 10 shows the sketch of force-time history for trawl boards and beam trawls pull-over force on the pipeline [3]. The force-time history applies for both horizontal and vertical pull-over force, F_p and F_z . The fall time for trawl boards may be taken as 0.6s. Unless the total pull-over time is less than this, the fall time should be equal to total time and assumed the force build-up time is 0.1s [3].

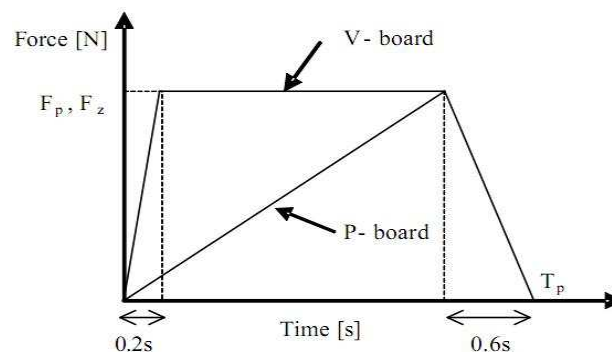


Figure 2 - 10 Force-time history for trawl boards pull-over forces [3].

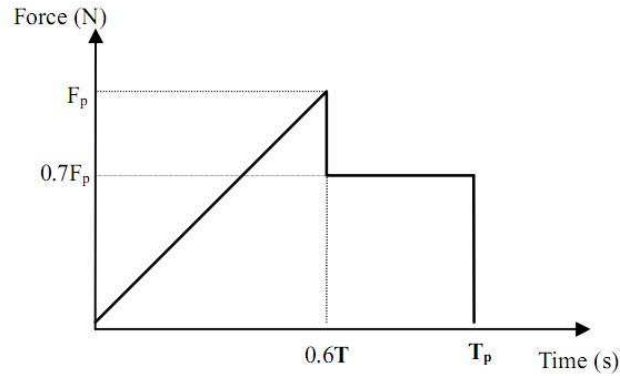


Figure 2 - 11 Force-time history for beam trawls pull-over forces [3].

b) Clump Weight

The pull-over duration of the roller type clump weight can be calculated as:

$$T_p = \frac{F_p}{(k_w \cdot V)} + \frac{\delta_p}{V}$$

As for trawl boards and beam trawls, the value of δ_p/V is unknown prior to analysis. Therefore, it is assumed that $\frac{\delta_p}{V} = 0.1 \left(\frac{F_p}{k_w \cdot V} \right)$ in the analysis and the pull-over duration equation becomes:

$$T_p = \frac{F_p}{(k_w \cdot V)} (1 + 0.1)$$

The force-time history of the pull-over force for roller type clump weights is shown in Figure 2 - 12 below.

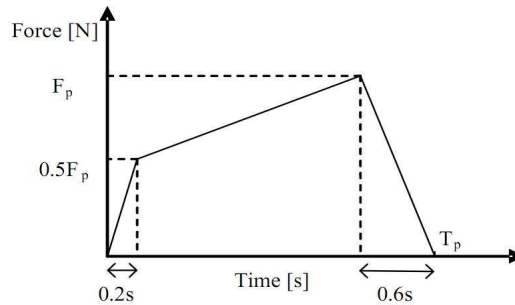


Figure 2 - 12 Force-time history for roller type clump weight pull-over forces [3]

2.7. DNV Combined Loading Criteria

The global buckling is not a failure mode in itself [3]. The global buckling may cause other failure modes e.g. local buckling, fracture and fatigue. Trawl gears pull-over loads may cause global buckling on the pipeline. Hence, the pipe shall be checked for different failure modes, know as pipe integrity checks [3].

The displacement controlled condition is defined in section D600 DNV OS-F101 [1], in which the structural response is primarily governed by imposed geometric displacement. Trawl gears pull-over loads induce lateral buckling on pipeline is one of that structural response. The pipeline subjected to longitudinal compressive strain (bending and axial) and internal overpressure. The following condition shall be design to satisfy displacement controlled condition eq. 5.29 [1] for pipeline with $D/t_2 \leq 45$ and $p_i \geq p_e$.

$$\varepsilon_{sd} \leq \frac{\varepsilon_c(t_2, P_{min} - P_e)}{\gamma_\varepsilon}$$

- Where ε_{sd} = design compressive strain
 = $\varepsilon_F \gamma_F \gamma_c + \varepsilon_E \gamma_E + \varepsilon_I \gamma_F \gamma_c + \varepsilon_A \gamma_A \gamma_c$
- $\varepsilon_c(t, p_{min}-p_e)$ = characteristic strain capacity
 = $0.78 \left(\frac{t}{D} - 0.01 \right) \left(1 + 5 \frac{P_{min}-P_e}{P_b(t) \cdot 2/\sqrt{3}} \right) (\alpha_h)^{-1.5} \alpha_{gw}$
- p_{min} = minimum internal pressure that can be continuously sustained with the associated strain
- α_h = maximum allowed yield to tensile ratio $\left(\frac{R_{t0.5}}{R_m} \right)_{max}$, Table 7-5 and 7-11 [1]
- α_{gw} = girth weld factor, section 13 E1000 [1].
- γ_ε = strain resistance factor, Table 5-8 [1]

Chapter 3 Methodology

3.1. General

This section gives detailed description of the methodology used in this thesis works, including the preparation and working procedures of the case study. All calculation works, working procedures, methodology are prepared based on Subsea 7 Design Guideline for Lateral Buckling CEO1PD-P-GU-127 [7] and Subsea 7 Design Guideline for Pipeline Expansion CEO1PD-P-GU-126 [8] in accordance with DNV OS F101 [1], DNV RP F110 [2], DNV RP F111 [3] and ANSYS v13 (mechanical APDL) Manuals [14].

In order to study and understand the global response of the pipeline from trawl gear pull-over loads, a finite element analysis is carried out using general finite element software ANSYS v13 (Mechanical APDL). Section 3.3 Finite Element Model gives detailed description about pipeline model, seabed model, and pull-over loads in ANSYS mechanical APDL. The descriptions of load cases in the finite element analysis are presented in section 3.4. Load Cases. And section 3.5 Finite Element Analysis gives detailed procedure including the sequence of trawl pull-over finite element analysis.

Some preparation works need to be carried out prior to start the finite element analysis. Section 3.2 gives detailed description about preparation works that include verification of pipeline end expansion, Hobbs's critical buckling forces calculation and pull-over forces and duration calculations. All the preparation calculations are carried out using general calculation software MathCAD v13.

3.2. Preparation Works

3.2.1. Pipeline End Expansion

This part of preparation works calculates the end expansion and effective axial force on the pipeline. The end expansion and effective axial force occur due to internal pressure, product temperature profile along the pipeline and also external pressure.

The end expansion calculation is made based on Subsea 7 Design Guideline for Pipeline Expansion CEO1PD-P-GU-126 [8] and DNV OS F101 [1]. The expansion results from calculation are used as comparison with the expansion results from the ANSYS model. The pipeline and seabed models in the ANSYS are considered to be accepted if the results are within $\pm 10\%$ difference.

In this calculation, the pipe is assumed laid on a flat seabed. The pipeline parameters that are used in this preparation work are presented in Table 4-1 and 4-2 in section 4.2. The pipeline operating data are presented in Table 4-4 in section 4.4. All values for soil friction factors are given in Table 4 - 6 in chapter 4. Axial soil friction factor of 0.5 was selected as best estimate for seabed condition.

Detailed MathCAD calculation of the pipeline end expansion is given in Appendix A-1.

3.2.2. Hobbs' Critical Buckling Force

This part of preparation works calculates the critical buckling force for each mode shapes. The pipeline can buckle into a number of different alternative post-buckled shapes. Each mode requires a different minimum axial force for the onset of lateral buckling. The critical buckling forces are calculated based on the analytical method of Hobbs [9] as presented in section 2.5.4 in accordance to Subsea 7 Design Guideline for Lateral Buckling Analysis CEO1PD-P-GU-126 [8]. The results from Hobbs' critical buckling forces calculation are used as comparison with the results from the finite element analysis.

The Hobbs' critical buckling forces are calculated based on best estimate axial friction factors and several lateral friction factors. All values for soil friction factors are given in Table 4 - 6 in chapter 4. Axial soil friction factor of 0.5 was selected as best estimate for seabed condition. The pipeline parameters that are used in this preparation work are presented in Table 4-1 and 4-2 in section 4.2. The pipeline operating data are presented in Table 4-4 in section 4.4.

Detailed MathCAD calculation of the Hobbs' critical buckling forces is given in Appendix A-2.

3.2.3. Pull-Over Forces and Duration

The pull-over forces from different types of trawl gears are calculated in this part of preparation works. This part also estimates the duration of pull-over forces that are going to be applied on the pipeline. There are four types of trawl gears are considered as presented in Table 4-7 section 4.7. All the trawl gears data are taken from DNV RP F111 [3]. These are trawl gears that are commonly used in the North Sea and the Norwegian Sea.

The maximum horizontal and vertical forces and its respective duration from each trawl gear are calculated using MathCAD spreadsheet. The horizontal and vertical forces from each trawl gear are then compared to select one force combination that can represent the other trawl pull-over forces and will be applied in the pull-over finite element analysis.

Detailed MathCAD calculation of pull-over forces is given in Appendix A-3.

3.3. Finite Element Model

This section gives detailed description of the finite element model, including the assumptions that are used. The finite element software ANSYS v13 (Mechanical APDL) is used to carry out pull-over finite element analysis for the three stages of "initial condition", "during pull-over loads duration" and "after pull-over loads duration".

3.3.1. Pipeline Model

The pipeline is modeled as a 2 km straight pipeline and laid on the flat seabed as shown in Figure 3-1. The main features of the pipeline model are as follow:

- A 3-D 2-node PIPE288 element from ANSYS Mechanical APDL element is used to model the pipeline. The pipe material is defined as element attribute. Figure 3 - 1 shows PIPE288 element geometry and Figure 3 - 3 shows PIPE288 as pipe element in ANSYS model.

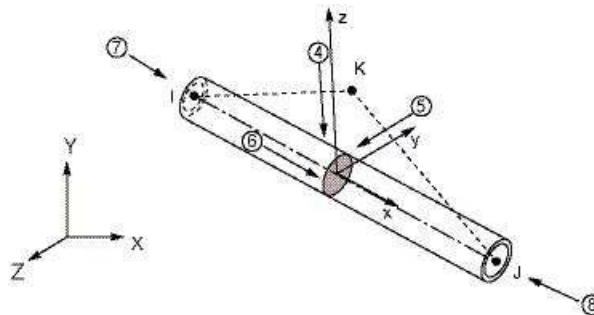


Figure 3 - 1 PIPE288 Geometry [14]

- The PIPE288 is set to follow thin-pipe theory by setting the value of KEYOPT (4) into 1. By applying this theory, a plain stress state in the pipe wall is assumed.
- The non-linear state of stress is taken into account by defining the stress-strain curve based on yield stress and ultimate strength. The stress-strain curve is defined into the model by using "TB" command for temperatures of 20°C and 100°C. The stress-strain curve is presented in figure 4-2.

- PIPE288 element is also well-suited for large rotation as per DNV RP F110 Section 4.5 recommendation [3].
- PIPE288 element also takes into account the de-rated yield stress for material properties of pipe SMLS 450 as per DNV recommendation. Figure 4-1 gives description of the de-rated yield stress of the pipe.
- The PIPE288 element is meshed by 1.2OD element size. This meshed element size gives better bending and displacement distribution in the buckle region.
- Insulation and coating properties are defined as additional weight on the pipeline. The insulation and coating density is taken as 910 kg/m^3 .
- The operating temperature on the pipeline is defined as element body loads and varies linearly through wall gradient by setting the value of Key Option 1 to 0.
- The internal and external pressures are assumed to cause loads on end caps by setting the value of Key Option 6 to 0.
- The pipe is laid on XZ-plane and the water depth is measured in Y-direction. Figure 3 - 3 shows the pipeline model in the ANSYS.

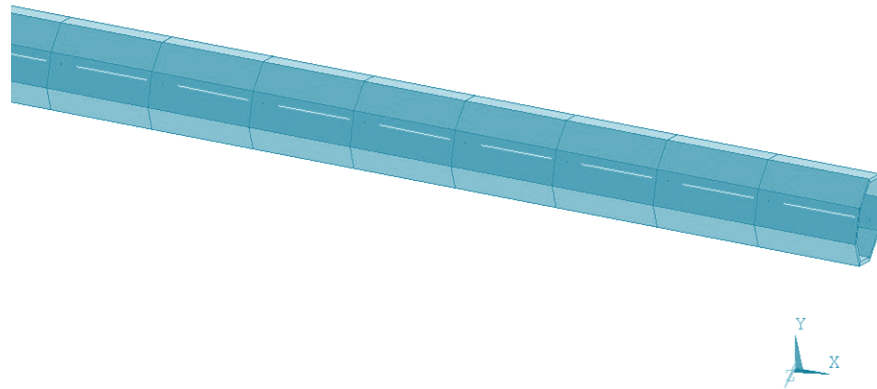


Figure 3 - 2 Pipe element using PIPE288 in ANSYS.

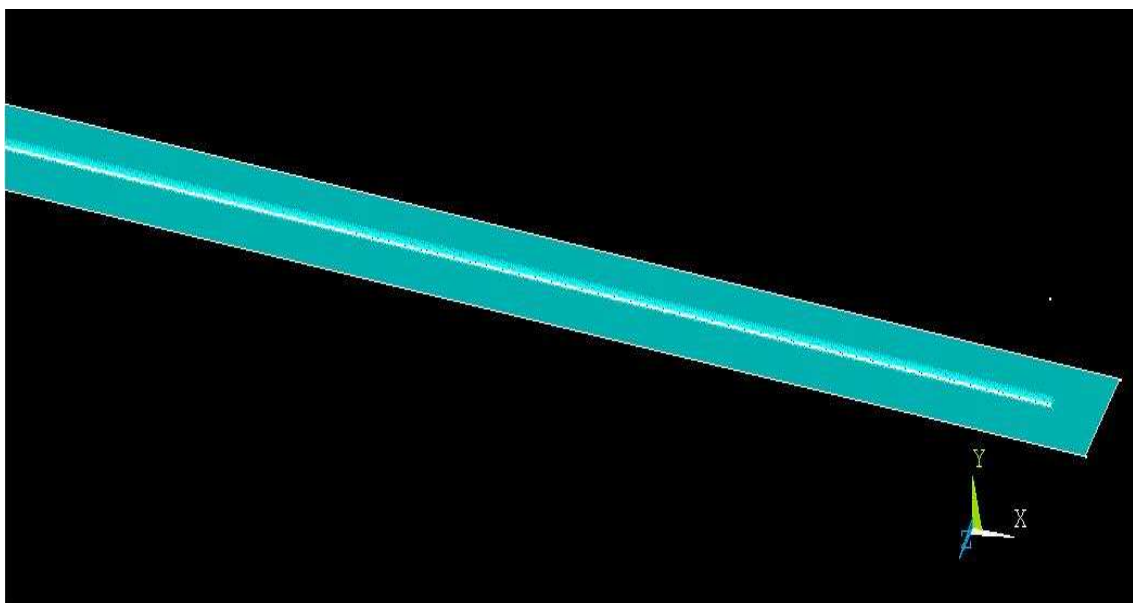


Figure 3 - 3 Pipeline Model in ANSYS

3.3.2. Seabed Model

In the ANSYS model, the seabed is defined using element CONTA175 for contact pair and also element TARGE170 for target surface. The main features of the seabed model are as follow:

- TARGE170 is used to represent rigid target surface for the associated 3-D node-to-surface contact element i.e. CONTA175. Figure Figure 3 - 4 shows the geometry of TARGE170.
- TARGE170 is defined as rigid target surface by define 4 nodes at the corner of the target surface and setting the segment type or shape into "QUAD" using "TSHAP" command. Figure 3 - 5 shows the segment type of TARGE170.
- A contact pair using 3-D node-to-surface CONTA175 is established between the seabed (TARGE170), which is the master surface, and the pipeline elements which form the slave surface.

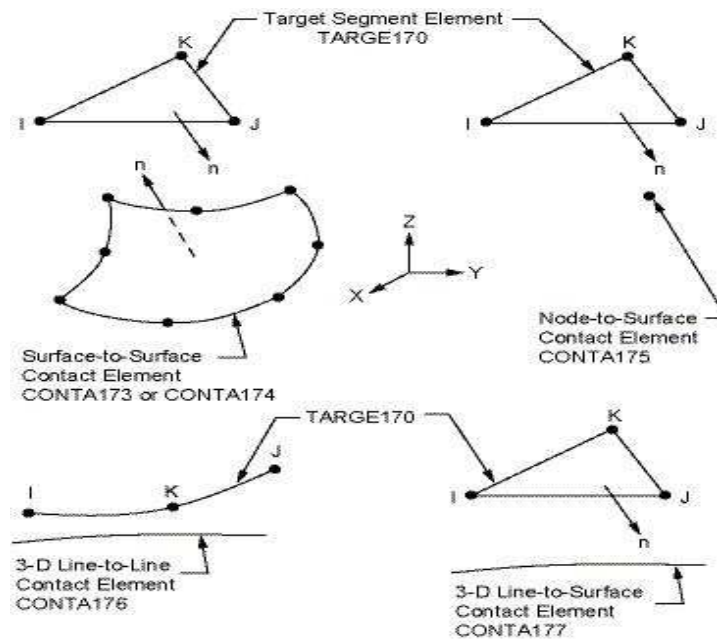


Figure 3 - 4 TARGE170 Geometry [14]

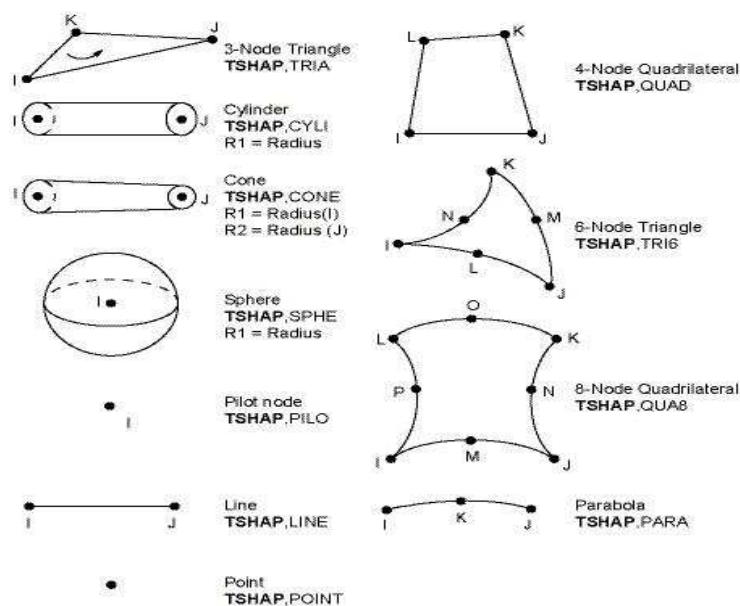


Figure 3 - 5 TARGE170 Segment Types [14]

- CONTA175 supports orthotropic Coulomb friction, a pipe-seabed interaction model with two different friction factors in axial and lateral directions. The orthotropic friction is defined using “TB,FRIC,” command by setting the value of “TBOPT” into “ORTHO”. The axial and lateral friction factors are defined using “TBDATA” command.

3.3.3. Initial Imperfection

In real life the pipeline will have some lateral imperfection. The lateral imperfections are introduced in the pipeline due to the pipe-lay vessel sway motion during installation process and due to seabed irregularities. In this thesis work, the pipeline is assumed as perfectly straight pipeline and laid on a flat seabed. Hence, there is no imperfection introduced in the finite element analysis model.

3.3.4. Soil Friction

The soil frictional is modeled based on Coulomb’s law using orthotropic friction model. The orthotropic friction model is based on two coefficients of soil friction, axial friction and lateral friction, to model different stick-slip behavior in different directions. The coefficients of friction (axial and lateral) are assumed constant through the analysis. Section 3.3.2 gives description about soil friction in ANSYS model.

The value of axial and lateral friction factors that are used in the analysis are presented in Table 4 - 6 section 4.6. The analysis is based on six scenarios of pull-over force and lateral soil friction coefficient as described in Table 3 - 1 section 3.3. These six scenarios also cover six combinations of axial and lateral soil friction factors.

3.3.5. Pull-over loads

The trawl gears pull-over loads are calculated as per section 2.6. The trawl gears pull-over loads are defined as a point load on the pipeline at mid of pipeline. The horizontal and vertical pull-over loads are applied based on force-time history from the section 4.8 hence a transient analysis is chosen. This type of analysis is used to determine the response of a structure under the action of any time-dependent loads.

This method involves building tables of load versus time using array parameters. Two tables are defined for horizontal and vertical pull-over forces and its respective force-time history in the ANSYS model. The loads are linearly interpolated (ramped) for each substep from the values of the previous load step to the values of this load step.

The pull-over forces are applied as force loads at nodes. The mid node 1490 is chosen as the node for force loads. The horizontal pull-over load is applied as force at node in positive global Z-direction (lateral). Meanwhile, the vertical pull-over load is applied as force at node in negative global Y-direction (downward). Figure 3 - 6 shows the pull-over forces that are applied on pipeline.

To apply the load histories on the pipeline and obtain the solution, a “Do-loops” command is constructed in the ANSYS model. “DO” and “ENDDO” are used in this command. Time start is defined at 2s. Time end is defined at 2.9s. A value of 0.1s is defined as time increment. A value of 10 is set to the number of substeps to be taken for each load step and automatic time stepping is used.

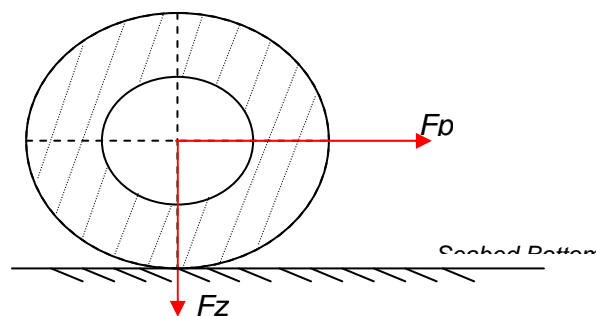


Figure 3 - 6 Pull-over Forces on Pipeline

After pull-over loads duration, the pull-over forces at node 1490 are applied as 0kN. The time start is set to 3s and the time end is set to 8s. A value of 0.5s is set as the time increment value. A “Do-loops” command is also used at the “after pull-over duration” period.

3.4. Load Cases

The assessment of trawl pull-over triggering global buckling is based on FE analyses for a set of trawl pull-over loads and pipe-soil resistances. Refer to section 6.3.2 in DNV RP F110 [2], the lateral soil friction and trawl pull-over load are defined by the soil-trawl matrix as shown in Figure 3 - 7 below. f_L is the lateral soil resistance force-displacement curve as presented in Table 4 - 6. F_T is the trawl load taken from section 4.8. Indices UB and LB indicate upper and lower bound value specified typically as a mean value ± 2 standard deviation and index BE indicates a “best-estimate” [2].

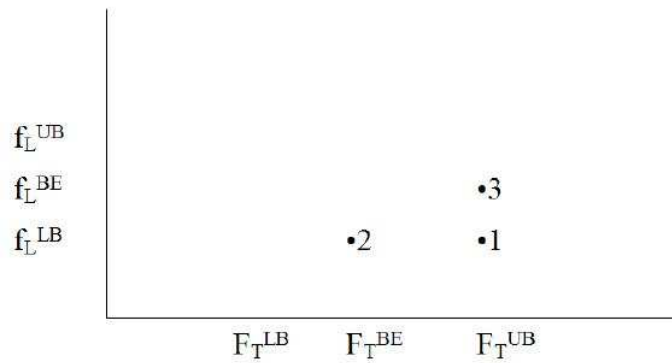


Figure 3 - 7 Combined lateral soil resistance and trawl load matrix [2].

Section 6.3.2 DNV RP F110 [2] recommends to use three scenarios in finite element analysis i.e. (F_T^{UB}, f_L^{LB}) denoted as •1, (F_T^{BE}, f_L^{LB}) denoted as •2 and (F_T^{UB}, f_L^{BE}) denoted as •3 in the Figure 3 - 7. The value of F_T^{LB} , F_T^{BE} and F_T^{UB} are presented in Table 2 - 2. These three scenarios are performed as follows:

- If global buckling not occur for scenario •1 using (F_T^{UB}, f_L^{LB}) and neither of scenarios •2 or •3 experience global buckling, hence *No Buckling* condition is obtained.
- If either scenarios •2 or •3 experience global buckling hence *Maybe Buckling* (SLS/ALS) condition is obtained.
- If both scenarios •2 or •3 experience global buckling hence *Buckling* condition is obtained. These load cases are applied for each type of trawl boards.

Table 3 - 1 Scenarios of lateral soil resistance and trawl pull-over loads

Load Case	Parameter	
	Trawl Load, F_p	Lateral Soil Resistance, μ_L
1	1.0 F_p	0.3
2	0.8 F_p	0.3
3	1.0 F_p	0.5
4	1.0 F_p	0.5
5	0.3 F_p	0.7
6	0.8 F_p	0.5

In addition to the DNV recommendation scenarios, this thesis work also considers three additional scenarios. These additional scenarios are included to carry out a sensitivity study for various pull-over loads and lateral soil friction on trawl pull-over. The six load case scenarios are listed in Table 3 - 1 above.

3.5. Finite Element Analysis

The finite element analysis is performed with a 2km straight pipeline under pressure and temperature corresponding to the trawl pull-over loads. Detailed finite element analysis is carried out for assessing the in-service and the post buckled behavior of the pipeline sections under operational conditions. The finite element analysis is carried out for six load cases as presented in Table 3 - 1. The stresses, strains, forces and bending moment from the analysis have to be checked against the acceptance criteria specified in the design code.

The finite element analysis is divided into 2 steps i.e. initial condition step and trawl gear pull-over analysis step. The initial analysis includes modeling the pipeline, laying the pipe on the seabed, applying boundary and operational condition on the pipeline. The initial condition step is set up from time 0s to 2s.

While, the trawl gear pull-over analysis is nonlinear-transient finite element analysis applying the pull-over forces on the pipeline based on force-time history as presented on section 4.8. The trawl gear pull-over analysis its self is divided into two periods of duration. From time 2.0s to 2.9s, the trawl gear pull-over analysis is set up as during pull-over duration period. The pull-over loads and its corresponding pull-over duration is applied in this period. The global response of pipeline that is induced by pull-over loads is analyzed.

From time 3s to 8s, the trawl gear pull-over analysis is set up as after pull-over duration period. The after pull-over loads duration period is analyzed post-buckling condition on pipeline and its governing factors post the application of pull-over loads. The pipe may continue to expand and buckle to establish its equilibrium state.

Detail description about applying pull-over forces and its corresponding pull-over duration in ANSYS model is presented in section 3.3.5. The ANSYS scripts for pull-over finite element are presented in appendix B.

3.5.1. Initial Condition Step

The initial condition step is from time 0s to 2s. It has scopes to model a 2 km long pipeline laying on the seabed, apply the boundary condition, end pipe condition and operating temperature-pressure on the pipeline. The analysis steps in the initial condition step are applied in the following sequence.

Table 3 - 2 Initial Condition Time Steps

Time Start	Time End	STEP Title	Description
0	1	Pipeline laid on seabed condition	<ul style="list-style-type: none"> • Call the pipeline model (pipe submerged weight and content weight are applied) • Lay pipeline on the seabed • Set boundary condition (fixed) for both end of pipeline • Select all elements associated with the pipeline • Apply external hydrostatic pressure on pipeline
1	2	Apply Operating Temperature and Pressure	<ul style="list-style-type: none"> • Select all elements associated with the pipeline • Apply operational pressure as surface loads on pipeline • Apply operational temperature different as element body force on pipeline (Top-Tamb)

3.5.2. Pull-over Analysis

The trawl gear pull-over analysis is performed to study the effect of trawl gear pull-over loads to the global response of subsea pipeline. The pull-over forces from a trawl gear may cause a straight pipeline under high compressive force to buckle or may induce imperfection from which a buckle may form during operation. The trawl pull-over loads are applied in the analysis in the following sequence.

Table 3 - 3 Trawl Gear Pull-over Analysis Time Steps

Time Start	Time End	STEP Title	Description
2	2.9	During Pull-over Loads Duration	<ul style="list-style-type: none"> • Set the number of substeps to be taken for each load step • Define Start Time, End Time, and Time Increment for “Do-loops” operation • Select node at mid of the pipeline (node 1490) • Apply horizontal and vertical pull-over forces as force on node as per force versus time history • Save the results in the data base file
3	8	After Pull-over Loads Duration	<ul style="list-style-type: none"> • Set the number of substeps to be taken for each load step • Define Start Time, End Time, and Time Increment for “Do-loops” operation • Apply no pull-over forces on pipeline • Save the results in the data base file

Chapter 4 Case Study

4.1. General

This section presents the basic data required for detailed FE analyses to check their susceptibility to lateral buckling due to trawl gear pull-over loads. The pipeline data and operating parameter are based on reasonable assumptions. The trawl gears data are based on DNV RP F111 [3].

4.2. Pipeline Parameter

This section gives a summary of material, dimension and operation condition of the subsea pipeline used in this thesis. Table 4 - 1 presents the line pipe data and material properties that are used in the analysis in this thesis.

Table 4 - 1 Pipe Design Data and Material Properties

Parameter	Unit	Value
Outside diameter	mm	559
Wall Thickness	mm	25.4
Corrosion Allowance	mm	3
Pipe Material Grade	-	DNV-450
Steel Density	kg/m ³	7850
SMYS	MPa	450
SMTS	MPa	535
Poisson ratio (ν)	-	0.3
Young's Modulus (E)	GPa	207
Thermal Expansion Coef.(α)	°C ⁻¹	1.17E-05
Temp. De-rating factor, $f_{u,temp}$	MPa	See section 4.3

Table 4 - 2 gives detail data for corrosion/thermal insulation coating and concrete weight coating on the pipeline to give realistic model in the analysis.

Table 4 - 2 Coating Parameter

Parameter	Unit	Value
Insulation Thickness	mm	5
Insulation Density	kg/m ³	910
Concrete Coating Thickness	mm	0
Concrete Coating Density	kg/m ³	2400

4.3. Pipe Material Yield Stress

For the analysis, the DNV SMLS 450 is used and the material properties refer to DNV OS F101 [1] including the de-rating of SMYS yield strength with temperature as shown in Figure 4 - 1. The yield stress de-rating of pipe material will be build into the FE models.

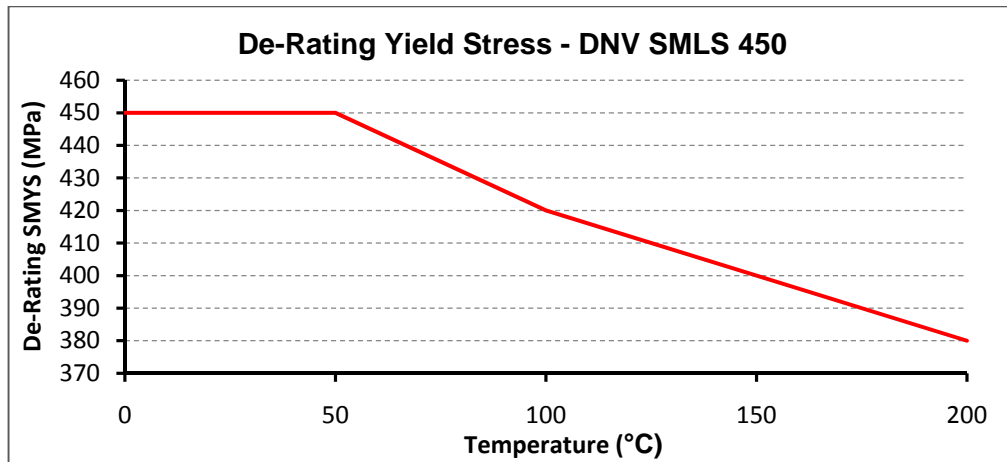


Figure 4 - 1 Pipe Material Yield Stress De-Rating [1]

In addition to that, the stress-strain curves for the material shall take into account the non-linear state of stress and strain [2]. The FE analyses will therefore be performed using the user defined stress strain curves. The stress-strain curves to be used in the analyses are shown in Figure 4 - 2. The yield stress is defined as the elastic strain of approximately 0.2% [1]. The yield plateau is limited to 2% strain and stress-strain curve beyond 2% strain is approximated up to SMTS.

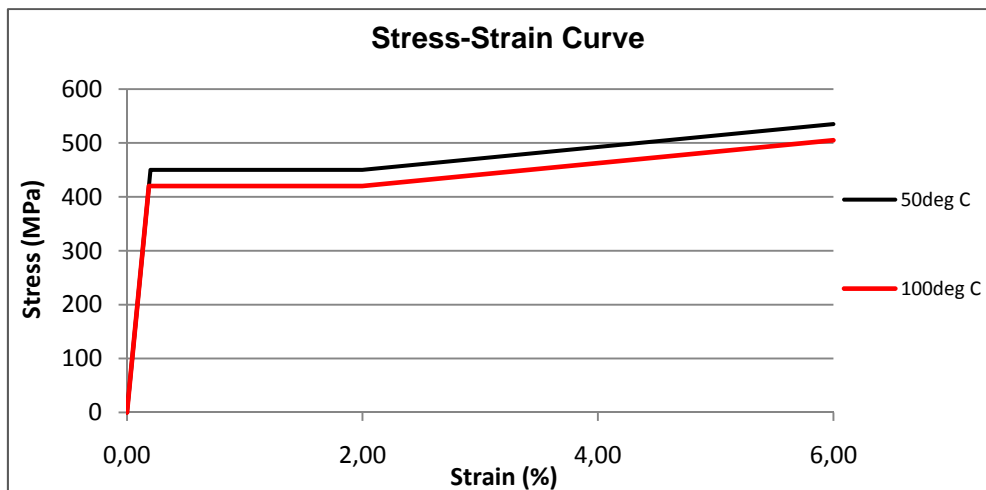


Figure 4 - 2 Steel Pipe Stress-Strain Curve

Numerical summary of the stress strain curve shows in Table 4 - 3 below.

Table 4 - 3 Stress-Strain Data

Parameter	Temperature							
	Below 50 °C				100 °C			
Strain	0.000	0.217	2.000	6.000	0	0.203	2.000	6.000
Stress	0	450	450	535	0	420	420	505

4.4. Operating Data

Table 4 - 4 gives the summary of the operational data used in the analysis. All the data are assumed with reasonable value to get proper model. The pipe is assumed to be filled with oil product.

Table 4 - 4 Operating Parameters

Parameter	Unit	Value
Content Density (Oil)	kg/m ³	900
Design Pressure	MPa	15
Operating Temperature	°C	100
Ambient Temperature	°C	5

4.5. Environmental Data

Table 4 - 5 shows the environmental data used in the analysis. Refer to section 6.3.2 DNV RP F110 [2], no waves and currents data are used in the analysis. The hydrodynamics loads are not included in the calculation as they may reduce the lateral pipe-soil resistance due to lift effects [2].

Table 4 - 5 Environmental Data

Parameter	Unit	Value
Seawater Density	kg/m ³	1027
Water Depth	m	100

4.6. Soil Data

The pipeline is assumed laid on clay flat (even) seabed. The soil properties are assumed constant along the pipeline. The axial and lateral friction factors are given in Table 4 - 6 below.

Table 4 - 6 Friction Factors

Parameter		Value
Axial friction		0.5
Lateral Friction	LB	0.3
	BE	0.5
	UB	0.7
Soil Mobilization		2mm – 4mm

4.7. Trawl Gear Parameter

This section gives the data of trawl gears used in the FE analysis. The data are considered for trawl gears that are commonly used in the North Sea and the Norwegian Sea. The trawl gears data are taken from DNV RP F111 [3]. There are four types of trawl gears that are considered in the analysis, i.e. polyvalent & rectangular trawl board, industrial v-shape trawl gear, beam trawl board, and roller type clump weight [3]. From all these type of trawl gears, only one type of trawl gears will be used in the finite element analysis which is considered to adequately represent the cases.

Table 4 - 7 Trawl Gears Data [3]

Parameter	Unit	Trawl Gears Type			
		Polyvalent & Rectangular	Industrial V-board	Beam Trawl	Clump Weight
Steel Mass, m_t	kg	4500	5000	5500	9000
Dimension Lxh	m	4.5 x 3.5	4.9 x 3.8	17.0 ³⁾	2)
Effective impact velocity	m/s	$2.8C_h^{1)}$	$1.8C_h^{1)}$	3.4	2.8
In plane stiffness, k_i	MN/m	500	500	-	4200
Bending board stiffness, k_b	MN/m	10	10	-	-
Hydrodynamic added mass, m_a	kg	$2.14m_t$	$2.90m_t$	1500	3140
Pull-Over Duration Coeff. C_T	-	2.0	2.0	1.5	-

Note:

- 1) The factor C_h is given in figure 4-2
- 2) Typical dimension of the largest clump weight of 9T are $L = 4$ m wide (i.e. length of roller) by 0.76m dia. cross section.
- 3) Beam Trawl length (i.e. distance between outside of each shoe)

The value of factor C_h , span height correction factor for the effective pull-over velocity is given in Figure 4 - 3. The pipeline is laid on flat seabed hence it is assumed no pipeline span occurs. The C_h value for polyvalent and rectangular is 0.85 and for industrial v-board is 1.0.

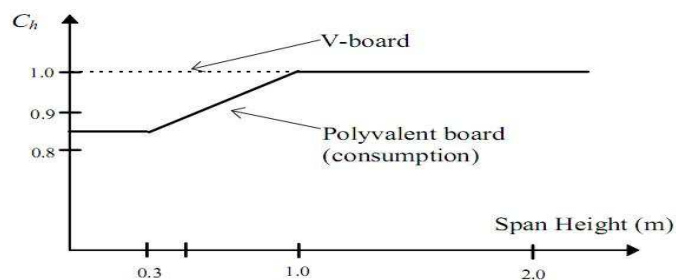


Figure 4 - 3 C_h coefficient for effect of span height on impact velocity [3]

4.8. Pull-over Loads and Durations

During the interaction with the trawl gears, the pipeline is subjected to substantial horizontal and vertical forces from trawl gears. The horizontal and vertical loads used in the analysis are calculated based on section 4 in DNV RP F111 [3] and presented in Appendix A-3. Table 4 - 8 summarized the horizontal and vertical loads calculated in Appendix A-3.

Table 4 - 8 Pull-over Horizontal and Vertical Loads and Durations

Parameter	Unit	Trawl Gears Type			
		Polyvalent & Rectangular	Industrial V-board	Beam Trawl	Clump Weight
Max. Horizontal Force	kN	101.97	64.18	321.47	305.96
Max. Vertical (upward) Force	kN	-	-	-	56.49 ²⁾
Max. Vertical (downward) Force	kN	61.22	32.09	-	66.49 ²⁾
Pull-over duration	s	0.687	0.672	1.337	1.03

Note:

- 1) Vertical acting force assumed to have the same force-time history as corresponding horizontal force.
- 2) Should be considered if the upward or the downward force will give the most critical load combination.

The horizontal and vertical pull-over loads are applied based on the force-time history as recommended in section 4.5 and 4.6 [3]. The force-time histories for each trawl gears type that are calculated in appendix A-3 are shown below.

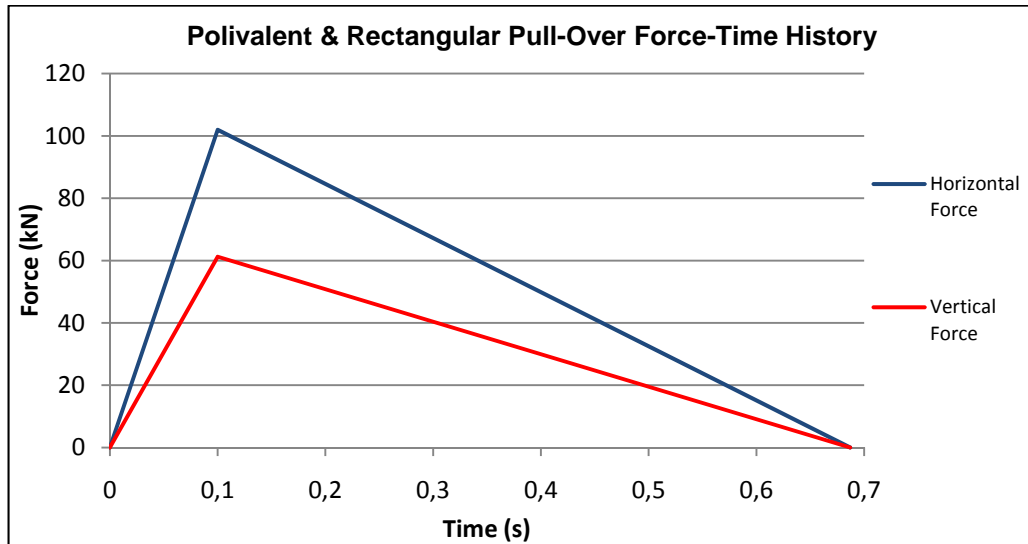


Figure 4 - 4 Polyvalent & rectangular pull-over force-time history

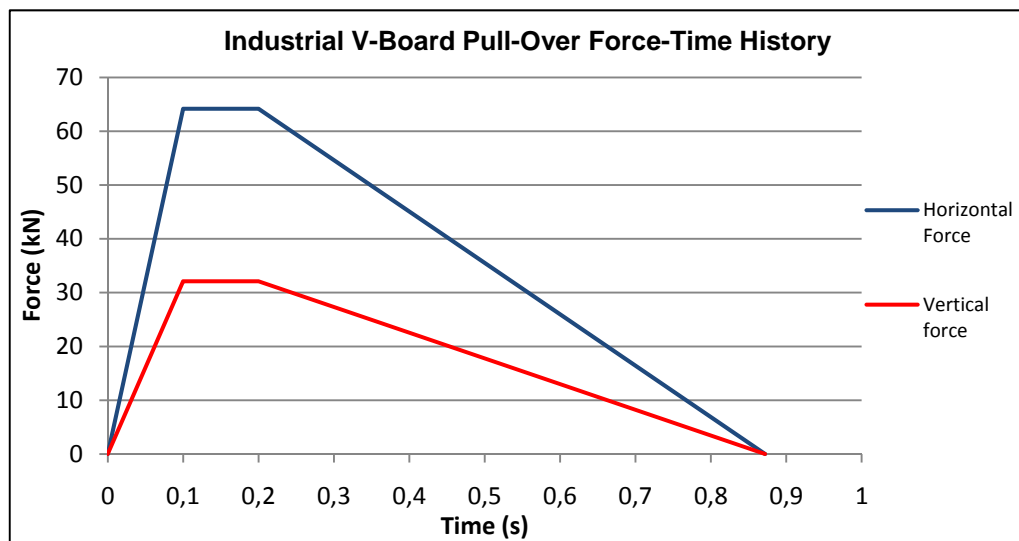


Figure 4 - 5 Industrial v-board pull-over force-time history

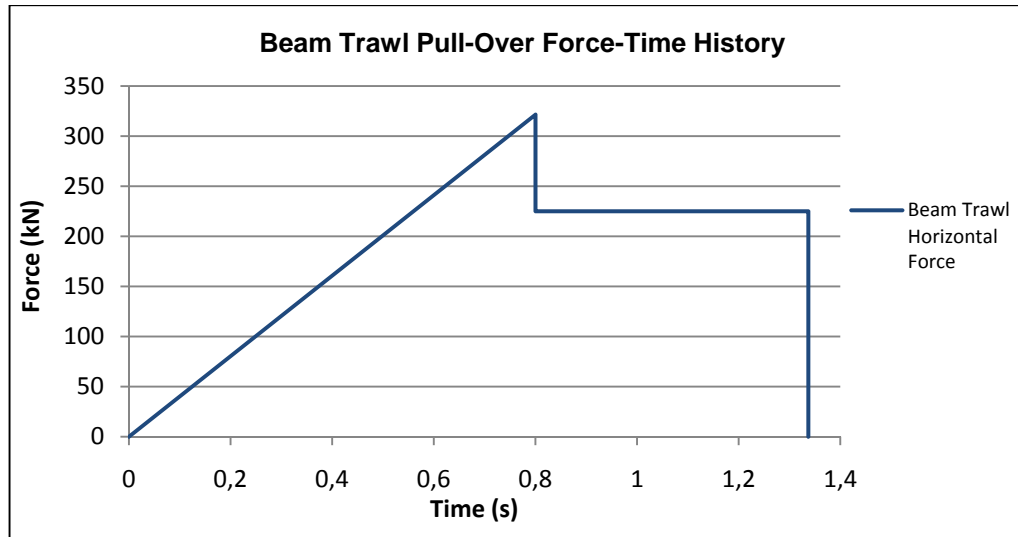


Figure 4 - 6 Beam trawl pull-over force-time history

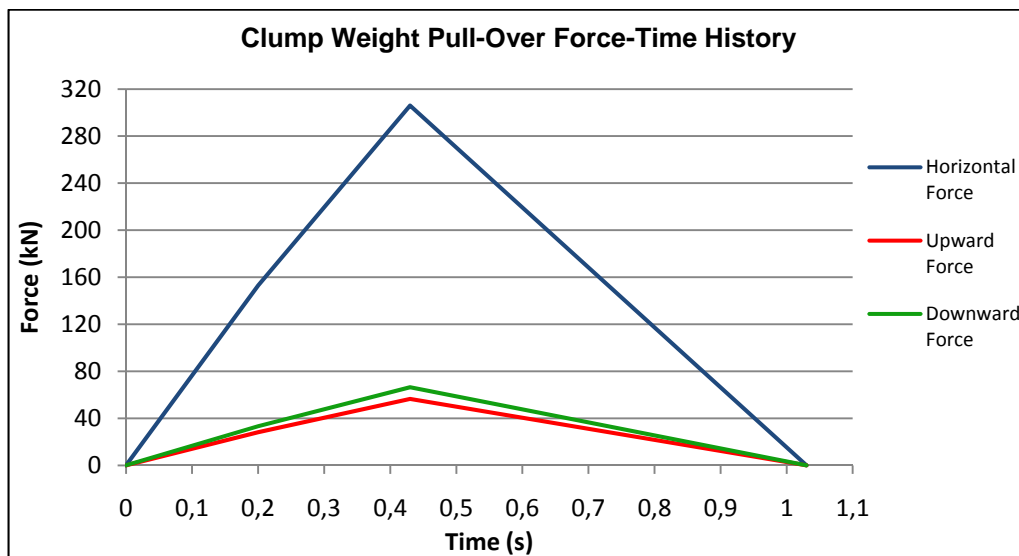


Figure 4 - 1 Clump Weight Pull-Over Force-Time History

4.9. Displacement Controlled Condition

This section presents the factors for DNV displacement controlled condition code check as per DNV OS F101 [1] and DNV RP F110 [2].

4.9.1. Safety Factors

The material strength factor (α_u), material resistance factor (γ_m) and safety class resistance factor (γ_{sc}) are given in Table 4 - 9 taken from DNV OS F101 [1].

Table 4 - 9 Safety factors

Load Scenario	α_u	γ_m	γ_{sc}	α_{fab}	γ_e	γ_C	α_h
Operation	0.96	1.15	1.14	1.0	2.50	1.07	0.93

4.9.2. Load Combinations and Load Effect Factors

Load combinations with the corresponding load effect factors (γ_F , γ_E , γ_A , γ_p) are given in Table 4 - 10 refer to Table 4-4 [1].

Table 4 - 10 Load combinations and load effect factors

Limit state category		Functional Loads	Environmental Loads	Accidental Loads
		γ_F	γ_E	γ_A
SLS & ULS	a	1.2	-	-
	b	1.1	-	-

Note:

- a. shall only be considered for scenarios where system effects are present.
- b. for local scenarios and shall always be considered.

Chapter 5 Result & Discussion

This chapter presents the results along with the discussion of the thesis work. In general, this chapter shows the results for model validation and the Hobbs analytical method for calculating the critical buckling forces. This chapter also presents the results for each load cases during and post pull-over analysis i.e. pipeline profile, the bending moments and forces distribution, the effective axial force distribution and the equivalent strain distribution along the pipeline and the DNV displacement controlled code checked.

The discussion about the analysis results and governing factors also will be presented later in this chapter.

5.1. Model Validation

Table 5 - 1 presents the pipeline end expansion from MathCAD Model Validation spreadsheet and FE model. The comparison of end expansion between MathCAD spreadsheet and ANSYS model are to check the finite element model in the ANSYS as describe in section 3.2.1 in this thesis report.

Table 5 - 1 Pipeline End Expansion

Parameter	Unit	MathCAD spreadsheet	FE model
End expansion with soil resistance	m	2.39	2.41
End expansion without soil resistance	m	2.80	2.71

As presented in table above, the difference of pipeline end expansion between MathCAD spreadsheet and finite element model is less than 10%. Hence, it is assumed that the finite element model is modeled properly and gives the behavior as expected. It also shows that the contact surface exists and the soil resistance is working.

Detailed MathCAD pipeline end expansion is presented in Appendix A-1.

5.2. Effective Axial Force

Table 5 - 2 shows the maximum friction force at mid of pipeline and the fully restrained axial force calculated based on DNV OS F101 [1]. These values are only for comparison purposes.

Table 5 - 2 Friction Force and Axial Restrained Force

Parameter	Unit	MathCAD spreadsheet
Max. Friction Force ¹⁾	kN	1294
Fully Restrained Axial Force	kN	10775

Note :

1) Maximum value at mid of pipeline (KP 1.0)

Detailed MathCAD calculation is presented in Appendix A-1.

5.3. Hobbs’s Critical Buckling Limiting Load

The values presented in Table 5 - 3 are extracted from MathCAD Lateral Buckling Verification spreadsheets. The MathCAD calculations are presented in Appendix A-2. These values are presented for comparison with the results reached in the presented FE analyses. The Hobbs’s Critical Buckling Forces are calculated based analytical method from Hobbs paper [9] and Subsea 7 Lateral Buckling Design Guideline [7]. The critical buckling force is calculated for lateral soil friction value of 0.3, 0.5 and 0.7 for each mode.

Table 5 - 3 Hobbs’s Critical Buckling Force

Buckle Mode	Unit	MathCAD spreadsheet		
		$\mu_{Lat}: 0.3$	$\mu_{Lat}: 0.5$	$\mu_{Lat}: 0.7$
Mode 1	kN	2086.6	2751.0	3299.1
Mode 2	kN	2022.2	2662.7	3192.9
Mode 3	kN	1991.1	2620.0	3140.2
Mode 4	kN	1991.3	2619.2	3135.5
Mode 5	kN	2612.9	3373.2	3991.2

Figure 5 - 1 shows the buckle length calculated using Hobbs's analytical method for each buckle modes. The graph also shows the minimum axial force to instigate a buckle at a given mode.

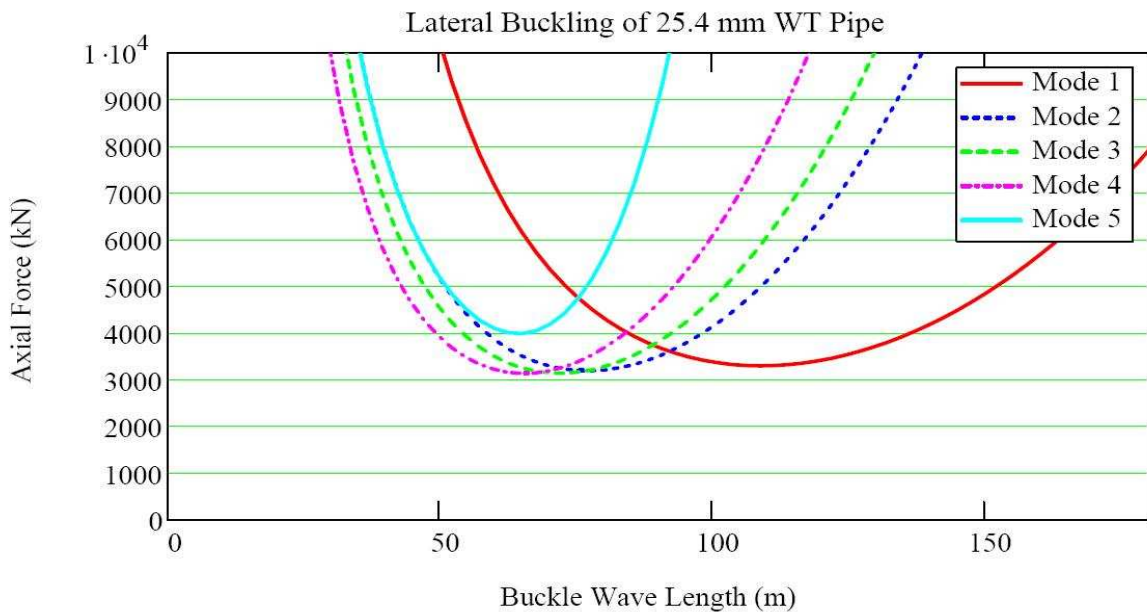


Figure 5 - 1 Hobbs’s Buckle Length Vs Axial force for each buckle modes for lateral soil friction of 0.7

5.4. Trawl Boards Pull-Over Analysis Results

5.4.1. Lateral Displacement

a) During Pull-over Loads Duration (t:2.0s-2.9s)

This section shows the lateral (Z-direction) displacement from load case 1 to load case 6 during pull-over load. The pull-over force was applied start at time 2s in the nonlinear transient analysis using ANSYS mechanical APDL. The pull over duration for the polyvalent & rectangular trawl board is 0.687s as presented in section 4.8.

Figure 5 - 2 gives results of the lateral (Z-direction) displacement from KP 0.738 to KP 1.21 for load case 1 (above) and load case 4 (below). These KPs are selected as these are the location with significant displacement results. Both load cases used 100% pull-over forces with different values of lateral soil friction factor. Load case 1 used *lateral lower bound soil friction factor* of 0.3 meanwhile load case 4 used *lateral upper bound friction factor* 0.7. The graph shows lateral displacement of the pipeline from 2.0s to 2.9s for every 0.1s time step increment.

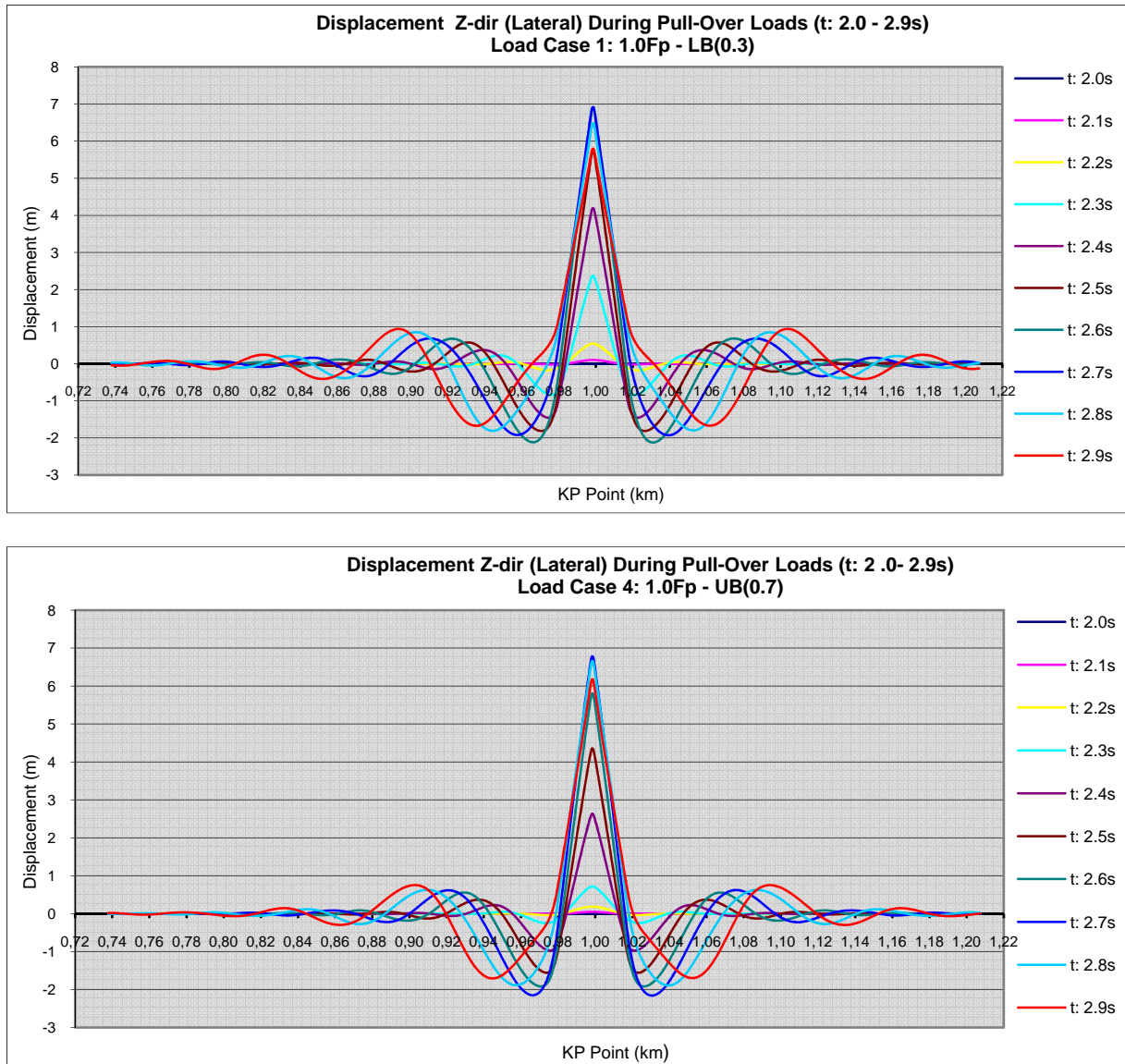


Figure 5 - 2 Lateral displacement during pull-over loads duration (t:2.0-2.9s)

Load Case 1(above): 100% pull-over forces with lower bound soil friction factor: 0.3

Load Case 4 (below): 100% pull-over forces with upper bound soil friction factor: 0.7

From Figure 5 - 2, the pipeline buckles into an indefinite series of half waves with different buckle amplitudes. However, both left and right side of the buckles show identical form with the maximum buckle amplitude is located at the point where the pull-over force is applied, i.e. at KP 1.0.

From Figure 5 - 2a, it is shown that the pipeline moves in lateral direction of 2.37m at time 2.3s. The displacement continuously increases to 4.18m at 2.4s, 5.73m at 2.5s, and 6.89m at 2.6s. The apex of the buckle reaches its maximum lateral displacement of 6.91m at time 2.7s. Afterward, the maximum displacement decreases to 5.79m at time 2.9s. For load case 1, the apex of the buckle occurs at the pull-over force location, i.e. at KP 1.0.

Figure 5 - 2b shows the lateral pipeline movement for load case 4. From the analysis, load case 4 also shows similar behavior as load case 1. The pipeline moves in lateral direction of 0.72m at time 2.3s. The displacement continuously increases to 2.62m at 2.4s, 4.34m at 2.5s, and 5.79m at 2.6s. The apex of the buckle reaches its maximum lateral displacement of 6.77m at 2.7s. Afterward, the maximum displacement decreases to 6.17m at time 2.9s. Similar as in load case 1, the apex of the buckle also occurs at the pull-over force location, i.e. at KP 1.0 for load case 4.

From the analysis for load cases 2, 3, and 6, the lateral displacements also show similar behavior as in load case 1 and 4. The lateral displacement graph during pull-over load for load cases 2, 3 and 6 are presented in appendix C.

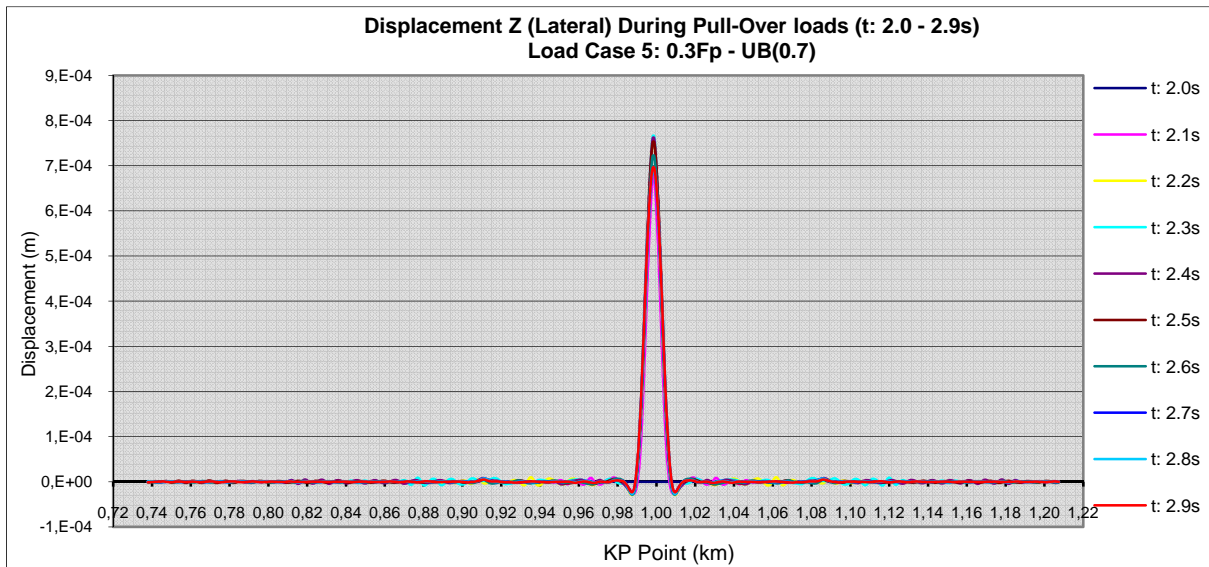


Figure 5 - 3 Lateral displacement during pull-over loads duration (t:2.0-2.9s) for load case 5.

Figure 5 - 3 shows the pipeline lateral displacement for load case 5. In this load case, only 30% of pull-over forces are applied in combination with the upper bound lateral soil friction coefficient. As shown in the graph, the pipeline only moves laterally in very small displacement, less than 1mm. This situation shows that no lateral buckling occurred and that the pipeline is still in straight line. The maximum lateral displacement for load case 5 is 7.66×10^{-4} m at time 2.3s. Similar with the other load cases, the maximum displacement also occurs at the point where the force is applied.

The summary of lateral displacement for all load cases is tabulated in Table 5 - 4 below.

Table 5 - 4 Pipeline lateral (Z-direction) displacement during pull-over loads duration

Load Case	1	2	3	4	5	6
Pull-over Factor	1.0	0.8	1.0	1.0	0.3	0.8
Lateral Soil friction	0.3	0.3	0.5	0.7	0.7	0.5
Time (s)	Displacement (m)					
2.0	2.66E-19	2.30E-19	1.54E-19	1.52E-19	1.13E-19	1.32E-19
2.1	0.10	0.08	0.08	0.05	6.77E-04	0.05
2.2	0.55	0.40	0.35	0.18	7.60E-04	0.24
2.3	2.37	1.92	1.70	0.72	7.66E-04	1.09
2.4	4.18	3.76	3.63	2.62	7.61E-04	3.09
2.5	5.73	5.32	5.25	4.34	7.53E-04	4.76
2.6	6.89	6.58	6.58	5.79	7.22E-04	6.14
2.7	6.91	6.74	6.88	6.77	6.85E-04	6.81
2.8	6.47	6.36	6.55	6.65	6.90E-04	6.57
2.9	5.79	5.70	5.92	6.17	6.95E-04	6.00

b) After Pull-Over Loads Duration (time: 3.0s – 8.0s)

As previously discussed, the pull-over forces start to be applied at time 2s in the nonlinear transient analysis using ANSYS mechanical APDL. The pull over duration for the polyvalent & rectangular trawl board is 0.687s as mentioned in section 4.8. This section shows the result of the lateral (Z-direction) displacement after the pull-over load forces are no longer applied, i.e. from time 3.0s to 8.0s. This section also shows the results for load case 1 to load case 6. The lateral movement behaviors of the pipeline after the application of pull-over load are shown in Figure 5 - 4 and Figure 5 - 5. The lateral displacements are summarized in Table 5-5.

From Figure 5 - 4, the pipeline still has indefinite series of half waves with different buckle amplitude. Both left and right sides of the buckle shows identical buckle form with the maximum buckle amplitude located at the point where the pull-over force is applied. These buckled forms only exist until time 4.0s. After time 4.0s, the buckle form is transformed to mode 3 refer to Hobbs' buckle modes. The shoulder parts of the main buckle wave become almost straight line.

Figure 5 - 4a shows the lateral movements of the pipeline post the pull-over load application for load case 1. The graph shows that at 3.0s, the maximum displacement of pipeline is 5.66m. This value is less than the maximum displacement at time 2.9s which is 5.79m. Afterward, the maximum displacement starts to increase continuously to 6.94m at 3.5s and become constant at 7.2m from 5.0s to 8.0s.

Load case 4 also shows similar lateral movement behavior as Load case 1. As shown in Figure 5 - 4b, the maximum displacement at 3.0s is 5.5m. This value is less than the maximum displacement at time 2.9s which is 6.17m. Afterward, the maximum displacement starts to increase continuously to 6.73m at 3.5s and become constant at 6.88m from 4.5s to 8.0s.

From the analysis, load case 2, 3 and 6 also show similar behavior as in load case 1 and 4. The lateral displacement graphs after the pull-over load for load cases 2, 3 and 6 are presented in appendix C.

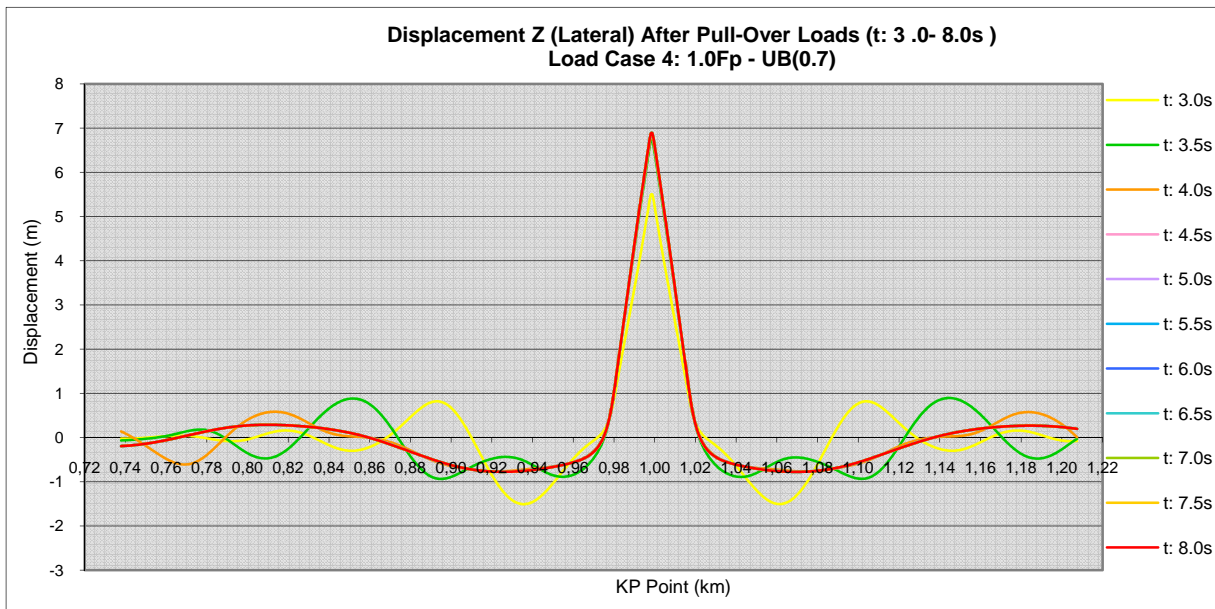
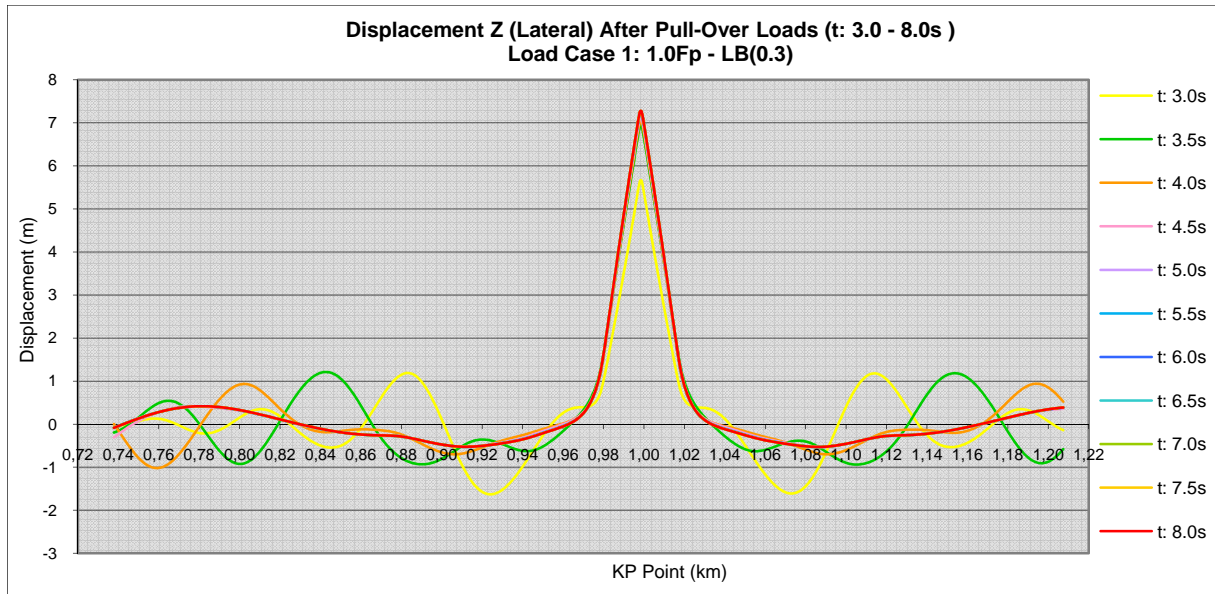


Figure 5 - 4 Lateral displacement after pull-over loads duration (t:3.0-8.0s)
Load Case 1(above): 100% pull-over forces with lower bound soil friction factor: 0.3
Load Case 4 (below): 100% pull-over forces with upper bound soil friction factor: 0.7

Figure 5 - 5 shows the pipeline lateral displacement for load case 5. As shown in the graph, the pipeline moves laterally only from KP 0.98 to KP 1.02 while the rest of the pipeline does not move laterally. The pipeline has constant maximum lateral displacement at $6.9 \times 10^{-4} \text{m}$ from time 3.0s to 8.0s.

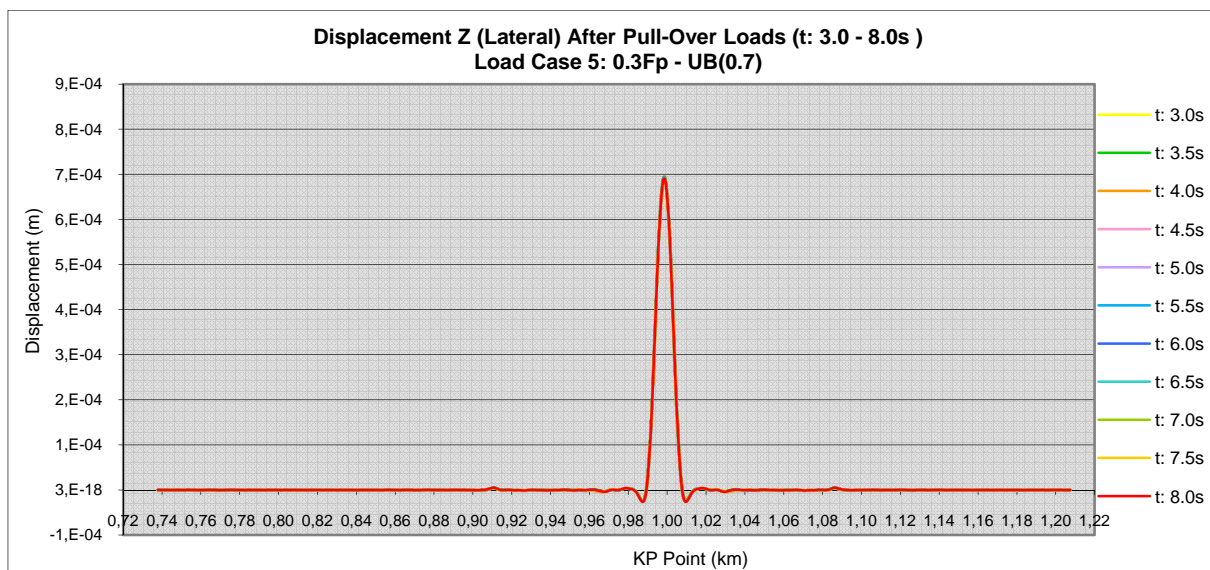


Figure 5 - 5 Lateral displacement after pull-over loads duration (t:3.0-8.0s) for load case 5.

The summary of lateral displacement after pull-over loads duration for all load cases is tabulated in Table 5 - 5 below.

Table 5 - 5 Pipeline lateral (Z-direction) displacement after pull-over loads duration

Load Case	1	2	3	4	5	6
Pull-over Factor	1.0	0.8	1.0	1.0	0.3	0.8
Lateral Soil friction	0.3	0.3	0.5	0.7	0.7	0.5
time (s)	Displacement (m)					
3.0	5.66	5.40	5.49	5.50	6.94E-04	5.36
3.5	6.94	6.63	6.83	6.73	6.94E-04	6.67
4.0	7.04	6.70	6.95	6.81	6.90E-04	6.79
4.5	7.13	6.78	7.03	6.87	6.87E-04	6.87
5.0	7.20	6.84	7.08	6.88	6.88E-04	6.92
5.5	7.24	6.88	7.10	6.88	6.91E-04	6.93
6.0	7.26	6.90	7.11	6.88	6.93E-04	6.94
6.5	7.26	6.90	7.11	6.88	6.91E-04	6.94
7.0	7.27	6.91	7.11	6.88	6.89E-04	6.94
7.5	7.27	6.91	7.11	6.88	6.88E-04	6.94
8.0	7.27	6.91	7.11	6.88	6.89E-04	6.94

5.4.2. Axial Displacement

a) During Pull-over Loads Duration (t:2.0s-2.9s)

This section gives results of axial (X-direction) displacement for load case 1 to load case 6 during pull-over load duration. The axial displacement values are extracted from the finite element analysis results. The pull-over force starts to be applied at time 2s in the nonlinear transient analysis using ANSYS mechanical APDL. The pull over duration for the polyvalent & rectangular trawl board is 0.687s as mentioned in section 4.8.

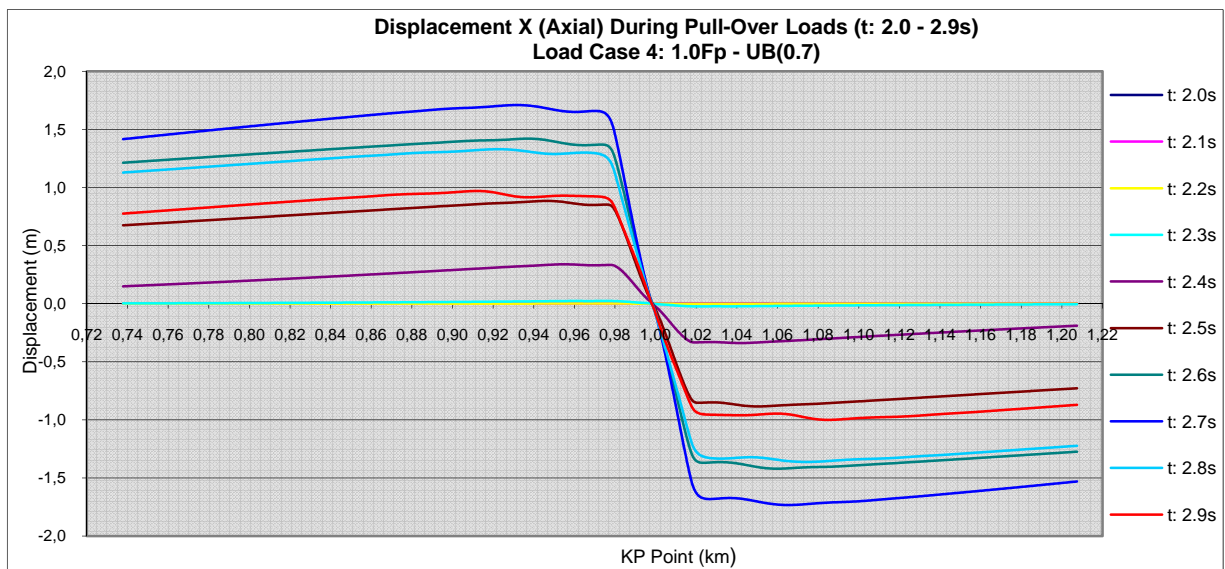
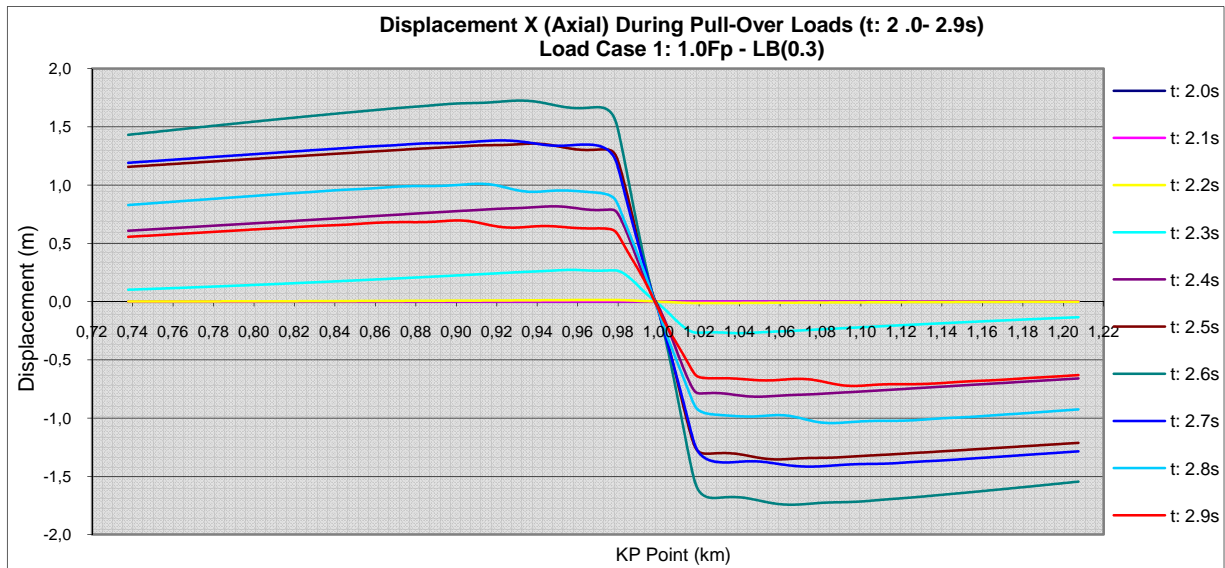


Figure 5 - 6 Axial displacement during pull-over loads duration (t:2.0-2.9s)
Load Case 1(above): 100% pull-over forces with lower bound soil friction factor: 0.3
Load Case 4 (below): 100% pull-over forces with upper bound soil friction factor: 0.7

Figure 5 - 6 gives results of the axial (X-direction) displacement from KP 0.738 to KP 1.21 for load cases 1 (above) and 4 (below). These KPs are selected as these are the location with significant results. The graph shows the axial displacement of the pipeline from time 2.0s to 2.9s for every 0.1s time step increment. Both load cases applied 100% of the pull-over force combine with lateral soil friction factor of 0.3 for load case 1 and 0.7 for load case 4.

Figure 5 - 6a & b show that the slip regions have identical axial displacement along the pipeline for every time steps. The axial displacement increases gradually from the end of the pipeline to the mid of pipeline until it reaches the maximum value at approximately KP 0.94 and 1.06. Then, it drops significantly to 0m for every time steps at the pull-over force applied location, i.e. at KP 1.0.

The pipeline axial displacement for load case 1 increases continuously from time 2.3s until it reaches the maximum axial displacement of 1.73m at time 2.6s as shown in Figure 5-7a. Afterward, the maximum axial displacement decreases to 0.696m at 2.9s.

Unlike load case 1, the pipeline axial displacement for load case 4 increases significantly from 0.34m at time 2.4s and continue to increase until it reaches maximum axial displacement of 1.71m at time 2.7 as shown in Figure 5 - 6b. Afterward, the maximum axial displacement decreases to 0.97m at 2.9s.

From the analysis, load cases 2, 3 and 6 also show similar behavior as in load case 1 and 4. The axial displacement graph during the pull-over load for load case 2, 3 and 6 are presented in appendix C.

Figure 5 - 7 shows the axial displacement of the pipeline for load case 5. As shown in the graph, the pipeline has considerable axial displacement for KP 0.92 to KP 1.06 compared to the rest of the pipeline, while the axial displacement of the pipeline drops to 0m at KP 1.0. For load case 5, the maximum axial displacement is 2.54×10^{-4} m at time 2.3s and gradually decreases to 2.08×10^{-4} m at 2.9s.

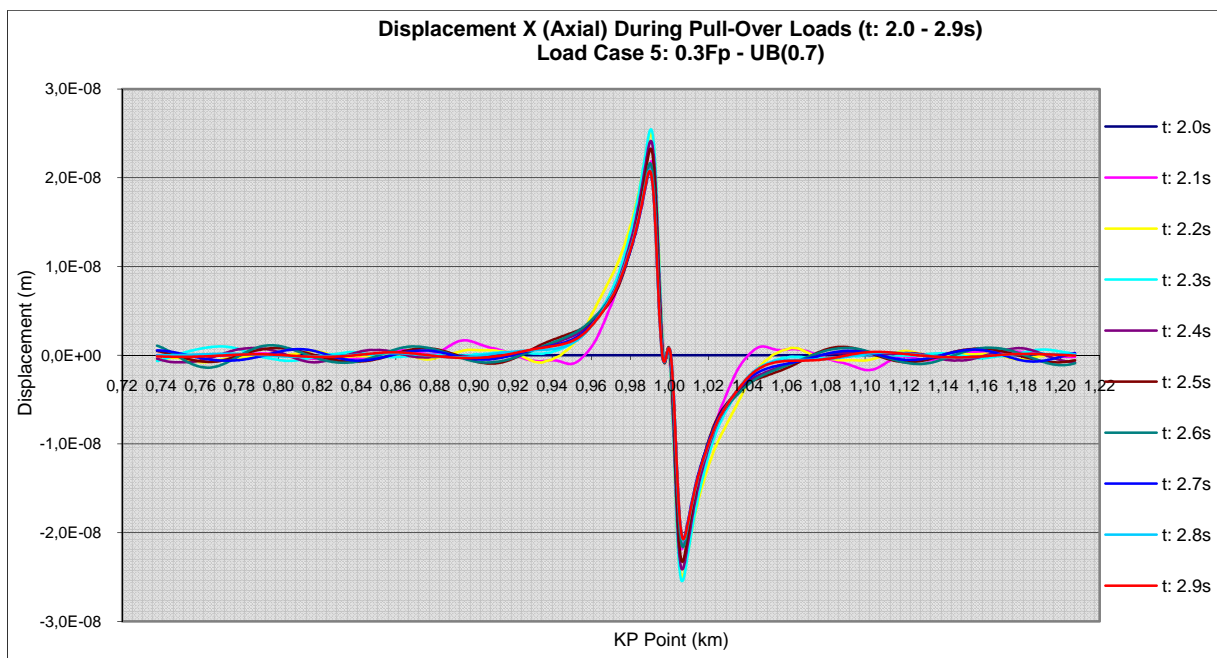


Figure 5 - 7 Axial displacement during pull-over loads duration (t:2.0-2.9s) for load case 5.

The summary of pipeline axial displacement during the pull-over loads duration is presented in Table 5 - 6.

Table 5 - 6 Pipeline axial (X-direction) displacement during pull-over loads duration

Load Case	1	2	3	4	5	6
Pull-over Factor	1.0	0.8	1.0	1.0	0.3	0.8
Lateral Soil friction	0.3	0.3	0.5	0.7	0.7	0.5
time (s)	Displacement (m)					
2.0	8.45E-13	8.33E-13	1.77E-12	3.46E-12	3.46E-12	1.77E-12
2.1	2.89E-04	1.72E-04	1.43E-04	4.57E-05	2.19E-08	5.90E-05
2.2	1.30E-02	6.64E-03	4.62E-03	9.68E-04	2.50E-08	1.81E-03
2.3	0.27	0.18	0.15	2.32E-02	2.54E-08	5.43E-02
2.4	0.82	0.72	0.65	0.34	2.41E-08	0.48
2.5	1.36	1.25	1.19	0.89	2.32E-08	1.03
2.6	1.73	1.70	1.68	1.42	2.16E-08	1.55
2.7	1.38	1.46	1.52	1.71	2.07E-08	1.64
2.8	1.01	1.07	1.12	1.33	2.09E-08	1.22
2.9	6.96	0.74	0.79	0.97	2.08E-08	0.88

b) After Pull-over Loads Duration (t:3.0s-8.0s)

This section gives results of axial (X-direction) displacement for load case 1 to load case 6 after pull-over load duration from time 3.0s to 8.0s in every 0.5s time steps increment.

Figure 5 - 8a & b show that the axial displacement on the pipeline has similar behavior as the behavior during pull-over load duration. The slip regions of the buckle have identical axial displacement along the pipeline for every time steps. The axial displacement increases gradually from the end of the pipeline to the mid of pipeline until it reaches the maximum displacement at approximately KP 0.98 on the left side and KP 1.02 on the right side. The axial displacement decreases significantly to 0m at the pull-over force location, i.e. at KP 1.0 for every time step increment.

The axial displacement for load case 1 continuously increases after time 2.9s. At time 3.0s, the maximum axial displacement is 0.733m and increases to 0.985m at 4.5s. The displacement becomes constant at 1m from time 5.0s to 8.0s. Meanwhile for load case 4, the axial displacement decreases from 0.88m at time 2.9s to 0.64m at time 3.0s. Afterward, the axial displacement increases to 0.98m at time 3.5s and becomes constant at approximately 1.08m until time 8.0s.

From the analysis, load cases 2, 3 and 6 also show similar behavior as in load case 1 and 4. The axial displacement graph during the pull-over load for load case 2, 3 and 6 are presented in appendix C.

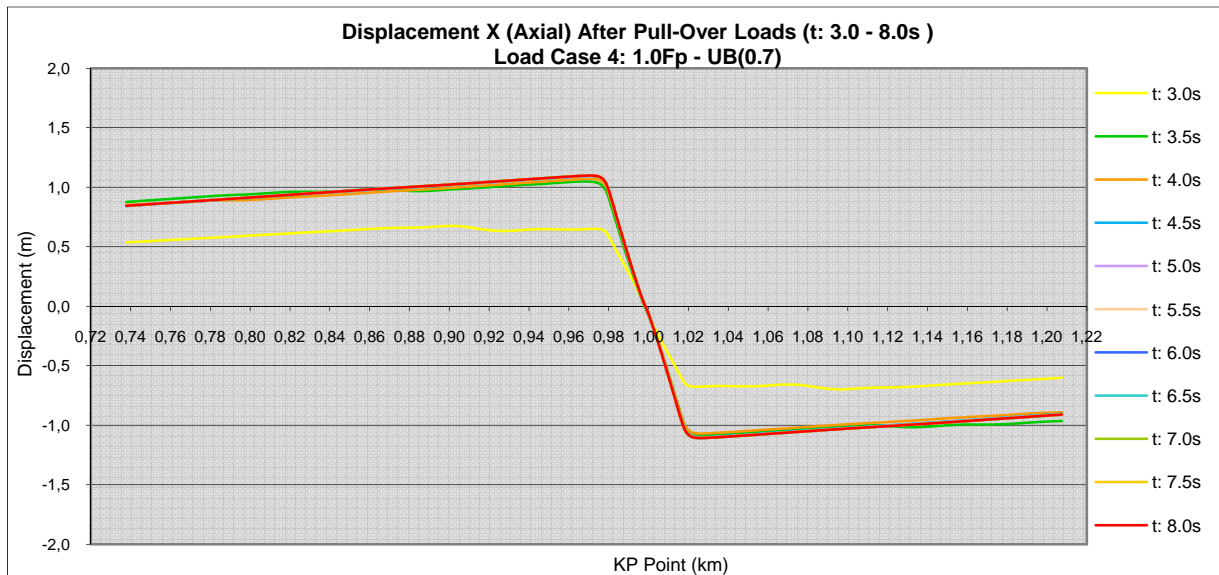
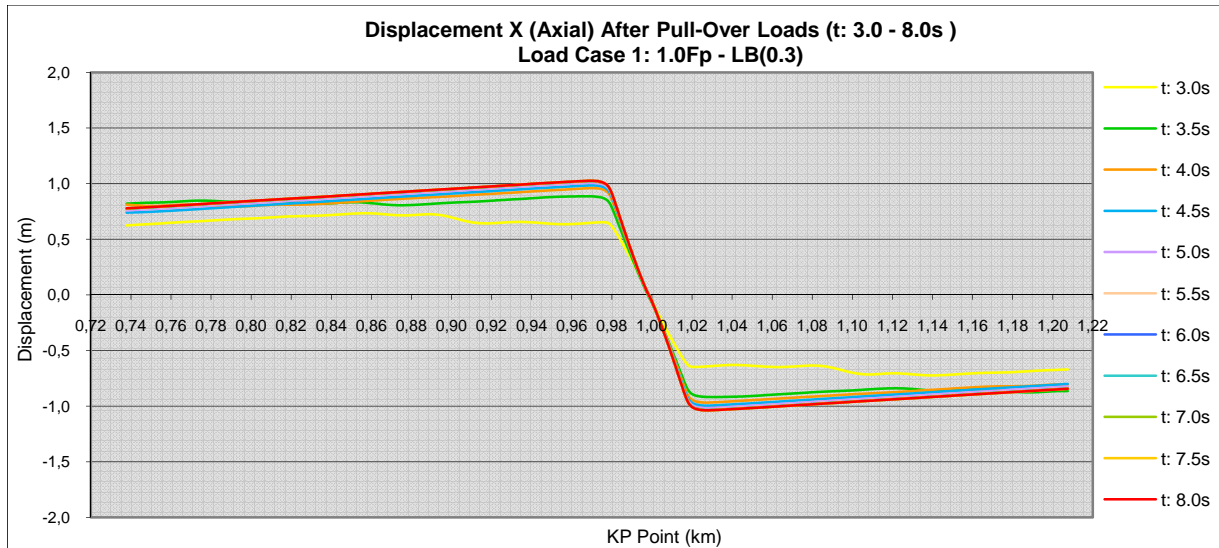


Figure 5 - 8 Axial displacement after pull-over loads duration (t:3.0-8.0s)
Load Case 1(above): 100% pull-over forces with lower bound soil friction factor: 0.3
Load Case 4 (below): 100% pull-over forces with upper bound soil friction factor: 0.7

Figure 5 - 9 shows the axial displacement of the pipeline for load case 5. As shown in the graph, the pipeline has significant axial displacement at location KP 0.99 to KP 1.01. The graph also shows that the axial displacement of the pipe drops to 0m at KP 1.0. The maximum axial displacement after pull-over load duration is constant at 2.06×10^{-4} m.

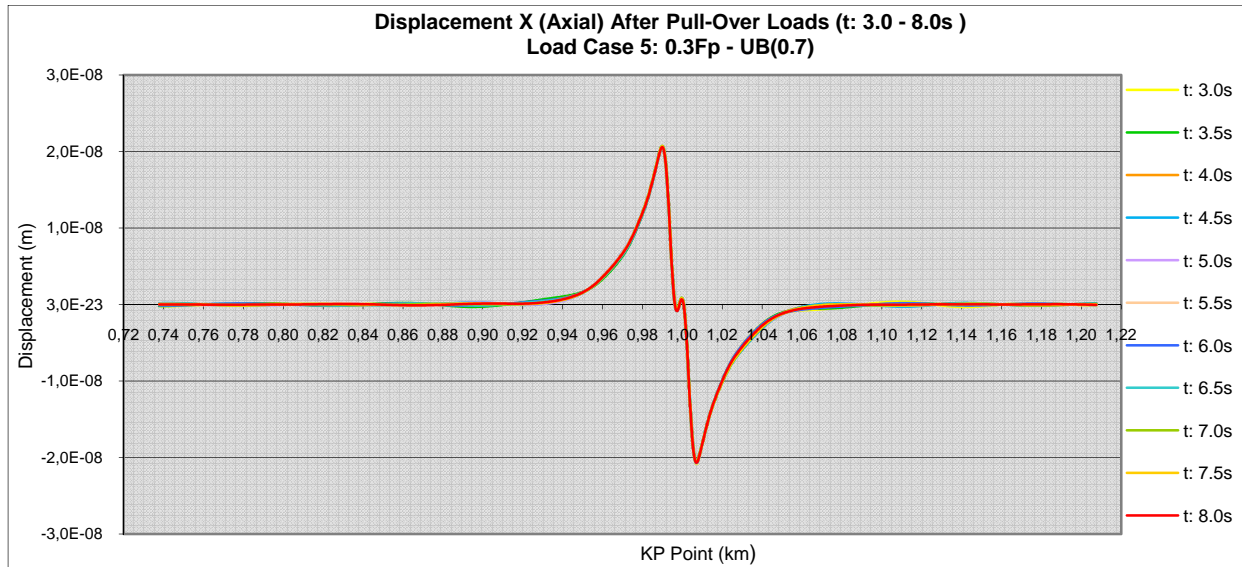


Figure 5 - 9 Axial displacement after pull-over load duration (t:3.0-8.0s) for load case 5.

The summary of axial displacement after pull-over loads duration is tabulated in Table 5 - 7.

Table 5 - 7 Pipeline axial (X-direction) displacement after pull-over loads duration

Load Case	1	2	3	4	5	6
Pull-over Factor	1.0	0.8	1.0	1.0	0.3	0.8
Lateral Soil friction	0.3	0.3	0.5	0.7	0.7	0.5
time (s)	Displacement (m)					
3.0	0.73	0.69	0.67	0.68	2.07E-08	0.64
3.5	0.89	0.90	0.95	1.05	2.06E-08	0.98
4.0	0.96	0.97	1.03	1.07	2.06E-08	1.03
4.5	0.99	0.98	1.05	1.09	2.07E-08	1.06
5.0	1.01	1.01	1.07	1.10	2.06E-08	1.07
5.5	1.02	1.02	1.07	1.10	2.05E-08	1.08
6.0	1.02	1.03	1.08	1.10	2.05E-08	1.08
6.5	1.02	1.03	1.08	1.10	2.06E-08	1.08
7.0	1.02	1.03	1.08	1.10	2.07E-08	1.08
7.5	1.03	1.03	1.08	1.10	2.07E-08	1.08
8.0	1.03	1.03	1.08	1.10	2.05E-08	1.08

5.4.3. Bending Moments

a) During Pull-Over Loads Duration (t:2.0s-2.9s)

This section gives results of bending moments for load case 1 to load case 6 during pull-over load duration. The bending moments are extracted from the finite element analysis results. The pull-over force

starts to be applied at time 2s in the nonlinear transient analysis using ANSYS mechanical APDL. The pull over duration for the polyvalent & rectangular trawl board is 0.687s as mentioned in section 4.8.

Figure 5 - 10 gives results of the bending moments from KP 0.738 to KP 1.21 for load cases 1 (above) and 4 (below). These KPs are selected as these are the location with significant results. The graph shows the bending moments at the pipeline from time 2.0s to 2.9s for every 0.1s time step increment. Both load cases applied 100% of the pull-over force combine with lateral soil friction factor of 0.3 for load case 1 and 0.7 for load case 4.

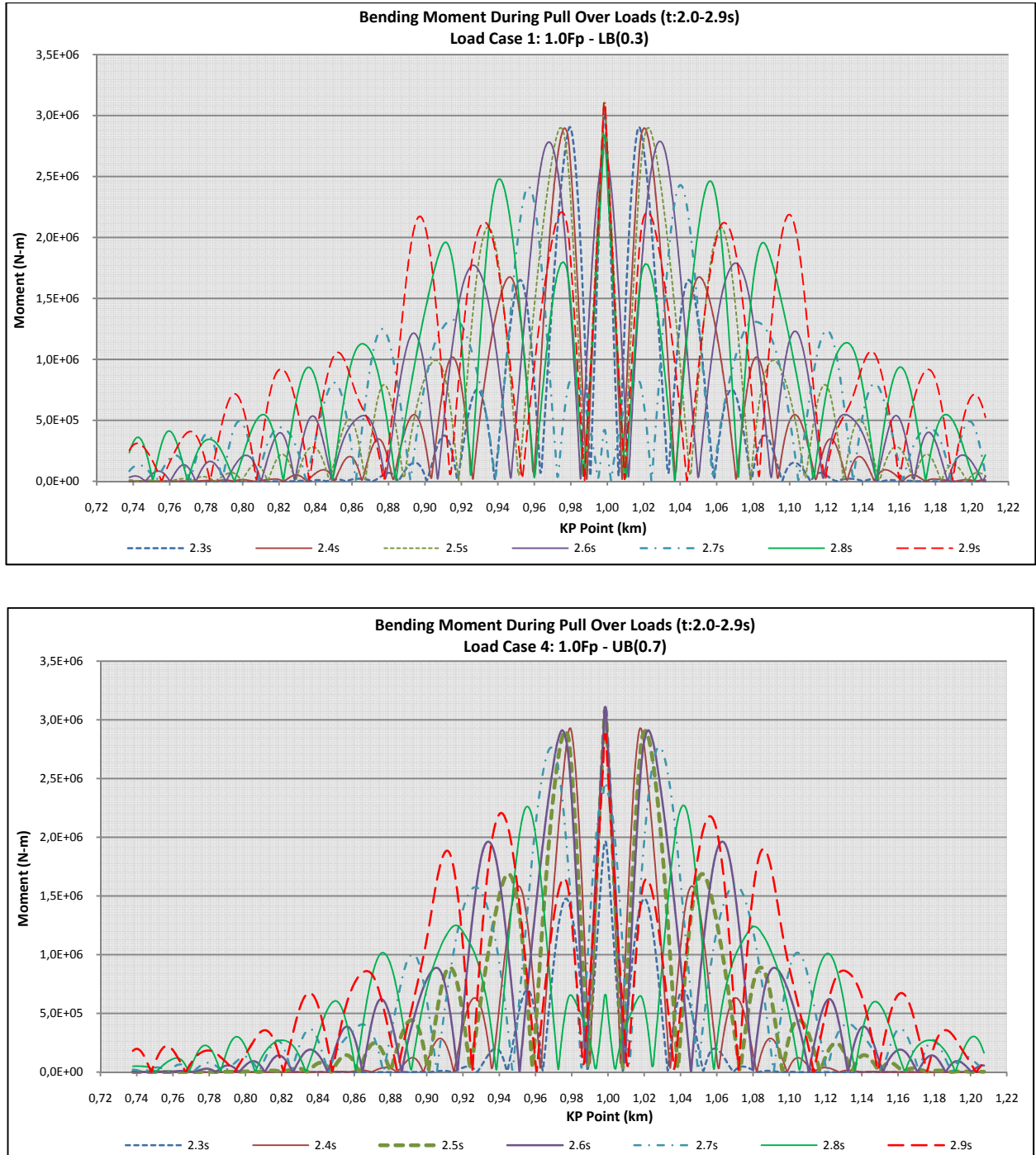


Figure 5 - 10 Bending moments during pull-over loads duration (t:2.0-2.9s)
Load Case 1(above): 100% pull-over forces with lower bound soil friction factor: 0.3
Load Case 4 (below): 100% pull-over forces with upper bound soil friction factor: 0.7

Figure 5 - 10a shows the bending moments on the pipeline for load case 1. The graph shows that the bending moments during the pull-over load has maximum value at pull-over force location, i.e. at KP 1.0. The graph also shows that the bending moment's distribution at the left and the right side are identical.

The bending moments increases significantly from time 2.0s to 2.3s. At time 2.3s, the maximum bending moment is 3013.2 kN-m and it increases to 3102.2 kN-m at time 2.5s. The bending moments decreases to 2430 kN-m at 2.7s and increases again to 3103.4 kN-m at 2.9s. The bending moment at time 2.9s is the maximum bending moment for load case 1. All max bending moments occur at pull-over force location, i.e. at KP 1.0.

Figure 5 - 10b shows the bending moments on the pipeline for load case 4. The bending moment's distribution shows the same behavior with load case 1. The bending moment increases significantly from 2.0s to 2.4s. The maximum bending moment at 2.4s is 3030 kN-m at KP 1.0. It continues to increase to the value of 3110 kN-m at 2.6s. This is the maximum bending moment for load case 4. Then, the bending moment goes down to 2270 kN-m at 2.8s. At 2.9s, the maximum bending moment is 2880 kN-m at KP 1.0.

As shown in Figure 5 - 10, the maximum bending moment for load case 1 and 4 are occurred at KP 1.0. This is the location of pull-over force. The graph shows that during pull-over load duration, the maximum bending moment is not always occurred at KP 1.0. The maximum value at certain time steps might be located at the slip region. But, the maximum bending moment for each load case is always occurred at KP 1.0.

The same bending moments distribution also happen at load case 2, 3, and 6, except load case 5. There is no lateral buckling occurred in load case 5. The bending moment's distribution graph for load case 2, 3, 5 and 6 are also presented in appendix D. The summary of bending moments during the pull-over load is tabulated in Table 5 - 8 below.

Table 5 - 8 Pipeline bending moments during pull-over loads duration

Load Case	1	2	3	4	5	6
Pull-over Factor	1.0	0.8	1.0	1.0	0.3	0.8
Lateral Soil friction	0.3	0.3	0.5	0.7	0.7	0.5
time (s)	Moment (kN-m)					
2.0	3.5E-13	4.0E-13	3.57E-13	3.6E-13	3.49E-13	3.7E-13
2.1	612.0	484.6	452.2	314.2	21.60	341.2
2.2	1730.0	1455.8	1330.7	808.8	21.03	996.0
2.3	3013.2	2948.9	2864.6	1960.6	20.17	2378.1
2.4	3071.6	3056.8	3056.9	3025.2	18.35	3039.7
2.5	3102.2	3091.9	3094.7	3075.0	16.51	3079.9
2.6	2787.7	3056.4	3101.9	3105.1	14.72	3106.4
2.7	2429.6	2495.0	2582.4	2769.9	11.51	2727.0
2.8	2836.2	2517.5	2312.7	2272.5	11.44	2201.9
2.9	3103.4	3094.6	3090.6	2877.5	11.52	3006.3

b) After Pull-over Loads Duration (t:3.0s-8.0s)

This section shows the bending moments from KP 0.738 to KP 1.21 for load case 1 to load case 6 after pull-over load duration. The graphs show the distribution of bending moments from time 3.0s to 8.0s every 0.5s time steps.

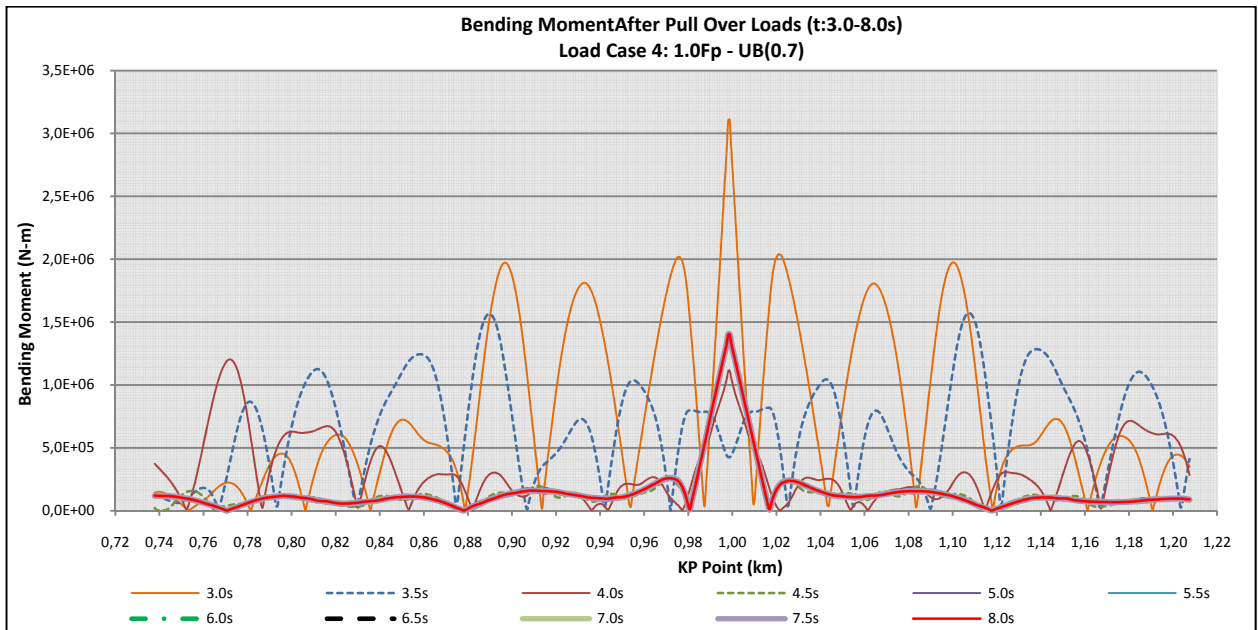
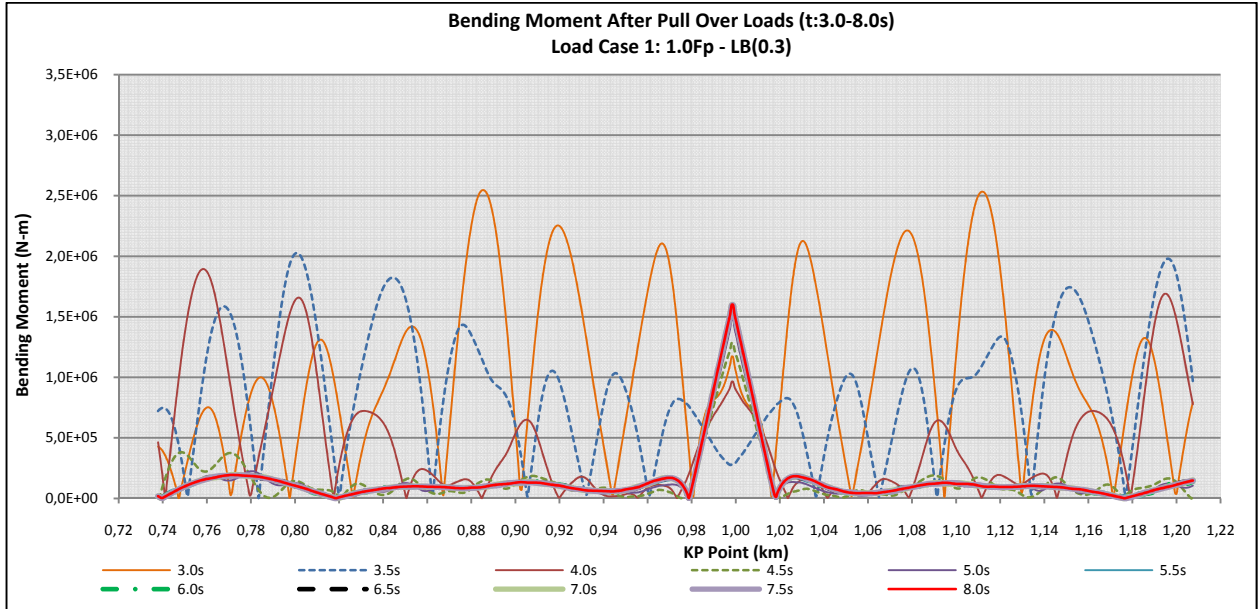


Figure 5 - 11 Bending moments after pull-over loads duration (t:3.0-8.0s)
Load Case 1 (above): 100% pull-over forces with lower bound soil friction factor: 0.3
Load Case 4 (below): 100% pull-over forces with upper bound soil friction factor: 0.7

Figure 5 - 11a shows the bending moments distribution for load case 1. The graph shows that at 3.0s, the maximum bending moment of 2546.4 kN-m is not occurred at KP 1.0. This value is occurred at KP 0.89. The maximum bending moment gradually goes down to 1280 kN-m at 4.5s. Then, it increases to 1580.2 kN-m at 6.5s and constant until 8.0s.

Figure 5 - 11a shows that the distribution of bending moment outside KP 0.98 to KP 1.02 is much smaller and almost flat than the maximum value at the buckle region. At the buckle region from KP 0.98 to 1.02, the bending moments have steep distribution. These distributions consist with the lateral displacement on the pipeline in the same KP range.

Figure 5 - 11b shows the distribution of bending moment for load case 4. The bending moment's distribution shows the same behavior distribution with load case 1, except for time 3.0s. At 3.0s, the maximum bending moment is occurred at KP 1.0. At this time, the bending moment reaches maximum value of 3110 kN-m as at 2.6s. Then, the bending moment goes down drastically to 1200 kN-m at 4.0s and constant at 1400 kN-m since 6.0s until 8.0s.

As for load case 1, the distribution of bending moment for load case 4 outside KP 0.98 to KP 1.02 is much smaller and almost flat than the bending moment at the buckle region. At the buckle region from KP 0.98 to 1.02, the bending moments have steep distribution. These distributions consist with the distribution of lateral displacement on the pipeline.

The similar bending moment distribution also found for load case 2, 3 and 6. For load case 5, the distribution of bending moment is very small and almost flat along the pipeline since no lateral buckling is occurred. The graph for load case 2, 3 and 6 are also presented in appendix C. The Summary of bending moments after the pull-over load is tabulated in Table 5 - 9.

Table 5 - 9 Pipeline bending moments after pull-over loads duration

Load Case	1	2	3	4	5	6
Pull-over Factor	1.0	0.8	1.0	1.0	0.3	0.8
Lateral Soil friction	0.3	0.3	0.5	0.7	0.7	0.5
time (s)	Moment (kN-m)					
3.0	2546.4	2493.6	2278.0	3108.4	11.5	2921.1
3.5	2026.9	1977.7	1568.6	1572.1	11.5	1624.6
4.0	1894.1	1906.6	1600.6	1203.6	11.5	1611.3
4.5	1894.1	1906.6	1575.7	1387.6	11.5	1506.6
5.0	1281.0	1265.6	1657.4	1396.9	11.5	1598.3
5.5	1480.9	1418.2	1653.0	1391.2	11.5	1622.4
6.0	1546.0	1508.9	1672.4	1400.0	11.5	1615.2
6.5	1580.2	1528.2	1681.2	1397.3	11.5	1624.1
7.0	1586.7	1553.8	1681.4	1404.7	11.5	1618.7
7.5	1594.6	1562.6	1680.1	1401.0	11.5	1623.7
8.0	1592.9	1566.6	1681.1	1399.2	11.5	1622.3

5.4.4. Effective Axial Force

a) During Pull-over Loads Duration (t:2.0s-2.9s)

This section presents the effective axial force on the pipeline for load case 1 to load case 6 during pull-over load duration. The graphs show the effective axial for from KP 0.738 to KP 1.21 for every 0.1s time steps. The effective axial forces are calculated from the true axial forces based on the effective axial force

formulae on DNV OS F101 [1]. The values of true axial forces are extracted from the finite element analysis results

Figure 5 - 12 shows the effective axial force for load case 1 and 4. Both of the load case shows the similar distribution of effective axial force along the pipeline. The negative sign indicates the pipeline is under compressive force. At time 2.0s, the effective axial force is $-1.01 \times 10^4 \text{ kN}$. The effective axial force significantly drops to the average value of $-3.7 \times 10^3 \text{ kN}$ at 2.3s for load case 1 and at 2.4s at load case 4. Then, it continuously increases and reaches equilibrium level at $6.7 \times 10^3 \text{ kN}$ at time 2.9s.

As shown in the graph, there is small tip around KP 1.0, where the pull-over load is applied. This small tip starts to appear when the effective axial force reached the average value of $-3.7 \times 10^3 \text{ kN}$. After that, the scale of small tip is constant along the rest of pull-over load duration.

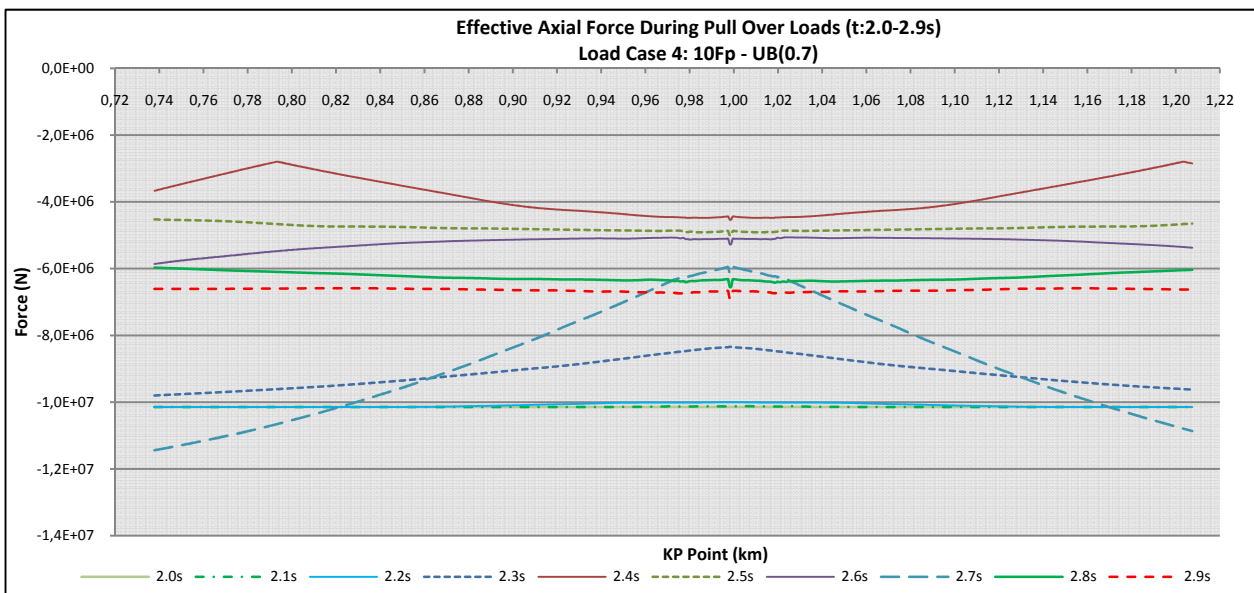
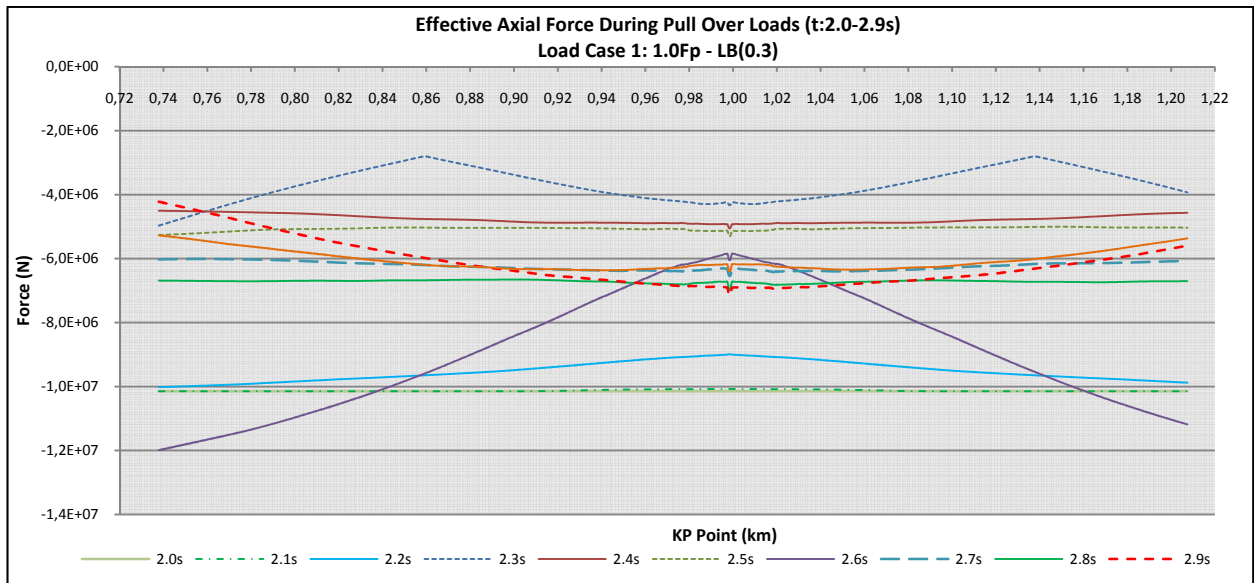


Figure 5 - 12 Effective axial force during pull-over loads durations (t:2.0-2.9s)
Load Case 1(above): 100% pull-over forces with lower bound soil friction factor: 0.3
Load Case 4 (below): 100% pull-over forces with upper bound soil friction factor: 0.7

b) After Pull-over Loads Duration (t:3.0-8.0s)

This section presents the effective axial force for load case 1 to load case 6 after pull-over load duration. The graphs show the effective axial for from KP 0.738 to KP 1.21 for every 0.5s time steps. The effective axial forces are calculated from the true axial forces based on the effective axial force formulae on DNV OS F101 [1]. The values of true axial forces are extracted from the finite element analysis results.

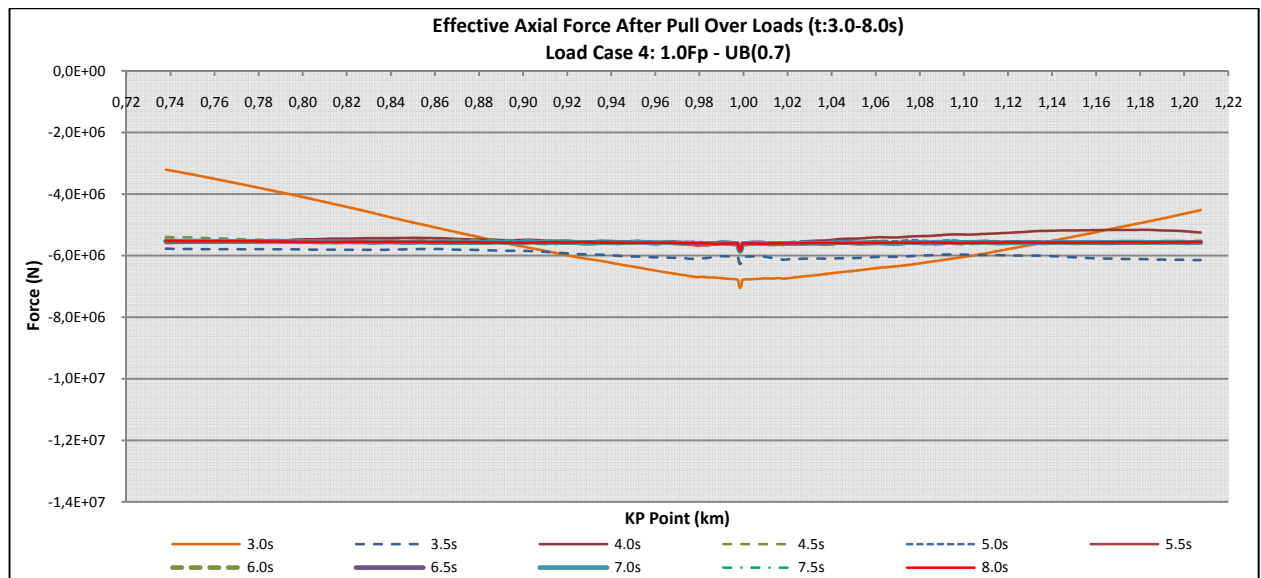
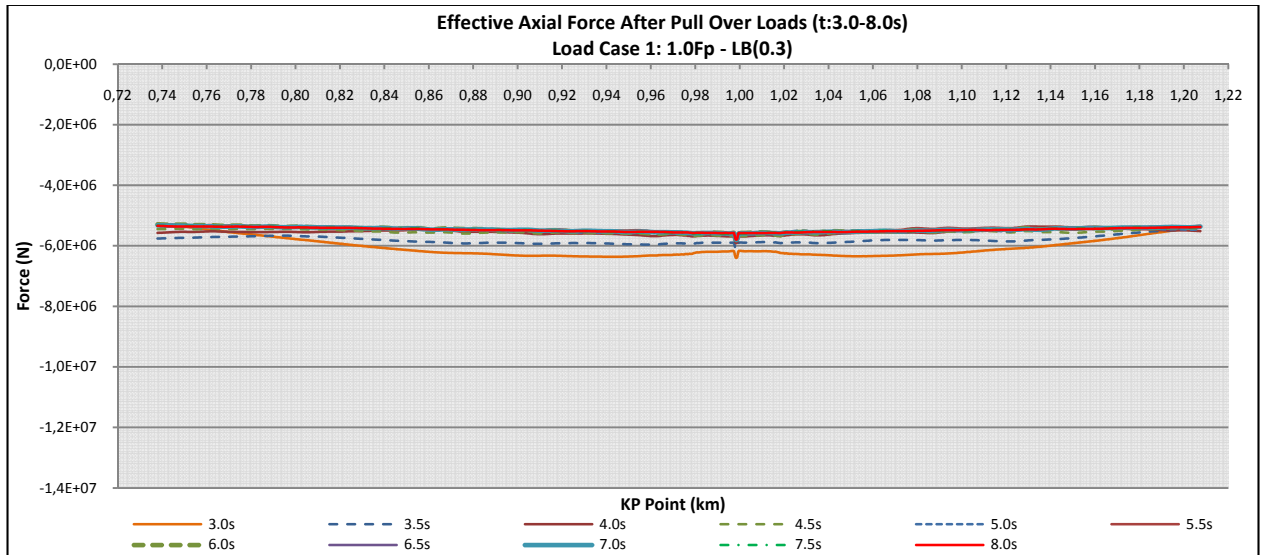


Figure 5 - 13 Effective axial force after pull-over loads duration (t:3.0-8.0s)
Load Case 1(above): 100% pull-over forces with lower bound soil friction factor: 0.3
Load Case 4 (below): 100% pull-over forces with upper bound soil friction factor: 0.7

Figure 5 - 13 shows the effective axial force for load case 1 and 4. Both of the load case shows the similar distribution of effective axial force along the pipeline. The negative effective axial force indicates the pipeline is under compressive force.

The graphs show both load case 1 and 4 have reached equilibrium level of effective axial force since time 4s. At time 8.0s, the average effective axial force is -5.6×10^3 kN. As seen on the graph, the small tip at KP 1.0 still exists till time 8.0s.

5.4.5. Equivalent Strain

a) During Pull-over Loads Duration (t:2.0s-2.9s)

This section presents the equivalent strain for load case 1 to load case 6 during pull-over load duration. The equivalent strain values are extracted from the finite element analysis results. The graphs show the equivalent strain for from KP 0.738 to KP 1.21 for every 0.1s time steps.

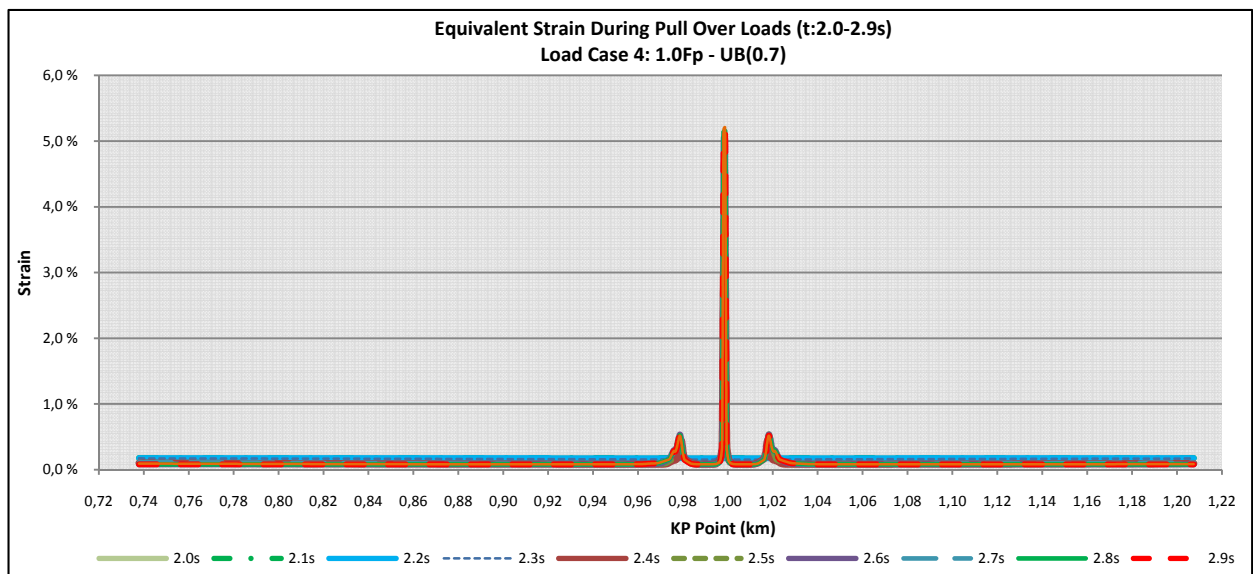
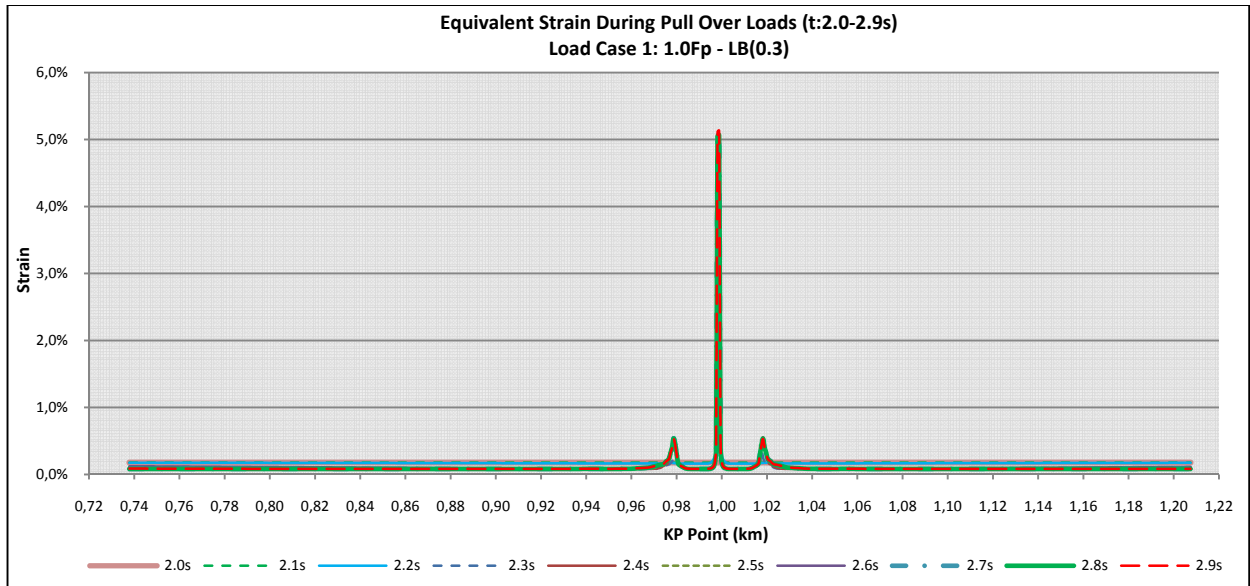


Figure 5 - 14 Equivalent strain during pull-over loads duration (t:2.0-2.9s)
Load Case 1(above): 100% pull-over forces with lower bound soil friction factor: 0.3
Load Case 4 (below): 100% pull-over forces with upper bound soil friction factor: 0.7

Figure 5 - 14 shows the equivalent strain on the pipeline during pull-over load duration for load case 1 and 4. From Figure 5 - 14a above, the maximum equivalent strain at 2.0s is 0.18%. The maximum equivalent strain increases significantly to 3.2% at 2.3s and continues to increase to 5.08% at 2.6s. The maximum equivalent strain remind constant at 5.08% until time 2.8s before it reaches a value of 5.13% at 2.9s. This is the maximum equivalent strain for load case 1 during pull-over load duration.

From Figure 5 - 14b, the maximum equivalent strain reaches 3.26% at time 2.4s from 0.18% at 2.0s. It gradually increase to 5.16% at 2.7s before it goes down to 5.13% at 2.9s. This is the maximum strain for load case 4 during pull-over load duration. The maximum equivalent strain is occurred at KP 1.0 for all time steps.

The summary of equivalent strain during the pull-over load duration is tabulated in Table 5 - 10 below. The graphs for load case 2, 3 and 6 are also presented in appendix C.

Table 5 - 10 Equivalent strain during pull-over loads duration

Load Case	1	2	3	4	5	6
Pull-over Factor	1.0	0.8	1.0	1.0	0.3	0.8
Lateral Soil friction	0.3	0.3	0.5	0.7	0.7	0.5
time (s)	Equivalent Strain (%)					
2.0	0.18	0.18	0.18	0.18	0.18	0.18
2.1	0.18	0.18	0.18	0.18	0.18	0.18
2.2	0.41	0.24	0.21	0.18	0.18	0.18
2.3	3.16	2.79	2.83	0.70	0.18	1.64
2.4	4.17	3.78	3.81	3.26	0.18	3.32
2.5	4.94	4.73	4.82	4.31	0.18	4.44
2.6	5.08	4.96	5.14	5.04	0.18	4.99
2.7	5.08	4.95	5.13	5.16	0.18	4.99
2.8	5.06	4.93	5.12	5.15	0.18	4.99
2.9	5.13	4.98	5.14	5.13	0.18	4.96

b) After Pull-over Loads Duration (t:3.0-8.0s)

This section presents the equivalent strain for load case 1 to load case 6 after pull-over load duration. The graphs show the equivalent strain for from KP 0.738 to KP 1.21 for every 0.5s time steps.

Figure 5 - 15 shows the equivalent strain after the pull-over duration for load case 1 and 4. The graphs show the identical pattern with the equivalent strain graphs during pull-over load duration.

For load case 1, the maximum equivalent strain at time 3.0s is 5.18% and constant at this value till time 4.5s. Then, the equivalent strain increases to 5.19% at 5.0s till 8.0s.

For load case 4, the maximum equivalent strain at time 3.0s is 5.21%. Then, the equivalent strain increases to 5.23% at 3.5s till 8.0s.

The equivalent strain graphs for load case 2, 3 and 6 are also presented in appendix C.

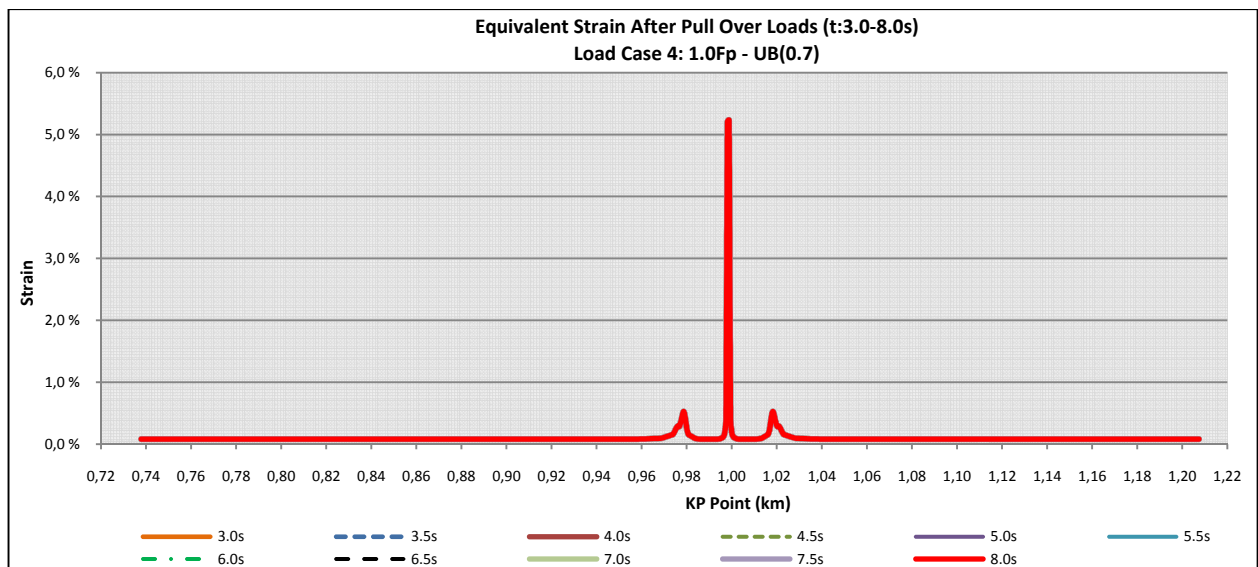
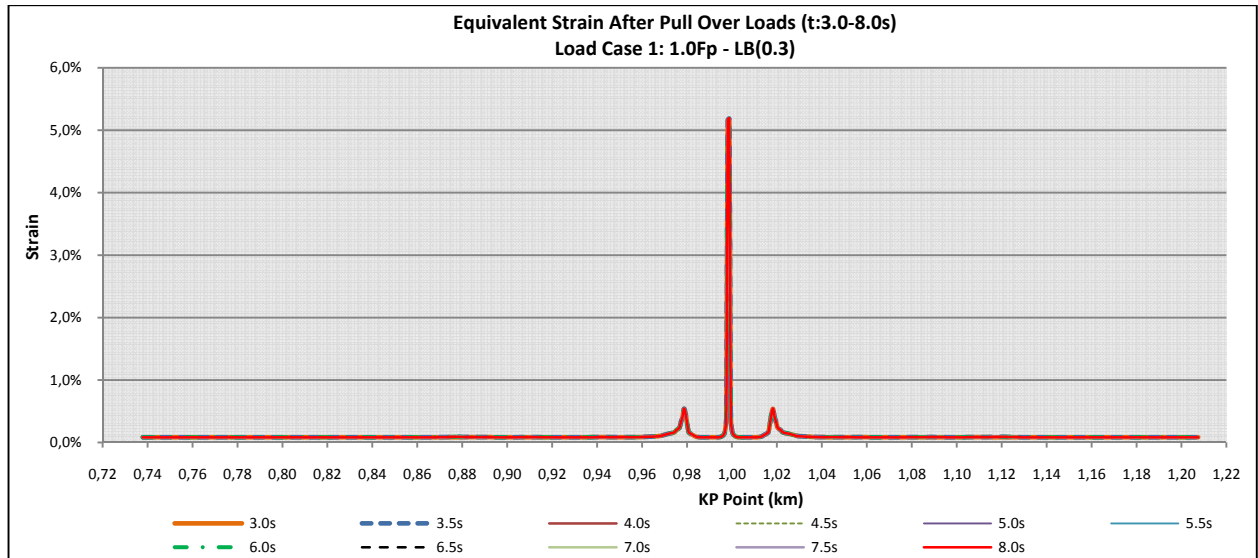


Figure 5 - 15 Equivalent strain after pull-over loads duration (t:3.0-8.0s)
Load Case 1(above): 100% pull-over forces with lower bound soil friction factor: 0.3
Load Case 4 (below): 100% pull-over forces with upper bound soil friction factor: 0.7

The Summary of equivalent strain after pull-over loads duration is tabulated in Table 5 - 11.

Table 5 - 11 Pipeline equivalent strain after pull-over loads duration

Load Case	1	2	3	4	5	6
Pull-over Factor	1.0	0.8	1.0	1.0	0.3	0.8
Lateral Soil friction	0.3	0.3	0.5	0.7	0.7	0.5
time (s)	Equivalent Strain (%)					
3.0	5.18	5.04	5.22	5.21	0.18	5.07
3.5		5.05	5.23	5.23		5.09
4.0						
4.5						
5.0	5.19				5.05	
5.5						
6.0						
6.5						
7.0						
7.5						
8.0						

5.5. Discussion

5.5.1. During Pull-over Loads Duration (t: 2.0s – 2.9s)

As presented in section 5.4, the pull-over analysis shows that the pull-over force from trawl board induces lateral buckling on HT/HP pipeline. During pull-over load duration, the pull-over force pushes the pipeline to move laterally resulting in lateral buckling at the point where the pull-over force is applied. It also induces several small buckle shapes on the pipeline as shown in Figure 5 - 2 and Figure 5 - 4. The lateral displacement on the pipeline increases based on the increment of the pull-over force magnitude. Meanwhile, the magnitude of pull-over force varies based on the time history of pull-over force.

The pipeline starts to move laterally immediately after the pull-over force is applied. The pipeline continues to expand laterally until it reaches the maximum displacements during pull-over duration at time 2.7s. The buckle amplitudes of the buckle region and its slip regions can be seen in Figure 5 - 2.

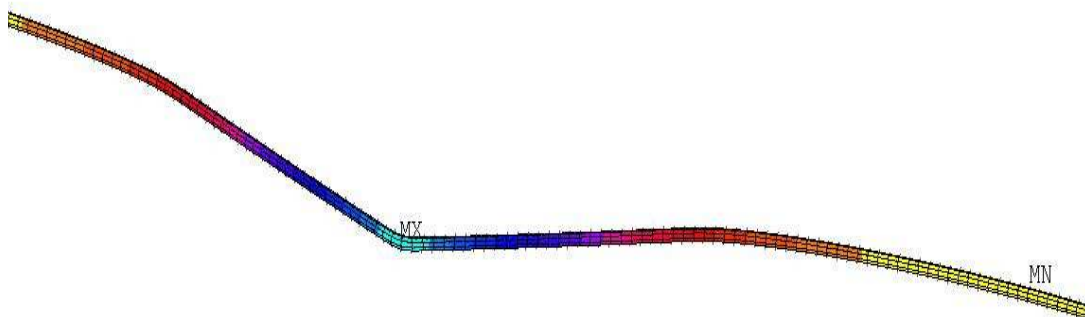


Figure 5 - 16 FEA result: pipeline lateral buckling profile for load case 1

This phenomenon can also be indicated from the effective axial forces distribution on pipeline. From Figure 5-13a, the pipeline releases a large effective compressive force immediately after the application of full pull-over force i.e. from time 2.2s to 2.3s. The effective axial force at time 2.2s is approximately $-10 \times 10^3 \text{ kN}$ and reduces to the average of $-3.8 \times 10^3 \text{ kN}$ at time 2.3s. The effective axial force significantly becomes less as the result of the forming of buckle due to pull-over force on the pipeline.

The pipeline expands significantly from time 2.3s to 2.6s as shown in Figure 5 - 6a. The slip region continues to expand and feed into the buckle region. Since the pipeline is under compression, it will deform globally in order to reduce the compression force and to find a new equilibrium shape. As the pull-over force continuously pushes the pipeline in lateral direction, the compressive axial force at the slip regions increases significantly. From Figure 5 - 12a, it is shown that at time 2.6s, the compressive axial force at the slip regions is higher than the force at buckle region. This significant increment of the effective axial force at the slip region is caused by pipeline's axial expansion due to thermal and pressure loads.

At time 2.7s, the pipeline lateral displacement reaches its maximum value and the effective axial force at the slip and the buckle regions become flat. As the pull-over forces disappear, pipeline axial expansion also decreases as shown in Figure 5 - 6a. These conditions cause the buckle amplitude to decrease as shown in Figure 5 - 2 and Figure 5 - 17.

The summary of maximum lateral displacement of the pipeline for all load cases is presented in Table 5 - 12. The table shows the maximum lateral displacement during the pull-over load duration and after the pull-over load duration.

Table 5 - 12 Summary of maximum lateral displacement

Load Case No.	Pull-Over Factor	Lateral Soil Friction (μ_{lat})	Maximum Lateral Displacement (m)	
			During Pull-Over Loads	After Pull-Over Loads
1	1.0	0.3	6.91	7.27
2	0.8	0.3	6.74	6.91
3	1.0	0.5	6.88	7.11
4	1.0	0.7	6.77	6.88
5	0.3	0.7	7.66E-04	6.94E-04
6	0.8	0.5	6.81	6.94

5.5.2. After Pull-over Loads Duration (t: 3.0s-8.0s)

Figure 5 - 4 shows the pipeline's lateral displacement after pull-over load duration i.e. from time 3.0s to 8.0s. From Figure 5 - 4, it can be seen that the buckle further increases after pull-over forces are no longer applied. At time 3.0s and 3.5s, several small buckles still appear at the slip region as seen during pull-over load duration. Afterward, the buckle amplitudes at the slip region close to the buckle region become less apparent at time 3.5s. This indicates that the slip region still continue to expand and feed into the buckle until time 3.5s.

This phenomenon can also be clearly indicated from the pipeline axial displacement (pipeline expansion) as shown in Figure 5 - 8a for load case 1. It can be seen that the axial displacement decreases from time 2.6s until 3.0s before it starts increasing from time 3.0s. This condition shows that the axial feed-in from the slip region into the buckle increases. The slip regions expand axially and deform globally in order to become straight pipeline. This deformation at the slip regions pushes the buckle to expand even further as the buckle length is longer than the straight length.

From Figure 5 - 13, it is also shown that the compressive force along the pipeline is reduced and becomes constant. The pipeline continuously deforms to release the compressive force until it reaches the equilibrium shape. This is described by higher effective compressive force at time 3.0s compared to at time 5.0s. The pipeline reaches the average effective axial force of $-5.5 \times 10^3 \text{ kN}$ at time 5.0s and becomes constant at this level until time 8.0s.

5.5.3. Buckle Amplitude

Table 5 - 12 and Figure 5 - 17 show that the maximum lateral displacement after pull-over loads duration is higher than the displacement during pull-over loads duration. For load case 1, the maximum lateral displacement during pull-over loads duration is 6.91m. The displacement then increased to 7.27m after pull-over loads duration and becomes constant at this value until time 8.0s. Similar trend also applies to load case 4, the maximum lateral displacement during pull-over loads duration is 6.77m and continuously increased to 6.88m after pull-over loads duration.

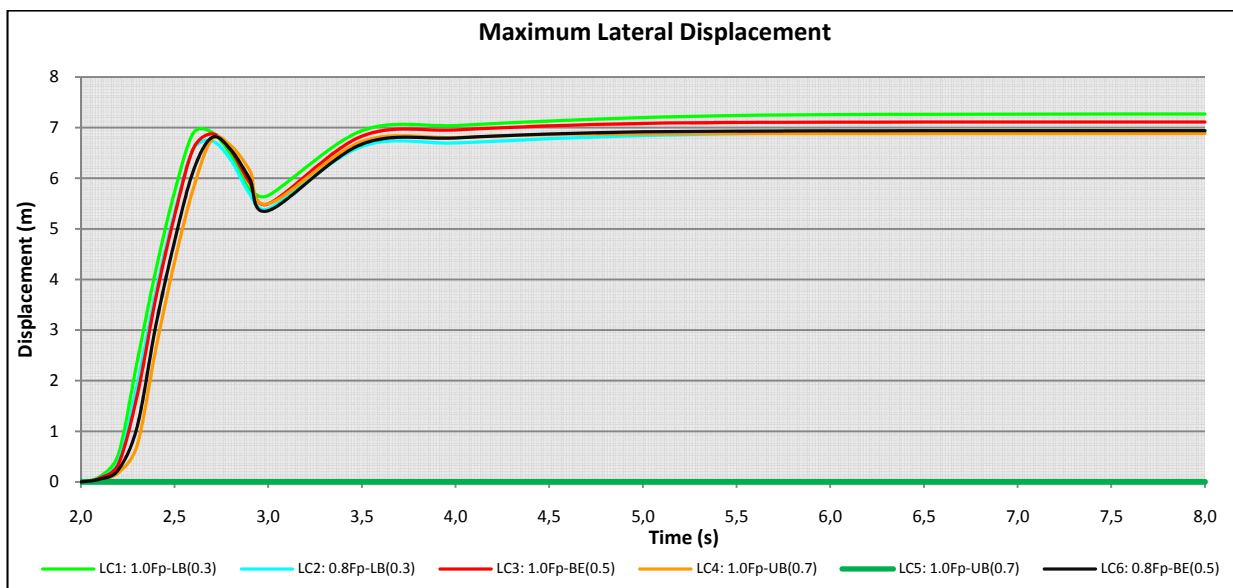


Figure 5 - 17 Pipeline maximum lateral displacement from time 2.0s to 8.0s

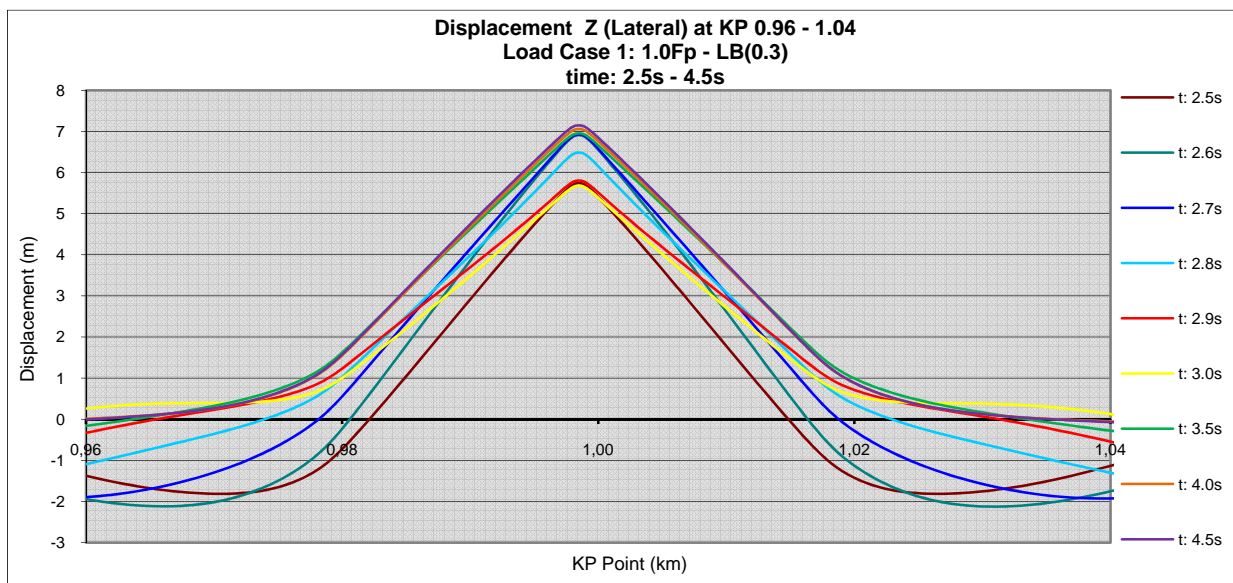


Figure 5 - 18 Pipeline lateral displacement at buckle region from time 2.5 to 4.5s for load case 1.

As shown in Figure 5 - 17, the pipeline tends to shrink at the end of pull-over loads duration when the pull-over forces are no longer applied. Afterward, the pipeline tends to expand and increase the buckle amplitude of the lateral buckling before it reaches the equilibrium form. This trend is also applicable for load cases 2, 3 and 6, except for load case 5 where no lateral buckling was occurred. The same trend can also be seen in Figure 5 - 18 showing the pipeline's lateral displacement at KP 0.96 to 1.04 from time 2.5s to time 4.5s.

This phenomenon can be clearly explained by the effective axial force distribution on pipeline. Figure 5 - 12 shows that when the pull-over loads are applied, the effective axial force on the pipeline decreases significantly. This can be seen by the changes of the effective axial force from the average value of -9.5×10^3 kN at time 2.2s and drops to the average value of -3.7×10^3 kN at time 2.3s (negative value indicates compression force). The pull-over forces push the pipeline to move laterally and trigger lateral buckling. As the lateral buckle is developed, the effective axial force on the pipeline will reduce.

After time 2.3s, the effective axial force on pipeline significantly increases until it reaches the average value of -6.3×10^4 kN at time 2.7s. Afterward, the increment becomes less. At time 2.8s, the average value of axial force is -6.7×10^3 kN. At this point, the effective axial force becomes the governing force on pipeline.

In Figure 5 - 12, at time 2.6s, the compressive axial force at the slip region are developed significantly compared to the effective axial force at the buckle region. This makes the compressive axial forces at the slip region feed into the buckle region. The significant increment on compressive axial force at time 2.6s causes the pipeline to expand even more and reaches the maximum lateral displacement during pull-over load duration at 2.7s.

The pull-over force continuously pushes the pipeline away laterally with decreasing magnitude of force and become 0 kN at time 2.7s. In the same time, the compressive axial forces that feed into the buckle region become less since the pipeline releases the compression axial force as the result of large deflection on the buckle region. The absent of pull-over forces and less compressive axial force that feed into the buckle cause the pipeline to lose the governing force to continuously move laterally. This makes the pipeline tends to shrink from time 2.7s to 3.0s. The contraction on pipeline is affected by the elasticity of the steel pipe material.

The axial displacement on the pipeline starts to increase from time 3.0s. This indicates the increment of the axial feed-in on the buckle. The pipeline will expand furthermore as shown in Figure 5 - 8 and obtain new equilibrium state in order to reduce the compression by deforming globally. As shown in Figure 5 - 4 and Figure 5 - 17, the pipeline reaches the new equilibrium form at time 4.0s. The post-buckling profile of pipeline can be seen in Figure 5 - 4 as well for load case 1 and 4. The post-buckling profile of pipeline for load cases 2, 3, 5 and 6 can be seen in appendix C.

5.5.4. Lateral Soil Friction

As presented in Table 5 - 4, the maximum lateral displacement or the buckle amplitude for load cases 1, 3 and 4 have no significant difference during pull-over load duration. Load cases 1, 3 and 4 apply 100% of the pull-over forces with various lateral soil friction factors. By using lateral soil friction of 0.3, load case 1 has maximum lateral displacement of 6.91m. For load case 3, the maximum displacement of 6.88m achieved by using lateral soil friction of 0.5. Meanwhile, load case 4 has the maximum lateral displacement of 6.77 with lateral soil friction of 0.7.

The maximum lateral displacement during pull-over duration for load case 2 is 6.74m and for load case 6 is 6.81m. Both of the load cases apply 80% of the pull-over force. The lateral soil friction of 0.3 was used in load case 2. While, the lateral soil friction of 0.5 was used in load case 4.

The results above explain that during pull-over duration, the lateral soil friction does not give significant effect on the lateral displacement. With the variation of the lateral soil friction factor from 0.3 to 0.7, the pipeline will deform into almost similar maximum displacement on the same magnitude of pull-over force.

The variation of lateral soil friction factor only gives variation on the “built-up” rapidity of lateral buckling on the pipeline during pull-over load.

As shown in Figure 5 - 17, the graph for load case 1 at time 2.0s to 2.7s has steeper slope compared to load case 3 and 4. This trend shows that buckles are developed faster on soil with less lateral soil friction factor, since buckle in load case 1 was developed faster compared to load cases 3 and 4. Smaller friction factor makes the pipeline to move even easier in lateral direction due to pull-over forces.

This phenomenon can also be seen in Table 5 - 4. Load case 1 shows more increment on the displacement compared to load case 3 and 4. For example at time 2.3s, the lateral displacement on load case 1 reaches up to 2.37m compared to load case 3 that reaches only 1.70m. Having smaller lateral soil friction factor, load case 1 reaches 40% as far as load case 3. This trend can also be seen on load case 4.

After pull-over duration, the variation of lateral soil friction factor gives significant effect for lateral buckling. Figure 5 - 17 shows that load case 1 has higher buckle amplitude compared to load cases 3 and 4. Referring to Table 5 - 12, the maximum value of buckle amplitude for load case 1 is 7.27m and 7.11m for load case 3 and 6.88m for load case 4. The maximum buckle amplitude for load case 1 increases 0.36m from the maximum buckle amplitude during pull-over loads duration. While, the increment for load case 3 is 0.23m and 0.11m for load case 4. Hence, smaller lateral soil friction factor gives higher lateral displacement in after pull-over loads duration.

The variations on the lateral soil friction factors do not give significant effect on the development of equivalent strain. Further discussion regarding this topic is presented in section 5.5.6

5.5.5. Bending Moments

Figure 5 - 10 shows that the bending moment at the buckle region has higher value than the slip region. The maximum bending moment during pull-over load duration occurs at the apex of the buckle. During pull-over load duration, the maximum bending moment for load case 1 is 3103.4 kN-m at time 2.9s. While for load case 4, the maximum bending moment is 3105.1 kN-m at time 2.6s. Both of the maximum bending moments occur at the apex of the buckle.

However, this situation is not applicable for every time steps. In some of the time steps, the maximum bending moments do not occur at the apex of the buckle. For example, for load case 1 at time 2.7s, the maximum bending moment of 2429.6 kN-m occurs at KP 1.04. And also for load case 4 at time 2.7s, the maximum bending moment of 2769.9 kN-m occurs at KP 1.04. But, these values of bending moment are less than the maximum bending moment during pull-over load duration.

From the pull-over finite element analysis, it is also found that the maximum bending moment does not occur at the same time with the maximum lateral displacement. As mentioned above, the maximum bending moment for load case 1 occurs at time 2.9s. Meanwhile, the maximum lateral displacement for load case 1 occurs at time 2.7s. For load case 4, the maximum bending moment occurs at time 2.6s meanwhile the maximum lateral displacement occurs at time 2.7s.

This phenomenon also found on the “after pull-over load” duration. For load case 1, the maximum bending moment occurs at time 3.0s. Meanwhile, the maximum lateral displacement for load case 1 occurs at time 7.0s. Also for load case 4, the maximum bending moment occurs at time 3.0s. Meanwhile the maximum lateral displacement occurs at time 5.0s.

This situation shows that the pull-over forces induce high bending moments on the pipeline during pull-over duration. The high bending moment is caused due to the concentrated pull-over force. It is also caused by the pipe’s need to breakout from the soil before sliding and the stiffness of the steel pipe. Hence, there will be a peak resistance from the soil friction and the pipe itself against the lateral displacement due to the pull-over force. After the pipe breaks out its peak resistance point, the soil friction resistance will become less and the pipe will move more easily in lateral direction until it reaches maximum lateral displacement. Thus, the bending moment at this period decreases.

As mentioned in section 5.5.3, the pipe tends to shrink when the pull-over force is disappeared. When the pipe starts to shrink, the soil frictional resistance will exist in opposite direction. The contraction on the pipe and the soil frictional resistance will increase the bending moment.

After pull-over duration, the bending moment at the buckle region tends to decrease. The global deformation on pipeline i.e. buckles laterally into a new equilibrium state that causes the buckle to be more relax. The deformation will reduce the compression and the bending moment as seen in Figure 5 - 11. The bending moment will become constant in some level. The maximum bending moment occurs at the apex of the buckle.

Table 5 - 13 shows the summary of the maximum bending moment and the maximum equivalent strain for each load cases.

Table 5 - 13 Summary of maximum bending moments, equivalent strain and DNV code check

Load Case No.	Pull-Over Factor	Lateral Soil Friction (μ_{lat})	Max. Bending moment (kN-m)	Max. Equivalent Strain (%)	DNV Disp. Controlled Utility Code Check
1	1.0	0.3	3104	5.13	1.36
2	0.8	0.3	3095	4.98	1.32
3	1.0	0.5	3091	5.14	1.36
4	1.0	0.7	3108	5.23	1.39
5	0.3	0.7	14.7	0.18	0.05
6	0.8	0.5	3106	5.09	1.35

5.5.6. Equivalent Strain

Figure 5 - 14 and Table 5 - 10 show the strain development on the pipeline during pull-over load. The equivalent strain on load case 1 significantly increases from 0.18% at time 2.0s and 2.1s to 3.16% at time 2.3s. Afterward, the equivalent strain continuously increases until it reaches 5.13% at 2.9s. After pull-over duration, the equivalent strain becomes constant at 5.18% from time 3.0s to 4.5s and slightly increased to 5.19% until time 8.0s.

This phenomenon also found on load cases 3 and 4. The equivalent strain significantly increases at time 2.3s for load case 3 and at time 2.4s for load case 4. The equivalent strain at the end of pull-over duration for both load cases also reaches above 5.0%. Load cases 2 and 6 also shows similarly increasing trend on the equivalent strain even though the strain does not reach over 5.0% by the end of pull-over duration.

From the results above, the increasing equivalent strains at time 2.3s or 2.4s showing that the pull-over force induce the excessive equivalent strain. And the maximum equivalent strain occurs at the location of pull-over force which is at the apex of the buckle. This situation shows that the concentrated pull-over forces pull the pipeline to move laterally and deform into plastic region.

The lateral soil friction does not give any significant effect on the equivalent strain during pull-over load duration. As seen in Table 5 - 13, the variation of lateral soil friction does not give any difference on the equivalent strain at the apex location. Load cases 1, 3 and 4 have approximately 5,13% equivalent strain regardless the variation of lateral soil friction factor applied. The equivalent strains on the buckle are also built up almost in the same rapidity compared to load case 2 and 6 that have higher soil friction factor.

5.5.7. DNV Displacement Controlled Checked

The DNV displacement controlled was carried out to check the integrity of the pipeline in the post-buckling condition. The performed code checks were according to the DNV-OS-F101 2007 version [1]. The DNV displacement controlled checked is carried out using Pipeline Engineering Tool (PET) version 3.0.1 developed by Det Norske Veritas (DNV). Detailed calculations are presented in Appendix D.

Table 5 - 13 shows the summary of the maximum equivalent strain and the utility code check from the DNV displacement controlled. The utility code check gives values above 1.0 for load cases 1, 2, 3, 4, and 6. All of these load cases have found that the pull-over force induces lateral buckling on pipeline. It is shown that none of the load case passed the DNV displacement controlled criteria. The equivalent strain on the lateral buckling induced by trawl gears pull-over load are above the allowable strain as per DNV displacement controlled criterion in DNV OS F101 [1]. The post buckling pipeline integrity is not give sufficient safety.

Chapter 6 Conclusion and Further Works

This chapter of the thesis report will give brief summary of analysis results and also present the conclusion of the thesis work. The conclusions are made based on the finite element analysis results presented in chapter 5. The further works regarding the subject of this thesis also present later in this chapter.

6.1. Summary

The objective of this thesis is to study and understand the pipeline's global response on pipe-trawl gears interaction on high pressure-high temperature subsea pipeline. The pipeline is susceptible to lateral buckling induced by the trawl gears pull-over loads. To get better understanding of global response of the pipeline as a result of trawl gears pull-over loads, a finite element analysis is carried out. A non-linear transient analysis type is used to perform the pull-over finite element analysis on the pipeline. The finite element analysis results can be summarized as follow:

1. The finite element analysis results indicate that the pipeline moves in lateral direction caused by the pull-over loads. The trawl gears pull-over forces pull the pipeline to deform laterally and induce the lateral buckling. Based on the analysis results that are discussed in section 5.5, the magnitude of 100% and 80% of the pull-over forces used in the analysis are proved to cause lateral buckling on pipeline. At some magnitude, the pull-over force may not enough to pull the pipeline to deform laterally and induce lateral buckling.
2. The maximum lateral displacements after pull-over loads duration are higher than the maximum lateral displacement during pull-over loads duration. Table 5 - 12 presents the summary of maximum lateral displacement for all load cases during and after pull-over loads duration. The maximum lateral displacement caused by trawl gears pull-over are located at the pull-over forces location i.e. KP1.0.
3. The measurement of lateral displacement in the buckle region indicates that during pull-over loads duration, the buckle amplitude is governed by the magnitude of pull-over loads. The summary of maximum lateral displacement with respect to the magnitude of pull-over forces can be seen in Table 5 - 12. The table shows that the longer buckle amplitude is measured on the load case with higher pull-over force magnitude.
4. The effective compression forces have contribution in the process of build up the lateral buckling. The effective compression forces at the slip region feed into the buckle and cause the buckle continues to expand. This situation is occurred during and after pull-over loads duration.
5. After pull-over duration, the effective axial force on the pipeline and the lateral soil friction factors govern the lateral buckling on the pipeline. The pipeline expands further longer on the smaller soil friction factor compare to the higher lateral soil friction with similar effective axial force on pipeline.
6. The results show that the buckle expands furthermore after the pull-over loads are no longer applied. The maximum buckle amplitudes after pull-over loads duration are longer than during pull-over loads duration. The results also indicates that with higher pull-over forces, the buckle amplitudes after pull over loads duration may expand even longer compare to the buckle amplitude during pull-over loads duration.
7. The finite element analysis results shows that the pipeline tends to shrink at the end of pull-over loads duration. When the pull-over forces are no longer applied, the pipeline in the buckle region shrinks into certain level in some duration. Afterward, the pipeline starts to expand and continue to move in lateral direction until reaches the equilibrium form. This situation is discussed in section 5.5.3 and also shown in Figure 5 - 17.

8. During pull-over loads duration, the maximum lateral displacement has no significant difference on load cases 1, 3 and 4. Those load cases used the same magnitude of pull-over forces with the variation of lateral soil friction. It is also shown on load cases 2 and 6. In contrary with that, after the pull-over loads duration, load cases 1, 3, and 4 show different maximum lateral displacement. With smaller lateral soil friction factor, the buckle expands longer compare to the load case with higher lateral soil friction after pull-over loads duration
9. The finite element analysis shows that the maximum bending moment is occurred at the pull-over forces location during pull-over load duration. The bending moments after pull-over load duration are gradually decreased until reach the equilibrium state.
10. The results also show that the similar magnitude of pull-over forces gives similar maximum bending moments on pipeline regardless the value of lateral soil friction. This finding is discussed in section 5.5.5. The summary of maximum bending moments on pipeline for all load cases is presented in Table 5 - 13.
11. The finite element results show that the equivalent strain in the buckle reaches approximately 5.0% at the apex of the buckle during pull-over loads duration and constant in this level after pull-over loads duration. The results also shows that similar magnitude of pull-over forces gives similar maximum equivalent strain on pipeline regardless the value of lateral soil friction. This finding is discussed in section 5.5.6. The summary of equivalent strain for all load cases is presented in Table 5 - 13.
12. As recommended in DNV RP F110 [2], the integrity of the pipeline should be check depend on the outcome from the finite element analysis as discussed in section 3.4 in this thesis report. A DNV displacement controlled condition check is carried out to perform the pipeline integrity check. Table 5 - 13 shows the results from DNV displacement controlled check. From this table, the utility code check ratio for all load cases are above 1.3 except for load case 5, which no lateral buckling occurs.

6.2. Conclusion

From the results presented in Chapter 5 and the summary that are discussed in the previous section, the following conclusions are made:

1. The pipeline is strongly susceptible to lateral buckling that is induced by trawl gears pull-over loads. The pull-over forces from the trawl gears pull the pipeline to deform in lateral direction. The magnitude of pull-over forces will govern the lateral displacement, bending moments and equivalent strain on the pipeline.
2. The lateral soil friction does not give sufficient effect on the buildup of lateral buckling during pull-over duration. In contrary to this, lateral soil friction gives significant effect for lateral buckling in the after pull-over loads duration.
3. The lateral soil friction does not give sufficient effect on maximum bending moments and equivalent strain development for all analysis time (during and after pull-over loads duration).
4. The pipe integrity check does not satisfy the DNV displacement controlled condition. It shows that the high pressure/high temperature subsea pipeline cannot stand the lateral buckling induced by the trawl gears pull-over loads.

6.3. Further Works

Further studies should be carried out with different dimension of pipeline as well as the variation of operating temperature and pressure on pipeline. This way, a better conclusion can be verified. This also can show the global response of the pipeline on which interact with the trawl gears more accurate.

A full comparison of lateral and axial soil friction combinations for various pull-over loads and duration should also be considered. The results from the finite element analysis show that the combination of lateral and axial soil friction may give different response on the pipeline.

The comparison which is carried out in this pull-over analysis is still very limited. Hence, it does not completely represent the actual condition.

References

1. Det Norkse, V., *Offshore Standard F101: Submarine Pipeline Systems*, October 2010, Norway
2. Det Norkse, V., *Recommended Practice F110: Global Buckling of Submarine Pipelines – Structural Design due to High Temperature/High Pressure*, October 2007, Norway
3. Det Norkse, V., *Recommended Practice F111: Interference between Trawl Gear and Pipelines*, October 2010, Norway
4. Lee, J., *Introduction to Offshore Pipeline and Risers*, 2007
5. Guo, B., *Offshore pipelines*. 2005, Amsterdam: Elsevier/GPP. XX, 281 s.
6. Karunakaran, D., *Lecture notes in MOK-160 Pipeline and Risers*. 2010, University of Stavanger: Stavanger, Norway.
7. Subsea 7, *Design Guidelines for Lateral Buckling Analysis*, Doc.No.CEO1PD-P-GU-127, December 2007
8. Subsea 7, *Design Guidelines for Pipeline Expansion*, Doc.No.CEO1PD-P-GU-126, November 2007
9. Hobbs R.E., “*In Service Buckling of Heated Pipelines*”, ASCE Journal of Transportation Engineering, Vol. 110, No 2, 175-189, March 1984.
10. Kien, Lim K., Ming, Lau S., Maschner, E., *Design of High Temperature/High Pressure (HT/HP) Pipeline against Lateral Buckling.*, J P Kenny Wood Group Sdn. Bhd., Kuala Lumpur, Malaysia.
11. Kaye, D., *Lateral Buckling of Subsea Pipelines: Comparison between Design and Operation*. ASPECT 1966, 155-174. Aberdeen, UK.
12. Moshagen, H., Kjeldsen, Soren P., *OTC 3782: Fishing Gear Loads and Effects on Submarine Pipelines*. 12th Offshore Technology Conference, May 1980, Houston.
13. SAFEBUK JIP, 2010 [cited 2001, 22nd April], available from: <http://www.safebuck.com/project.asp>
14. ANSYS inc., “ANSYS User Manuals released 13.0”, 2010
15. JEE, [cited 2011, 8th June] available from: http://www.jee.co.uk/Industry_specialists/Fishing_interaction/Fishing_interaction.html
16. Simrad News Bulletin, *Simrad receives historic orders of trawls system*, www.simrad.com, Horten, Norway, April 2009.
17. Mhara, Bord Iascaigh (Irish Sea Fisheries Board), 2003, *Fishing Methods*. [cited 2011, 8th June], available from: http://www.bim.ie/templates/fishing_methods.asp?node_id=408

18. Casson, *A tough week*, May 4th, 2010, [cited 2011, 8th June], available from:
<http://www.sustainablesushi.net/tag/overfishing/>
19. Chevron, *Amberjack Pipeline Company LLC to Install 136 Mile Jack/St. Malo Oil Export Pipeline*, December 14, 2010, [cited 2011, 8th June], available from:
http://www.facebook.com/note.php?note_id=473134995185&comments
20. Wikipedia, April 22nd, 2011. *Fishing trawler*, [cited 2011, 8th June], available from:
[\[http://en.wikipedia.org/wiki/Fishing_trawler\]](http://en.wikipedia.org/wiki/Fishing_trawler)
21. Peace, Green., *Beam trawling in the North Sea*, [cited 2011, 8th June], available from:
<http://archive.greenpeace.org/comms/cbio/beam.html>
22. R D Galbraith, *A Rice after E S Strange*, "An Introduction to Commercial Fishing Gear and Methods Used in Scotland", FRS Marine Laboratory, Aberdeen, 2004

Appendix A

Preparation Works

Appendix A-1

Pipeline End Expansion

Pipeline End Expansion Calculation

Master Thesis - Offshore Technology, University of Stavanger - Norway

Date : 2 April 2011

Author : Iswan Herlianto

Description :

This MathCAD sheet is for calculating pipeline end expansion of rigid pipeline under temperature and pressure loading. The purpose is validating the result of ANSYS Model of Lateral Buckling on rigid pipeline made by the author for his master thesis.

The calculation is based on Subsea 7 Guideline: CEO1PD-P-GU-126 Pipeline Expansion Design Guideline and DNV OS

Units : MPa \equiv 1N \cdot mm⁻² g \equiv 9.81 \cdot m \cdot s⁻²

Water depth

WD := 100m

Pipeline Data :

Pipeline Outside Diameter

OD := 559mm

Wall Thickness

tkwall := 25.4mm

External Coating Thickness

t_ext := 5mm

Concrete Coating Thickness

t_conc := 0mm

Length of pipeline

L := 2000m

Material Properties :

Pipeline :

Pipe Steel Density

DENS := 7850 kg \cdot m⁻³

SMYS Steel Pipe

SMYS := 450MPa

Steel Pipe Young's Modulus

E := 207000MPa

Steel Pipe Thermal Expansion Coeff.

α := 1.17 \cdot 10⁻⁵ \cdot C⁻¹

Steel Poisson Ratio

ν := 0.3

Insulation or Coating :

Insulation or Coating Density

P_EXT := 910 \cdot kg \cdot m⁻³

Concrete Coating Density

P_CONC := 2400 \cdot kg \cdot m⁻³

Operating Parameters :

Sea Water Density

RHO_W := 1027 \cdot kg \cdot m⁻³

Max Content Density

DENSFL := 900 \cdot kg \cdot m⁻³

Design Pressure

Pres_d := 15MPa

Operating Pressure

Pres_op := 15MPa

Hydrotest Pressure

Pres_hyd := 0MPa

Ambient Temperature

T_amb := 5 \cdot C

Operating Temperature

T_op := 100 \cdot C

EXTERNAL LOADS :

Bending moment

M_b := 0kN \cdot m

Axial Force

N_a := 0kN

Residual Lay Tension

N_{lay} := 0kN

SOIL PROPERTIES :

Axial Friction Factor

μ_{axial} := 0.5

Lateral Friction Factor

$\mu_{lateral}$:= 0.3

SAFETY FACTORS :

Usage Factor for Hoop Stress

$$\beta_h := 0.72$$

Usage Factor for Longitudinal Stress

$$\beta_l := 0.8$$

Usage Factor for Longitudinal Stress

$$\beta_c := 0.9$$

PARAMETER CALCULATION :

Effective Pipe Diameter

$$D_{EFF} := OD + 2 \cdot (t_{ext} + t_{conc})$$

Internal Diameter

$$ID := OD - 2 \cdot tk_{wall}$$

Cross-sectional Area of steel pipe

$$AS := \frac{\pi}{4} \cdot (OD^2 - ID^2)$$

Cross-sectional Area of External Coat.

$$AS_{EXT} := \frac{\pi}{4} \cdot [(OD + 2 \cdot t_{ext})^2 - OD^2]$$

Cross-sectional Area of Concrete Coat.

$$AS_{CONC} := \frac{\pi}{4} \cdot [(OD + 2 \cdot t_{ext} + 2 \cdot t_{conc})^2 - (OD + 2 \cdot t_{ext})^2]$$

Pipe Steel Mass

$$M_{STEEL} := AS \cdot DENS$$

External Coating Mass

$$M_{EXT} := AS_{EXT} \cdot P_{EXT}$$

Concrete Coating Mass

$$M_{CONC} := AS_{CONC} \cdot P_{CONC}$$

Content Mass

$$M_{CONT} := \left(\frac{\pi}{4} \cdot ID^2 \right) \cdot DENS_{FL}$$

Water Content Mass

$$M_{WATER} := \left(\frac{\pi}{4} \cdot ID^2 \right) \cdot RHO_W$$

Bouyancy Mass

$$M_{BUOY} := \left(\frac{\pi}{4} \cdot D_{EFF}^2 \right) \cdot RHO_W$$

Pipeline Total Mass (Weight in Air)

$$M_{WALL} := M_{STEEL} + M_{EXT} + M_{CONC}$$

Submerged Mass (weight in Water)

$$M_{SUB} := M_{WALL} - M_{BUOY}$$

Steel Pipe Dry Weight

$$W_{dry} := M_{WALL} \cdot g$$

$$W_{dry} = 3358.063 \text{ N} \cdot \text{m}^{-1}$$

Content Weight

$$W_{CONT} := M_{CONT} \cdot g$$

Flooded Weight

$$W_{WATER} := M_{WATER} \cdot g$$

Empty Pipe Submerged Weight

$$W_{SUB} := M_{SUB} \cdot g$$

$$W_{SUB} = 796.212 \text{ N} \cdot \text{m}^{-1}$$

Equivalent Density

$$EQ_{DEN} := \frac{M_{WALL}}{AS}$$

Coating Equivalent Density (Insulation & Concrete Coating)

$$DENSIN := \frac{t_{ext} \cdot P_{EXT} + t_{conc} \cdot P_{CONC}}{t_{ext} + t_{conc}}$$

Coating Thickness (Insulation & Concrete Coating)

$$TKIN := t_{ext} + t_{conc}$$

coating Area (Insulation & Concrete Coating)

$$AREA_{IN} := AS_{EXT} + AS_{CONC}$$

Moment Of Inertia of steel pipe cross section

$$I_s := \frac{\pi}{64} \cdot (OD^4 - ID^4)$$

Section Modulus of steel pipe

$$Z_s := \frac{I_s}{\frac{OD}{2}}$$

Temperature Difference

$$\Delta T := (T_{op} - T_{amb})$$

CALCULATION :

END EXPANSION

Fully Constrained Axial Force $F_{\text{anchor}} := (\pi \cdot \text{ID} \cdot t_{\text{kwall}}) \cdot E \cdot \alpha \cdot \Delta T + \frac{\text{Pres_op} \cdot \pi \cdot \text{ID}^2}{4} \cdot (1 - 2 \cdot \nu)$ $F_{\text{anchor}} = 1.055 \times 10^4 \text{ kN}$

Friction Force (Restraining Force) $f_{\text{fric}} := \mu_{\text{axial}} \cdot (W_{\text{SUB}} + W_{\text{CONT}}) \cdot 1\text{m}$ $f_{\text{fric}} = 1.294 \times 10^3 \text{ N}$

Total Longitudinal Strain $\text{Strain} := \alpha \cdot \Delta T + \frac{\text{Pres_op} \cdot \text{ID}}{2 \cdot t_{\text{kwall}}} \cdot \frac{1 - 2 \cdot \nu}{E}$ $\text{Strain} = 1.401 \times 10^{-3}$

Pipeline end expansion without soil resistance $L_{\text{exp1}} := L \cdot \text{Strain}$ $L_{\text{exp1}} = 2.803 \text{ m}$

Pipeline end expansion with soil resistance $L_{\text{exp2}} := \frac{(F_{\text{anchor}} - f_{\text{fric}}) \cdot L}{AS \cdot E}$ $L_{\text{exp2}} = 2.393 \text{ m}$

PLOT :

Input Temperature Profile

Number of Input Points $n := 15$ $i := 0..n-1$

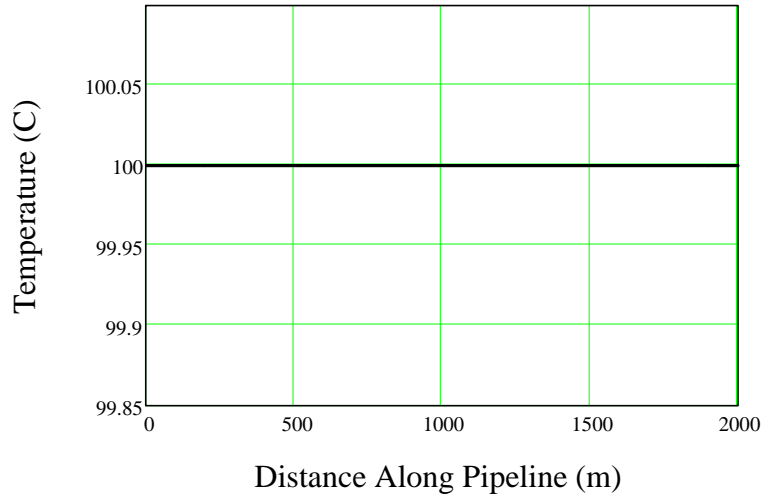
KPStep := 10m

Number of Temperature Input Points
Product Corresponding
Temperature KP Point

$T_i :=$	$Kp_i :=$
T_op	0-m
T_op	200-m
T_op	400-m
T_op	600m
T_op	800-m
T_op	900-m
T_op	1000-m
T_op	1200-m
T_op	1400-m
T_op	1500-m
T_op	1600-m
T_op	1700m
T_op	1800-m
T_op	1900m
T_op	2000m

Note : For non-linear temp. profiles use more input points. Linear temp. profiles only require inlet and outlet points.

Temperature Profile



Input Water Depth Profile

Number of Input Points $nw := 2$

$iw := 0..nw-1$

Water Depth Corresponding KP point

$WDw_{iw} :=$	$KPw_{iw} :=$
100-m	0-m
100-m	2000-m

$WDw(x) := \text{linterp}(KPw, WDw, x)$

Effective Axial Force Derivation - Restrained Flowline

Define functions with KP:

$x := Kp_0, KPStep.. Kp_{n-1}$

Define Temperature Difference with KP

$\Delta T_i := T_i - T_{amb}$

$Temp(x) := \text{linterp}(Kp, \Delta T, x)$

Define External Pressure with KP

$Po(x) := RHO_W \cdot g \cdot WDw(x)$

Define Local Design Pressure with KP

$Pin(x) := Pres_op + DENSFL \cdot g \cdot WDw(x)$

Define Pressure Difference with KP

$\Delta P(x) := Pin(x) - Po(x)$

Thermal Expansion Force with KP

$Ft(x) := -E \cdot AS \cdot \alpha \cdot Temp(x)$

Poisons Force with KP

$Fp(x) := v \cdot \Delta P(x) \cdot AS \cdot \frac{OD - tkwall}{2 \cdot tkwall}$

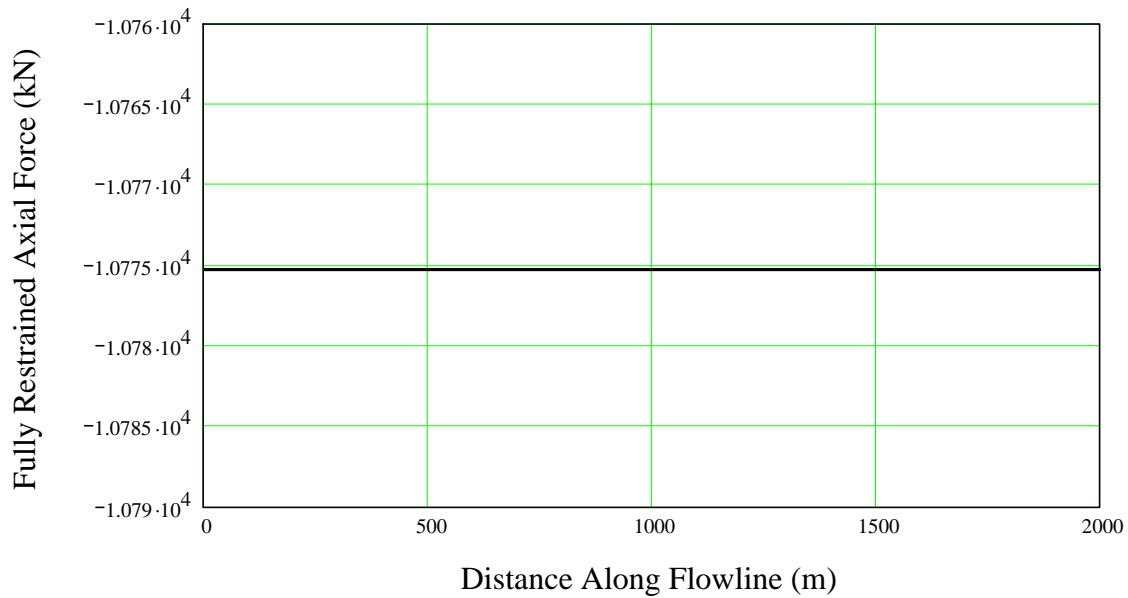
Endcap Force with KP

$Fe(x) := \frac{\pi}{4} \cdot (Pin(x) \cdot ID^2 - Po(x) \cdot OD^2)$

Fully Restrained Axial Force with KP

$Fr(x) := Nlay - Fe(x) + Fp(x) + Ft(x)$

Plot of Fully Restrained Axial Force vs KP



Effective Axial Force - Partially Restrained Flowline

Flowline Length

$$L := K_{p_{n-1}} \quad L = 2 \text{ km}$$

Maximum Friction Force
(at mid of pipeline)

$$P_{fmax} := \mu_{axial} \cdot (W_{SUB} + W_{CONT}) \cdot \frac{L}{2}$$

Friction Force with Length at Hot End

$$PfH(x) := \mu_{axial} \cdot (W_{SUB} + W_{CONT}) \cdot x \cdot (-1)$$

Friction Force with Length at Cold End

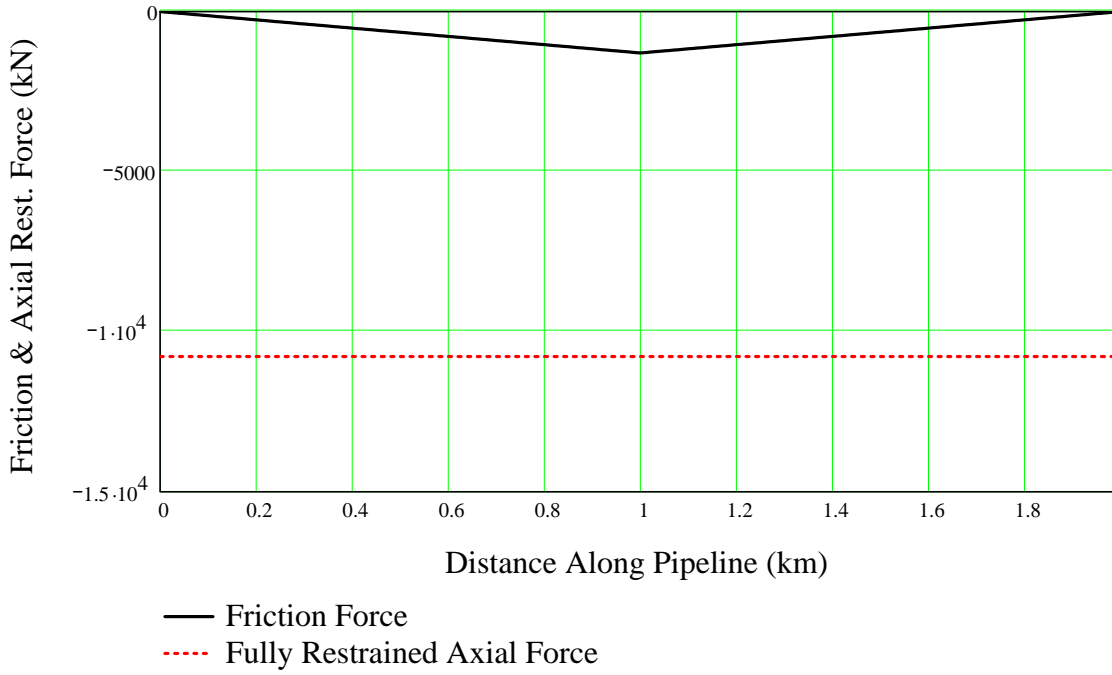
$$PfC(x) := \mu_{axial} \cdot (W_{SUB} + W_{CONT}) \cdot (x - L)$$

Logic Step to Calculate Friction Restraint Along Full Length

$$P_{fmax} = 1293.555 \text{ kN}$$

$$Pf(x) := \text{if}(PfH(x) > PfC(x), PfH(x), PfC(x))$$

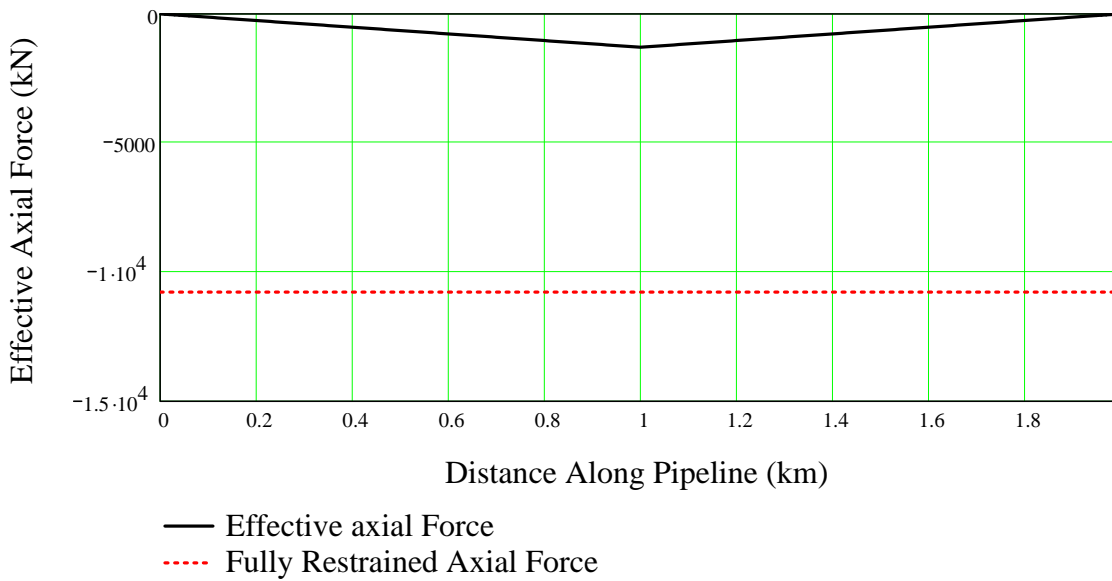
Friction and Fully Rest. Axial Force



Logic statement to plot friction force if less than full restraint force i.e. effective axial force is the less of friction force or full restraint force.

Effective Axial Force $P_{eff}(x) := \text{if}(P_f(x) < F_r(x), F_r(x), P_f(x))$
 $P_{buck}(x) := \text{if}(P_{eff}(x) < 0, P_{eff}(x), -10 \cdot N)$

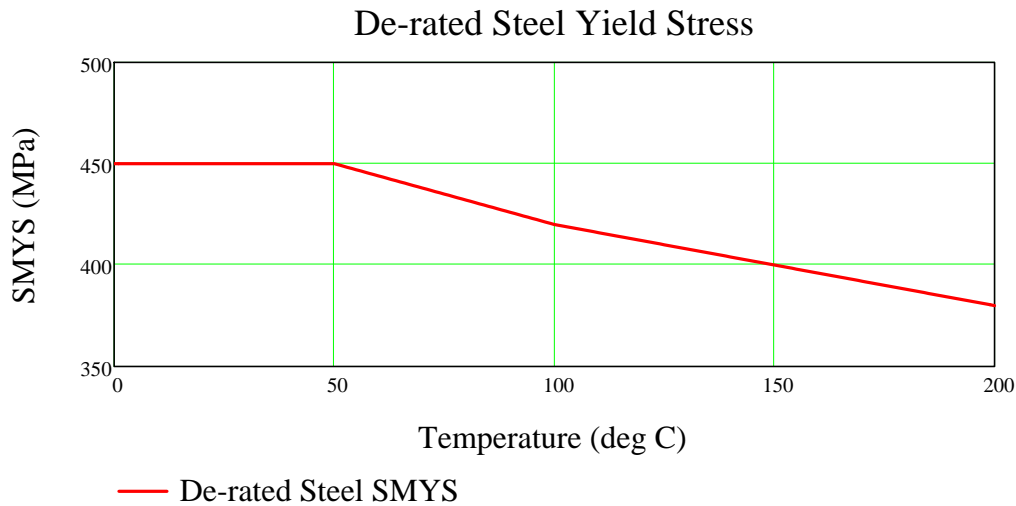
Effective Axial Force



PLOT : Stress-Strain Curve

T := 0C, 1C.. 200C

$$\text{SMYS}(T) := \begin{cases} \text{SMYS} & \text{if } T \leq 50\text{C} \\ \text{SMYS} - \left[\left[\frac{3(T - 50\text{C})}{5} \right] \cdot \frac{\text{MPa}}{\text{C}} \right] & \text{if } 50\text{C} < T \leq 100\text{C} \\ \text{SMYS} - \left[\left[\frac{(T - 100\text{C})}{2.5} \right] \cdot \frac{\text{MPa}}{\text{C}} + 30\text{MPa} \right] & \text{otherwise} \end{cases}$$



SMYS(T_{op}) = 420MPa

RESULT SUMMARY :

PIPELINE PARAMETERS:

ID = 0.508 m

D_{EFF} = 0.569 m

TKIN = 5 mm

AS = 0.043 m²

AS_{EXT} = 8.859 × 10⁻³ m²

AS_{CONC} = 0 m²

AREAIN = 8.859 × 10⁻³ m²

M_{STEEL} = 334.248 kg·m⁻¹

M_{EXT} = 8.062 kg·m⁻¹

M_{CONC} = 0 kg·m⁻¹

M_{CONT} = 182.558 kg·m⁻¹

M_{WATER} = 208.319 kg·m⁻¹

M_{BUOY} = 261.147 kg·m⁻¹

M_{WALL} = 342.31 kg·m⁻¹

M_{SUB} = 81.163 kg·m⁻¹

W_{CONT} = 1790.897 N·m⁻¹

W_{WATER} = 2043.613 N·m⁻¹

W_{SUB} = 796.212 N·m⁻¹

Appendix A-2

Hobbs' Critical Buckling

Pipeline Lateral Buckling Calculation

This MATHCAD sheet calculates the lateral buckling characteristics of a laterally unrestrained pipeline due to axial loads.

Limitations:

1. Consideration of concrete coating is NOT currently implemented in buckling calculations
2. Critical buckling array is for two pipe sizes only - with location fixed.
3. No consideration is given to lateral restraints other than seabed friction.

References:

1. Hobbs, R. E., 'In service buckling of heated pipelines', Journal of transport engineering, Vol 110, No. 2, March 1984.
2. DNV RP F104 - Mechanical Pipeline Couplings, 1999

Load case: **Lateral Soil friction 0.3**

User Inputs

Yellow fields - user input

NOTE THAT FOR THE PURPOSES OF THE CALCULATIONS PRESENTED HEREIN, KP 0 HAS BEEN DEFINED AS BEING AT THE HOT END

Define KP for Variables

$$KP := 2\text{km}$$

Input KP Step size

$$KPStep := 10\text{m}$$

Define range of Kp variable

$$x := 0, KPStep.. KP$$

Define (x) in terms of xi
(counter)

$$xi := 0, 1.. \frac{KP}{KPStep}$$

Pipeline Parameters

External Pipeline Diameter

$$De := 559\text{mm}$$

Wall Thickness

$$WT(x) := \begin{cases} 25.4\text{mm} & \text{if } x < 1\text{km} \\ 25.4\text{mm} & \text{if } x \geq 1\text{km} \end{cases}$$

Corrosion Allowance

$$CA := 3\text{mm}$$

(Corrosion Allowance is used in OSF101
Interaction ratio calculations only)

Young's Modulus of Pipe Material

$$E := 207000\text{MPa}$$

Steel Density

$$\rho_{st} := 7850\text{kg}\cdot\text{m}^{-3}$$

Specified Minimum Yield Strength

$$SMYS := 450\text{N}\cdot\text{mm}^{-2}$$

$$SMTS := 535\text{MPa}$$

Coefficient of Thermal Expansion

$$\alpha := 1.17\cdot 10^{-5}\cdot\text{C}^{-1}$$

Poisson's Ratio

$$\nu := 0.3$$

Coating Parameters

Corrosion Coating Density

$$\rho_{cc} := 910\text{kg}\cdot\text{m}^{-3}$$

Corrosion Coating Thickness

$$T_{cor} := 5\text{mm}$$

Pipeline Lateral Buckling Calculation

▢ Conc. Coat Parameters - NotUsed

Environmental Parameters

Density of Water

$$\rho_{\text{water}} := 1027 \cdot \text{kg} \cdot \text{m}^{-3}$$

Water Depth

$$n_w := 2$$

$$i_w := 0..(n_w - 1)$$

KPw_{i_w} :=

0km
2km

WDw_{i_w} :=

100m
100m

Installation Temperature

$$T_o := 5\text{C}$$

▢

Axial Friction Factor

$$\mu(x) := \begin{cases} 0.5 & \text{if } x < 1\text{km} \\ 0.5 & \text{if } x \geq 1\text{km} \end{cases}$$

Lateral Friction Factor

$$\mu_{\text{lat}}(x) := \begin{cases} 0.3 & \text{if } x < 1\text{km} \\ 0.3 & \text{if } x \geq 1\text{km} \end{cases}$$

Operational Parameters

Contents Density

$$\rho_{\text{cont}} := 910 \cdot \text{kg} \cdot \text{m}^{-3}$$

Internal Pressure

$$P_i := 15\text{MPa}$$

Lay Tension:

$$T_{\text{lay}} := 0\text{KN}$$

Calculations Section

▢ Define Functions for Variables

Concrete coating Thickness $T_{\text{con}}(x) := \text{linterp}(KP_{\text{conc}}, T_{\text{conc}}, x)$

Water Depth $WD(x) := \text{linterp}(KP_w, WD_w, x)$

Total Outside Diameter $Do(x) := De + 2 \cdot (T_{\text{cor}} + T_{\text{con}}(x) + T_{\text{mar}})$

Internal Diameter $Di(x) := De - 2 \cdot WT(x)$

Steel Area $A_{\text{st}}(x) := \frac{\pi}{4} \cdot (De^2 - Di(x)^2)$

Steel Mass $M_{\text{st}}(x) := A_{\text{st}}(x) \cdot \rho_{\text{st}}$

Corrosion Coating Area $Acc := \frac{\pi}{4} \cdot [(De + 2 \cdot T_{\text{cor}})^2 - De^2]$

Corrosion Coating Mass $M_{\text{cc}} := Acc \cdot \rho_{\text{cc}}$

Concrete Coating Area $A_{\text{con}}(x) := \frac{\pi}{4} \cdot [(De + 2 \cdot T_{\text{cor}} + 2 \cdot T_{\text{con}}(x))^2 - (De + 2 \cdot T_{\text{cor}})^2]$

Pipeline Lateral Buckling Calculation

Concrete Coating Mass $M_{con}(x) := A_{con}(x) \cdot \rho_{con}$

Mar.Growth Area $A_{mar}(x) := \frac{\pi}{4} \cdot \left[(De + 2 \cdot T_{cor} + 2 \cdot T_{con}(x) + 2 \cdot T_{mar})^2 - (De + 2 \cdot T_{con}(x) + 2 \cdot T_{cor})^2 \right]$

Marine Growth Mass $M_{mar}(x) := A_{mar}(x) \cdot \rho_{mar}$

Contents Mass $M_{cont}(x) := \frac{\pi}{4} \cdot Di(x)^2 \cdot \rho_{cont}$

Buoyancy Force $F_b(x) := \frac{\pi}{4} \cdot Do(x)^2 \cdot \rho_{water} \cdot g$

Submerged Weight $W_s(x) := (M_{st}(x) + M_{cc} + M_{con}(x) + M_{cont}(x) + M_{mar}(x)) \cdot g - F_b(x)$

Second Moment of Area of steel section $I(x) := \frac{\pi}{64} \cdot (De^4 - Di(x)^4)$

Define Functions for Variables

Lateral Buckling assessment

Define Functions as per Ref [1]

Define Constants for lateral buckling modes (Ref 1 Table 1)

	0	1	2	3	4	5
k =	"Mode"	"K1"	"K2"	"K3"	"K4"	"K5"
1	1	80.76	$6.391 \cdot 10^{-5}$	0.5	$2.407 \cdot 10^{-3}$	$6.938 \cdot 10^{-2}$
2	2	39.478	$1.743 \cdot 10^{-4}$	1	$5.532 \cdot 10^{-3}$	0.109
3	3	34.06	$1.668 \cdot 10^{-4}$	1.294	$1.032 \cdot 10^{-2}$	0.143
4	4	28.2	$2.144 \cdot 10^{-4}$	1.608	$1.047 \cdot 10^{-2}$	0.148
5	"inf"	39.478	$4.705 \cdot 10^{-5}$	$4.705 \cdot 10^{-5}$	$4.495 \cdot 10^{-3}$	$5.066 \cdot 10^{-2}$

Case 1 - Infinite mode lateral buckling

Buckle Wave Length $L_{bar}(x, \phi) := \left[\frac{2.7969 \cdot 10^5 \cdot (E \cdot I(x))^3}{(\phi \cdot W_s(x))^2 \cdot A_{st}(x) \cdot E} \right]^{0.125}$ Ref 1, Eq 22

$$L_{bar}(1 \cdot km, \mu_{lat}(1km)) = 79.61 \text{ m}$$

Axial Force in Buckle $P_{buck}(x, L) := 4 \cdot \pi^2 \cdot \frac{E \cdot I(x)}{L^2}$ Ref 1, Eq 20

$$W_s(1km) = 2.606 \frac{kN}{m}$$

Axial force due to thermal expansion: $P_{o_inf}(x, L, \phi) := P_{buck}(x, L) + 4.7050 \cdot 10^{-5} \cdot A_{st}(x) \cdot E \cdot \left(\frac{\phi \cdot W_s(x)}{E \cdot I(x)} \right)^2 \cdot L^6$ Ref 1, Eq 21

Case 2 - All buckling modes

Arguments in the following functions are defined as follows:

- x - location of interest [m]
- L - Buckle Wave Length [m]
- modeb - buckling mode (1 to 4 for first four modes, 5 for infinite mode)
- f - Lateral Friction Factor
- P - Axial Force

Axial force in buckle $P_{buck}(x, L, modeb) := k_{modeb} \cdot 1 \cdot \frac{E \cdot I(x)}{L^2}$ Ref 1, Eq 26

Pipeline Lateral Buckling Calculation

Axial force due to thermal expansion:

Ref 1, Eq 27

$$P_o(x, L, modeb, \phi) := \begin{cases} P_{buck}(x, L, modeb) \dots & \text{if } modeb < 5 \\ + k_{modeb, 3} \cdot \phi \cdot W_s(x) \cdot L \cdot \left[1 + k_{modeb, 2} \cdot A_{st}(x) \cdot E \cdot \phi \cdot W_s(x) \cdot \frac{L^5}{(E \cdot I(x))^2} \right]^{0.5} - 1 & \\ P_{o_inf}(x, L, \phi) & \text{otherwise} \end{cases}$$

Maximum Buckle Amplitude: $y_{max}(x, L, modeb, \phi) := k_{modeb, 4} \cdot \phi \cdot \frac{W_s(x)}{E \cdot I(x)} \cdot L^4$ Ref 1, Eq 28

Maximum Bending Moment in Buckle: $M_{max}(x, L, modeb, \phi) := k_{modeb, 5} \cdot \phi \cdot W_s(x) \cdot L^2$ Ref 1, Eq 29

Maximum Slope: $y_{maxbar}(x, L, \phi) := 0.01267 \cdot \left(\phi \cdot \frac{W_s(x)}{E \cdot I(x)} \cdot L^3 \right)$ Ref 1, Eq 25

Define a function, which for a given mode, location and friction factor, returns an array with the following format:

- Col 1 - Buckle Length
- Col 2 - Required axial force to cause buckle with length in column 1

Note that for data processing purposes, all outputs are nondimensionalised within this routine (In MATHCAD all elements of an array must have the same or no units).

$$\text{buck_array}(x, modeb, \phi) := \begin{cases} LL \leftarrow Lbar(x, \phi) \\ ntest \leftarrow 500 \\ \text{for } i \in 0..ntest \\ \quad mult \leftarrow i \cdot \frac{20}{ntest} + 0.05 \\ \quad L_{test} \leftarrow LL \cdot mult \\ \quad PP \leftarrow P_o(x, L_{test}, modeb, \phi) \\ \quad \Delta T \leftarrow \left(E \cdot A_{st}(x) \cdot \frac{\alpha}{PP} \right)^{-1} \\ \quad out_{i, 0} \leftarrow \frac{L_{test}}{m} \\ \quad out_{i, 1} \leftarrow \frac{PP}{(kg \cdot m \cdot sec^{-2}) \cdot 1000} \end{cases} \text{out}$$

Define a routine that, given a matrix of Buckle length vs. Axial force, will calculate the minimum axial force to instigate a buckle at a given mode. Output is a vector with the following values:

- 0 - Critical Buckle Length
- 1 - Critical Temperature for buckle (assuming fixed pipeline)
- 2 - Critical buckling load

$$T_P_crit(x, modeb, \phi) := \begin{cases} L_{array} \leftarrow \text{buck_array}(x, modeb, \phi)^{\langle 0 \rangle} \\ P_{array} \leftarrow \text{buck_array}(x, modeb, \phi)^{\langle 1 \rangle} \\ P_{crit} \leftarrow \min(P_{array}) \\ L_{crit_index} \leftarrow \text{match}(P_{crit}, P_{array})_0 \\ L_{crit} \leftarrow L_{array}_{L_{crit_index}} \\ out_0 \leftarrow L_{crit} \\ out_1 \leftarrow P_{crit} \end{cases} \text{out}$$

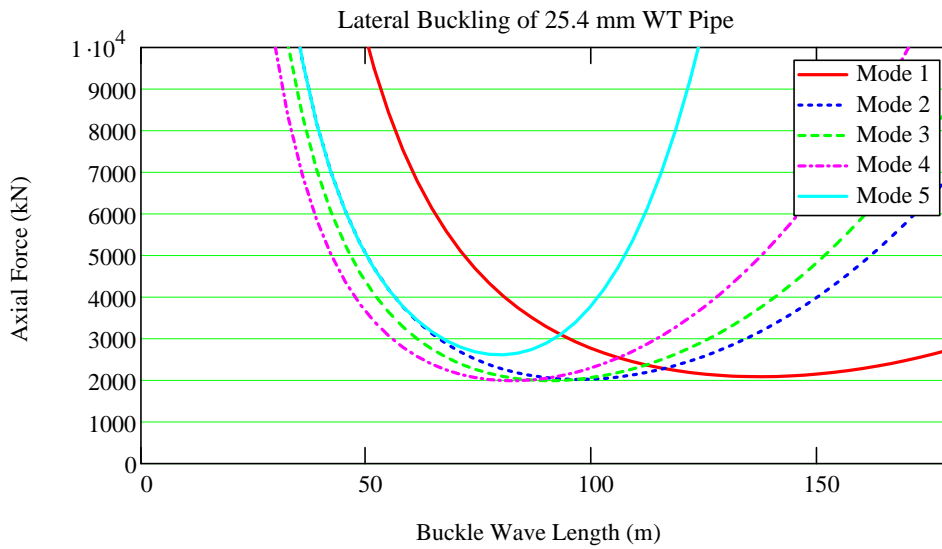
test_data_a := buck_array(1000m, 1, μ_{lat}(1000m)) test_data_b := buck_array(1000m, 2, μ_{lat}(1000m))

test_data_c := buck_array(1000m, 3, μ_{lat}(1000m)) test_data_d := buck_array(1000m, 4, μ_{lat}(1000m))

test_data_e := buck_array(1000m, 5, μ_{lat}(1000m))

Pipeline Lateral Buckling Calculation

Define Functions as per Ref [1]



Calculate Critical buckling temperature and axial force for the specified lateral friction coefficient and a range of modes (The critical buckling temperature is changes only with pipe wall thickness and Friction factor):

$$aa := \min(\text{test_data_a}^{\langle 1 \rangle}) \quad aa = 2086.565$$

$$bb := \min(\text{test_data_b}^{\langle 1 \rangle}) \quad bb = 2022.127$$

$$cc := \min(\text{test_data_c}^{\langle 1 \rangle}) \quad cc = 1991.012$$

$$dd := \min(\text{test_data_d}^{\langle 1 \rangle}) \quad dd = 1991.269$$

$$ee := \min(\text{test_data_e}^{\langle 1 \rangle}) \quad ee = 2612.846$$

$$\text{MinBuckleForce} := \min(\text{test_data_a}^{\langle 1 \rangle}, \text{test_data_b}^{\langle 1 \rangle}, \text{test_data_c}^{\langle 1 \rangle}, \text{test_data_d}^{\langle 1 \rangle}, \text{test_data_e}^{\langle 1 \rangle})$$

$$\text{MinBuckleForce} = 1991.012$$

This MATHCAD sheet calculates the lateral buckling characteristics of a laterally unrestrained pipeline due to axial loads.

Limitations:

1. Consideration of concrete coating is NOT currently implemented in buckling calculations
2. Critical buckling array is for two pipe sizes only - with location fixed.
3. No consideration is given to lateral restraints other than seabed friction.

References:

1. Hobbs, R. E., 'In service buckling of heated pipelines', Journal of transport engineering, Vol 110, No. 2, March 1984.
2. DNV RP F104 - Mechanical Pipeline Couplings, 1999

Load case: **Lateral Soil friction 0.5**

User Inputs Yellow fields - user input

NOTE THAT FOR THE PURPOSES OF THE CALCULATIONS PRESENTED HEREIN, KP 0 HAS BEEN DEFINED AS BEING AT THE HOT END

Define KP for Variables	KP := 2km
Input KP Step size	KPStep := 10m
Define range of Kp variable	x := 0, KPStep.. KP
Define (x) in terms of xi (counter)	xi := 0, 1.. $\frac{KP}{KPStep}$

Pipeline Parameters

External Pipeline Diameter	De := 559·mm
Wall Thickness	WT(x) := $\begin{cases} 25.4\text{mm} & \text{if } x < 1\text{km} \\ 25.4\text{mm} & \text{if } x \geq 1\text{km} \end{cases}$

Corrosion Allowance	CA := 3mm
---------------------	-----------

(Corrosion Allowance is used in OSF101 Interaction ratio calculations only)

Young's Modulus of Pipe Material	E := 207000·MPa
Steel Density	$\rho_{st} := 7850 \cdot \text{kg} \cdot \text{m}^{-3}$
Specified Minimum Yield Strength	SMYS := 450·N·mm ⁻²
	SMTS := 535MPa

Coefficient of Thermal Expansion	$\alpha := 1.17 \cdot 10^{-5} \cdot \text{C}^{-1}$
----------------------------------	--

Poisson's Ratio	v := 0.3
-----------------	----------

Coating Parameters

Corrosion Coating Density	$\rho_{cc} := 910 \cdot \text{kg} \cdot \text{m}^{-3}$
Corrosion Coating Thickness	Tcor := 5·mm

Pipeline Lateral Buckling Calculation

▢ Conc. Coat Parameters - NotUsed

Environmental Parameters

Density of Water

$$\rho_{\text{water}} := 1027 \cdot \text{kg} \cdot \text{m}^{-3}$$

Water Depth

$$n_w := 2$$

$$i_w := 0..(n_w - 1)$$

KPw_{i_w} :=

0km
2km

WDw_{i_w} :=

100m
100m

Installation Temperature

$$T_o := 5\text{C}$$

▢

Axial Friction Factor

$$\mu(x) := \begin{cases} 0.5 & \text{if } x < 1\text{km} \\ 0.5 & \text{if } x \geq 1\text{km} \end{cases}$$

Lateral Friction Factor

$$\mu_{\text{lat}}(x) := \begin{cases} 0.5 & \text{if } x < 1\text{km} \\ 0.5 & \text{if } x \geq 1\text{km} \end{cases}$$

Operational Parameters

Contents Density

$$\rho_{\text{cont}} := 910 \cdot \text{kg} \cdot \text{m}^{-3}$$

Internal Pressure

$$P_i := 15\text{MPa}$$

Lay Tension:

$$T_{\text{lay}} := 0\text{KN}$$

Calculations Section

▢ Define Functions for Variables

Concrete coating Thickness $T_{\text{con}}(x) := \text{linterp}(KP_{\text{conc}}, T_{\text{conc}}, x)$

Water Depth $WD(x) := \text{linterp}(KP_w, WD_w, x)$

Total Outside Diameter $Do(x) := De + 2 \cdot (T_{\text{cor}} + T_{\text{con}}(x) + T_{\text{mar}})$

Internal Diameter $Di(x) := De - 2 \cdot WT(x)$

Steel Area $A_{\text{st}}(x) := \frac{\pi}{4} \cdot (De^2 - Di(x)^2)$

Steel Mass $M_{\text{st}}(x) := A_{\text{st}}(x) \cdot \rho_{\text{st}}$

Corrosion Coating Area $Acc := \frac{\pi}{4} \cdot [(De + 2 \cdot T_{\text{cor}})^2 - De^2]$

Corrosion Coating Mass $M_{\text{cc}} := Acc \cdot \rho_{\text{cc}}$

Concrete Coating Area $A_{\text{con}}(x) := \frac{\pi}{4} \cdot [(De + 2 \cdot T_{\text{cor}} + 2 \cdot T_{\text{con}}(x))^2 - (De + 2 \cdot T_{\text{cor}})^2]$

Pipeline Lateral Buckling Calculation

Concrete Coating Mass $M_{con}(x) := A_{con}(x) \cdot \rho_{con}$

Mar.Growth Area $A_{mar}(x) := \frac{\pi}{4} \cdot \left[(De + 2 \cdot T_{cor} + 2 \cdot T_{con}(x) + 2 \cdot T_{mar})^2 - (De + 2 \cdot T_{con}(x) + 2 \cdot T_{cor})^2 \right]$

Marine Growth Mass $M_{mar}(x) := A_{mar}(x) \cdot \rho_{mar}$

Contents Mass $M_{cont}(x) := \frac{\pi}{4} \cdot Di(x)^2 \cdot \rho_{cont}$

Buoyancy Force $F_b(x) := \frac{\pi}{4} \cdot Do(x)^2 \cdot \rho_{water} \cdot g$

Submerged Weight $W_s(x) := (M_{st}(x) + M_{cc} + M_{con}(x) + M_{cont}(x) + M_{mar}(x)) \cdot g - F_b(x)$

Second Moment of Area of steel section $I(x) := \frac{\pi}{64} \cdot (De^4 - Di(x)^4)$

Define Functions for Variables

Lateral Buckling assessment

Define Functions as per Ref [1]

Define Constants for lateral buckling modes (Ref 1 Table 1)

	0	1	2	3	4	5
k =	"Mode"	"K1"	"K2"	"K3"	"K4"	"K5"
1	1	80.76	$6.391 \cdot 10^{-5}$	0.5	$2.407 \cdot 10^{-3}$	$6.938 \cdot 10^{-2}$
2	2	39.478	$1.743 \cdot 10^{-4}$	1	$5.532 \cdot 10^{-3}$	0.109
3	3	34.06	$1.668 \cdot 10^{-4}$	1.294	$1.032 \cdot 10^{-2}$	0.143
4	4	28.2	$2.144 \cdot 10^{-4}$	1.608	$1.047 \cdot 10^{-2}$	0.148
5	"inf"	39.478	$4.705 \cdot 10^{-5}$	$4.705 \cdot 10^{-5}$	$4.495 \cdot 10^{-3}$	$5.066 \cdot 10^{-2}$

Case 1 - Infinite mode lateral buckling

Buckle Wave Length $L_{bar}(x, \phi) := \left[\frac{2.7969 \cdot 10^5 \cdot (E \cdot I(x))^3}{(\phi \cdot W_s(x))^2 \cdot A_{st}(x) \cdot E} \right]^{0.125}$ Ref 1, Eq 22

$$L_{bar}(1 \cdot km, \mu_{lat}(1km)) = 70.066 \text{ m}$$

Axial Force in Buckle $P_{buck}(x, L) := 4 \cdot \pi^2 \cdot \frac{E \cdot I(x)}{L^2}$ Ref 1, Eq 20

$$W_s(1km) = 2.606 \frac{kN}{m}$$

Axial force due to thermal expansion: $P_{o_inf}(x, L, \phi) := P_{buck}(x, L) + 4.7050 \cdot 10^{-5} \cdot A_{st}(x) \cdot E \cdot \left(\frac{\phi \cdot W_s(x)}{E \cdot I(x)} \right)^2 \cdot L^6$ Ref 1, Eq 21

Case 2 - All buckling modes

Arguments in the following functions are defined as follows:

- x - location of interest [m]
- L - Buckle Wave Length [m]
- modeb - buckling mode (1 to 4 for first four modes, 5 for infinite mode)
- f - Lateral Friction Factor
- P - Axial Force

Axial force in buckle $P_{buck}(x, L, modeb) := k_{modeb} \cdot 1 \cdot \frac{E \cdot I(x)}{L^2}$ Ref 1, Eq 26

Pipeline Lateral Buckling Calculation

Axial force due to thermal expansion:

Ref 1, Eq 27

$$P_o(x, L, modeb, \phi) := \begin{cases} P_{buck}(x, L, modeb) \dots & \text{if } modeb < 5 \\ + k_{modeb, 3} \cdot \phi \cdot W_s(x) \cdot L \cdot \left[1 + k_{modeb, 2} \cdot Ast(x) \cdot E \cdot \phi \cdot W_s(x) \cdot \frac{L^5}{(E \cdot I(x))^2} \right]^{0.5} - 1 & \\ P_{o_inf}(x, L, \phi) & \text{otherwise} \end{cases}$$

Maximum Buckle Amplitude: $y_{max}(x, L, modeb, \phi) := k_{modeb, 4} \cdot \phi \cdot \frac{W_s(x)}{E \cdot I(x)} \cdot L^4$ Ref 1, Eq 28

Maximum Bending Moment in Buckle: $M_{max}(x, L, modeb, \phi) := k_{modeb, 5} \cdot \phi \cdot W_s(x) \cdot L^2$ Ref 1, Eq 29

Maximum Slope: $y_{maxbar}(x, L, \phi) := 0.01267 \cdot \left(\phi \cdot \frac{W_s(x)}{E \cdot I(x)} \cdot L^3 \right)$ Ref 1, Eq 25

Define a function, which for a given mode, location and friction factor, returns an array with the following format:

- Col 1 - Buckle Length
- Col 2 - Required axial force to cause buckle with length in column 1

Note that for data processing purposes, all outputs are nondimensionalised within this routine (In MATHCAD all elements of an array must have the same or no units).

```

buck_array(x, modeb, phi) :=
  LL ← Lbar(x, phi)
  ntest ← 500
  for i ∈ 0..ntest
    mult ← i ·  $\frac{20}{ntest}$  + 0.05
    L_test ← LL · mult
    PP ← P_o(x, L_test, modeb, phi)
    ΔT ←  $\left( E \cdot Ast(x) \cdot \frac{\alpha}{PP} \right)^{-1}$ 
    out_i_0 ←  $\frac{L_{test}}{m}$ 
    out_i_1 ←  $\frac{PP}{(kg \cdot m \cdot sec^{-2}) \cdot 1000}$ 
  out
  
```

Define a routine that, given a matrix of Buckle length vs. Axial force, will calculate the minimum axial force to instigate a buckle at a given mode. Output is a vector with the following values:

- 0 - Critical Buckle Length
- 1 - Critical Temperature for buckle (assuming fixed pipeline)
- 2 - Critical buckling load

```

T_P_crit(x, modeb, phi) :=
  L_array ← buck_array(x, modeb, phi) <sup>(0)</sup>
  P_array ← buck_array(x, modeb, phi) <sup>(1)</sup>
  P_crit ← min(P_array)
  L_crit_index ← match(P_crit, P_array)
  L_crit ← L_array <sub>L_crit_index</sub>
  out_0 ← L_crit
  out_1 ← P_crit
  out
  
```

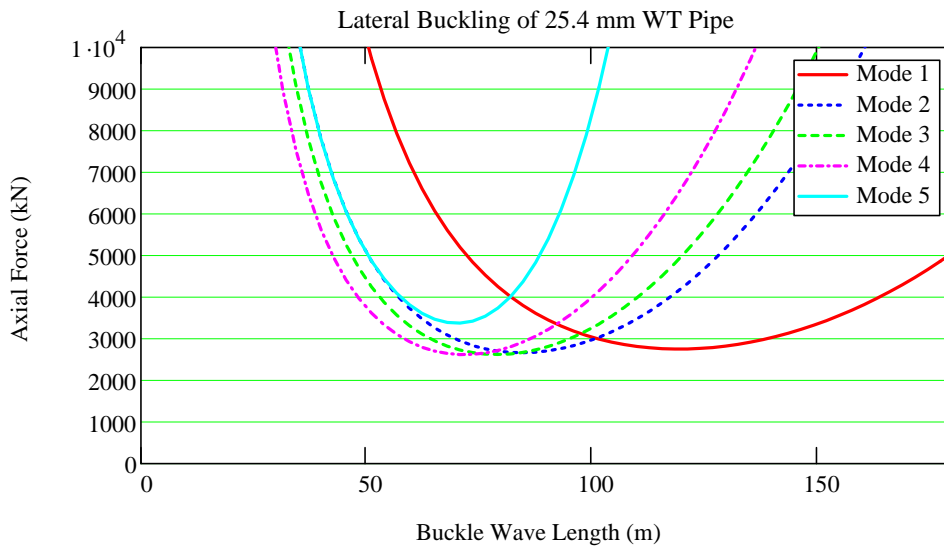
test_data_a := buck_array(1000m, 1, μ_{lat}(1000m)) test_data_b := buck_array(1000m, 2, μ_{lat}(1000m))

test_data_c := buck_array(1000m, 3, μ_{lat}(1000m)) test_data_d := buck_array(1000m, 4, μ_{lat}(1000m))

test_data_e := buck_array(1000m, 5, μ_{lat}(1000m))

Pipeline Lateral Buckling Calculation

Define Functions as per Ref [1]



Calculate Critical buckling temperature and axial force for the specified lateral friction coefficient and a range of modes (The critical buckling temperature is changes only with pipe wall thickness and Friction factor):

$$aa := \min(\text{test_data_a}^{\langle 1 \rangle}) \quad aa = 2751.023$$

$$bb := \min(\text{test_data_b}^{\langle 1 \rangle}) \quad bb = 2662.686$$

$$cc := \min(\text{test_data_c}^{\langle 1 \rangle}) \quad cc = 2619.992$$

$$dd := \min(\text{test_data_d}^{\langle 1 \rangle}) \quad dd = 2619.175$$

$$ee := \min(\text{test_data_e}^{\langle 1 \rangle}) \quad ee = 3373.169$$

$$\text{MinBuckleForce} := \min(\text{test_data_a}^{\langle 1 \rangle}, \text{test_data_b}^{\langle 1 \rangle}, \text{test_data_c}^{\langle 1 \rangle}, \text{test_data_d}^{\langle 1 \rangle}, \text{test_data_e}^{\langle 1 \rangle})$$

$$\text{MinBuckleForce} = 2619.175$$

Pipeline Lateral Buckling Calculation

This MATHCAD sheet calculates the lateral buckling characteristics of a laterally unrestrained pipeline due to axial loads.

Limitations:

1. Consideration of concrete coating is NOT currently implemented in buckling calculations
2. Critical buckling array is for two pipe sizes only - with location fixed.
3. No consideration is given to lateral restraints other than seabed friction.

References:

1. Hobbs, R. E., 'In service buckling of heated pipelines', Journal of transport engineering, Vol 110, No. 2, March 1984.
2. DNV RP F104 - Mechanical Pipeline Couplings, 1999

Load case: **Lateral Soil friction 0.7**

User Inputs **Yellow fields - user input**

NOTE THAT FOR THE PURPOSES OF THE CALCULATIONS PRESENTED HEREIN, KP 0 HAS BEEN DEFINED AS BEING AT THE HOT END

Define KP for Variables	KP := 2km
Input KP Step size	KPStep := 10m
Define range of Kp variable	x := 0, KPStep.. KP
Define (x) in terms of xi (counter)	xi := 0, 1.. $\frac{KP}{KPStep}$

Pipeline Parameters

External Pipeline Diameter	De := 559·mm
Wall Thickness	$WT(x) := \begin{cases} 25.4\text{mm} & \text{if } x < 1\text{km} \\ 25.4\text{mm} & \text{if } x \geq 1\text{km} \end{cases}$

Corrosion Allowance	CA := 3mm
---------------------	-----------

(Corrosion Allowance is used in OSF101 Interaction ratio calculations only)

Young's Modulus of Pipe Material	E := 207000·MPa
Steel Density	$\rho_{st} := 7850 \cdot \text{kg} \cdot \text{m}^{-3}$
Specified Minimum Yield Strength	$SMYS := 450 \cdot \text{N} \cdot \text{mm}^{-2}$
	SMTS := 535MPa

Coefficient of Thermal Expansion	$\alpha := 1.17 \cdot 10^{-5} \cdot \text{C}^{-1}$
----------------------------------	--

Poisson's Ratio	v := 0.3
-----------------	----------

Coating Parameters

Corrosion Coating Density	$\rho_{cc} := 910 \cdot \text{kg} \cdot \text{m}^{-3}$
Corrosion Coating Thickness	Tcor := 5·mm

Pipeline Lateral Buckling Calculation

▢ Conc. Coat Parameters - NotUsed

Environmental Parameters

Density of Water

$$\rho_{\text{water}} := 1027 \cdot \text{kg} \cdot \text{m}^{-3}$$

Water Depth

$$n_w := 2$$

$$i_w := 0..(n_w - 1)$$

KPw_{i_w} :=

0km
2km

WDw_{i_w} :=

100m
100m

Installation Temperature

$$T_o := 5\text{C}$$

▢

Axial Friction Factor

$$\mu(x) := \begin{cases} 0.5 & \text{if } x < 1\text{km} \\ 0.5 & \text{if } x \geq 1\text{km} \end{cases}$$

Lateral Friction Factor

$$\mu_{\text{lat}}(x) := \begin{cases} 0.7 & \text{if } x < 1\text{km} \\ 0.7 & \text{if } x \geq 1\text{km} \end{cases}$$

Operational Parameters

Contents Density

$$\rho_{\text{cont}} := 910 \cdot \text{kg} \cdot \text{m}^{-3}$$

Internal Pressure

$$P_i := 15\text{MPa}$$

Lay Tension:

$$T_{\text{lay}} := 0\text{KN}$$

Calculations Section

▢ Define Functions for Variables

Concrete coating Thickness $T_{\text{con}}(x) := \text{linterp}(KP_{\text{conc}}, T_{\text{conc}}, x)$

Water Depth $WD(x) := \text{linterp}(KP_w, WD_w, x)$

Total Outside Diameter $Do(x) := De + 2 \cdot (T_{\text{cor}} + T_{\text{con}}(x) + T_{\text{mar}})$

Internal Diameter $Di(x) := De - 2 \cdot WT(x)$

Steel Area $A_{\text{st}}(x) := \frac{\pi}{4} \cdot (De^2 - Di(x)^2)$

Steel Mass $M_{\text{st}}(x) := A_{\text{st}}(x) \cdot \rho_{\text{st}}$

Corrosion Coating Area $Acc := \frac{\pi}{4} \cdot [(De + 2 \cdot T_{\text{cor}})^2 - De^2]$

Corrosion Coating Mass $M_{\text{cc}} := Acc \cdot \rho_{\text{cc}}$

Concrete Coating Area $A_{\text{con}}(x) := \frac{\pi}{4} \cdot [(De + 2 \cdot T_{\text{cor}} + 2 \cdot T_{\text{con}}(x))^2 - (De + 2 \cdot T_{\text{cor}})^2]$

Pipeline Lateral Buckling Calculation

Concrete Coating Mass $M_{con}(x) := A_{con}(x) \cdot \rho_{con}$

Mar.Growth Area $A_{mar}(x) := \frac{\pi}{4} \cdot \left[(De + 2 \cdot T_{cor} + 2 \cdot T_{con}(x) + 2 \cdot T_{mar})^2 - (De + 2 \cdot T_{con}(x) + 2 \cdot T_{cor})^2 \right]$

Marine Growth Mass $M_{mar}(x) := A_{mar}(x) \cdot \rho_{mar}$

Contents Mass $M_{cont}(x) := \frac{\pi}{4} \cdot Di(x)^2 \cdot \rho_{cont}$

Buoyancy Force $F_b(x) := \frac{\pi}{4} \cdot Do(x)^2 \cdot \rho_{water} \cdot g$

Submerged Weight $W_s(x) := (M_{st}(x) + M_{cc} + M_{con}(x) + M_{cont}(x) + M_{mar}(x)) \cdot g - F_b(x)$

Second Moment of Area of steel section $I(x) := \frac{\pi}{64} \cdot (De^4 - Di(x)^4)$

Define Functions for Variables

Lateral Buckling assessment

Define Functions as per Ref [1]

Define Constants for lateral buckling modes (Ref 1 Table 1)

	0	1	2	3	4	5
k =	"Mode"	"K1"	"K2"	"K3"	"K4"	"K5"
1	1	80.76	$6.391 \cdot 10^{-5}$	0.5	$2.407 \cdot 10^{-3}$	$6.938 \cdot 10^{-2}$
2	2	39.478	$1.743 \cdot 10^{-4}$	1	$5.532 \cdot 10^{-3}$	0.109
3	3	34.06	$1.668 \cdot 10^{-4}$	1.294	$1.032 \cdot 10^{-2}$	0.143
4	4	28.2	$2.144 \cdot 10^{-4}$	1.608	$1.047 \cdot 10^{-2}$	0.148
5	"inf"	39.478	$4.705 \cdot 10^{-5}$	$4.705 \cdot 10^{-5}$	$4.495 \cdot 10^{-3}$	$5.066 \cdot 10^{-2}$

Case 1 - Infinite mode lateral buckling

Buckle Wave Length $L_{bar}(x, \phi) := \left[\frac{2.7969 \cdot 10^5 \cdot (E \cdot I(x))^3}{(\phi \cdot W_s(x))^2 \cdot A_{st}(x) \cdot E} \right]^{0.125}$ Ref 1, Eq 22

$$L_{bar}(1 \cdot km, \mu_{lat}(1km)) = 64.413 \text{ m}$$

Axial Force in Buckle $P_{buck}(x, L) := 4 \cdot \pi^2 \cdot \frac{E \cdot I(x)}{L^2}$ Ref 1, Eq 20

$$W_s(1km) = 2.606 \frac{kN}{m}$$

Axial force due to thermal expansion: $P_{o_inf}(x, L, \phi) := P_{buck}(x, L) + 4.7050 \cdot 10^{-5} \cdot A_{st}(x) \cdot E \cdot \left(\frac{\phi \cdot W_s(x)}{E \cdot I(x)} \right)^2 \cdot L^6$ Ref 1, Eq 21

Case 2 - All buckling modes

Arguments in the following functions are defined as follows:

- x - location of interest [m]
- L - Buckle Wave Length [m]
- modeb - buckling mode (1 to 4 for first four modes, 5 for infinite mode)
- f - Lateral Friction Factor
- P - Axial Force

Axial force in buckle $P_{buck}(x, L, modeb) := k_{modeb} \cdot 1 \cdot \frac{E \cdot I(x)}{L^2}$ Ref 1, Eq 26

Pipeline Lateral Buckling Calculation

Axial force due to thermal expansion:

Ref 1, Eq 27

$$P_o(x, L, modeb, \phi) := \begin{cases} P_{buck}(x, L, modeb) \dots & \text{if } modeb < 5 \\ + k_{modeb, 3} \cdot \phi \cdot W_s(x) \cdot L \cdot \left[1 + k_{modeb, 2} \cdot Ast(x) \cdot E \cdot \phi \cdot W_s(x) \cdot \frac{L^5}{(E \cdot I(x))^2} \right]^{0.5} - 1 & \\ P_{o_inf}(x, L, \phi) & \text{otherwise} \end{cases}$$

Maximum Buckle Amplitude: $y_{max}(x, L, modeb, \phi) := k_{modeb, 4} \cdot \phi \cdot \frac{W_s(x)}{E \cdot I(x)} \cdot L^4$ Ref 1, Eq 28

Maximum Bending Moment in Buckle: $M_{max}(x, L, modeb, \phi) := k_{modeb, 5} \cdot \phi \cdot W_s(x) \cdot L^2$ Ref 1, Eq 29

Maximum Slope: $y_{maxbar}(x, L, \phi) := 0.01267 \cdot \left(\phi \cdot \frac{W_s(x)}{E \cdot I(x)} \cdot L^3 \right)$ Ref 1, Eq 25

Define a function, which for a given mode, location and friction factor, returns an array with the following format:

- Col 1 - Buckle Length
- Col 2 - Required axial force to cause buckle with length in column 1

Note that for data processing purposes, all outputs are nondimensionalised within this routine (In MATHCAD all elements of an array must have the same or no units).

```

buck_array(x, modeb, phi) :=
  LL ← Lbar(x, phi)
  ntest ← 500
  for i ∈ 0..ntest
    mult ← i · 20 / ntest + 0.05
    L_test ← LL · mult
    PP ← P_o(x, L_test, modeb, phi)
    ΔT ← (E · Ast(x) · α / PP)-1
    outi, 0 ← L_test / m
    outi, 1 ← PP / (kg m sec-2) · 1000
  out
  
```

Define a routine that, given a matrix of Buckle length vs. Axial force, will calculate the minimum axial force to instigate a buckle at a given mode. Output is a vector with the following values:

- 0 - Critical Buckle Length
- 1 - Critical Temperature for buckle (assuming fixed pipeline)
- 2 - Critical buckling load

```

T_P_crit(x, modeb, phi) :=
  L_array ← buck_array(x, modeb, phi)<0>
  P_array ← buck_array(x, modeb, phi)<1>
  P_crit ← min(P_array)
  L_crit_index ← match(P_crit, P_array)
  L_crit ← L_arrayL_crit_index
  out0 ← L_crit
  out1 ← P_crit
  out
  
```

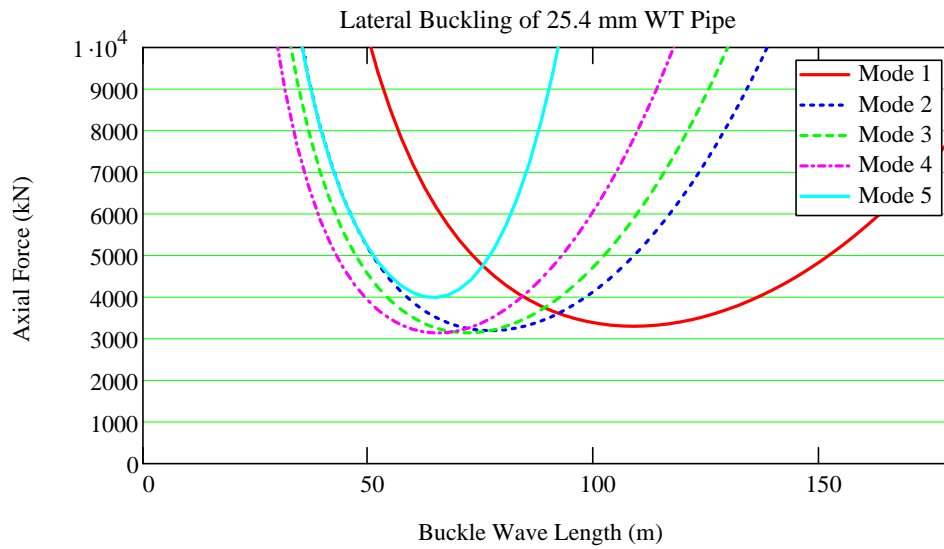
test_data_a := buck_array(1000m, 1, μ_{lat}(1000m)) test_data_b := buck_array(1000m, 2, μ_{lat}(1000m))

test_data_c := buck_array(1000m, 3, μ_{lat}(1000m)) test_data_d := buck_array(1000m, 4, μ_{lat}(1000m))

test_data_e := buck_array(1000m, 5, μ_{lat}(1000m))

Pipeline Lateral Buckling Calculation

Define Functions as per Ref [1]



Calculate Critical buckling temperature and axial force for the specified lateral friction coefficient and a range of modes (The critical buckling temperature is changes only with pipe wall thickness and Friction factor):

$$aa := \min(\text{test_data_a}^{\langle 1 \rangle}) \quad aa = 3299.063$$

$$bb := \min(\text{test_data_b}^{\langle 1 \rangle}) \quad bb = 3192.871$$

$$cc := \min(\text{test_data_c}^{\langle 1 \rangle}) \quad cc = 3140.2$$

$$dd := \min(\text{test_data_d}^{\langle 1 \rangle}) \quad dd = 3135.52$$

$$ee := \min(\text{test_data_e}^{\langle 1 \rangle}) \quad ee = 3991.188$$

$$\text{MinBuckleForce} := \min(\text{test_data_a}^{\langle 1 \rangle}, \text{test_data_b}^{\langle 1 \rangle}, \text{test_data_c}^{\langle 1 \rangle}, \text{test_data_d}^{\langle 1 \rangle}, \text{test_data_e}^{\langle 1 \rangle})$$

$$\text{MinBuckleForce} = 3135.52$$

Appendix A-3

Pull-Over Forces and Durations

Trawl Gears Pull-over Forces and Durations Calculation

Master Thesis - Offshore Technology, University of Stavanger - Norway

Date : 5 April 2011

Author : Iswan Herlianto

Description :

This MathCAD spreadsheet will calculate the impact energy and pull-over load to be used as load input in ANSYS FEA Model.

The trawl gears data are based Table 2-1 DNV RP F111[3]. The calculations are based on DNV RP F111[3].

UNITS :

DESIGN DATA :

Pipeline Data :

Pipeline Outside Diameter	OD := 559mm
Wall Thickness	tkwall := 25.4mm
Corrosion Allowance	tcorr := 3mm
Length of pipeline	$L := 2000\text{m}$
Pipe wall thickness (stress calculation)	$t_s := \text{tkwall} - \text{tcorr}$

Material Properties :

Pipeline : SML 450I U

Pipe Steel Density	DENS := $7850\text{kg}\cdot\text{m}^{-3}$
SMYS Steel Pipe	SMYS := 450MPa
SMTS Steel Pipe	SMTS := 535MPa
Steel Pipe Young's Modulus	E := 207000MPa

Insulation or Coating :

External Coating Thickness	t_ext := 5mm
Insulation or Coating Density	P_EXT := $910\cdot\text{kg}\cdot\text{m}^{-3}$
Concrete Coating Thickness	t_conc := 0mm
Concrete Coating Density	P_CONC := $2400\cdot\text{kg}\cdot\text{m}^{-3}$
Effective Pipe Diameter	$D_{\text{EFF}} := \text{OD} + 2\cdot(\text{t}_{\text{ext}} + \text{t}_{\text{conc}})$ D_EFF = 0.569 m

Operating Parameters :

Max Content Density (OIL)	DENSFL := $900\cdot\text{kg}\cdot\text{m}^{-3}$
Design Pressure	Pres_d := 15MPa
Operating Pressure	Pres_op := 15MPa
Hydrotest Pressure	Pres_hyd := 0MPa
Operating Temperature	T_op := 100C

Environmental Data :

Sea Water Density	RHO_W := $1027\cdot\text{kg}\cdot\text{m}^{-3}$
Ambient Temperature	T_amb := 5C
Water depth	WD := 100m

Soil Properties :

Axial Friction Factor	$\mu_{\text{axial}} := 0.5$
Lateral Friction Factor	$\mu_{\text{lateral}} := 0.3$

Safety Criteria :

Fluid Category	B
Location Class	1
Safety Class	Normal
Load Effect Factor	$\gamma := 1.1$
Conditional Load Effect Factor	$\gamma_c := 1.07$
Functional Load Factor	$\gamma_f := 1$

Note :

The load effect loading factor, γ_c , is to be applied on the vertical component of the pipeline response from the trawl pull-over load, i.e. to the moment acting about the horizontal axis perpendicular to the pipeline axis.

The functional load factor, γ_f , is to be applied to the total pipeline response from the pull-over load, i.e. both the axial force and moment response from the pull-over load.

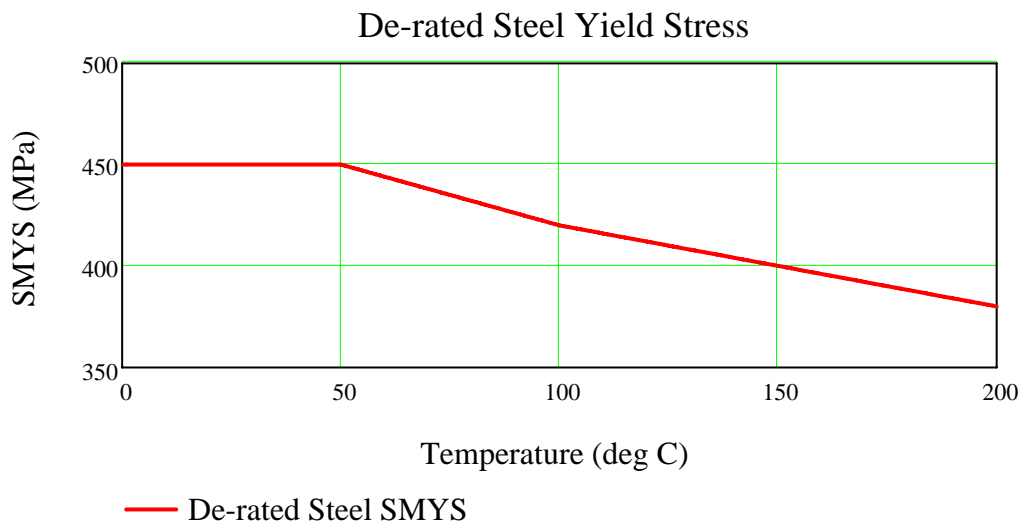
Reduction Factors: (figure 3-3 DNV RP F111 depending on the pipe diameter and soil type)

Added	$R_{fa} := 0.25$
mass	
Steel	$R_{fs} := 0.55$
mass	

PLOT : Steel Material Strength

$T := 0C, 1C.. 200C$

$$SMYS(T) := \begin{cases} SMYS & \text{if } T \leq 50C \\ SMYS - \left[\left[\frac{3(T - 50C)}{5} \right] \cdot \frac{MPa}{C} \right] & \text{if } 50C < T \leq 100C \\ SMYS - \left[\left(\frac{T - 100 \cdot C}{2.5} \right) \cdot \frac{MPa}{C} + 30MPa \right] & \text{otherwise} \end{cases}$$



$SMYS(T_{op}) = 420 \text{ MPa}$

$f_{y_{temp}} := SMYS(T_{op})$

TRAWL GEARS DATA :

Additional data

Span height	$H_{SP} := 0m$	(no span, span height = 0m)
Warp line diameter	$dw := 38mm$	
Warp line length	$lw := 3 \cdot WD$	
The Warp Line stiffness	$k_w := \frac{3.5 \cdot 10^7 N}{lw}$	(eq. 4.9 DNV RP F111)

1) POLIVALENT & RECTANGULAR

Design Parameters (Table 3.1 DNV RP F111)

Trawl board length	$l_{PR} := 4.5m$	
Trawl board height	$h_{PR} := 3.5m$	
Steel mass	$m_{tPR} := 4500kg$	
In plane stiffnes	$k_{iPR} := 500 \cdot 10^6 N \cdot m^{-1}$	
In plane stiffnes	$k_{bPR} := 10 \cdot 10^6 N \cdot m^{-1}$	
Direction on Impact	$\phi_{PR} := 45$	
Ch factor based n span height	$Ch_{PR} := 0.85$	(no span, span height = 0m)
Impact Velocity	$v_{PR} := 2.8 \cdot m \cdot s^{-1}$	
Hydrodynamic added mass	$m_{aPR} := 2.14 \cdot m_{tPR}$	$m_{aPR} = 9630 kg$
Coefficient for Pull-over duration	$C_T := 2$	(eq. 4.21 section 4.5)

Impact Energy Analysis : (conservative)

Absorbed Impact Energy :

Due to the impacting steel mass (eq. 3.1 DNV RP F111)

$$Es_{PR} := R_{fs} \cdot \frac{m_{tPR}}{2} \cdot (Ch_{PR} \cdot v_{PR})^2 \quad Es_{PR} = 7009.695 J$$

Due to the hydrodynamic mass (eq. 3.3 DNV RP F111)

$$\text{The impacting force} \quad Fb_{PR} := Ch_{PR} \cdot v_{PR} \cdot (m_{aPR} \cdot k_{bPR})^{0.5} \quad Fb_{PR} = 738.567 kN$$

$$\text{Impact Energy} \quad Ea_{PR} := \min \left[R_{fa} \cdot \frac{2 \cdot Fb_{PR}^3}{75 \cdot fy_{temp} \cdot t_s^3}, \frac{m_{aPR}}{2} \cdot (Ch_{PR} \cdot v_{PR})^2 \right] \quad Ea_{PR} = 1354.679 J$$

$$\text{Maximum Absorbed Energy} \quad E_{PR} := \max(Es_{PR}, Ea_{PR}) \quad E_{PR} = 7009.695 J$$

Pull-Over Parameter Calculation :

Pull-over Load (section 4.3 DNV RP F111)

$$\text{Dimensionless Height} \quad H_{PR} := \frac{H_{sp} + 0.5 \cdot D_{EFF} + 0.2m}{0.5 \cdot h_{PR}} \quad (\text{eq. 4.5 DNV RP F111})$$

$$\text{The Empirical Coefficient as function of trawl gear type and some geometrical parameters} \quad C_{F,PR} := 8 \cdot \left(1 - e^{-0.8 H_{PR}} \right) \quad (\text{eq. 4.3 DNV RP F111})$$

$$\text{Maximum Pull-over force} \quad F_{PPR} := C_{F,PR} \cdot v_{PR} \cdot (m_{tPR} \cdot k_w)^{0.5} \quad (\text{eq. 4.2 DNV RP F111})$$

$$\text{Maximum downward acting force} \quad Fz_{PR} := F_{PPR} \cdot \left(0.2 + 0.8 \cdot e^{-2.5 \cdot H_{PR}} \right) \quad (\text{eq. 4.10 DNV RP F111})$$

Pull-over Load Duration (section 4.5 DNV RP F111)

$$\text{Pull-over duration} \quad T_{pPR} := C_T \cdot C_{F,PR} \cdot \left(\frac{m_{tPR}}{k_w} \right)^{0.5} \cdot (1 + 0.1) \quad T_{pPR} = 0.687 \text{ s}$$

Note:

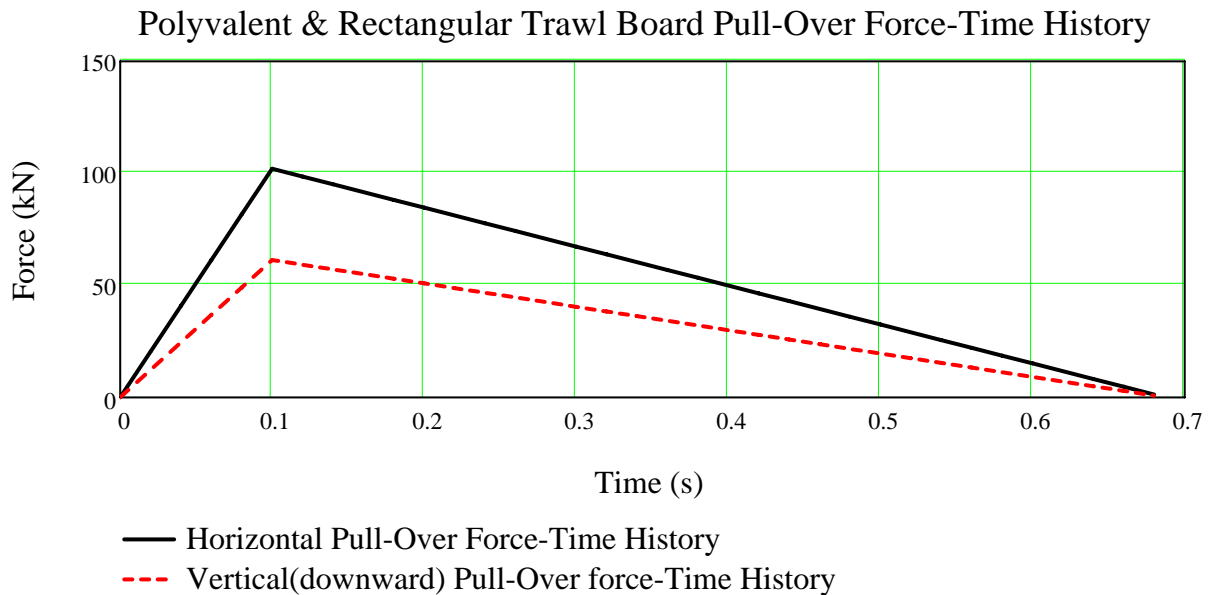
$\delta p/v$ is assumed as $T_p/10$. see explanation in section 4.5 DNV RP F111.

The fall time for trawl boards may be taken as 0.6s, unless the pull-over given by Eq 4.20 is less than this, in which case the fall time should be equal to the total time but still allowing for some force build-up say 0.1s.[DNV RP F111]

PLOT : Force-Time history for Polyvalent and Rectangular trawl board pull-over force on pipeline

$$t := 0 \cdot s, 0.02s .. T_{pPR}$$

$$F_{pPR}(t) := \begin{cases} F_{pPR} \cdot \frac{t}{0.1s} & \text{if } 0s \leq t < 0.1s \\ F_{pPR} - \frac{F_{pPR} \cdot (t - 0.1s)}{T_{pPR} - 0.1s} & \text{otherwise} \end{cases} \quad F_{zPR}(t) := \begin{cases} F_{zPR} \cdot \frac{t}{0.1s} & \text{if } 0s \leq t < 0.1s \\ F_{zPR} - \frac{F_{zPR} \cdot (t - 0.1s)}{T_{pPR} - 0.1s} & \text{otherwise} \end{cases}$$



Result Summary : (for one trawl board)

Maximum Pull-over force	$F_{pPR} = 101.968 \text{ kN}$
Maximum downward acting force	$F_{zPR} = 61.222 \text{ kN}$
Pull-over duration	$T_{pPR} = 0.687 \text{ s}$
	$F_{pPR}(0.1s) = 101.968 \text{ kN}$
	$F_{pPR}(T_{pPR} - 0.6s) = 88.433 \text{ kN}$

2) INDUSTRIAL V-BOARD

Design Parameters (Table 3.1 DNV RP F111)

Trawl board length	$l_I := 4.9\text{m}$	
Trawl board height	$h_I := 3.8\text{m}$	
Steel mass	$m_{tI} := 5000\text{kg}$	
In plane stiffnes	$k_{iI} := 500 \cdot 10^6 \text{N} \cdot \text{m}^{-1}$	
In plane stiffnes	$k_{bI} := 10 \cdot 10^6 \text{N} \cdot \text{m}^{-1}$	
Direction on Impact	$\phi_I := 0$	
Ch factor based n span height	$Ch_I := 1$	
Impact Velocity	$v_I := 1.8 \cdot \text{m} \cdot \text{s}^{-1}$	
Hydrodynamic added mass (for up to 1500kg)	$m_{aI} := 2.9 \cdot m_{tI}$	$m_{aI} = 14500 \text{ kg}$
Coefficient for Pull-over duration	$C_{T,I} := 2$	(eq. 4.21 section 4.5)

Impact Energy Analysis : (conservative)

Absorbed Impact Energy

: Due to the impacting steel mass (eq. 3.1 DNV RP F111)

$$Es_I := R_{fs} \cdot \frac{m_{tI}}{2} \cdot (Ch_I v_I)^2 \quad Es_I = 4455 \text{ J}$$

Due to the hydrodynamic mass (eq. 3.3 DNV RP F111)

The impacting force	$Fb_I := Ch_I v_I (m_{aI} k_{bI})^{0.5}$	$Fb_I = 685.42 \text{ kN}$
---------------------	--	----------------------------

Impact Energy	$Ea_I := \min \left[R_{fa} \cdot \frac{2 \cdot Fb_I^3}{75 \cdot fy_{temp} \cdot t_s^3}, \frac{m_{aI}}{2} \cdot (Ch_I v_I)^2 \right]$	$Ea_I = 1082.769 \text{ J}$
---------------	---	-----------------------------

Maximum Absorbed Energy

$$E_I := \max(Es_I, Ea_I) \quad E_I = 4455 \text{ J}$$

Pull-Over Parameter Calculation :

Pull-over Load (section 4.3 DNV RP F111)

Dimensionless Height

$$H_I := \frac{H_{sp} + 0.5 \cdot D_{EFF} + 0.2\text{m}}{0.5 \cdot h_I} \quad (\text{eq. 4.5 DNV RP F111})$$

The Empirical Coefficient as function of trawl gear type and some geometrical parameters.

$$C_{F,I} := 8 \cdot \left(1 - e^{-0.8 H_I} \right) \quad (\text{eq. 4.3 DNV RP F111})$$

Maximum Pull-over force

$$Fp_I := C_{F,I} v_I (m_{tI} k_w)^{0.5} \quad (\text{eq. 4.2 DNV RP F111})$$

Maximum downward acting force

$$Fz_I := \frac{Fp_I}{2} \quad (\text{eq. 4.11 DNV RP F111})$$

Pull-over Load Duration (section 4.5 DNV RP F111)

Pull-over duration

$$Tp_I := C_T \cdot C_{F,I} \left(\frac{m_{tI}}{k_w} \right)^{0.5} \cdot (1 + 0.1) \quad Tp_I = 0.672 \text{ s}$$

Note:

$\delta p/v$ is assumed as $Tp/10$. see explanation in section 4.5 DNV RP F111.

The fall time for trawl boards may be taken as 0.6s, unless the pull-over given by Eq 4.20 is less than this, in which case the fall time should be equal to the total time but still allowing for some force build-up say 0.1s.[DNV RP F111]

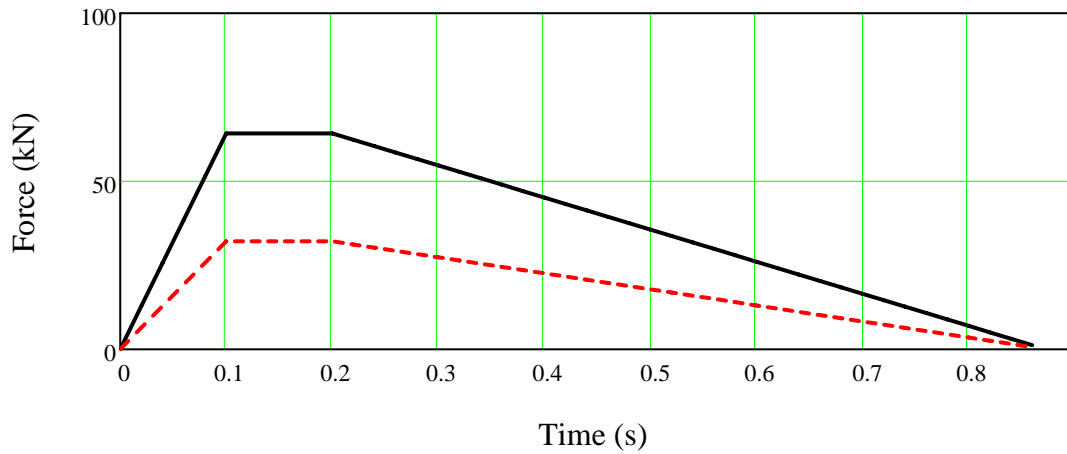
PLOT : Force-Time history for V-board pull-over force on pipeline

$$t := 0 \cdot s, 0.02s \dots T_{pI} + 0.2s$$

$$F_{pI}(t) := \begin{cases} F_{pI} \frac{t}{0.1s} & \text{if } 0s \leq t < 0.1s \\ F_{pI} & \text{if } 0.1s \leq t < 0.2s \\ F_{pI} - \frac{F_{pI}(t - 0.2s)}{T_{pI}} & \text{otherwise} \end{cases}$$

$$F_{zI}(t) := \begin{cases} F_{zI} \frac{t}{0.1s} & \text{if } 0s \leq t < 0.1s \\ F_{zI} & \text{if } 0.1s \leq t < 0.2s \\ F_{zI} - \frac{F_{zI}(t - 0.2s)}{T_{pI}} & \text{otherwise} \end{cases}$$

V-Board Pull-Over Force-Time History



— Horizontal Pull-Over Force-Time History
 - - - Vertical(downward) Pull-Over force-Time History

Result Summary : (for one trawl board)

Maximum Pull-over force	$F_{pI} = 64.181 \text{ kN}$
Maximum downward acting force	$F_{zI} = 32.09 \text{ kN}$
Pull-over duration	$T_{pI} = 0.672 \text{ s}$
	$F_{pI}(0.1s) = 64.181 \text{ kN}$
	$F_{pI}(0.2s) = 64.181 \text{ kN}$
	$F_{pI}(T_{pI} + 0.2s) = -0 \text{ kN}$

3) BEAM TRAWL BOARD

Design Parameters (Table 3.1 DNV RP F111)

Beam Trawl length	$l_B := 17\text{m}$	
Beam Trawl height	$h_B := 3.8\text{m}$	
Steel mass	$m_{tB} := 5500\text{kg}$	
Impact Velocity	$v_B := 3.4 \cdot \text{m} \cdot \text{s}^{-1}$	
Hydrodynamic added mass	$m_{aB} := 1500\text{kg}$	
Effective mass factor	$C_b := 0.5$	(Section 3.4.3)
Coefficient for Pull-over duration	$C_{T,w} := 1.5$	(eq. 4.21 section 4.5)
Number of warplines	$n_w := 3$	(eq. 4.9 section 4.3)

Impact Energy Analysis : (conservative)

Absorbed Impact Energy :

$$E_B := R_{fs} \cdot \frac{C_b}{2} \cdot (m_{tB} + m_{aB}) \cdot v_B^2 \quad (\text{eq. 3.7 section 3.4.3})$$

Pull-Over Parameter Calculation :

Pull-over Load (section 4.3 DNV RP F111)

The Empirical Coefficient as function of trawl gear type and some geometrical parameters without hoopbars

$$C_{F,B} := \begin{cases} 5.0 & \text{if } \frac{D_{EFF}}{0.2\text{m}} \leq 2 \\ 8.0 - 1.5 \frac{D_{EFF}}{0.2\text{m}} & \text{if } 2 < \frac{D_{EFF}}{0.2\text{m}} \leq 3 \\ 3.5 & \text{if } \frac{D_{EFF}}{0.2\text{m}} > 3 \end{cases} \quad (\text{eq. 4.8 DNV RP F111})$$

Note:

CF shall be taken as for beam trawls without hoop bars if it is not assured that all beam trawls in the relevant area have such bars installed.

Ha may be set to 0.2m if no better information available.

Maximum Pull-over force

$$F_{pB} := C_{F,B} \cdot v_B \cdot \left[(m_{aB} + m_{tB}) \cdot n_w \cdot k_w \right]^{0.5} \quad (\text{eq. 4.2 DNV RP F111})$$

Maximum downward acting force

$$F_{zB} := \frac{F_{pB}}{2} \quad (\text{eq. 4.10 DNV RP F111})$$

Pull-over Load Duration (section 4.5 DNV RP F111)

Pull-over duration

$$T_{pB} := C_T \cdot C_{F,B} \cdot \left(\frac{m_{tB}}{n_w \cdot k_w} \right)^{0.5} \cdot (1 + 0.1) \quad T_{pB} = 0.772 \text{ s}$$

Note:

$\delta p/v$ is assumed as $T_p/10$. see explanation in section 4.5 DNV RP F111.

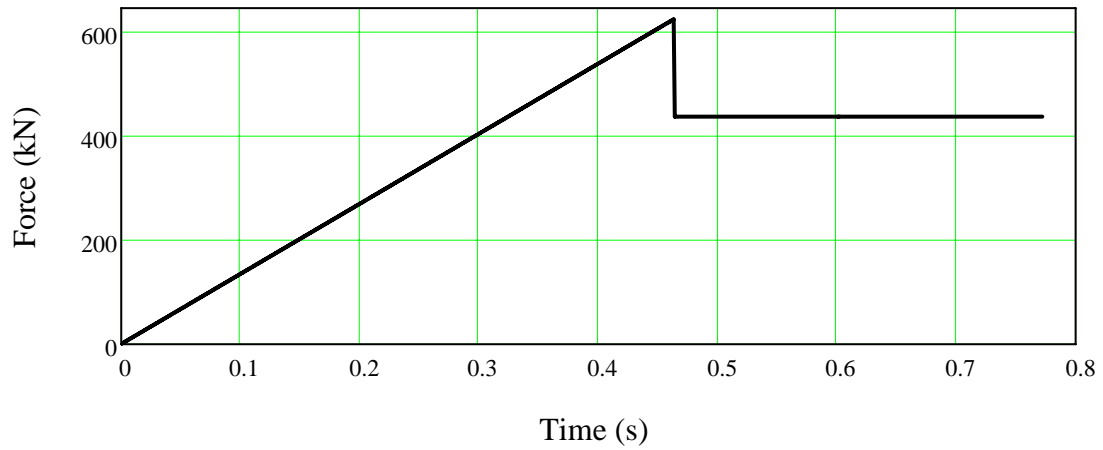
The fall time for trawl boards may be taken as 0.6s, unless the pull-over given by Eq 4.20 is less than this, in which case the fall time should be equal to the total time but still allowing for some force build-up say 0.1s.[DNV RP F111]

PLOT : Force-Time history for Beam Trawl Board pull-over force on pipeline

$$t := 0 \cdot \text{s}, 0.001 \text{s} \dots T_{pB}$$

$$F_{pb}(t) := \begin{cases} F_{pB} \cdot \frac{t}{0.6 T_{pB}} & \text{if } 0 \text{s} \leq t < 0.6 \cdot T_{pB} \\ 0.7 \cdot F_{pB} & \text{if } 0.6 \cdot T_{pB} \leq t < T_{pB} \\ 0 & \text{if } t \geq T_{pB} \end{cases}$$

Beam Trawl Board Pull-Over Force-Time History



— Horizontal Pull-Over Force-Time History

Result Summary : (total for both beam shoes)

Maximum Pull-over force

$$F_{pB} = 628.148 \text{ kN}$$

Pull-over duration

$$T_{pB} = 0.772 \text{ s}$$

$$F_{pb}(0\text{s}) = 0 \text{ N}$$

$$F_{pb}(0.6 \cdot T_{pB} - 0.001\text{s}) = 626.792 \text{ kN}$$

$$F_{pb}(0.6 \cdot T_{pB} + 0.001\text{s}) = 439.703 \text{ kN}$$

$$F_{pb}(T_{pB} - 0.001\text{s}) = 439.703 \text{ kN}$$

$$F_{pb}(T_{pB} + 0.001\text{s}) = 0 \text{ kN}$$

4) CLUMP WEIGHTS (ROLLER TYPE)

Design Parameters (Table 3.1 DNV RP F111)

Clump weight length	$l_{CW} := 4\text{m}$	
Clump weight height	$h_{CW} := 0.76\text{m}$	(diameter cross section)
Steel mass	$m_{tCW} := 9000\text{kg}$	
Impact Velocity	$v_{CW} := 2.8 \cdot \text{m} \cdot \text{s}^{-1}$	
In plane stiffness	$k_{iCW} := 4200 \cdot 10^6 \text{N} \cdot \text{m}^{-1}$	
Hydrodynamic added mass	$m_{aCW} := 3140\text{kg}$	

Note:

the added mass can be estimated as the mass of the displaced seawater volume, multiplied by a factor 2.29 for proximity to sea bed and a factor 0.8 for limited length, according to DNV RP C205.

Impact Energy Analysis : (conservative)

$$\text{Absorbed Impact Energy : } E_{CW} := R_{fs} \cdot (m_{tCW} + m_{aCW}) \cdot v_{CW}^2 \quad (\text{eq. 3.8 section 3.4.4})$$

Pull-Over Parameter Calculation :

Pull-over Load (section 4.3 DNV RP F111)

$$\begin{aligned} &\text{Distance from the reaction point to the} \\ &\text{centre of gravity of the clump weight} \\ &\text{(based on roller type clump weight drum dia.} \\ &\text{of 0.76m)} \end{aligned} \quad L_{\text{clump}} := 0.7\text{m} \quad (\text{Roller type, eq.4.14 section 4.4})$$

$$\text{Dimensionless Height} \quad h := \frac{H_{sp} + D_{\text{EFF}}}{L_{\text{clump}}} \quad (\text{eq. 4.13 DNV RP F111})$$

$$\text{Maximum Horizontal Pull-over force} \quad F_{pCW} := 3.9 \cdot m_{tCW} \cdot g \cdot (1 - e^{-1.8h}) \cdot \left(\frac{D_{\text{EFF}}}{L_{\text{clump}}} \right)^{-0.65} \quad (\text{eq. 4.12 DNV RP F111})$$

$$\text{Maximum downward pull-over force} \quad F_{zdCW} := 0.1 \cdot F_{pCW} - 1.1 \cdot m_{tCW} \cdot g \quad (\text{eq. 4.19 DNV RP F111})$$

$$\text{Maximum upward Pull-over force} \quad F_{zuCW} := 0.3 \cdot F_{pCW} - 0.4 \cdot m_{tCW} \cdot g \quad (\text{eq. 4.18 DNV RP F111})$$

Note:

In each case it should be considered if the upward or the downward force will give the most critical load combination.

Pull-over Load Duration (EQ. 4.23 Section 4.6 DNV RP F111)

$$\text{Pull-over duration} \quad T_{pCW} := \frac{F_{pCW}}{k_w \cdot v_{CW}} \cdot (1 + 0.1) \quad T_{pCW} = 1.03 \text{ s}$$

Note:

as for trawl boards and beam trawls, δp is the displacement of the pipe at the point of interaction which is unknown prior to the response simulation. Therefore, the value of $\delta p/v$ is assumed as $0.1x F_p/(k_w \cdot V)$. see explanation in section 4.6 DNV RP F111.

PLOT : Force-Time history for Clump Weight pull-over force on pipeline

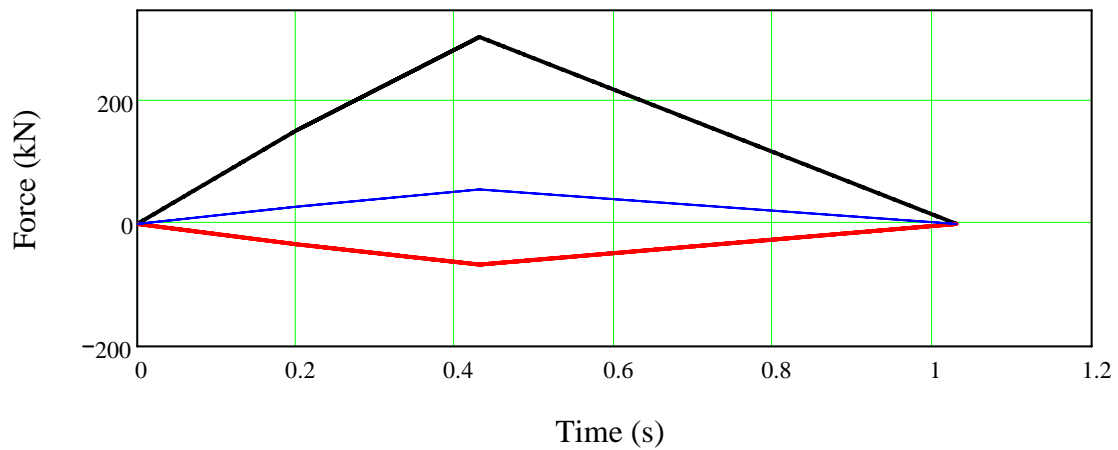
$$t := 0 \cdot \text{s}, 0.001 \text{s} .. T_{pCW}$$

$$F_{pcw}(t) := \begin{cases} 0.5 \cdot F_{pCW} \cdot \frac{t}{0.2\text{s}} & \text{if } 0\text{s} \leq t < 0.2\text{s} \\ \left[\frac{t - 0.2\text{s}}{(T_{pCW} - 0.6\text{s}) - 0.2\text{s}} \cdot 0.5 F_{pCW} \right] + 0.5 F_{pCW} & \text{if } 0.2\text{s} \leq t < T_{pCW} - 0.6\text{s} \\ F_{pCW} - \frac{F_{pCW} \cdot [t - (T_{pCW} - 0.6\text{s})]}{0.6\text{s}} & \text{otherwise} \end{cases}$$

$$F_{zdcw}(t) := \begin{cases} 0.5 \cdot F_{zd_{CW}} \cdot \frac{t}{0.2s} & \text{if } 0s \leq t < 0.2s \\ \left[\frac{t - 0.2s}{(T_{p_{CW}} - 0.6s) - 0.2s} \cdot 0.5F_{zd_{CW}} \right] + 0.5F_{zd_{CW}} & \text{if } 0.2s \leq t < T_{p_{CW}} - 0.6s \\ F_{zd_{CW}} - \frac{F_{zd_{CW}} \cdot [t - (T_{p_{CW}} - 0.6s)]}{0.6s} & \text{otherwise} \end{cases}$$

$$F_{zucw}(t) := \begin{cases} 0.5 \cdot F_{zu_{CW}} \cdot \frac{t}{0.2s} & \text{if } 0s \leq t < 0.2s \\ \left[\frac{t - 0.2s}{(T_{p_{CW}} - 0.6s) - 0.2s} \cdot 0.5F_{zu_{CW}} \right] + 0.5F_{zu_{CW}} & \text{if } 0.2s \leq t < T_{p_{CW}} - 0.6s \\ F_{zu_{CW}} - \frac{F_{zu_{CW}} \cdot [t - (T_{p_{CW}} - 0.6s)]}{0.6s} & \text{otherwise} \end{cases}$$

Clump Weight (Roller Type) Pull-Over Force-Time History



- Horizontal Pull-Over Force-Time History
- Vertical(downward) Pull-Over Force-Time History
- Vertical(upward) Pull-Over Force-Time History

Result Summary :

Maximum Pull-over force	$F_{p_{CW}} = 305.962 \text{ kN}$
Maximum downward pull-over force	$F_{zd_{CW}} = -66.49 \text{ kN}$
Maximum upward Pull-over force	$F_{zu_{CW}} = 56.485 \text{ kN}$
Pull-over duration	$T_{p_{CW}} = 1.03 \text{ s}$
	$F_{pcw}(0.2s) = 152.981 \text{ kN}$
	$F_{pcw}(T_{p_{CW}} - 0.6s) = 305.962 \text{ kN}$
	$F_{pcw}(T_{p_{CW}}) = 0 \text{ N}$

Appendix B

Finite Element Model

ANSYS Script

```

*****
!*
!* Title      : The Effect of Trawl Gear Impact Load
!*            : on Lateral Buckling of HT/HP Subsea Pipeline
!* Company   : Subsea 7 Norway
!* Date      : March 2011
!* Originator : Iswan Herlianto
!*           : Master Student in Offshore Tech. University of Stavanger, Norway
!*
*****
!* Description:
!* The respon analysis of lateral buckling on HT/HP subsea pipeline due
!* Trawl Gear Impact Loads
!*
!* Status/Comments:
!* See loadcomb.inp
!* - Pull-over load using *DO loops
!* - Results commands done
!* To do:
!*
!*
*****

! File Desc.: Model 22in pipeline
FINI
/CLEAR

*SET,LOADCASE,'Pol&Rect_LC4'

/TITLE,%LOADCASE%
!File Desc.: Polyvalent&Rectangular Trawl Pull-Over UB(1.0Fp) Vs Upper Bound Lateral friction(0.7)
/FILENAME,%LOADCASE%
/UNITS,MKS                                ! MKS system (m,kg,s,deg C)

#####
!#   Various parameters      # #   Unit are [m] [N] [Kg] [s] [deg C] #
#####

pi=4*ATAN(1.0)                ! Phi
g=9.81                        ! Gravitational Acceleration (m/s^2)
WD=100                         ! Water Depth (m)

/PREP7                          ! Enter model creation preprocessor
!ANTYPE,0,NEW                  ! 0=STATIC
ACEL,,g                        ! Define gravity

ET,1,PIPE288                   ! Pipe elements
SECTYPE,1,PIPE                 ! Define pipe section type
SECDATA,559E-3,25.4E-3        ! Define pipe section:OD,Tkwall [m]

ET,2,TARGE170                 ! Seabed element
ET,3,CONTA175                 ! Contact elements

!-----
!                               PIPELINE DATA
!-----
!#DIMENSION FOR WEIGHT CALCULATION

OD=559E-3                      ! Pipe Outer Diameter (m)
tkwall=25.4E-3                 ! Pipe Wall Thickness (m)
DI=OD-2*tkwall                 ! Pipe Inner Diameter (m)

L=2000                          ! Pipe Model Length (m)

t_ext=3E-3                     ! External Coating Thickness (m)
t_conc=0E-3                    ! Concrete Coating Thickness (m)
    
```


!#OPERATIONAL DATA

RHO_W=1027 ! Water Density (Kg/m³)
 DENSFL=900 ! Content Density OIL (Kg/m³)

Pres_d=15E6 ! Design Pressure (N/m²)
 Pres_op=15E6 ! Operating Pressure (N/m²)
 Pres_hyd=0E6 ! Hydrotest Pressure (N/m²)

T_amb=5 ! Ambient Temperature (deg C)
 T_op=100 ! Operating Temperature (deg C)

!R_lay= ! Residual Lay Tension

!#MATERIAL PROPERTIES

!MP,DENS,1,7850 ! Pipe Material density (Kg/m³)
 ! defined as equivalent density

MPTEMP,1,0,100 ! Define temperatures for Young's modulus
 MP,EX,1,207E9 ! Young's modulus (N/m²)

MP,ALPX,1,1.17E-5 ! Thermal expansion coefficient (/deg C)

MP,PRXY,1,0.3 ! Poisson ratio

!#COATING DENSITY

P_EXT=910 ! Insulation or Coating Density (Kg/m³)
 P_CONC=2400 ! Concrete Coating Density (Kg/m³)

!-----
 ! **DEFINE STRESS-PLASTIC STRAIN CURVE**
 !-----

TB,KINH,1,2,4 !PLASTIC ! Activate a data table (Multilinear kinematic
 ! hardening using von Mises or Hill plasticity)
 TBTEMP,20.0 ! Temperature = 20.0deg C
 TBPT,,0.0,0.0 ! Strain = 0.0000, Stress = 0.0
 TBPT,,0.002174,450E6 ! Strain = 0.2174%, Stress = 450E6 N/m²
 TBPT,,0.020,450E6 ! Strain = 2.0%, Stress = 450E6 N/m²
 !TBPT,,0.060,535E6 ! Strain = 6.0%, Stress = 535E6 N/m²
 TBTEMP,100.0 ! Temperature = 100.0deg C
 TBPT,,0.0,0.0 ! Strain = 0.0000, Stress = 0.0
 TBPT,,0.00203,420E6 ! Strain = 0.203%, Stress = 420E6 N/m²
 TBPT,,0.020,420E6 ! Strain = 2.0%, Stress = 420E6 N/m²
 !TBPT,,0.060,505E6 ! Strain = 6.0%, Stress = 505E6 N/m²

!# PLOT #

!-----
 TBLIST,KINH,1 ! List the data table
 /XRANGE,0,0.01 ! X-axis of TBPLOT to extend from varepsilon=0 to 0.01
 TBPLOT,KINH,1 ! Display the data table
 !FINISH ! Exit the preprocessor
 !/EOF

!-----
 ! SEABED DATA
 !-----

!DEFINE SEABED SOIL FRICTION

FRICLAX=0.5 ! Soil friction coefficient in axial direction
 FRICLLAT=0.7 ! Soil friction coefficient in lateral direction

TB,FRIC,2,,,ORTHO ! Define orthotropic soil friction
 TBDATA,1,FRICLAX,FRICLLAT

igap=0 ! Initial gap between pipeline and seabed
 !bgap=295-(d_coating/2) ! Gap between pipe to peak seabed profile point
 bgap=0 ! Gap between pipe to peak seabed profile point

```

!-----
!                                     PIPE SYSTEM PARAMETER CALCULATION
!-----

D_EFF=OD+2*(t_ext+t_conc)           ! Effective Pipe Diameter (m)
AS=pi*(OD**2-DI**2)/4              ! Cross-sectional Area of Pipe Steel (m^2)
AS_EXT=pi*((OD+2*t_ext)**2-OD**2)/4 ! Cross-sectional Area of External Coating (m^2)
AS_CONC=pi*((OD+2*t_ext+2*t_conc)**2-(OD+2*t_ext)**2)/4 ! Cross-sectional Area of Concrete Coating (m^2)

M_STEEL=AS*7850                    ! Pipe Steel Mass (Kg/m)
M_EXT=AS_EXT*P_EXT                 ! External Coating Mass (Kg/m)
M_CONC=AS_CONC*P_CONC             ! Concrete Coating Mass (Kg/m)
M_CONT=pi*(DI**2)*DENSFL/4        ! Content Mass (Kg/m)
M_WATE=pi*(DI**2)*RHO_W/4        ! Water Mass (Kg/m)

M_BUOY=pi*(D_EFF**2)*RHO_W/4     ! Buoyancy Mass (Kg/m)
MWALL=M_STEEL+M_EXT+M_CONC       ! Pipeline Total Mass (Kg/m) (weight on air)
M_SUB=MWALL-M_BUOY               ! Submerged Mass (Kg/m) (weight in water)

W_CONT=M_CONT*g                   ! Content Weight (N/m)
W_WATE=M_WATE*g                   ! Flooded Weight (N/m)
W_SUB=M_SUB*g                     ! Empty Pipe Submerged Weight (N/m)
EQ_DEN=M_SUB/AS                   ! Submerged pipe Equivalent Density (kg/m^3)

DENSIN=((t_ext*P_EXT)+(t_conc*P_CONC))/(t_ext+t_conc) ! Insulation Eqv. Density (Corr. & Concr. Coat.) (N/m)
TKIN=t_ext+t_conc                ! Insulation thickness (Corr. & Concr. Coat.) (m)
AREAIN=AS_EXT+AS_CONC            ! Insulation Area (Corrosion coat.& Concrete Coat.) (m^2)

!-----
! **APPLY WEIGHT ON PIPELINE**
!-----

MP,DENS,1,EQ_DEN                  ! Pipe Material density (Kg/m^3)
                                  ! using Equivalent Density for submerged weight
SECCONTROLS,M_CONT               ! added mass: Content(kg/m)

!-----
!                                     ELEMENT REAL CONSTANT
!-----
!# FOR PIPELINE !
!-----!

KEYOPT,1,1,0                      ! Temperature Through wall gradient
!KEYOPT,1,3,0                      ! linear shape functions
KEYOPT,1,4,1                      ! Thin Pipe Theory
KEYOPT,1,6,0                      ! Internal and External pressure cause loads on end caps
KEYOPT,1,7,0                      ! Output control for section forces/moments and strains/curvatures

KEYOPT,1,8,0                      ! Output control at integration points (1=Maximum and minimum
stresses/strains)
KEYOPT,1,9,2
KEYOPT,1,15,0                    ! One result for each section integration point

!-----!
!# SEABED      !
!-----!
R,22,,,1,0,2                    ! Define Normal Contact Stiffness Factor and Penetration Tolerance Factor
                                  ! (use ANSYS default)

KEYOPT,3,10,2                    ! Set option 10 (Contact Stiffnes Update) for element type 3 to 2 (Each
substep based on mean
                                  ! stress of underlying elements from the previous substep (pair based))
                                  ! Update stiffness automaticly based on maximum penetration
KEYOPT,3,2,1                    ! Penalty method, static stiffness of seabed
!KEYOPT,3,3,1                    ! Contact M0del: (0)Contact Force Based (1)Contact traction based
KEYOPT,3,4,2
!KEYOPT,3,5,3                    ! Either Close the gap or reduces initial penetration

```

```
!KEYOPT,3,9,4          ! 3=Include offset only (exclude initial geometrical penetration or gap) or
                       ! 4=gradually resolve
KEYOPT,3,10,2         !
KEYOPT,3,12,0        ! Behaviour of Contact Surface (0=standard)
```

```
!-----
!                PULL-OVER LOADS : Polyvalent & Rectangular Trawl Gears
!-----
```

```
!# Horizontal Pull-Over Force #
```

```
!-----
*DIM,HORFORCE,TABLE,4,1
HORFORCE(1,1)=0.0,101968,0.0,0.0      ! 1.0Fp: Horizontal Pull-over in column 1 [N]
HORFORCE(1,0)=2.0,2.1,2.7,3.0        ! Corresponding pull-over time in column 0 [sec]
HORFORCE(0,1)=1                       ! Zeroth row
```

```
!# Downward Pull-Over Force #
```

```
!-----
*DIM,VERFORCE,TABLE,4,1
VERFORCE(1,1)=0.0,-61222,0.0,0.0     ! Vertical ("-": Downward) Pull-over in column 1 [N]
VERFORCE(1,0)=2.0,2.10,2.7,3.0      ! Corresponding pull-over time in column 0 [sec]
VERFORCE(0,1)=1                       ! Zeroth row
```

```
!-----
!                PIPELINE MODELING
!-----
```

```
#####
!#      Generate Keypoints (m)                                     #
!#####
K,      1      ,      0.0      ,      0.0      ,      0.0
K,      2      ,      200.0    ,      0.0      ,      0.0
K,      3      ,      400.0    ,      0.0      ,      0.0
K,      4      ,      600.0    ,      0.0      ,      0.0
K,      5      ,      800.0    ,      0.0      ,      0.0
K,      6      ,      1000.0   ,      0.0      ,      0.0
K,      7      ,      1200.0   ,      0.0      ,      0.0
K,      8      ,      1400.0   ,      0.0      ,      0.0
K,      9      ,      1600.0   ,      0.0      ,      0.0
K,     10      ,      1800.0   ,      0.0      ,      0.0
K,     11      ,      2000.0   ,      0.0      ,      0.0
ant_k=11
```

```
!*****
!* Create nodes to describe local coordinate systems for ends *
!*****
```

```
K,     12      ,      -25.0    ,      0.0      ,      0.0
K,     13      ,      0.0      ,      25.0     ,      0.0
K,     14      ,      2025.0   ,      0.0      ,      0.0
K,     15      ,      2000.0   ,      25.0     ,      0.0
```

```
!*****
!* Create new coordinate systems for ends (11,12)*
!*****
```

```
CSKP, 11      ,0      ,1      ,12     ,13
CSKP, 12      ,0      ,11     ,14     ,15
```

```
CSYS,0          ! Activate the default coordinate system (0)
```

```

#####
!#      Generate Lines      #
#####

*DO,I,1,ant_k-1           ! Define line between two keypoints
    L,I,I+1
*ENDDO

#####
!#      Meshing            #
#####

ESIZE,1.2*OD              ! Element size of pipe

|*****
!* Meshing of straight pipe elements      *
|*****

LSEL,S,LINE,,1,10         ! Selecting straight pipe elements
TYPE,1                    ! Element type, material, constants
MAT,1
!REAL,11

LMESH,ALL                 ! Create mesh for straight elements

|-----
!                               SEABED MODELING
|-----
|*****
!* Meshing of seabed elements
|*****

! Define nodes for seabed area
N,    3001    ,    -15.0    ,    -igap    ,    15.0
N,    3002    ,     2015    ,    -igap    ,    15.0
N,    3003    ,     2015    ,    -igap    ,   -15.0
N,    3004    ,    -15.0    ,    -igap    ,   -15.0

!#DEFINE TARGET ELEMENT##
!-----

TYPE,2                     ! Select material and properties for seabed
MAT,2
REAL,22
TSHAPE,QUAD               ! SET TARGET SHAPE
E,3001,3002,3003,3004     ! Define Element

LSEL,S,LINE,,1,10         ! Select line (straight pipe element)
NSLL,,1                   ! Select nodes associated with those lines

TYPE,3                     ! Select element type 3
!INSEL,R,LOC,X,0          ! Reselect nodes (DOF) in X-direction
!INSEL,R,LOC,Y,0          ! Reselect nodes (DOF) in Y-direction
!INSEL,R,LOC,Z,0          ! Reselect nodes (DOF) in Z-direction
ESURF                     ! Generate contact elements overlaid on the free faces of existing
selected elements

ALLSEL                     ! - Seabed done
    
```

```

!-----
!                               MISC: END LOCAL COORDINATE
!-----

e1=NODE(KX(1),KY(1),KZ(1))      ! Rotate end nodes to local coordinate system
CSYS,11                          ! Identify end node and
NROTAT,e1                        ! change nodal coordinate system

e2=NODE(KX(ant_k),KY(ant_k),KZ(ant_k))  ! Identify end node and
CSYS,12                          ! change nodal coordinate system
NROTAT,e2

CSYS,0

GPLOT

!-----
!                               DISPLAY MODEL
!-----

/ESHAPE,1                         ! Display elements as solids
/TRIAD,rbot                       ! Display XYZ triad in right bottom corner
/PSYMB,NDIR,1                     ! Display nodal coord. system if other than globa

WAVES                             ! Initiates reordering for the solution phase
WSORT                             ! Sorts elements based on geometric sort
!WMID,YES

SAVE                              ! Save all current database information
PARSAV,ALL,param,txt             ! Save parameters to param.txt

FINISH                            ! Exit the preprocessor
!/EOF

#####
!#          SOLUTION PROCESSOR          #
#####

/CONFIG,NRES,20000
/SOLU                              ! Enter solution processor
ANTYPE,TRANS                       ! 0=STATIC

NLGEOM,ON                          ! Includes large deflection effects in a static or full transient analysis

NEQIT,1000                         ! Specifies the maximum number of equilibrium iterations for
                                   ! nonlinear analyses

AUTOTS,ON                          ! Automatic time stepping

NROPT,UNSYM                        ! Specifies the Newton-Raphson options in a static or full transient
                                   ! analysis
                                   ! (FULL or UNSYM= the stiffness matrix is updated at every
                                   ! equilibrium iteration)

NSUBST,10,20,10                   ! Specifies the number of substeps to be taken every load step (nbr
                                   ! this step, maximum number of
                                   ! substeps to be taken (i.e. min. time step), minimum number of
                                   ! step (i.e. max time step)

PSTRES,ON                          ! Calculate Prestress Effects
LNSRCH,on                          ! Linesearch-Alternative to adaptive descent

PARRES,,param,txt                 ! Read parameters from param.txt

TREF,T_amb                         ! Reference Temperature (deg C) for Thermal Strain Calculation

SFCUM,PRES,ADD                    ! Cumulative Surface Load On
CNCHECK,AUTO                       ! Adjust the initial status of contact pairs
    
```

```

|*****
!*                               LOAD STEPS
|*****

TIME,1                               ! Set the time for the end of the load step
/STITLE,1,PIPELINE LAID ON SEABED-INITIAL CONDITION

                                     ! Set Boundary Condition
D,e1,ALL                               ! Initial state: placed at initial positions, Fix End 1
D,e2,ALL
  !D,e2,UY,0                           ! Fix vertically End 2
  !D,e2,UZ,0                           ! Fix laterally End 2

ESEL,S,ENAME,,PIPE288
ESLL,S                               ! Selects all elemets associated with the lines
SFE,ALL,2,PRES,0,RHO_W*ACC*WD       ! Hydrostatic pressure @ 100m WD (N/m)

ALLSEL
SOLVE
SAVE

!FINI
!/EOF

|-----

TIME,2
/STITLE,1,APPLY OPERATING PRESSURE AND TEMPERATURE

5-POUT                               ! Surface Loads PIPE288: Pressures -- 1-PINT, 2-PX, 3-PY, 4-PZ,
                                     ! Select All lines
ESEL,S,ENAME,,PIPE288
ESLL,S                               ! Selects all elemets associated with the lines

SFE,ALL,1,PRES,0,Pres_op             ! Operating pressure @ 100m WD (N/m)
BFE,ALL,TEMP,1,(T_op-T_amb)         ! Operating Temperature 100deg C

ALLSEL
SOLVE
SAVE

!/DSCALE,all,10
!FINI
!/EOF

|-----

!TIME,3
/STITLE,1,APPLY PULL-OVER LOADS

NSUBST,30,50,10
TM_START=2+1E-1                       ! Starting time (must be > 0)
TM_END=2.9                             ! Ending time of the transient
TM_INCR=0.1                           ! Time increment
*DO,TM,TM_START,TM_END,TM_INCR       ! Do for TM from TM_START to TM_END in
                                     ! steps of TM_INCR
TIME,TM                               ! Time value
/STITLE,1,APPLY PULL-OVER LOADS AT TIME: %TM%
NSEL,S,NODE,,1490                     ! Select Node at Mid Pipeline
  F,ALL,FZ,HORFORCE(TM)              ! Time-varying force (at Mid pipeline)
  F,ALL,FY,VERFORCE(TM)
ALLSEL

```

```

SOLVE                                ! Initiate solution calculations
SAVE
*ENDDO

NSUBST,10,10,10
TM_START2=3                          ! Starting time (must be > 0)
TM_END2=8                             ! Ending time of the transient
TM_INCR2=0.5                          ! Time increment
*DO,TM2,TM_START2,TM_END2,TM_INCR2    ! Do for TM from TM_START to TM_END in
    ! steps of TM_INCR
    TIME,TM2                           ! Time value
    /STITLE,1,POST APPLIED PULL-OVER LOADS AT TIME: %TM2%
    NSEL,S,NODE,,1490                   ! Select Node at Mid Pipeline
    F,ALL,FZ,HORFORCE(TM)              ! Time-varying force (at Mid pipeline)
    F,ALL,FY,VERFORCE(TM)

ALLSEL
SOLVE                                ! Initiate solution calculations
SAVE
*ENDDO

!OUTPR,BASIC,1
PARSAV,ALL,param.txt

/DSCALE,all,10
FINI
!/EOF

|*****
|
|                                EXTRACT RESULTS
|*****
/POST1
/OUTPUT,RESULTS %LOADCASE%,OUT        ! Save file as RESULTS.OUT
*DO,i,2,2.9,0.1                       ! To Time:3
    SET,,,,i
    ESEL,S,ELEM,,1100,1800              ! Select Element number
    !ESEL,R,ENAME,,PIPE288              ! Reselect Element Name

    ! Extract Axial Force
    !ETABLE,FX,SMISC
    ETABLE,a1,SMISC,1                   !Node "I"
    ETABLE,b1,NMISC,14                  !Node "J"
    SABS,1
    SMAX,FX,a1,b1                       !Max Value Axial Force
    !SABS,0

    ! Extract Moments
    ETABLE,a2,SMISC,2                   !Node "I"
    ETABLE,b2,NMISC,15                  !Node "J"
    SABS,1
    SMAX,My,a2,b2                       !Max Value
    !SABS,0

    ETABLE,a3,SMISC,3                   !Node "I"
    ETABLE,b3,NMISC,16                  !Node "J"
    SABS,1
    SMAX,Mz,a3,b3                       !Max Value
    !SABS,0

    ! Display Result on Table
    !PRETAB,FX,My,Mz

    ETABLE,Eqv.Strain,EPTT,EQV          ! Extract Equivalent Total Strain
    ! Elastic+Plastic+Creep+Thermal Strains
    
```

! EXTRACT STRESSES

```

ETABLE,a4,SMISC,64
ETABLE,b4,SMISC,68
SABS,1
SMAX,HOOPStr,a4,b4                                ! Max Value HOOP Stress

ETABLE,a5,SMISC,31                                ! Node "I"
ETABLE,b5,SMISC,36                                ! Node "J"
SABS,1
SMAX,AXIALStr,a5,b5                                ! Max Value Stress due to Axial Load

ETABLE,a6,SMISC,34                                ! Node "I" Stress due to Bending moment
ETABLE,b6,SMISC,35
SABS,1
SMAX,bend1,a6,b6
!SADD,l1,a5,bend1

                                                    ! Node "J" Stress due to Bending moment

ETABLE,a7,SMISC,39
ETABLE,b7,SMISC,40
SABS,1
SMAX,bend2,a7,b7
!SADD,l2,a6,bend2

SMAX,LONGTDLStr,bend1,bend2                        ! Max Value Longitudinal Stress
                                                    ! due to bending moment

PRETAB,FX,My,Mz,HOOPStr,LONGTDLStr,AXIALStr,Eqv.Strain  ! Display Result on Table
  
```

*ENDDO

```

*DO,i,3,8,0.5                                     ! To Time:3 to 8
  SET,,,,i
  ESEL,S,ELEM,,1100,1800                           ! Select Element number
  !ESEL,R,ENAME,,PIPE288                           ! Reselect Element Name

                                                    ! Extract Axial Force

  !ETABLE,FX,SMISC
  ETABLE,a1,SMISC,1                                 !Node "I"
  ETABLE,b1,NMISC,14                               !Node "J"
  SABS,1
  SMAX,FX,a1,b1                                    !Max Value Axial Force
  !SABS,0

                                                    ! Extract Moments

  ETABLE,a2,SMISC,2                                 !Node "I"
  ETABLE,b2,NMISC,15                               !Node "J"
  SABS,1
  SMAX,My,a2,b2                                    !Max Value
  !SABS,0

  ETABLE,a3,SMISC,3                                 !Node "I"
  ETABLE,b3,NMISC,16                               !Node "J"
  SABS,1
  SMAX,Mz,a3,b3                                    !Max Value
  !SABS,0

                                                    ! Display Result on Table

  !PRETAB,FX,My,Mz

  ETABLE,Eqv.Strain,EPTT,EQV                       ! Extract Equivalent Total Strain
                                                    ! Elastic+Plastic+Creep+Thermal Strains
  
```

! EXTRACT STRESSES

```

ETABLE,a4,SMISC,64
ETABLE,b4,SMISC,68
SABS,1
  
```



```

SMAX,HOOPStr,a4,b4                                ! Max Value HOOP Stress

ETABLE,a5,SMISC,31                                ! Node "I"
ETABLE,b5,SMISC,36                                ! Node "J"
SABS,1
SMAX,AXIALStr,a5,b5                                ! Max Value Stress due to Axial Load

ETABLE,a6,SMISC,34                                ! Node "I" Stress due to Bending moment
ETABLE,b6,SMISC,35
SABS,1
SMAX,bend1,a6,b6
!SADD,l1,a5,bend1

                                                    ! Node "J" Stress due to Bending moment

ETABLE,a7,SMISC,39
ETABLE,b7,SMISC,40
SABS,1
SMAX,bend2,a7,b7
!SADD,l2,a6,bend2

SMAX,LONGTDLStr,bend1,bend2                       ! Max Value Longitudinal Stress
                                                    ! due to bending moment

PRETAB,FX,My,Mz,HOOPStr,LONGTDLStr,AXIALStr,Eqv.Strain  ! Display Result on Table

*ENDDO

/OUTPUT,DISPLACEMENT %LOADCASE%,OUT              ! Save file as RESULTS.OUT
*DO,i,2,2,9,0.1                                   ! To Time:3
SET,,,,,i
ESEL,S,ELEM,,1100,1800                            ! Select Element number
!ESEL,R,ENAME,,PIPE288                            ! Reselect Element Name

ETABLE,DispX,U,X
ETABLE,DispY,U,Y
ETABLE,DispZ,U,Z

PRETAB,DispX,DispY,DispZ
!PRETAB,DispY,DispZ

*ENDDO

*DO,i,3,8,0.5                                     ! To Time:3
SET,,,,,i
ESEL,S,ELEM,,1100,1800                            ! Select Element number
!ESEL,R,ENAME,,PIPE288                            ! Reselect Element Name

ETABLE,DispX,U,X
ETABLE,DispY,U,Y
ETABLE,DispZ,U,Z

PRETAB,DispX,DispY,DispZ
!PRETAB,DispY,DispZ

*ENDDO

/OUTPUT,
FINI
ALLSEL
/EOF
  
```

Appendix C

FE Analysis Result Graphs

Appendix C-1

Axial Displacement

(X – Direction)

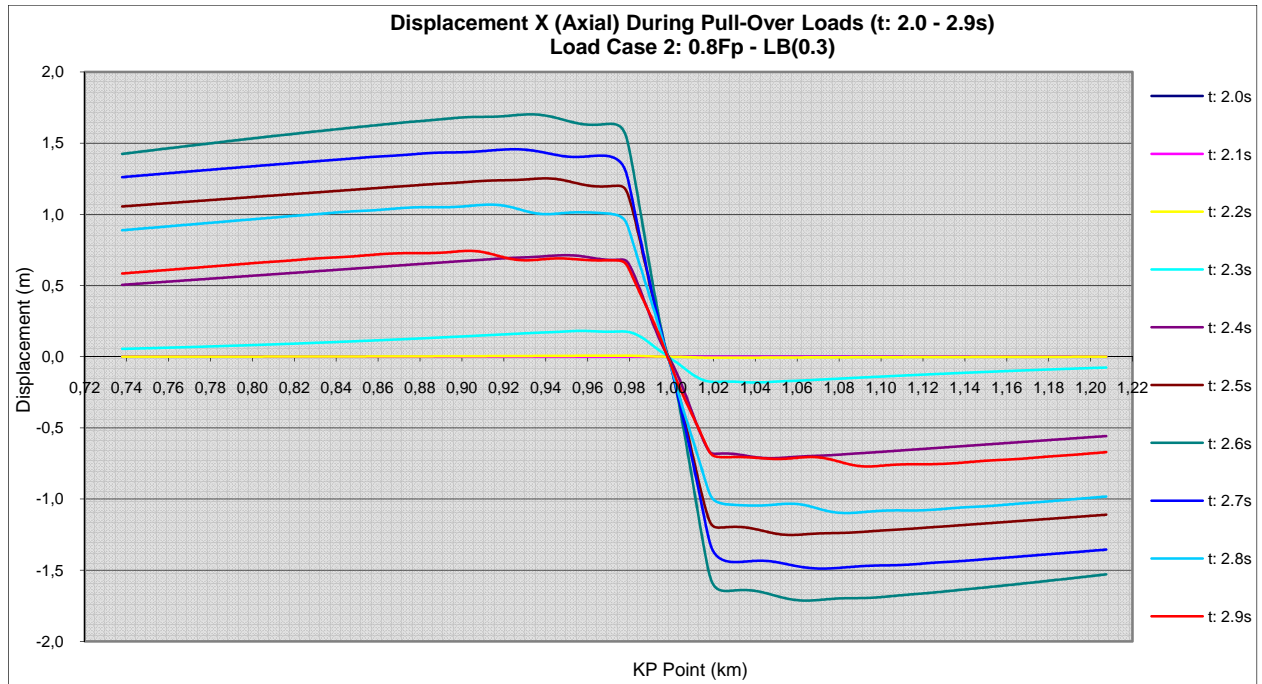


Figure C - 1 Axial displacement during pull-over loads duration (t:2.0-2.9s) for load case 2

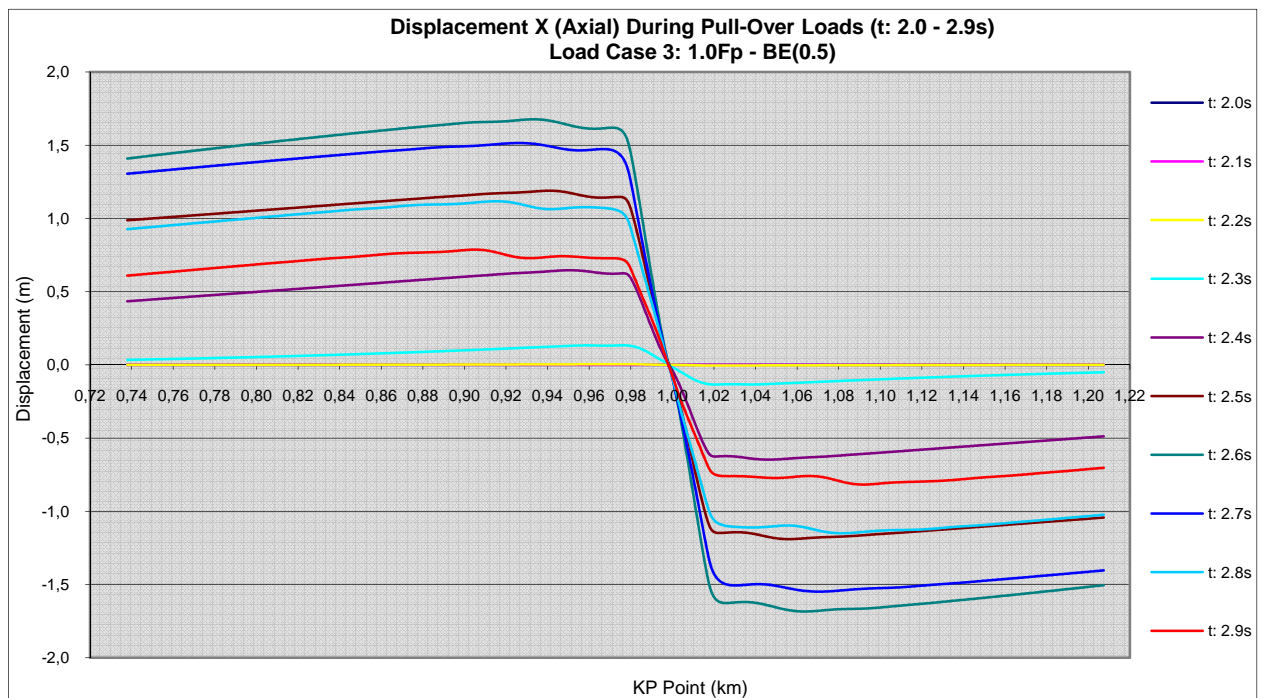


Figure C - 2 Axial displacement during pull-over loads duration (t:2.0-2.9s) for load case 3

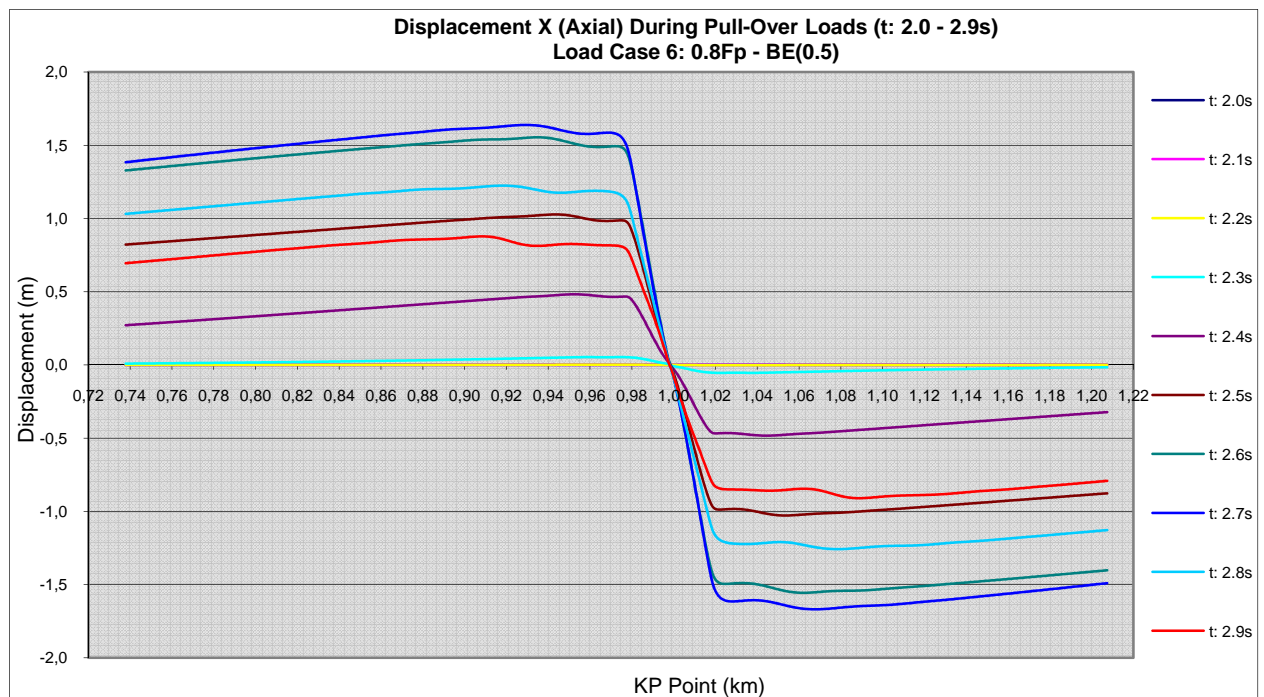


Figure C - 3 Axial displacement during pull-over loads duration (t:2.0-2.9s) for load case 6

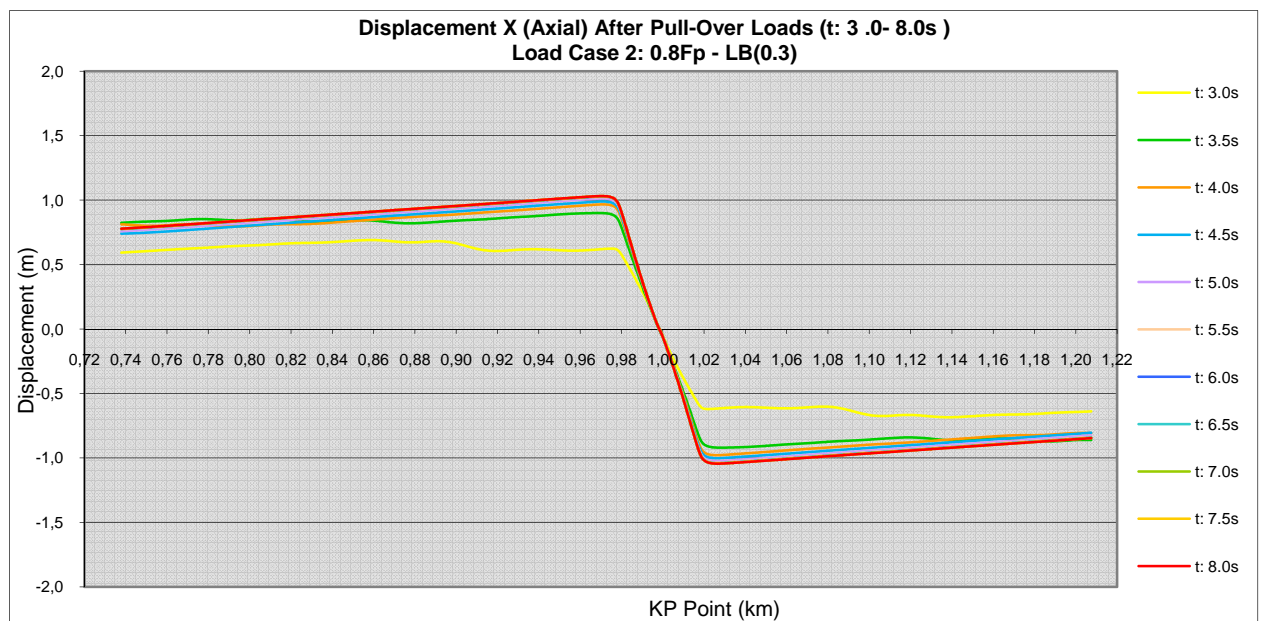


Figure C - 4 Axial displacement after pull-over loads duration (t:3.0-8.0s) for load case 2

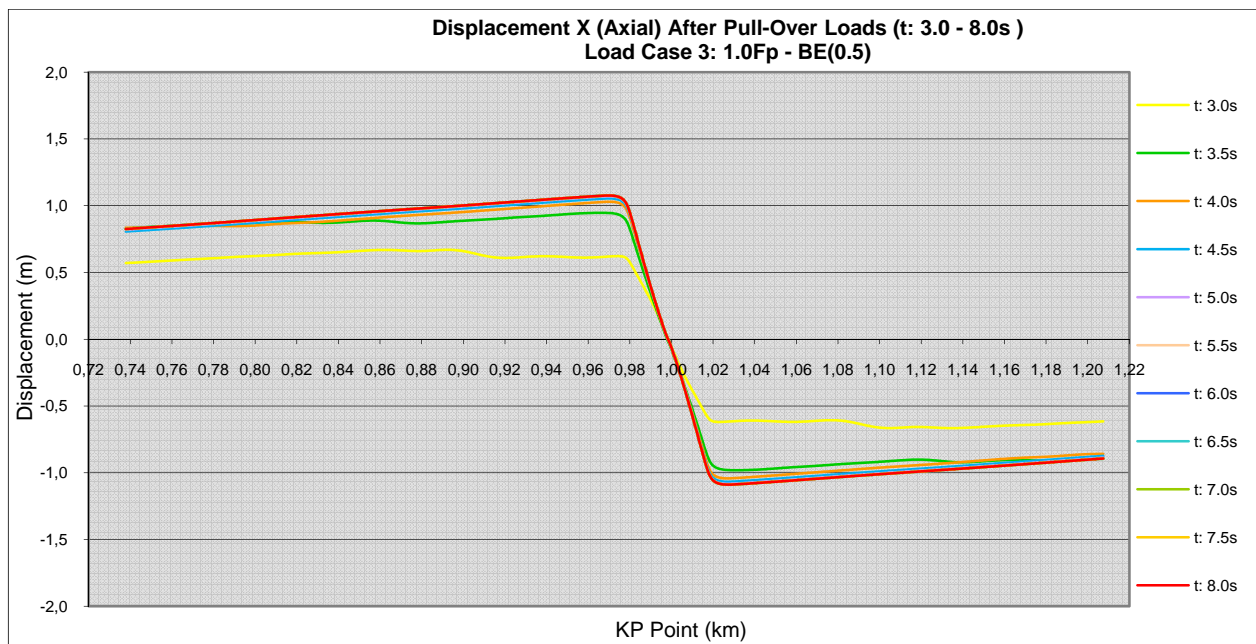


Figure C - 5 Axial displacement after pull-over loads duration (t:3.0-8.0s) for load case 3

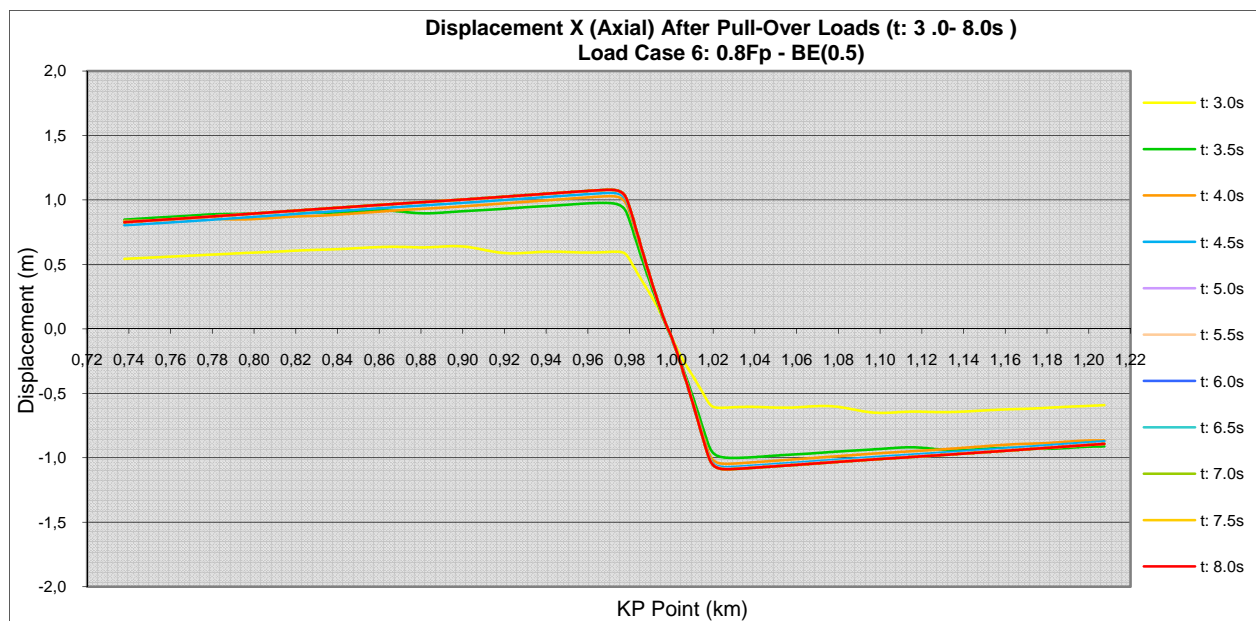


Figure C - 6 Axial displacement after pull-over loads duration (t:3.0-8.0s) for load case 6

Appendix C-2

Lateral Displacement

(Z – Direction)

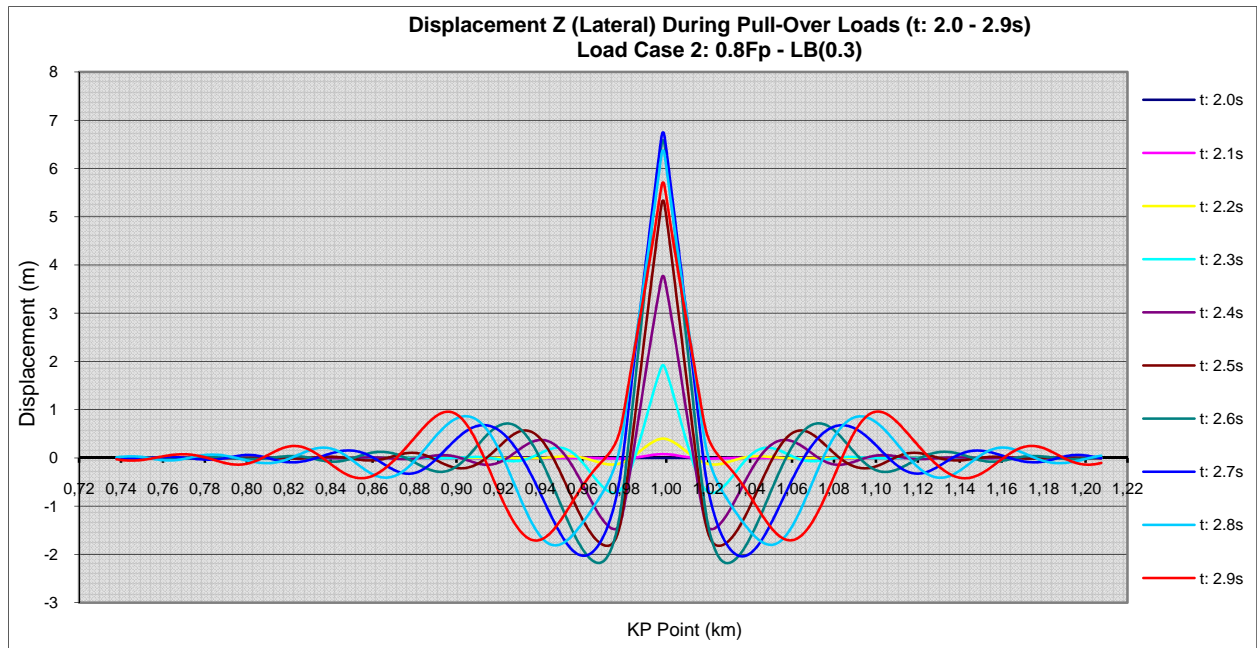


Figure C - 7 Lateral displacement during pull-over loads duration (t:2.0-2.9s) for load case 2

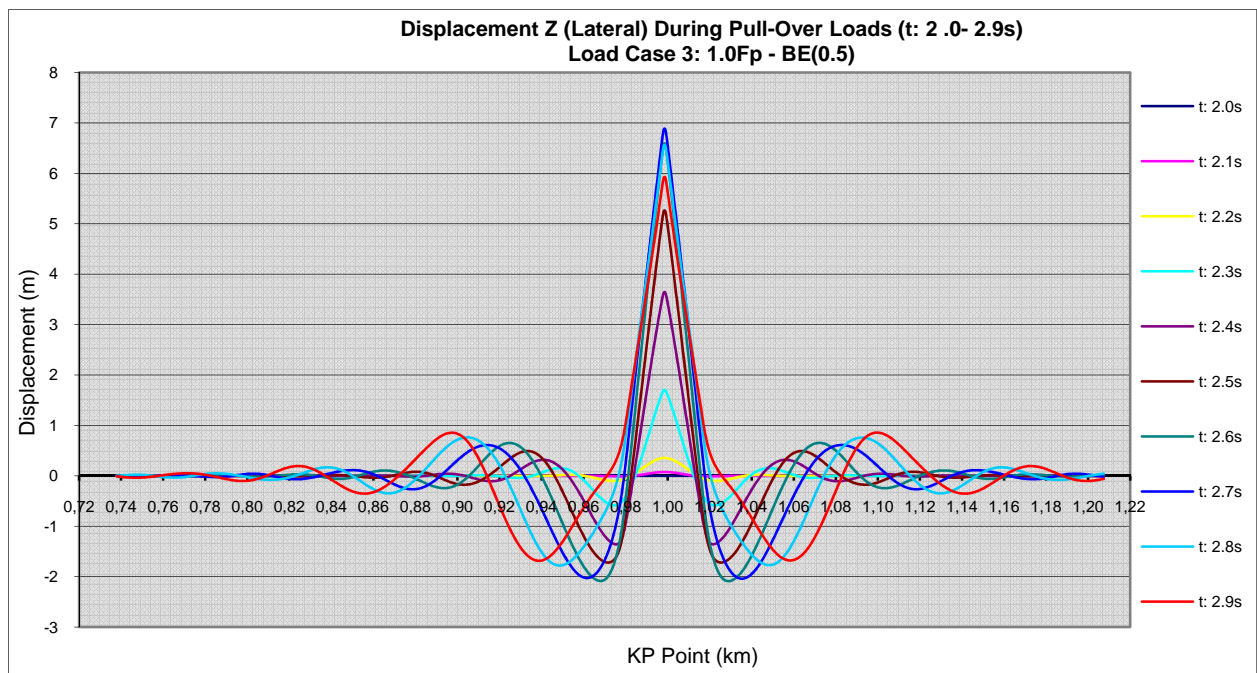


Figure C - 8 Lateral displacement during pull-over loads duration (t:2.0-2.9s) for load case 3

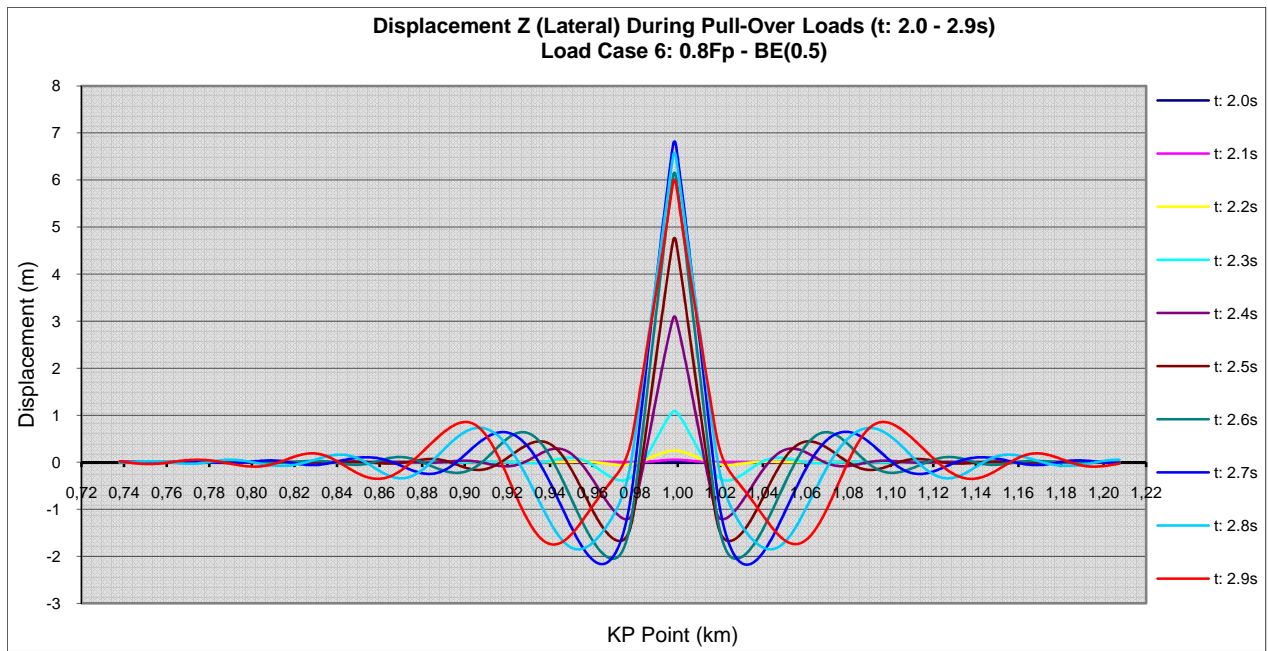


Figure C - 9 Lateral displacement during pull-over loads duration (t:2.0-2.9s) for load case 6

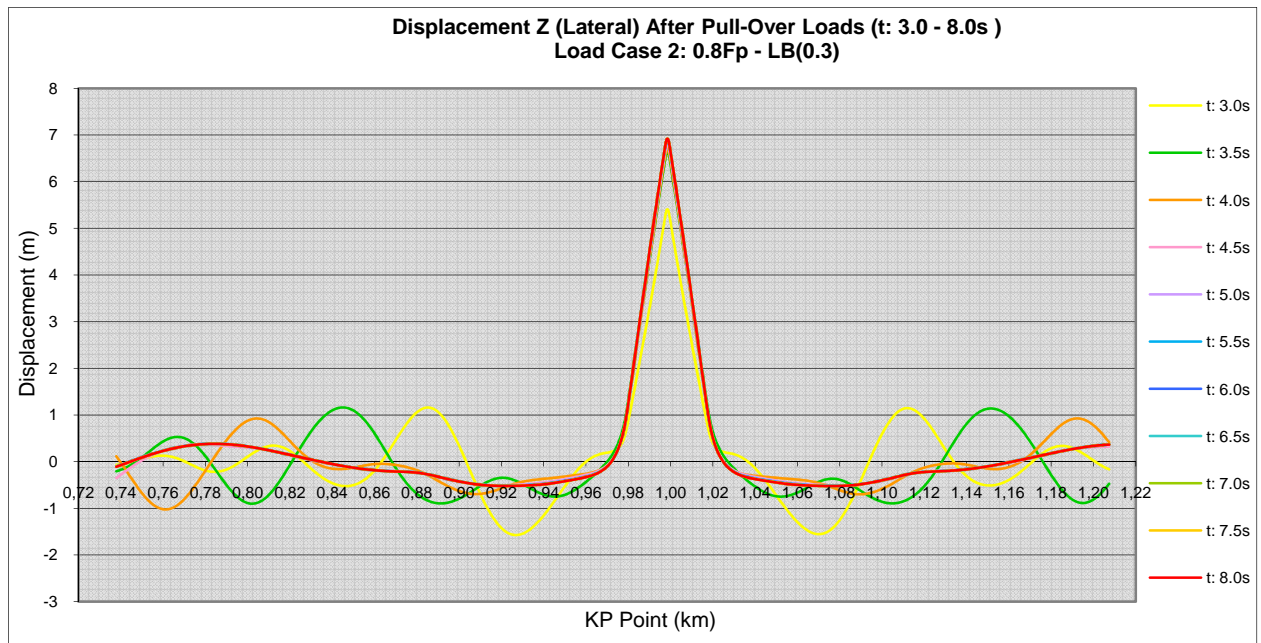


Figure C - 10 Lateral displacement after pull-over loads duration (t:3.0-8.0s) for load case 2

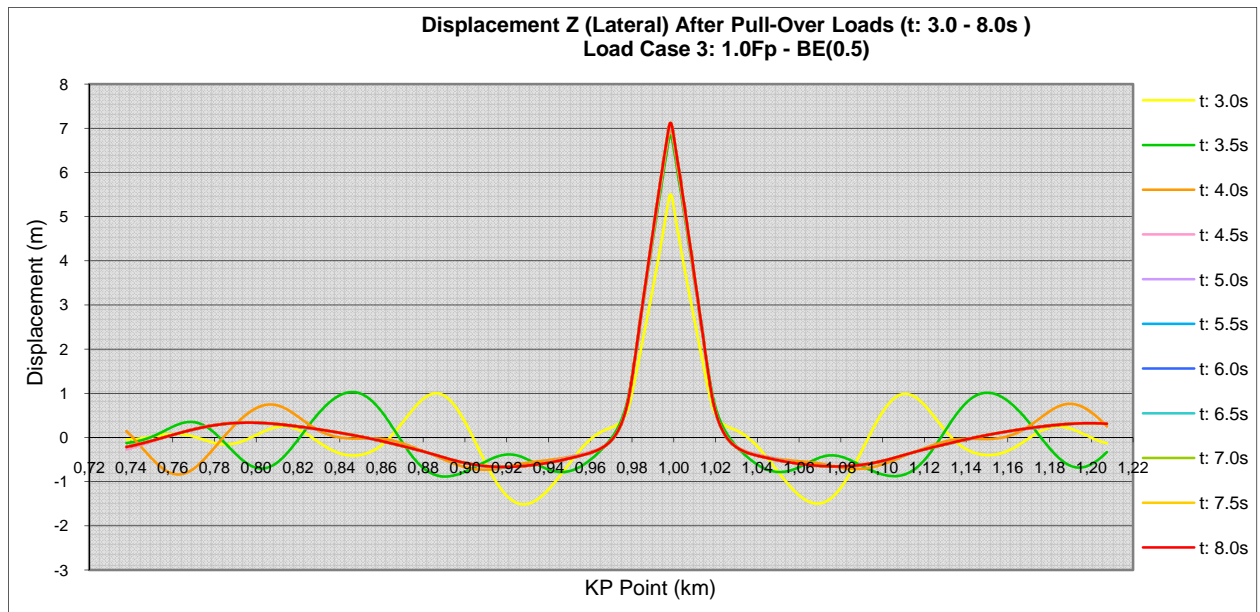


Figure C - 11 Lateral displacement after pull-over loads duration (t:3.0-8.0s) for load case 3

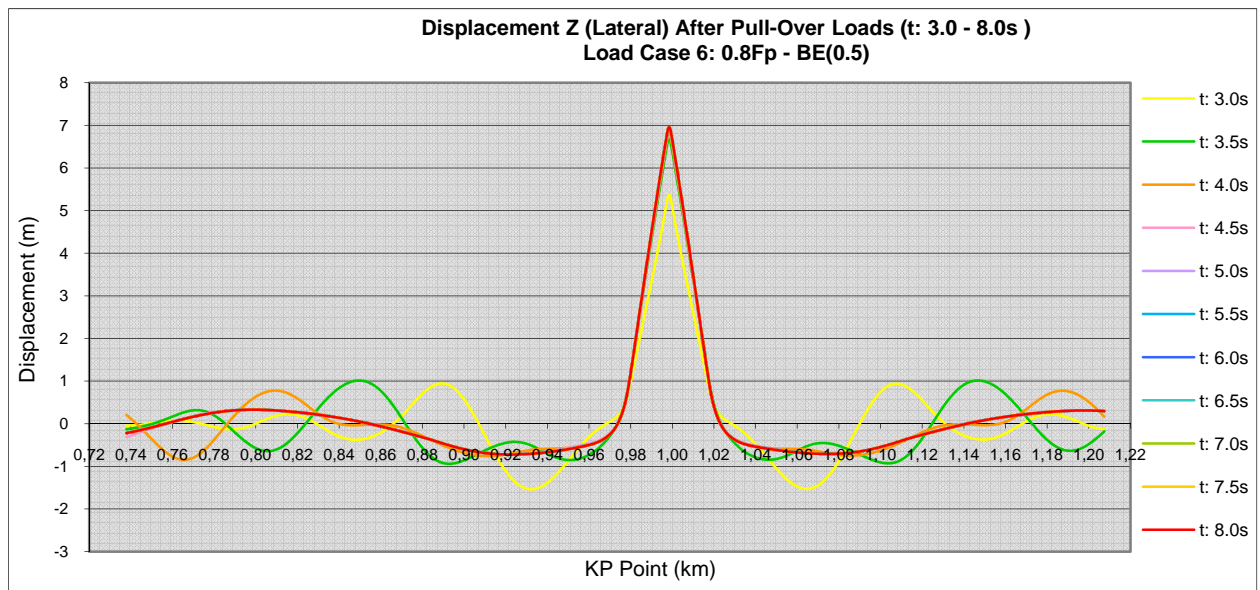


Figure C - 12 Lateral displacement after pull-over loads duration (t:3.0-8.0s) for load case 6

Appendix C-3

Bending Moment

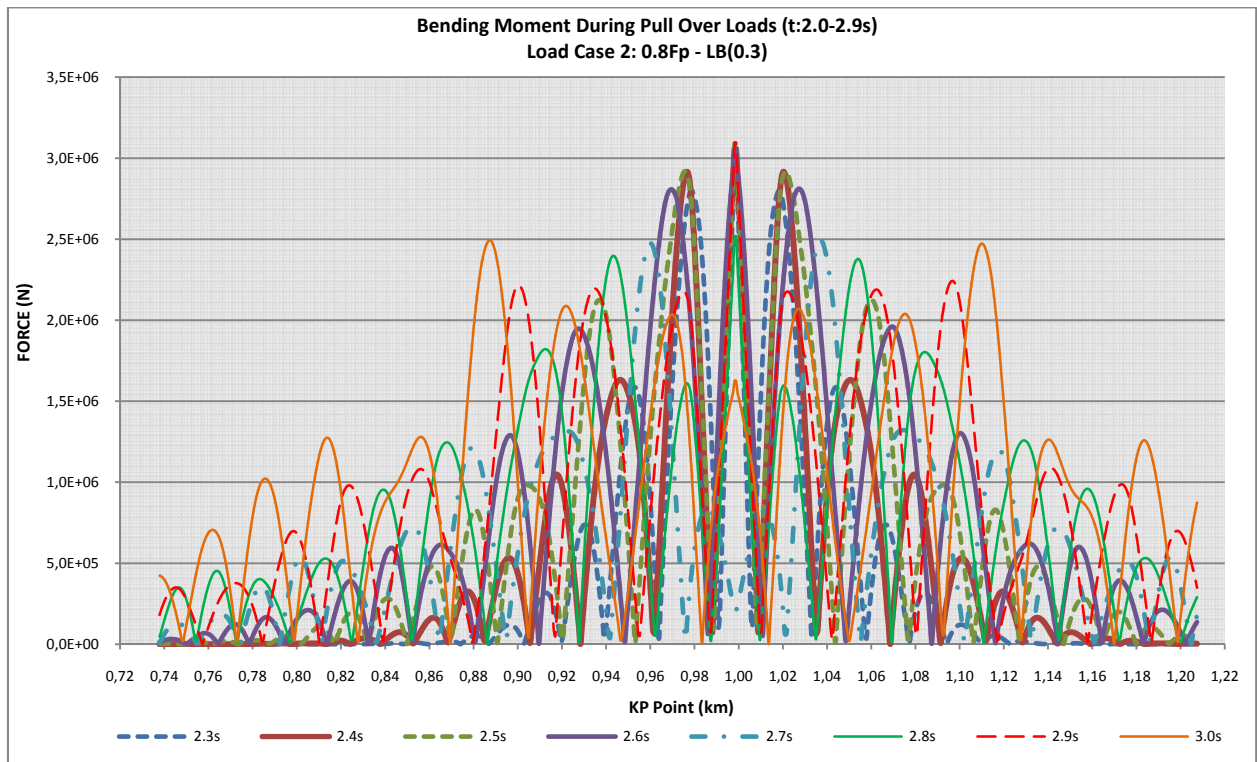


Figure C - 13 Bending moments during pull-over loads duration (t:2.0-2.9s) for load case 2

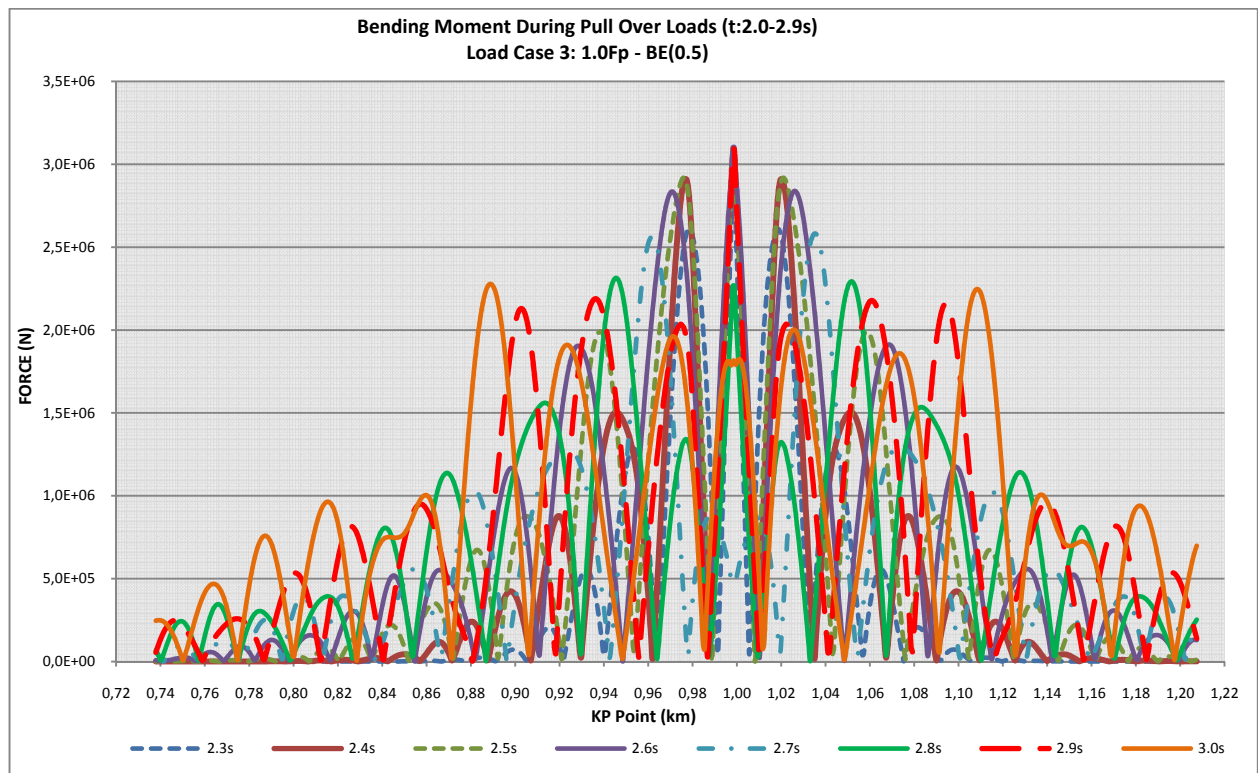


Figure C - 14 Bending moments during pull-over loads duration (t:2.0-2.9s) for load case 3

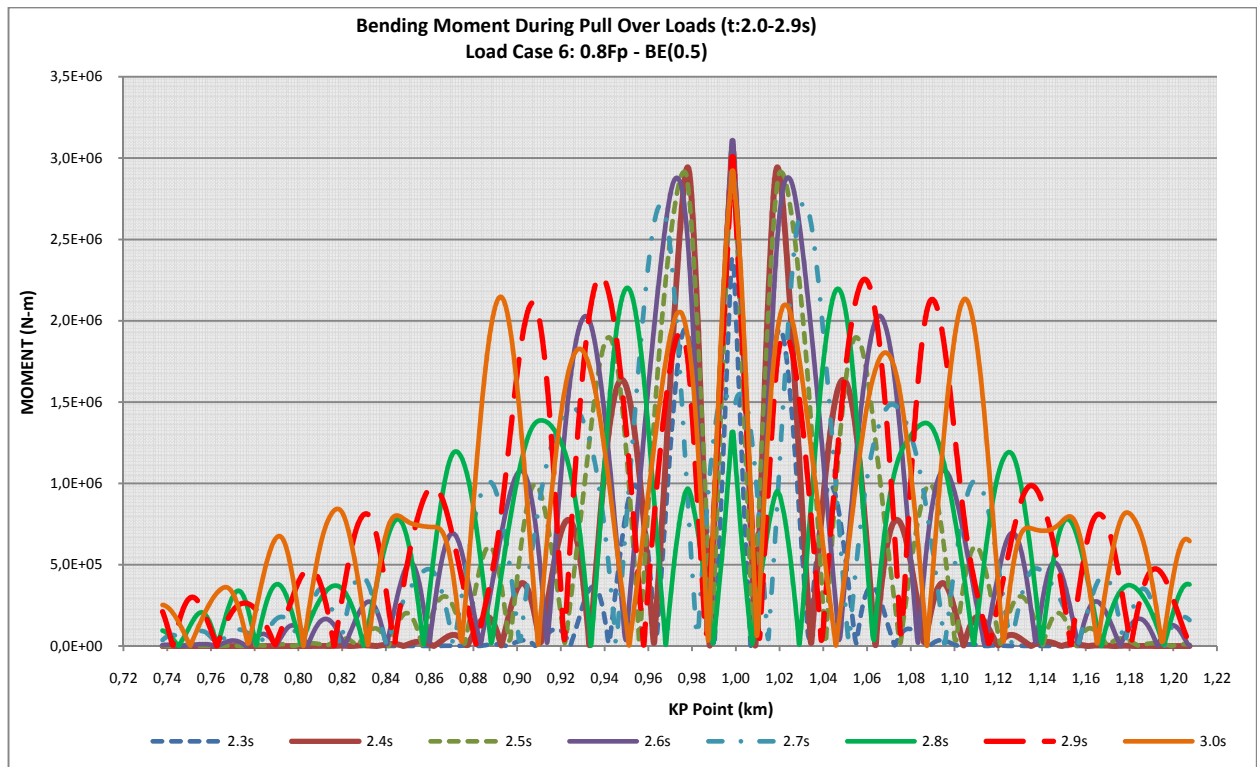


Figure C - 15 Bending moments during pull-over loads duration (t:2.0-2.9s) for load case 6

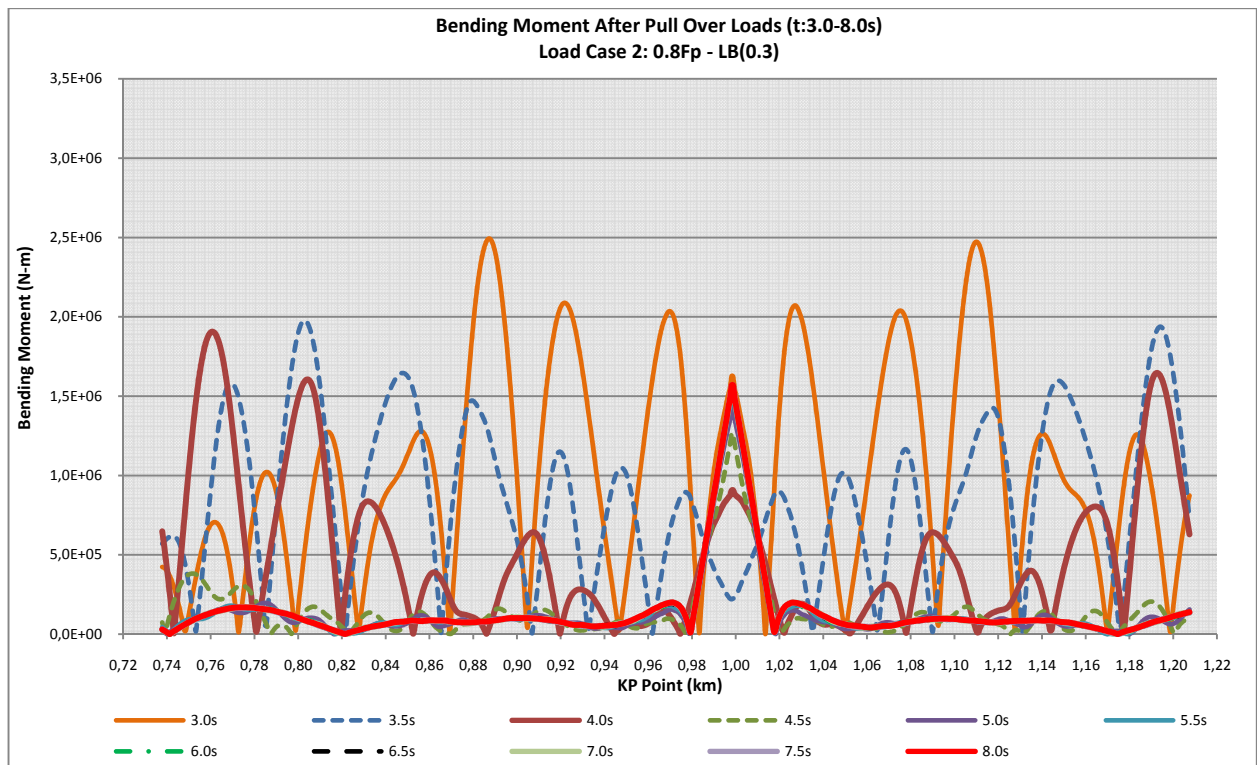


Figure C - 16 Bending moments after pull-over loads duration (t:3.0-8.0s) for load case 2

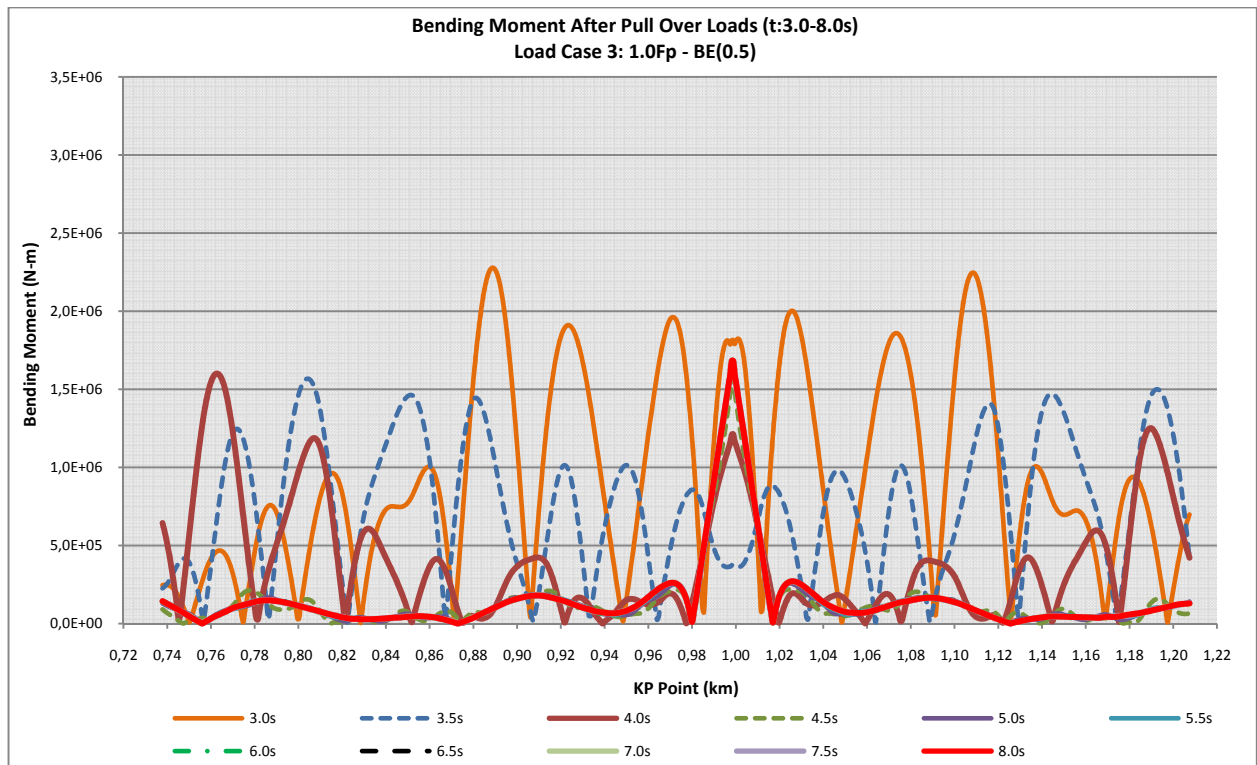


Figure C - 17 Bending moments after pull-over loads duration (t:3.0-8.0s) for load case 3

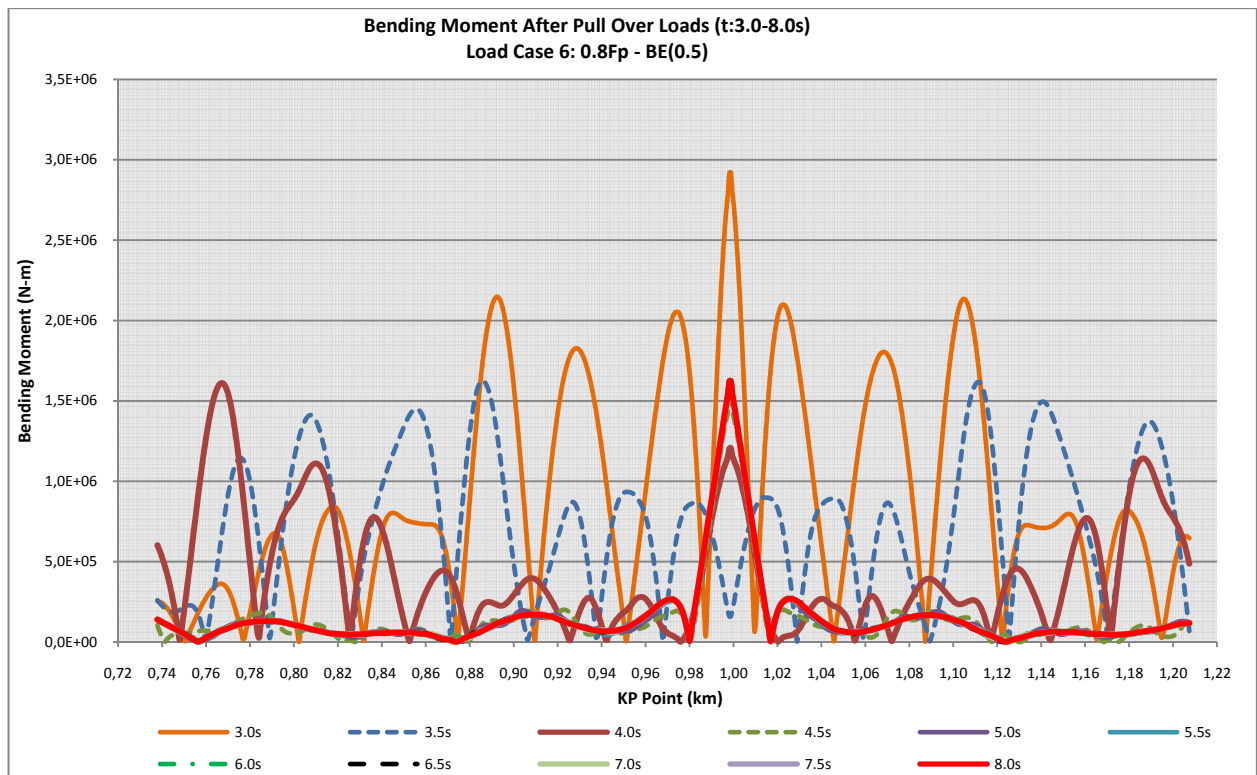


Figure C - 18 Bending moments after pull-over loads duration (t:3.0-8.0s) for load case 6

Appendix C-4

Effective Axial Force

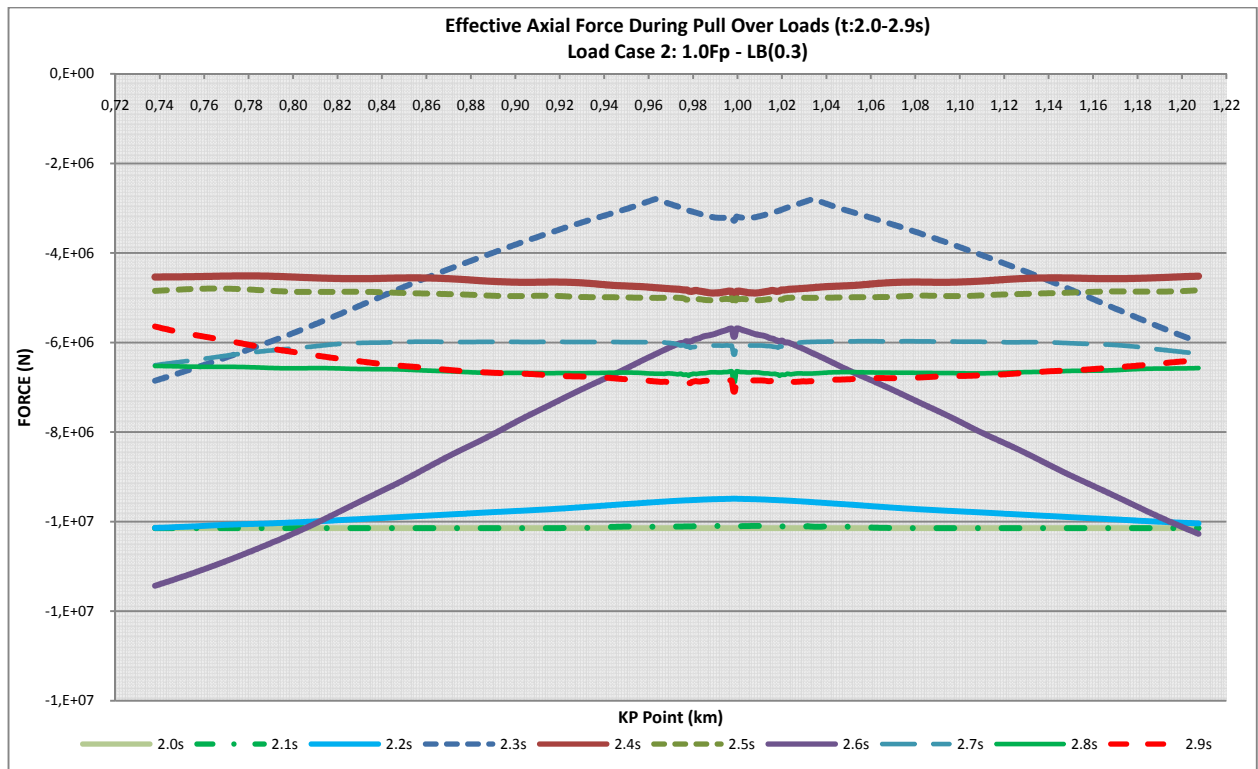


Figure C - 19 Effective axial force during pull-over loads durations (t:2.0-2.9s) for load case 2

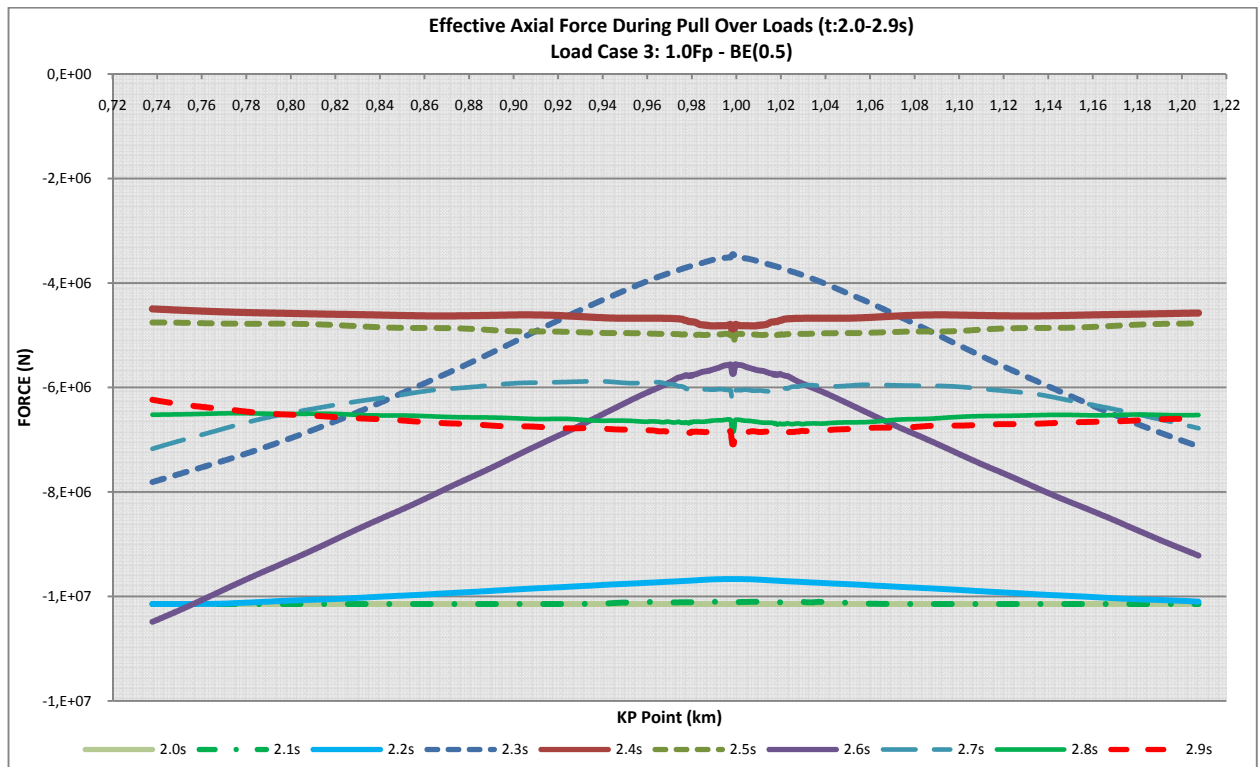


Figure C - 20 Effective axial force during pull-over loads durations (t:2.0-2.9s) for load case 3

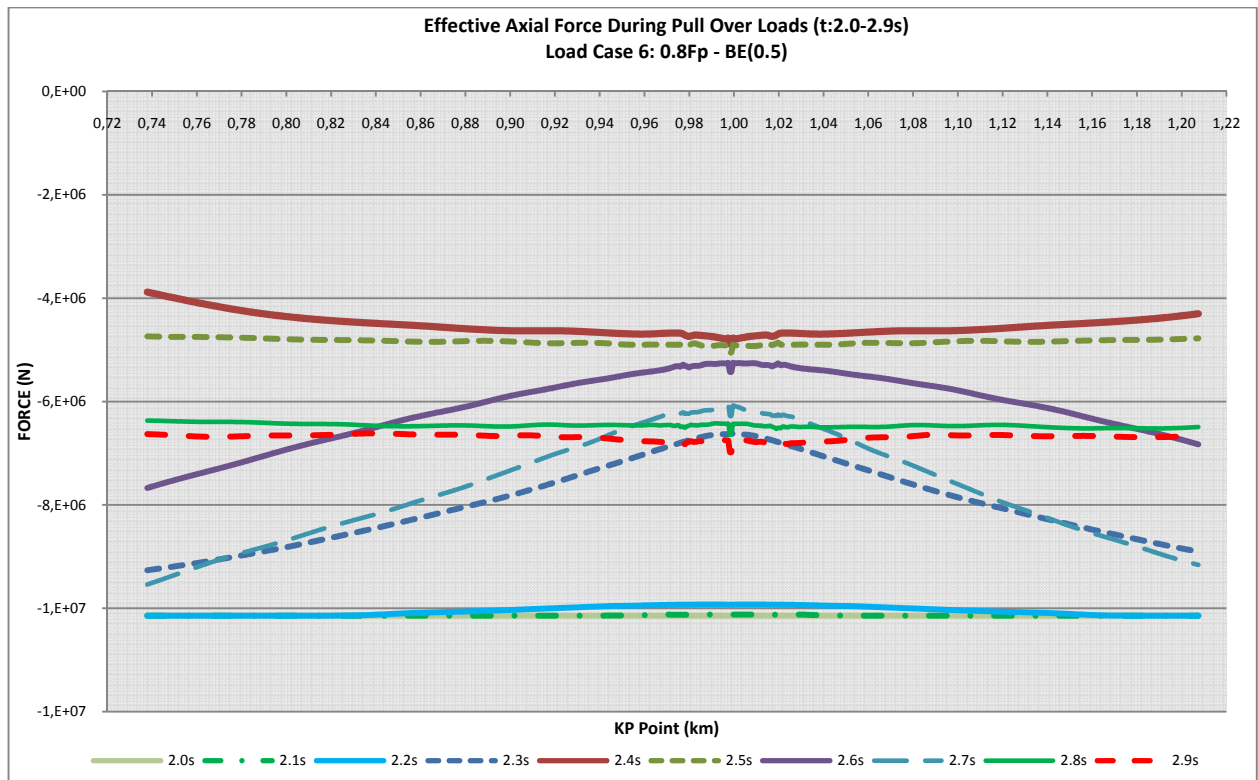


Figure C - 21 Effective axial force during pull-over loads durations (t:2.0-2.9s) for load case 6

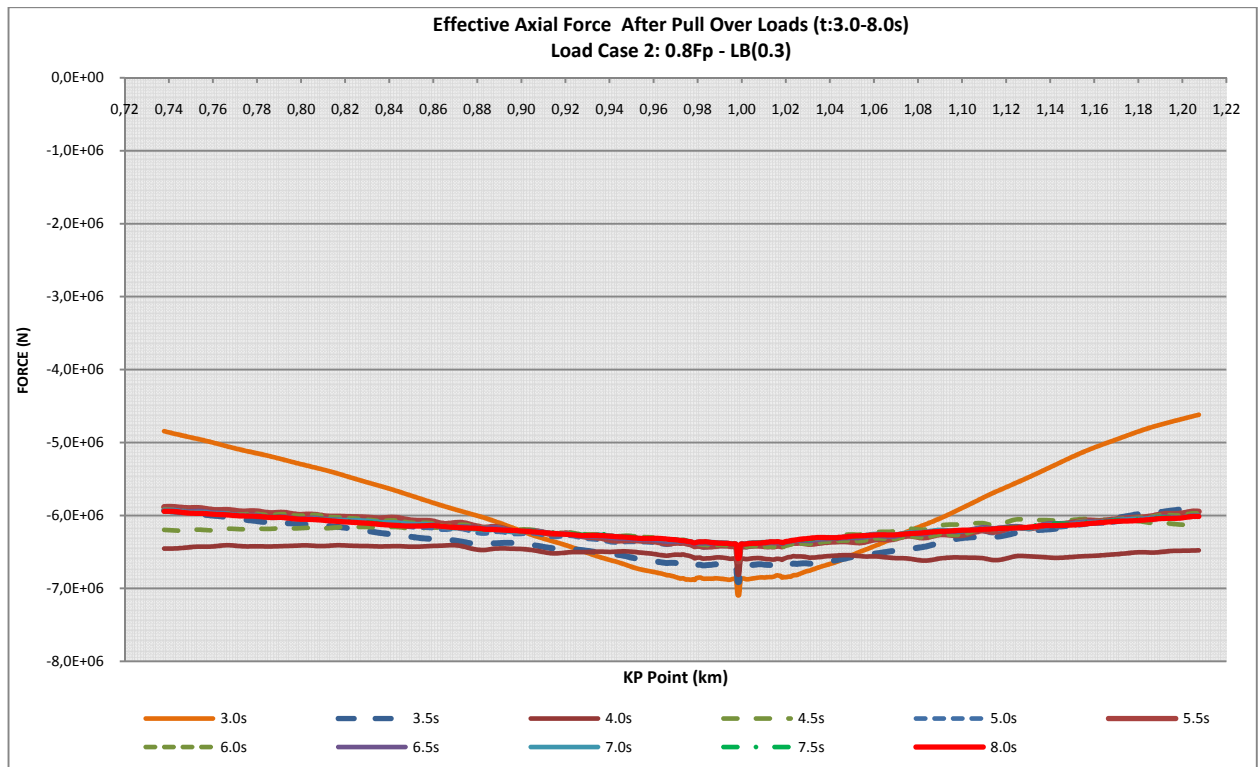


Figure C - 22 Effective axial force after pull-over loads duration (t:3.0-8.0s) for load case 2

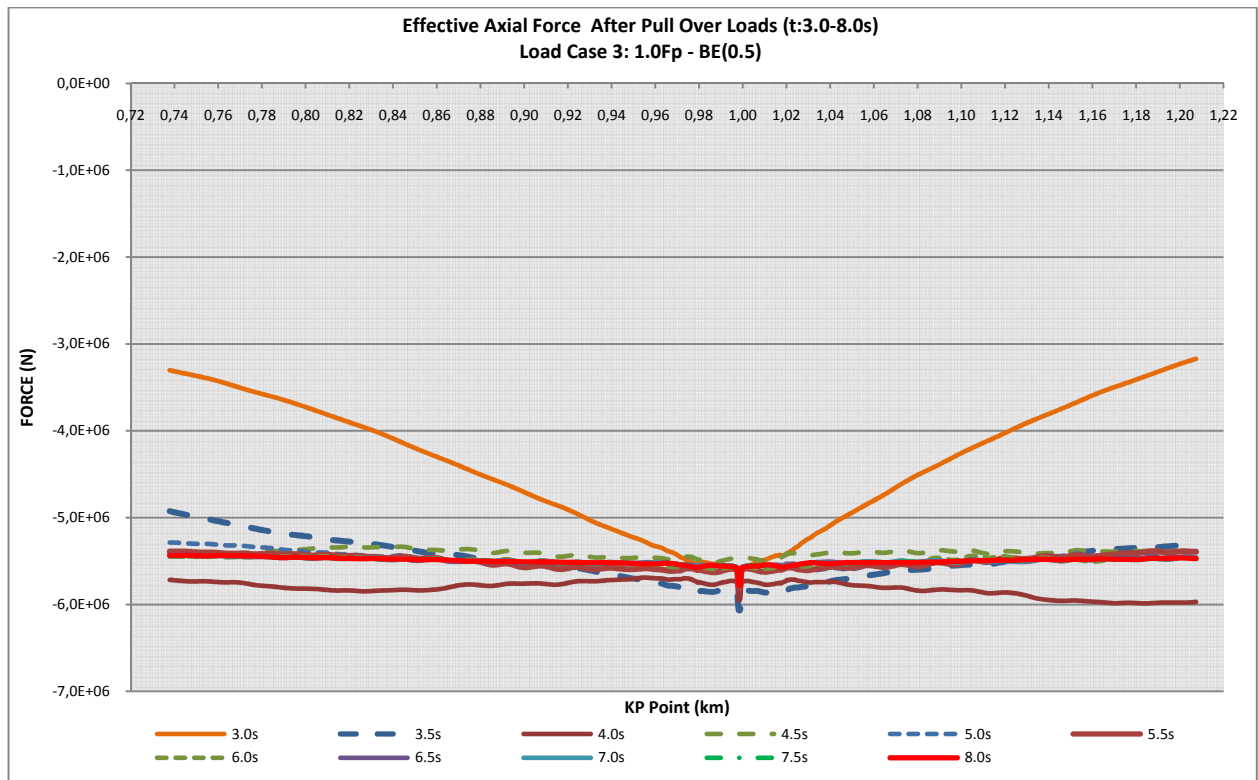


Figure C - 23 Effective axial force after pull-over loads duration (t:3.0-8.0s) for load case 3

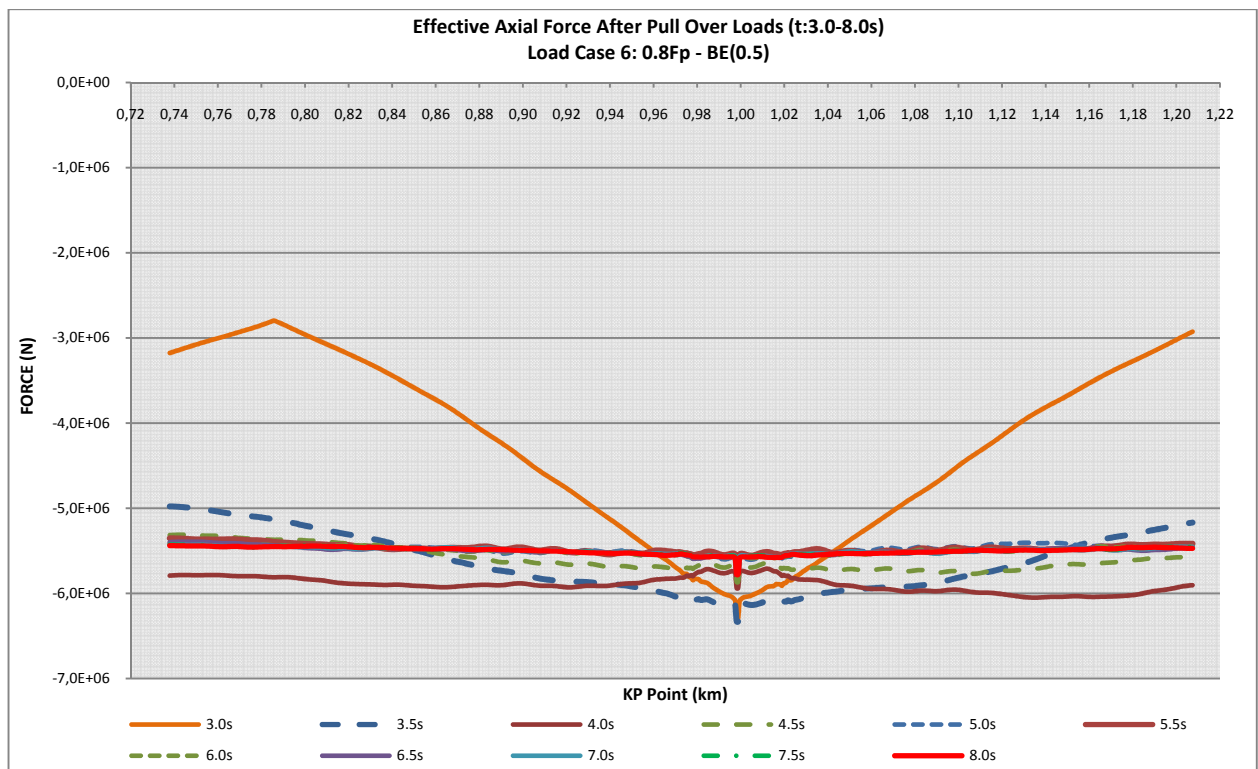


Figure C - 24 Effective axial force after pull-over loads duration (t:3.0-8.0s) for load case 6

Appendix C-5

Equivalent Strain

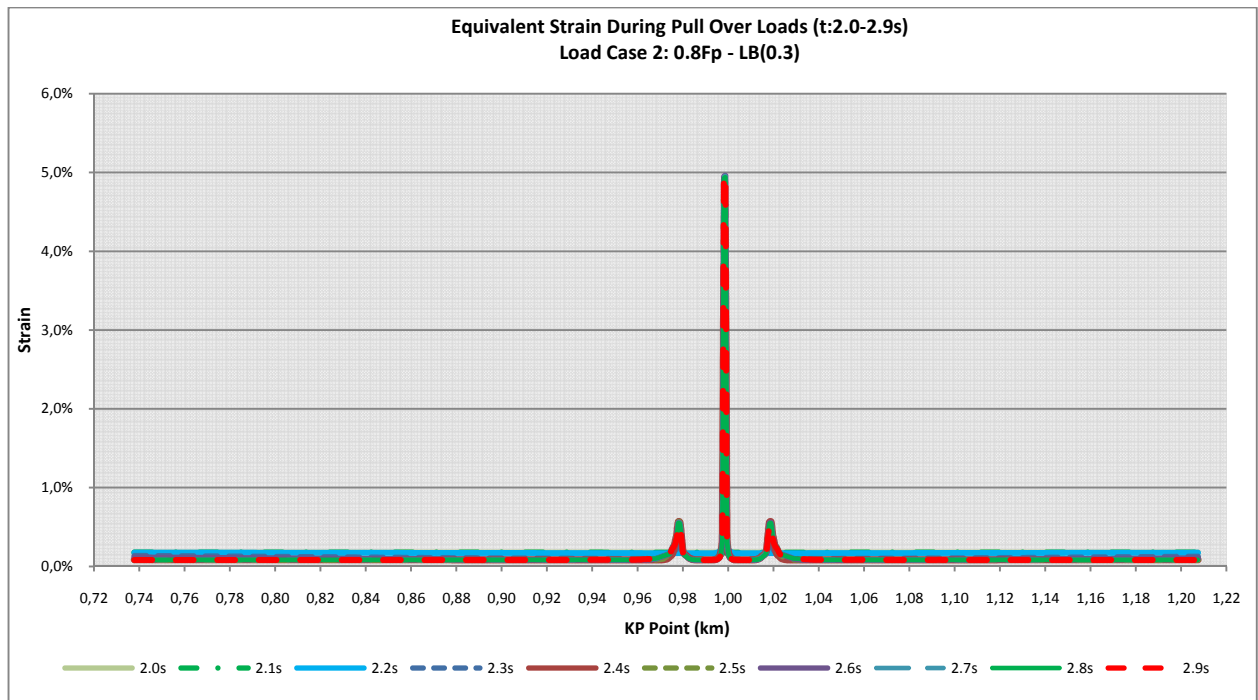


Figure C - 25 Equivalent strain during pull-over loads duration (t:2.0-2.9s) for load case 2

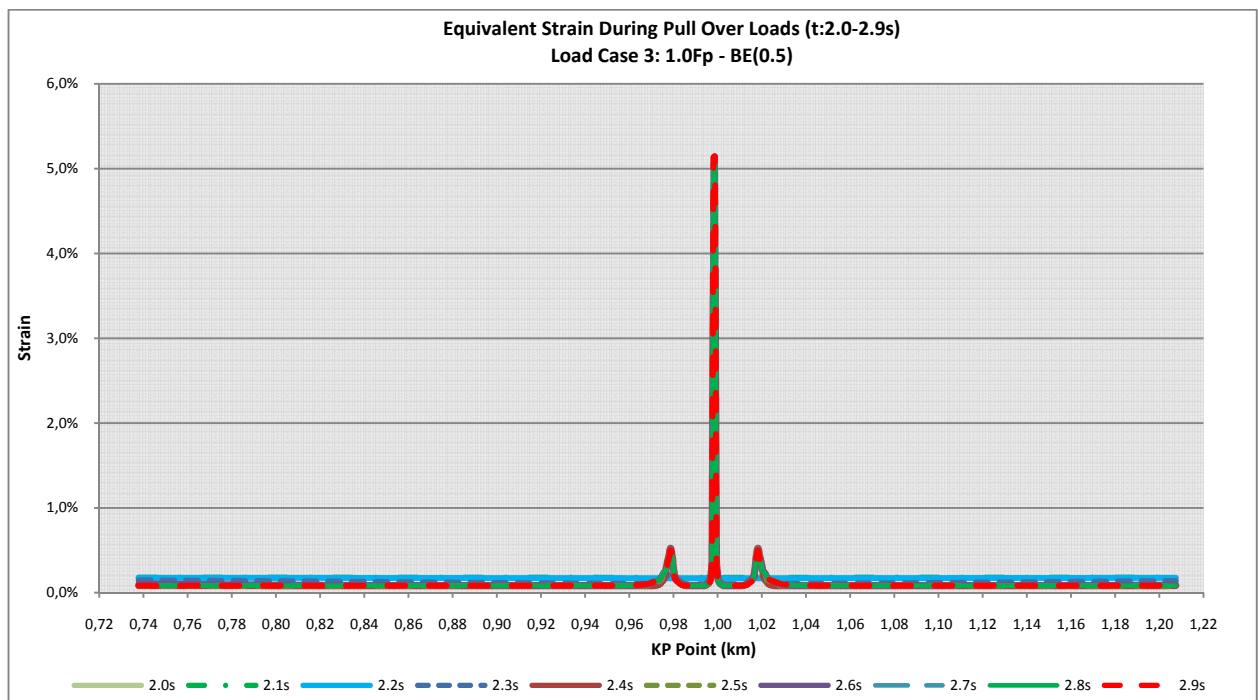


Figure C - 26 Equivalent strain during pull-over loads duration (t:2.0-2.9s) for load case 3

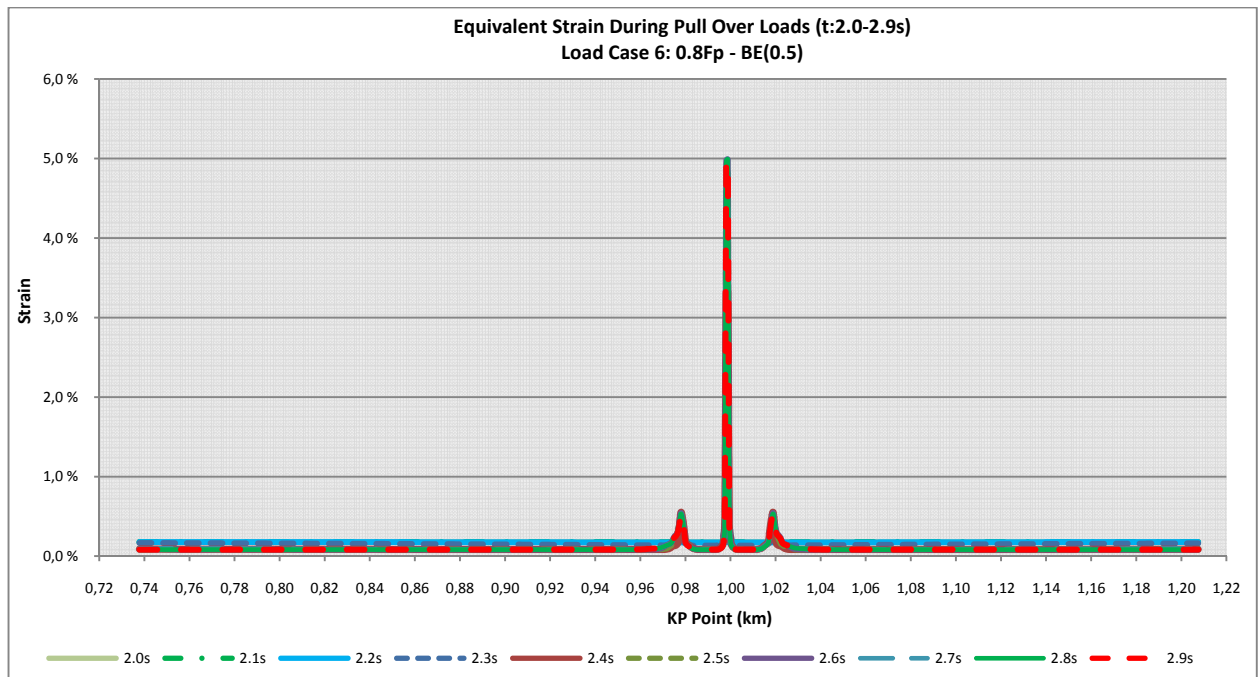


Figure C - 27 Equivalent strain during pull-over loads duration (t:2.0-2.9s) for load case 6

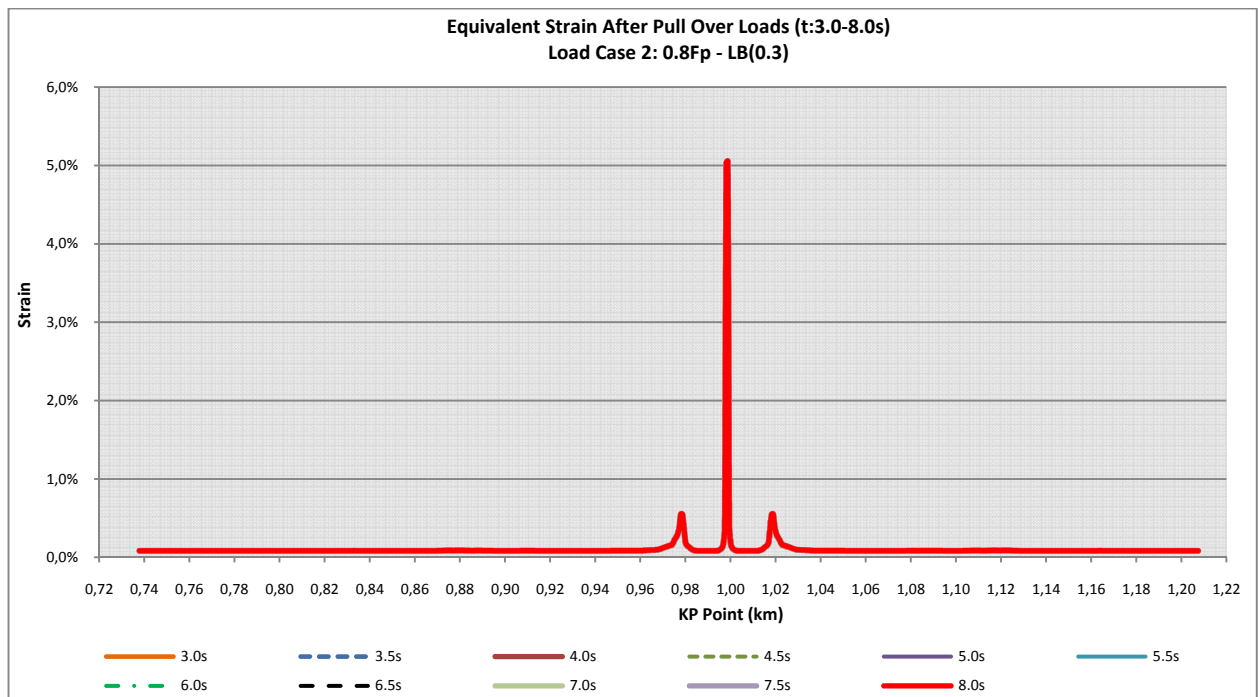


Figure C - 28 Equivalent strain after pull-over loads duration (t:3.0-8.0s) for load case 2

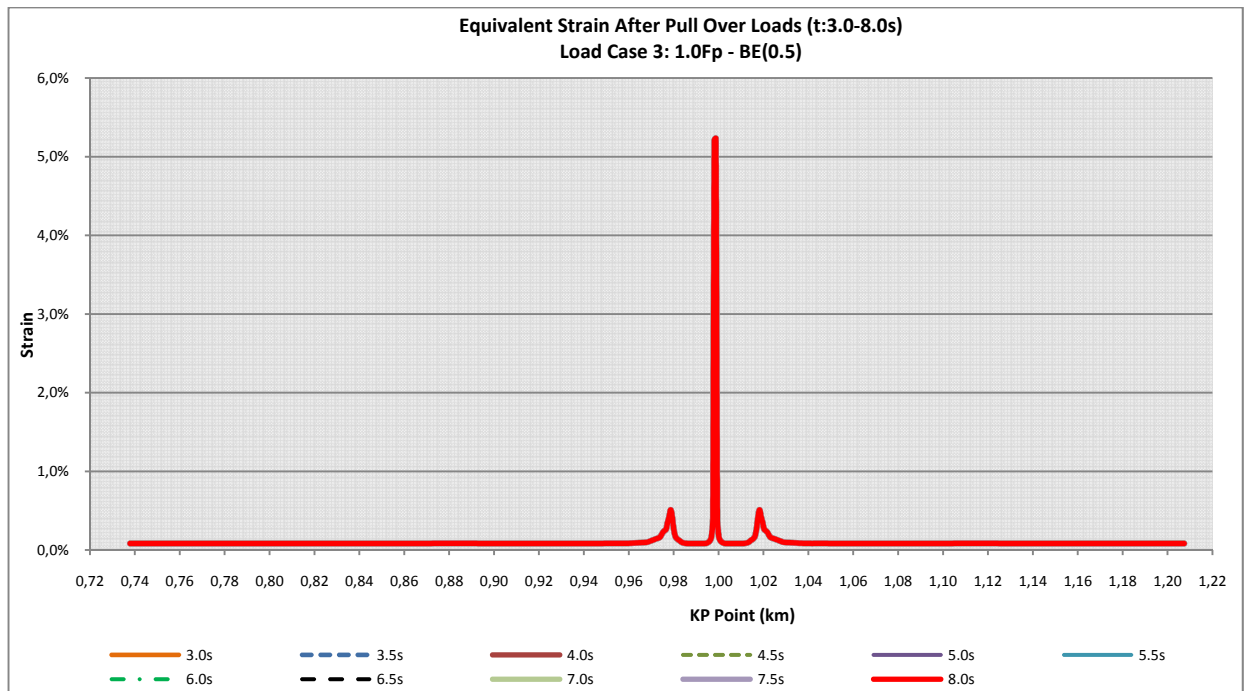


Figure C - 29 Equivalent strain after pull-over loads duration (t:3.0-8.0s) for load case 3

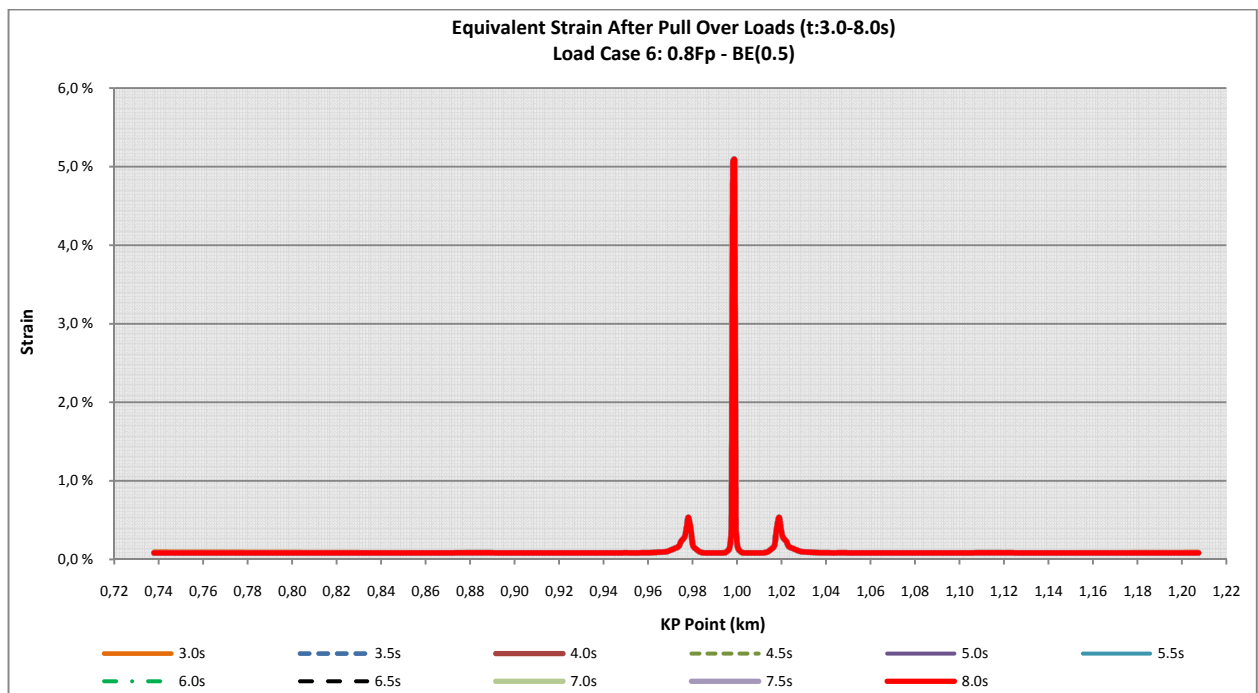


Figure C - 30 Equivalent strain after pull-over loads duration (t:3.0-8.0s) for load case 6

Appendix D

DNV Displacement Controlled Condition Code Check

DNV-OS-F101 - SUBMARINE PIPELINE SYSTEMS - 2007

Pipeline Engineering Tool (PET)

Load Combination - Displacement Controlled Condition

Project: PolRec LC1

Section: pipeline

KP Start: 0,000

KP End: 2,000

Date: 14.06.2011



RELEVANT INPUT PARAMETERS:			
Nominal outer steel diameter [mm]:		559,00	
Nominal steel wall thickness [mm]:		25,40	
Corrosion allowance [mm]:		3,00	
Ovality [%]:		1,50	
Girth weld factor [-]:		0,98	
Specified minimum yield stress [MPa]:		450,0	
Derating in yield stress due to temperature [MPa]:		30,0	
Young's modulus [GPa]:		207,0	
Poisson's ratio [-]:		0,30	
Yield to tensile ratio [-]:		0,93	
Material strength factor [-]:		1,00	
Internal pressure at reference level [bar] and reference level [m]:	150,0 @ -99,0		
Density of internal fluid [kg/m ³]:		900,0	
Depth [m]:		100,0	
Density of external fluid [kg/m ³]:		1027,0	
Load condition factor [-]:		0,80	
Functional and environmental moment [kNm]:	5,0 & 0,0		
Safety Class :		MEDIUM	
Corroded wall thickness :		NO	
Derated material properties :		YES	
INTERMEDIATE RESULTS:		Load comb. a	Load comb. b
Local internal pressure [bar]:		150,1	
External pressure [bar]:		10,1	
Characteristic yield stress [MPa]:		0,0	
Steel wall thickness used in code check [mm]:		0,00	
Design compressive strain [%]:	4,78		4,38
Design pressure [bar]:	0,0		0,0
Characteristic pressure containment resistance [bar]:		0,0	
Hoop stress [MPa]:		154,4	
Characteristic plastic strain capacity [%]:		8,29	
Resistance strain factor [-]:		2,50	
FINAL RESULTS:		Load comb. a	Load comb. b
Code check, utility with given wall thickness [-]:		1,44	1,32
Required nominal wall thicness [mm]:		46,52	40,33

DNV-OS-F101 - SUBMARINE PIPELINE SYSTEMS - 2007

Pipeline Engineering Tool (PET)

Load Combination - Displacement Controlled Condition

Project: PolRec LC2

Section: pipeline

KP Start: 0,000

KP End: 2,000

Date: 14.06.2011



RELEVANT INPUT PARAMETERS:			
Nominal outer steel diameter [mm]:		559,00	
Nominal steel wall thickness [mm]:		25,40	
Corrosion allowance [mm]:		3,00	
Ovality [%]:		1,50	
Girth weld factor [-]:		0,98	
Specified minimum yield stress [MPa]:		450,0	
Derating in yield stress due to temperature [MPa]:		30,0	
Young's modulus [GPa]:		207,0	
Poisson's ratio [-]:		0,30	
Yield to tensile ratio [-]:		0,93	
Material strength factor [-]:		1,00	
Internal pressure at reference level [bar] and reference level [m]:	150,0 @ -99,0		
Density of internal fluid [kg/m ³]:		900,0	
Depth [m]:		100,0	
Density of external fluid [kg/m ³]:		1027,0	
Load condition factor [-]:		0,80	
Functional and environmental moment [kNm]:	5,0 & 0,0		
Safety Class :		MEDIUM	
Corroded wall thickness :		NO	
Derated material properties :		YES	
INTERMEDIATE RESULTS:		Load comb. a	Load comb. b
Local internal pressure [bar]:		150,1	
External pressure [bar]:		10,1	
Characteristic yield stress [MPa]:		0,0	
Steel wall thickness used in code check [mm]:		0,00	
Design compressive strain [%]:	4,78		4,38
Design pressure [bar]:	0,0		0,0
Characteristic pressure containment resistance [bar]:		0,0	
Hoop stress [MPa]:		154,4	
Characteristic plastic strain capacity [%]:		8,29	
Resistance strain factor [-]:		2,50	
FINAL RESULTS:		Load comb. a	Load comb. b
Code check, utility with given wall thickness [-]:		1,44	1,32
Required nominal wall thicness [mm]:		46,52	40,33

DNV-OS-F101 - SUBMARINE PIPELINE SYSTEMS - 2007

Pipeline Engineering Tool (PET)

Load Combination - Displacement Controlled Condition

Project: PolRec LC3

Section: pipeline

KP Start: 0,000

KP End: 2,000

Date: 14.06.2011



RELEVANT INPUT PARAMETERS:			
Nominal outer steel diameter [mm]:	559,00		
Nominal steel wall thickness [mm]:	25,40		
Corrosion allowance [mm]:	3,00		
Ovality [%]:	1,50		
Girth weld factor [-]:	0,98		
Specified minimum yield stress [MPa]:	450,0		
Derating in yield stress due to temperature [MPa]:	30,0		
Young's modulus [GPa]:	207,0		
Poisson's ratio [-]:	0,30		
Yield to tensile ratio [-]:	0,93		
Material strength factor [-]:	1,00		
Internal pressure at reference level [bar] and reference level [m]:	150,0 @ -99,0		
Density of internal fluid [kg/m ³]:	900,0		
Depth [m]:	100,0		
Density of external fluid [kg/m ³]:	1027,0		
Load condition factor [-]:	0,80		
Functional and environmental moment [kNm]:	5,1 & 0,0		
Safety Class :	MEDIUM		
Corroded wall thickness :	NO		
Derated material properties :	YES		
INTERMEDIATE RESULTS:	Load comb. a	Load comb. b	
Local internal pressure [bar]:	150,1		
External pressure [bar]:	10,1		
Characteristic yield stress [MPa]:	0,0		
Steel wall thickness used in code check [mm]:	0,00		
Design compressive strain [%]:	4,93	4,52	
Design pressure [bar]:	0,0	0,0	
Characteristic pressure containment resistance [bar]:	0,0		
Hoop stress [MPa]:	154,4		
Characteristic plastic strain capacity [%]:	8,29		
Resistance strain factor [-]:	2,50		
FINAL RESULTS:	Load comb. a	Load comb. b	
Code check, utility with given wall thickness [-]:	1,49	1,36	
Required nominal wall thicness [mm]:	48,97	42,49	

DNV-OS-F101 - SUBMARINE PIPELINE SYSTEMS - 2007

Pipeline Engineering Tool (PET)

Load Combination - Displacement Controlled Condition

Project: PolRec LC4

Section: pipeline

KP Start: 0,000

KP End: 2,000

Date: 14.06.2011



RELEVANT INPUT PARAMETERS:			
Nominal outer steel diameter [mm]:		559,00	
Nominal steel wall thickness [mm]:		25,40	
Corrosion allowance [mm]:		3,00	
Ovality [%]:		1,50	
Girth weld factor [-]:		0,98	
Specified minimum yield stress [MPa]:		450,0	
Derating in yield stress due to temperature [MPa]:		30,0	
Young's modulus [GPa]:		207,0	
Poisson's ratio [-]:		0,30	
Yield to tensile ratio [-]:		0,93	
Material strength factor [-]:		1,00	
Internal pressure at reference level [bar] and reference level [m]:	150,0 @ -99,0		
Density of internal fluid [kg/m ³]:		900,0	
Depth [m]:		100,0	
Density of external fluid [kg/m ³]:		1027,0	
Load condition factor [-]:		0,80	
Functional and environmental moment [kNm]:	0,0 & 0,0		
Safety Class :		MEDIUM	
Corroded wall thickness :		NO	
Derated material properties :		YES	
INTERMEDIATE RESULTS:		Load comb. a	Load comb. b
Local internal pressure [bar]:		150,1	
External pressure [bar]:		10,1	
Characteristic yield stress [MPa]:		0,0	
Steel wall thickness used in code check [mm]:		0,00	
Design compressive strain [%]:	0,00		0,00
Design pressure [bar]:	0,0		0,0
Characteristic pressure containment resistance [bar]:		0,0	
Hoop stress [MPa]:		154,4	
Characteristic plastic strain capacity [%]:		8,29	
Resistance strain factor [-]:		2,50	
FINAL RESULTS:		Load comb. a	Load comb. b
Code check, utility with given wall thickness [-]:		1,49	1,36
Required nominal wall thicness [mm]:		48,97	42,49

DNV-OS-F101 - SUBMARINE PIPELINE SYSTEMS - 2007

Pipeline Engineering Tool (PET)

Load Combination - Displacement Controlled Condition

Project: PolRec LC5

Section: pipeline

KP Start: 0,000

KP End: 2,000

Date: 14.06.2011



RELEVANT INPUT PARAMETERS:			
Nominal outer steel diameter [mm]:	559,00		
Nominal steel wall thickness [mm]:	25,40		
Corrosion allowance [mm]:	3,00		
Ovality [%]:	1,50		
Girth weld factor [-]:	0,98		
Specified minimum yield stress [MPa]:	450,0		
Derating in yield stress due to temperature [MPa]:	30,0		
Young's modulus [GPa]:	207,0		
Poisson's ratio [-]:	0,30		
Yield to tensile ratio [-]:	0,93		
Material strength factor [-]:	1,00		
Internal pressure at reference level [bar] and reference level [m]:	150,0 @ -99,0		
Density of internal fluid [kg/m ³]:	900,0		
Depth [m]:	100,0		
Density of external fluid [kg/m ³]:	1027,0		
Load condition factor [-]:	0,80		
Functional and environmental moment [kNm]:	0,2 & 0,0		
Safety Class :	MEDIUM		
Corroded wall thickness :	NO		
Derated material properties :	YES		
INTERMEDIATE RESULTS:		Load comb. a	Load comb. b
Local internal pressure [bar]:	150,1		
External pressure [bar]:	10,1		
Characteristic yield stress [MPa]:	0,0		
Steel wall thickness used in code check [mm]:	0,00		
Design compressive strain [%]:	0,17	0,16	
Design pressure [bar]:	0,0	0,0	
Characteristic pressure containment resistance [bar]:	0,0		
Hoop stress [MPa]:	154,4		
Characteristic plastic strain capacity [%]:	8,29		
Resistance strain factor [-]:	2,50		
FINAL RESULTS:		Load comb. a	Load comb. b
Code check, utility with given wall thickness [-]:	0,05	0,05	
Required nominal wall thicness [mm]:	-1,00	5,58	

DNV-OS-F101 - SUBMARINE PIPELINE SYSTEMS - 2007

Pipeline Engineering Tool (PET)

Load Combination - Displacement Controlled Condition

Project: PolRec LC6

Section: pipeline

KP Start: 0,000

KP End: 2,000

Date: 14.06.2011



RELEVANT INPUT PARAMETERS:			
Nominal outer steel diameter [mm]:		559,00	
Nominal steel wall thickness [mm]:		25,40	
Corrosion allowance [mm]:		3,00	
Ovality [%]:		1,50	
Girth weld factor [-]:		0,98	
Specified minimum yield stress [MPa]:		450,0	
Derating in yield stress due to temperature [MPa]:		30,0	
Young's modulus [GPa]:		207,0	
Poisson's ratio [-]:		0,30	
Yield to tensile ratio [-]:		0,93	
Material strength factor [-]:		1,00	
Internal pressure at reference level [bar] and reference level [m]:	150,0 @ -99,0		
Density of internal fluid [kg/m ³]:		900,0	
Depth [m]:		100,0	
Density of external fluid [kg/m ³]:		1027,0	
Load condition factor [-]:		0,80	
Functional and environmental moment [kNm]:	5,1 & 0,0		
Safety Class :		MEDIUM	
Corroded wall thickness :		NO	
Derated material properties :		YES	
INTERMEDIATE RESULTS:		Load comb. a	Load comb. b
Local internal pressure [bar]:		150,1	
External pressure [bar]:		10,1	
Characteristic yield stress [MPa]:		0,0	
Steel wall thickness used in code check [mm]:		0,00	
Design compressive strain [%]:	4,89		4,48
Design pressure [bar]:	0,0		0,0
Characteristic pressure containment resistance [bar]:		0,0	
Hoop stress [MPa]:		154,4	
Characteristic plastic strain capacity [%]:		8,29	
Resistance strain factor [-]:		2,50	
FINAL RESULTS:		Load comb. a	Load comb. b
Code check, utility with given wall thickness [-]:		1,47	1,35
Required nominal wall thicness [mm]:		48,20	41,82